

Shear Behaviour of Disturbed Regions in Reinforced Concrete Beams with Corrosion Damaged Shear Reinforcement

by

Christopher Andrew Suffern

A thesis
presented to the University of Waterloo
in fulfillment of the
thesis requirement for the degree of
Masters of Applied Science
in
Civil Engineering

Waterloo, Ontario, Canada, 2008

©Christopher Andrew Suffern 2008

AUTHOR'S DECLARATION

I hereby declare that I am the sole author of this thesis. This is a true copy of the thesis, including any required final revisions, as accepted by my examiners.

I understand that my thesis may be made electronically available to the public.

Abstract

Corrosion of reinforcing steel is a major problem facing infrastructures owners with billions of dollars spent in repairing our aging infrastructure. One of the first steps in the repair process is to quantify the strength degradation in a reinforced concrete element caused by the corrosion of reinforcing steel. An understanding of the forces involved in the load carrying mechanisms is imperative; the transfer of shear forces in reinforced concrete beams is one of these load carrying mechanisms. The shear transfer mechanism is different near the end of beams, adjacent to point loads, and near changes in cross section. These regions are known as disturbed regions. Structural engineers have a good understanding of the shear transfer mechanism in disturbed regions. However, the effects of corroded shear reinforcement in these regions have not been widely investigated.

The current study is comprised of an experimental program and analytical strut and tie modeling aimed at quantifying the strength reduction that occurs in disturbed regions of reinforced concrete beams with corroded shear reinforcement. The feasibility of strengthening a beam with dry lay-up carbon fibre reinforced polymer (CFRP) to repair the damage caused by corrosion of the shear reinforcement was also investigated.

In the experimental study, a total of 16 reinforced concrete beams were cast. The specimens were 350 mm deep, 125 mm wide and 1850 mm long. Three shear-span to depth ratios (1.0, 1.5, 2.0) were selected. Each specimen was reinforced in flexure with two 25M bars and the shear reinforcement was 10M spaced at 150 mm on centre. The specimens were corroded for 21 days, 60 days, and 120 days corresponding to low, medium, and high corrosion levels. In addition, three specimens were constructed without shear reinforcement in the shear-span in order to compare the results from the corroded specimens. One specimen was also corroded to a high level and repaired with dry lay-up CFRP.

The specimens were corroded using an accelerated corrosion technique. There was evidence of cracking of the cover concrete in all specimens, and in the more severely corroded specimens delamination of the cover concrete was recorded. The stiffness of the corroded specimens was less than their corresponding control specimen, and a strength reduction was evident in most specimens. The maximum recorded strength reduction was 52% compared to the companion uncorroded specimen. It was revealed that a more critical case occurs when the corroded shear reinforcement was shifted during placement or was inclined closer to the direction of the compressive force flow. Also, it

was observed that the corroded shear reinforcement still provides limited ductility in comparison to the un-corroded reinforcement.

A strut and tie model was developed based on the experiments to explain the behaviour of disturbed regions with corroded shear reinforcement. The model consisted of direct and indirect struts. The effects of corrosion were expressed in terms of a reduction in the stirrup cross-section, a reduction of compressive strength due to corrosion cracking, and a reduction in the concrete cross section width. It was hypothesized that the corrosion crack width influences the concrete compressive strength in the strut; consequently, a mathematical model was developed that related the reduction in concrete compressive strength with corrosion crack width. Also, a relationship between reinforcing steel mass loss and corrosion crack width was utilized from the published literature. An effective cross section width was obtained by reducing the width by the damaged concrete cover. The results from these models were input into a strut and tie model as a reduction in concrete compressive strength. The output from the strut and tie model was the ultimate shear strength of the specimen. The developed models were compared with a model from the literature and compared with the experimental results.

The major contribution of this research is to allow designers to analyze disturbed regions with corroded shear reinforcement and determine the strength degradation; subsequently, one can determine what strengthening procedure would be most appropriate.

Acknowledgements

First and foremost, I would like to thank Dr. Khaled Soudki for his guidance and support throughout my studies. I always looked forward to and enjoyed our conversations.

I would like to acknowledge the Civil Engineering technical staff. Your technical knowledge and patience helped me complete the more challenging aspects of my research. I'd like to thank my graduate student colleagues and undergraduate research assistants that helped me with the laboratory work.

Finally, I would like to thank my family and friends for making this journey a little more fun and enjoyable.

Dedication

*To my
Mother, Father, and Sister
Thanks for the Love and Support*

Table of Contents

List of Figures	xii
List of Tables	xvi
Chapter 1 Introduction.....	1
1.1 General	1
1.2 Problem Statement.....	2
1.3 Research Objectives	2
1.4 Organization of Thesis	2
Chapter 2 Background and Literature Review	5
2.1 Introduction	5
2.2 Corrosion.....	5
2.2.1 Corrosion in Reinforced Concrete.....	5
2.2.2 Corrosion Initiators in Reinforced Concrete	6
2.2.2.1 Carbonation	6
2.2.2.2 Chloride Ingress.....	7
2.2.3 Macrocell and Microcell Corrosion.....	7
2.2.4 Factors Influencing Corrosion Rate in Reinforced Concrete	9
2.2.4.1 Initiation Phase	9
2.2.4.2 Propagation Phase	9
2.2.5 Formation of Rust.....	11
2.2.6 Strength of Corroded Reinforced Concrete	12
2.2.7 Accelerated Corrosion by Impressed Current	14
2.3 Shear in Reinforced Concrete.....	16
2.3.1 Beam and Arch Action	16
2.3.2 General Shear Models	17
2.3.2.1 Truss Analogy	17
2.3.2.2 Compression Field Theory	18
2.3.2.3 Strut and Tie Model.....	18
2.3.3 Deep Beam Shear Models	18
2.3.3.1 Bažant and Kim Model.....	19
2.3.3.2 Russo and Puleri Model.....	20
2.3.3.3 Matamoros and Wong Model.....	22

2.3.3.4 Russo, Venir, and Pauletta Model	24
2.4 Corrosion of Shear Reinforcement	26
Chapter 3 Experimental Program	34
3.1 Introduction	34
3.2 Test Program	34
3.3 Formwork Fabrication	35
3.4 Test Specimens	37
3.5 Material Properties	43
3.5.1 Concrete	43
3.5.2 Reinforcing and Stainless Steel	44
3.5.3 Carbon Fibre Reinforced Polymer System	44
3.6 Accelerated Corrosion	44
3.7 CFRP Strengthening	47
3.8 Test Setup and Instrumentation	47
3.8.1 Test Setup	47
3.8.2 Support System	48
3.8.3 Strain Measurement	50
3.8.4 Displacement Measurement	50
3.9 Mass Loss Analysis	51
3.9.1 Extraction of Reinforcing Steel	51
3.9.2 Gravimetric Mass Loss Analysis	52
Chapter 4 Experimental Results and Discussion	54
4.1 Introduction	54
4.2 Accelerated Corrosion Results	54
4.2.1 Corrosion Crack Widths	54
4.2.2 Reinforcing Steel Mass Loss	55
4.3 Monotonic Test Results	57
4.3.1 Experimental Results – $a/d = 1.0$	58
4.3.1.1 Cracking Load	59
4.3.1.2 Stiffness and Ductility	59
4.3.1.3 Ultimate Shear Strength	60
4.3.1.4 Crack Patterns and Modes of Failure	61

4.3.1.5 Diagonal Displacement	64
4.3.1.6 Reinforcing Steel Strain Behaviour.....	65
4.3.2 Experimental Results – $a/d = 1.5$	68
4.3.2.1 Cracking Load	69
4.3.2.2 Stiffness and Ductility	69
4.3.2.3 Ultimate Shear Strength	70
4.3.2.4 Crack Patterns and Modes of Failure	71
4.3.2.5 Reinforcing Steel Strain Behaviour.....	74
4.3.3 Experimental Results – $a/d = 2.0$	76
4.3.3.1 Cracking Load	77
4.3.3.2 Stiffness and Ductility	78
4.3.3.3 Ultimate Shear Strength	78
4.3.3.4 Crack Patterns and Modes of Failure	80
4.3.3.5 Diagonal Displacement	81
4.3.3.6 Reinforcing Steel Strain Behaviour.....	83
4.4 Feasibility of CFRP Repair	84
4.5 Summary	88
4.5.1 Un-corroded Specimens	88
4.5.1.1 Diagonal Cracking Load.....	88
4.5.1.2 Ultimate Shear Strength	88
4.5.1.3 Deflection at Failure	89
4.5.2 Corroded Specimens.....	90
4.5.2.1 Diagonal Cracking Load.....	90
4.5.2.2 Ultimate Shear Strength	92
4.5.2.3 Deflection at Failure	93
Chapter 5 Strut and Tie Modeling.....	95
5.1 Introduction	95
5.2 Design Codes.....	95
5.2.1 CSA A23.3-04	95
5.2.2 ACI 318-05.....	97
5.2.3 CEB-FIP Model Code 1990	99
5.3 Strut and Tie Model Evaluation	100

5.3.1 Model 1 – Direct Strut Mechanism	103
5.3.2 Model 2 – Direct and Indirect Strut Mechanism	105
5.3.3 Model 3 – Direct and Indirect Strut Mechanism with Effectiveness Factor	110
5.3.4 Discussion	112
Chapter 6 Effect of Corrosion in Strut and Tie Modelling.....	115
6.1 Introduction	115
6.2 Proposed Model.....	115
6.2.1 Mass Loss Model.....	116
6.2.2 Effective Concrete Strength	118
6.2.3 Linear Reduction Model.....	120
6.3 Effective Width Model.....	121
6.4 Model Evaluation	122
6.5 Application of Model	125
6.6 Discussion	125
Chapter 7 Conclusions and Recommendations	127
7.1 Introduction	127
7.2 Conclusions	127
7.2.1 Accelerated Corrosion.....	127
7.2.2 Effect of Corrosion	128
7.2.3 Effect of the presence of shear reinforcement.....	129
7.2.4 Effect of Shear-span to Depth Ratio.....	129
7.2.5 CFRP Repair.....	130
7.2.6 Strut and Tie Modelling.....	130
7.2.7 Effect of Corrosion in Strut and Tie Modelling	130
7.3 Recommendations	131
7.3.1 Specimen Fabrication	131
7.3.2 Accelerated Corrosion	131
7.3.3 Monotonic Testing.....	132
7.3.4 Repair Methods	132
Bibliography	133
Appendices	138
Appendix A Drawings.....	138

Appendix B Crack Width Drawings.....	152
Appendix C Material Tests and Mass Loss Analysis	163
Appendix D Specimen Strain Data.....	166
Appendix E Calculations.....	173
Appendix F Strut and Tie Model Validation	176
Appendix G Strut and Tie Models.....	183
Appendix H Corrosion Strut and Tie Model	220
Appendix I Case Study.....	245

List of Figures

Figure 2.1 Corrosion Process (Badawi, 2003).....	6
Figure 2.2 Microcell and Macrocell Corrosion (Badawi, 2003)	8
Figure 2.3 Volume of Rust (Liu and Weyers, 1998).....	12
Figure 2.4 Load Elongation Behaviour of Corroded Reinforcing Steel (Almusallam, 2001).....	13
Figure 2.5 Accelerated Corrosion Schematic	15
Figure 2.6 Shear Transfer Mechanisms (Russo and Puleri, 1997).....	19
Figure 2.7 Strut and Tie Models (Matamoros and Wong, 2003).....	22
Figure 2.8 Strength Coefficients (Matamoros and Wong, 2003)	23
Figure 2.9 Beam Elevation and Cross Section Kage et al. (1997)	27
Figure 2.10 Beam Loading and Crack Pattern Kage et al. (1997).....	27
Figure 2.11 Load-Deflection Plot Kage et al. (1997)	28
Figure 2.12 Beam Cross Section Regan and Kennedy Reid (2004).....	29
Figure 2.13 Beam Configuration Toongoenthong and Maekawa (2005)	29
Figure 2.14 Load Deflection Curves Toongoenthong and Maekawa (2005)	30
Figure 2.15 Load-Deflection Response Higgins and Farrow (2006)	31
Figure 2.16 Corrosion of Shear Stirrups Concrete Crack Pattern (Higgins et al., 2003)	32
Figure 3.1 Formwork Drawing.....	35
Figure 3.2 Upright Fabrication.....	36
Figure 3.3 Formwork Construction	37
Figure 3.4 Beam Cross Section	38
Figure 3.5 Beam Reinforcing	38
Figure 3.6 Beam Type.....	39
Figure 3.7 Stirrup Electrical Connection.....	40
Figure 3.8 Continuity Test.....	40
Figure 3.9 Reinforcing Steel Cages.....	41
Figure 3.10 Stainless Steel Tube Cathode	41
Figure 3.11 Concrete Dividers	42
Figure 3.12 Salted Concrete Distribution.....	42
Figure 3.13 Power Supplies.....	46
Figure 3.14 Corrosion Wiring Schematic.....	46
Figure 3.15 Anode and Cathode Connections	46

Figure 3.16 CFRP Application	48
Figure 3.17 Test Setup.....	48
Figure 3.18 Specimen Support System	49
Figure 3.19 Load Point System	49
Figure 3.20 Strain Gauge Application.....	50
Figure 3.21 Diagonal Displacement Setup.....	51
Figure 3.22 Stirrup Extraction.....	52
Figure 3.23 Mass Loss Analysis.....	53
Figure 4.1 Typical Corrosion Crack Pattern.....	54
Figure 4.2 Mass Loss Variation.....	56
Figure 4.3 Load-Deflection Behaviour $a/d = 1.0$	58
Figure 4.4 Inclined Corrosion Crack in Specimen M-1.0-R	61
Figure 4.5 Isolated and Continuous Cracks in Specimens M-1.0-R and L-1.0-R.....	62
Figure 4.6 Failure Crack Patterns $a/d = 1.0$	63
Figure 4.7 Crack Pattern in Specimen H-1.0-R.....	64
Figure 4.8 Diagonal Displacement Behaviour $a/d = 1.0$	65
Figure 4.9 Strain Behaviour of the Shear Reinforcement in Specimen 0-1.0-R	66
Figure 4.10 Strain Behaviour Longitudinal Reinforcement in Specimen 0-1.0-R.....	67
Figure 4.11 Strain Behaviour Longitudinal Reinforcement in Specimen L-1.0-R.....	67
Figure 4.12 Load-Deflection Behaviour $a/d = 1.5$	68
Figure 4.13 Failure Crack Patterns $a/d = 1.5$	72
Figure 4.14 Diagonal Displacement Behaviour $a/d = 1.5$	73
Figure 4.15 Diagonal Displacement Behaviour for Specimen 0-1.5-UR.....	73
Figure 4.16 Strain Behaviour in the Main Reinforcement Specimen L-1.5-R.....	75
Figure 4.17 Strain Behaviour of the Shear Reinforcement Specimen L-1.5-R.....	75
Figure 4.18 Strain Behaviour in the Shear Reinforcement Specimen 0-1.5-R.....	76
Figure 4.19 Load-Deflection Behaviour $a/d = 2.0$	77
Figure 4.20 Crack Pattern in Specimens L-2.0-R and M(L)-2.0-R.....	80
Figure 4.21 Diagonal Displacement $a/d = 2.0$	81
Figure 4.22 Failure Crack Patterns $a/d = 2.0$	82
Figure 4.23 Strain in Shear Reinforcement Specimen 0-2.0-R.....	84
Figure 4.24 Load-Deflection Behaviour of H-1.5-Repair	85

Figure 4.25 Crack Pattern at Failure and Crushing under CFRP Specimen H-1.5-Repair.....	86
Figure 4.26 Strain Behaviour of CFRP	87
Figure 4.27 Strain Behaviour of the Reinforcing Steel Specimen H-1.5-Repair	87
Figure 4.28 Diagonal Cracking Load for Control and Un-reinforced Specimens.....	88
Figure 4.29 Ultimate Shear Strength of Control and Un-reinforced Specimens	89
Figure 4.30 Deflection at Failure of Control and Un-reinforced Specimens	90
Figure 4.31 Diagonal Cracking Load versus Degree of Corrosion	91
Figure 4.32 Diagonal Cracking Load versus Shear-span to Depth Ratio.....	91
Figure 4.33 Shear Strength Vs. Degree of Corrosion.....	92
Figure 4.34 Shear Strength Vs. Shear-span to Depth Ratio	93
Figure 4.35 Deflection at Failure Vs. Degree of Corrosion	94
Figure 4.36 Deflection at Failure Vs. Shear-span to Depth Ratio.....	94
Figure 5.1 Crushing Strength of Concrete Strut (CSA A23.3-04, 2006)	96
Figure 5.2 Parabola-Rectangle Stress-Strain Diagram (CEB-FIP, 1990).....	99
Figure 5.3 Schematic of Stress from Uniform Stress Method (CEB-FIP, 1990)	100
Figure 5.4 Direct Strut Mechanism	103
Figure 5.5 Direct Strut Model Algorithm.....	104
Figure 5.6 Direct Strut Model Validation.....	105
Figure 5.7 Direct and Indirect Strut and Tie Model (CEB-FIP, 1999).....	106
Figure 5.8 Direct and Indirect Strut Mechanism	106
Figure 5.9 Angles at Node-Strut Connections.....	107
Figure 5.10 Direct and Indirect Model Algorithm	108
Figure 5.11 Calculation Algorithm for Lower or Upper Strut.....	109
Figure 5.12 Direct and Indirect Strut Model Validation	110
Figure 5.13 Direct and Indirect Strut (with Effectiveness Factor) Model Validation	111
Figure 5.14 Comparison of Models 2 and 3 with Shear-span to Depth ratio	112
Figure 5.15 Comparison of Models 2 and 3 with Concrete Strength	113
Figure 5.16 Comparison of Models 2 and 3 with Flexural Reinforcement Ratio	114
Figure 5.17 Comparison of Models 2 and 3 with Shear Reinforcement Ratio.....	114
Figure 6.1 Corrosion Model Flowchart.....	116
Figure 6.2 Average Corrosion Crack Width versus Mass Loss.....	118
Figure 6.3 Direct Strut and Tie Model	119

Figure 6.4 Linear Reduction Model	122
Figure 6.5 Model Comparison.....	124

List of Tables

Table 2.1 Beam Shear Classification.....	16
Table 3.1 Test Matrix	34
Table 3.2 Concrete Mix Design.....	43
Table 3.3 Concrete Compressive Strength	43
Table 3.4 Properties of CFRP System.....	44
Table 4.1 Corrosion Crack Widths.....	55
Table 4.2 Mass Loss Results	57
Table 4.3 Re-categorized Test Matrix	57
Table 4.4 Load-Deflection Behaviour Summary $a/d = 1.0$	58
Table 4.5 Stiffness $a/d = 1.0$	59
Table 4.6 Strength Reduction $a/d = 1.0$	61
Table 4.7 Strain in Reinforcing Steel at Ultimate Load $a/d = 1.0$	66
Table 4.8 Load-Deflection Behaviour Summary $a/d = 1.5$	68
Table 4.9 Stiffness $a/d = 1.5$	69
Table 4.10 Strength Reduction $a/d = 1.5$	70
Table 4.11 Strain in Reinforcing Steel at Ultimate Load $a/d = 1.5$	74
Table 4.12 Load-Deflection Behaviour Summary $a/d = 2.0$	77
Table 4.13 Stiffness $a/d = 2.0$	78
Table 4.14 Strength Reduction $a/d = 2.0$	79
Table 4.15 Strain in Reinforcing Steel at Ultimate Load $a/d = 2.0$	83
Table 5.1 Data Sets Summary	102
Table 6.1 Section Loss from Mass Loss Model	117
Table 6.2 Effective Concrete Strength from Measured Shear Strength	120
Table 6.3 Model 2 Results.....	124

Chapter 1

Introduction

1.1 General

Corrosion in reinforced concrete infrastructure is a major problem facing government decision makers. It has been estimated that corrosion of the American bridge infrastructure costs \$8.3 billion annually; in the United States 15% of bridge structures are structurally deficient due to the effects of corrosion (FHWA, 2002). It is evident from the recent bridge collapses of the de la Concorde overpass in Laval, Quebec (2006) and the I-35W Mississippi River Bridge in Minneapolis, Minnesota (2007) that attention has to be paid to our aging infrastructure.

Concrete and reinforcing steel together make a very good structural system; also, concrete protects the steel from corrosion due to its high alkalinity. The concrete's hydration reaction produces hydroxyl ions which contribute to the alkalinity of the concrete. The hydroxyl ions create a passive layer on the steel reinforcement. This passive oxide layer prevents the corrosion process from occurring (Broomfield, 1997; ACI 222, 2001). The corrosion process can commence when the environmental conditions disrupt the formation of the passive layer.

The corrosion process causes a loss of reinforcing steel section due to the migration of iron atoms into solution. A by-product of the corrosion process is rust; the volume of rust generation causes expansive forces which can cause cracks to form in the concrete. In addition, the generation of rust and reinforcing steel section loss can damage the bond between the steel reinforcement and the surrounding concrete. These effects can weaken reinforced concrete members.

Shear in reinforced concrete members is supported through two basic mechanisms: beam action and arch action. The type of mechanism depends on the span and depth of the beam. If the zone of the beam resists shear primarily through arch action then it is known as a "D" (disturbed) region. The other areas of the beam are known as "B" regions because they resist shear through beam action. The beam action mechanism resists shear through contributions from the concrete and reinforcing steel. The concrete resists shear through three components: shear in the compression zone, interlocking of the aggregate, and dowel action of the main reinforcement. The reinforcing steel resists the shear through tension in the shear stirrups. The arch action mechanism resists shear through compression in the concrete and tension in the main reinforcing steel.

There has been considerable research on the effects of corrosion on the flexural strength of beams and the bond strength between the reinforcing steel and the surrounding concrete. Also, researchers have developed numerous “design” equations for deep beams. The effect of corrosion on shear reinforcement (stirrups) has not been studied to a great extent; specifically, the effect of corrosion on deep beams is not well understood.

1.2 Problem Statement

Corrosion of reinforcing steel plagues structures such as bridges and parking garages. Disturbed regions can be found in pier structures and at the end of girders in a bridge. The de-icing chemicals that are used on bridges for winter maintenance contain chloride ions. It is these chloride ions that depassivate the reinforcing steel and allow the corrosion process to commence. The result is section loss in the reinforcing steel, cracking in the concrete, and spalling of the concrete cover. The current study is focused on determining the effect of corrosion on the shear strength of disturbed regions.

1.3 Research Objectives

Previous studies on the effects of corrosion on shear reinforcement are limited. To the author’s knowledge no one has studied the effect of corrosion of shear reinforcement in deep beams with varying the shear span to depth ratio. The current study is composed of experimental investigation and analytical modelling. Based on an assessment of the available literature in Chapter 2, the objectives of the current study are as follows:

- Quantify the effect of corrosion of shear reinforcement has on reinforced concrete deep beams.
- Investigate the effect of corrosion on beams with varying shear-span to depth ratio.
- Evaluate the feasibility of utilizing CFRP fabric to restore the strength of beams with corroded shear reinforcement.
- Develop a model that quantifies the shear strength of reinforced concrete deep beams with corroded shear reinforcement.

1.4 Organization of Thesis

The current study is composed of experimental and analytical work designed to investigate the shear strength of disturbed regions with corroded shear reinforcement. The experimental work involved

corroding the shear reinforcement in reinforced concrete beam specimens that were 350 mm deep x 125 mm wide x 1500 mm long. The beam specimens were tested to failure after the accelerated corrosion process was complete. The analytical portion of the study involved developing a strut and tie model that explicitly included the shear reinforcement. In addition, models were developed that modified the input parameters for the strut and tie model to predict the strength of disturbed regions with corrosion damaged shear reinforcement.

In Chapter 2, the background material on corrosion and shear behaviour in reinforced concrete is provided. A review of the current literature available on the shear behaviour of reinforced concrete beams with damaged shear reinforcement is provided.

The methodology used in the experimental program is presented in Chapter 3. The test matrix and the reinforcement details of the specimens are presented in this chapter. The details of the formwork that was constructed to cast the specimens are provided. The material properties of the concrete, reinforcing steel, and carbon fibre reinforced polymer (CFRP) system are supplied. Also, the methodology of the accelerated corrosion process, CFRP strengthening, test setup, and mass loss analysis are detailed.

In Chapter 4, the experimental results are presented. The corrosion crack widths and reinforcing steel mass loss results are summarized. The monotonic test results are divided into three sections based on the shear-span to depth ratio. The following parameters are examined in this chapter: cracking load, stiffness and ductility, ultimate shear strength, crack patterns and modes of failure, diagonal displacement, and reinforcing steel strain behaviour. The feasibility of using CFRP sheets to repair disturbed regions with corroded shear reinforcement is investigated.

The development of a strut and tie model capable of accurately predicting the strength of disturbed regions is presented in Chapter 5. A brief summary code provisions for strut and tie modelling is provided. Three strut and tie models are detailed; two of the strut and tie models incorporate the tension in the shear reinforcement. The accuracy of the strut and tie models is evaluated with published experimental results.

In Chapter 6, a method of modifying the strut and tie model inputs is present. The area of shear reinforcement, the concrete strength, and the cross section width are modified for the effects of corrosion. The mass loss in the shear reinforcement is correlated to corrosion crack width based on a published model. The corrosion crack width is used to reduce the strength of the concrete based on

the results from the experimental testing. In addition, the cross sectional width is reduced by width of the cover concrete. The modifications are input into a strut and tie model and compared with a published model.

The major conclusions and findings from the current study are provided in Chapter 7. Also, recommendations regarding the approach and methodology for future work in this area are provided.

Chapter 2

Background and Literature Review

2.1 Introduction

This study aims to examine the effects of corrosion of shear reinforcement on the structural performance of deep beams. This chapter will review the literature and present the background information on the corrosion process and shear behaviour in reinforced concrete. Investigations on the structural capacity of reinforced concrete deep beams with damaged shear reinforcement are presented. Finally, the research objectives of the current study are presented.

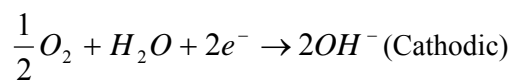
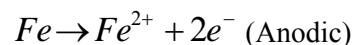
2.2 Corrosion

Corrosion can be thought of as the reverse of the metal formation process; this phenomena is sometimes referred to as “extractive metallurgy in reverse”(Jones, 1996). The corrosion of metals involving water is an electrochemical process; specifically, the process involves the formation of chemical compounds by chemical reaction and the transfer of electrons.

2.2.1 Corrosion in Reinforced Concrete

Corrosion is a naturally occurring process. The reinforcing steel, embedded in concrete, releases metallic iron into the surrounding pore solution (loss of steel cross section); the iron takes the form of ferrous ions in this solution. At the anode, the reaction that causes the iron to dissolve leaves an excess negative charge on the surface of the steel. These excess electrons flow to an area of lower electrical potential known as the cathode. At the cathode, oxygen and water react with the negative charge to form hydroxide ions. There must be a complete circuit for the corrosion process to continue; thus, ions flow through the pore water solution from the cathode to the anode. A schematic diagram is provided in Figure 2.1.

The anodic and cathodic reactions (Equation 2.1) take the following form:



Equation 2.1

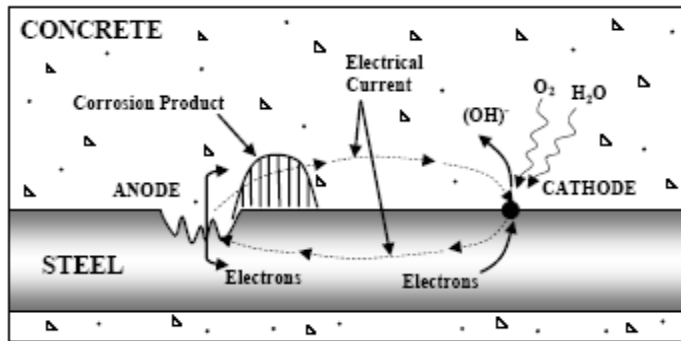


Figure 2.1 Corrosion Process (Badawi, 2003)

2.2.2 Corrosion Initiators in Reinforced Concrete

There are two primary mechanisms that accelerate the corrosion process: carbonation and chloride ingress. Carbonation is due to the ingress of carbon dioxide which reduces the alkalinity of the concrete. Chloride ions can penetrate into the concrete and accelerate the corrosion process. In Canada, the most likely cause of corrosion in reinforced concrete is chloride ingress. Carbonation is a comparatively slower process (ACI 222, 2001); carbonation is not as prevalent in Canada because of environmental factors. Carbonation affects structures that are constructed of poor quality concrete and are nearing the end of their service life. Chloride ingress affects structures much earlier in their services life; as a result, it is a more pervasive problem in Canadian structures because of the exposure to chloride based de-icing chemicals and salt spray in coastal environments. .

2.2.2.1 Carbonation

Carbon dioxide from the surrounding environment dissolves into the concrete pore water forming carbonic acid; the carbonic acid reacts with the calcium hydroxide in solution to form calcium carbonate neutralizing the concrete's alkalinity in the process. This reaction (Equation 2.2) is represented in chemical terms as follows (Broomfield, 1997):



When the concrete's alkalinity is lowered the protective oxide layer on the reinforcing steel becomes unstable; consequently, the corrosion process can commence. Carbonation induced

corrosion occurs in concrete that has a high water-cement ratio, and/or an insufficient depth of cover (ACI 222, 2001).

2.2.2.2 Chloride Ingress

Chlorides come from many sources, in the Canadian environment there are three main sources. Deicing salt is commonly used for winter maintenance; chlorides can be cast in, calcium chloride was commonly used as a set-accelerator although it is no longer prevalent or allowed in most structures; and salt exposure from the sea can cause chlorides to diffuse in concrete structures. Typically, the ingress of chlorides is thought to be due to a diffusion mechanism. A simplified way to express this relationship is provided by Equation 2.3. (Broomfield, 1997)

$$C(x,t) = C_i + (C_s - C_i) \left[1 - \frac{x}{\sqrt{12tD_o}} \right]^2 \quad \text{Equation 2.3}$$

$C(x,t)$ = chloride concentration

C_i = Initial oxygen concentration

C_s = Surface chloride concentration

x = depth

t = time

D_o = Chloride diffusion coefficient

Chloride ions attack the passive oxide layer that is developed on the outside of the reinforcing steel. However, due to the concrete's alkalinity this oxide layer can repair itself when it is breached. The chlorides can be a problem when the oxide layer cannot be repaired, this implies that there is a chloride threshold where the depassivation will occur and corrosion is initiated. This threshold is approximately 0.2% to 0.4% acid-soluble (total) chloride by weight of cement (Broomfield, 1997).

2.2.3 Macrocell and Microcell Corrosion

Macrocell corrosion is localized to areas of reinforcing steel separated by reinforcing which has not been depassivated. This type of corrosion generally occurs in chloride contaminated concrete. The anodic reaction occurs in an area that has been depassivated by chloride contamination; this anodic reaction is supported by a corresponding cathodic reaction which occurs on the passivated reinforcing

steel. It should be noted that the cathode to anode ratio in this case would be large compared to the other two types of corrosion; when the cathode to anode ratio is small than the corrosion process is slower. This type of reaction requires concrete that has a low resistivity; moisture and chloride contamination are known to lower the resistivity of concrete. Reinforced concrete slabs such as those found in parking structures and bridges can be susceptible to this type of corrosion. Chlorides from winter maintenance diffuse into the concrete surrounding the top layer of reinforcing steel; the bottom layer remains passivated and acts as the cathode (Figure 2.2). This type of corrosion is typically localized to areas where the wearing surface has broken sufficiently to allow ingress of moisture and chlorides to the level of the concrete. Macrocell corrosion can also occur in areas where the concrete cover has cracked (Schiessl and Raupach, 1997).

Microcell corrosion can be identified when the corrosion appears to be continuous over the length of the reinforcing steel. In this case, the anodic and cathodic reactions occur next to each other on the same reinforcing steel surface. The cathode and anode are separated by a very small, imperceptible distance (Figure 2.2). Since the cathode and anode are not separated by a large distance, the corrosion reaction can occur in concrete that has a higher resistivity compared to that for macrocell corrosion. The higher resistivity concrete is generally associated with a drier environment.

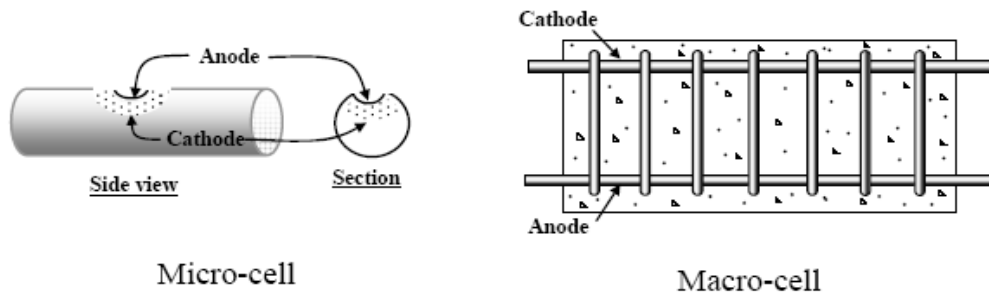


Figure 2.2 Microcell and Macrocell Corrosion (Badawi, 2003)

Pitting corrosion can be regarded as the most aggressive forms of microcell corrosion in reinforced concrete. This type of corrosion is more likely to occur in a chloride contaminated environment. The iron in the steel dissolves into solution at the site of the anode; this process occurs very quickly over a small area which forms a pit in the steel. In extreme cases, this type of corrosion can completely sever the reinforcing steel bar.

2.2.4 Factors Influencing Corrosion Rate in Reinforced Concrete

The corrosion reaction is a complex process influenced by a number of factors. Similarly, the rate at which the corrosion reaction occurs is affected by many items. Corrosion occurs in two stages over the service life of a structure. The first stage is initiation; the corrosion in this case is imperceptibly slow due to the presence of a passive layer. If the passive layer is interrupted by chloride ingress or carbonation then the second stage, known as propagation, can commence. Factors that influence corrosion rate during the propagation stage include: the ratio of the areas of the cathode and anode, the presence of moisture and oxygen, the corrosion potential, and polarization effects (limits the corrosion rate).

2.2.4.1 Initiation Phase

Concrete is naturally alkaline. This means there is an excess of hydroxide ions in solution; the result is that the reinforcing steel develops a passive layer. A “normal” passive layer is a thin metal oxide layer that slows the corrosion process. In reinforced concrete, this layer is thicker; this may be attributed to the fact that the passive layer is a combination of metal oxide and minerals from the surrounding concrete (Broomfield, 1997). Nevertheless, the passive layers acts in the same manner as a “normal” passive layer. The rate of corrosion in passivated steel is so slow that it could almost be considered non-existent. The initiation phase continues until an environmental effect such as chloride ingress or carbonation disrupts the passive layer.

2.2.4.2 Propagation Phase

Current density is a very important concept affecting the rate at which the corrosion process can proceed (Fraczek, 1987). The current density is ratio of the amount of current flowing through an anode to the area of the anode. The current density is related to the concept of cathode to anode ratio because as the current density increases the cathode to anode ratio also increases. This suggests that a small anodic area compared to the cathodic area can be critical in terms of rate of corrosion. Small anodic areas can occur at load induced cracks or at localized areas where moisture (allowing chloride ingress) collects such as along curbs on a bridge deck.

The corrosion potential is the potential energy within the corrosion cell; this potential energy is known as electromotive force. If there is electromotive force within the system then that is an indication that corrosion is occurring. The electromotive force is not an indication of the rate of

corrosion because of polarization effects. A potential difference will occur when there is an irregularity within the corrosion cell. If two different metals are in contact, then a corrosion potential can occur; an example of this would be an aluminium railing adjacent to reinforcing steel embedded in concrete. A concentration gradient can also cause a potential difference. Changes in the concentration of oxygen, moisture, or chloride over the depth of a bridge deck are a good example of this. In addition, these gradients can cause corrosion along a single reinforcing steel bar. In a bridge, moisture (and chlorides) tends to collect near the joints or near the curbs; this would cause a concentration gradient.

Polarization effects are conditions that limit the rate at which the corrosion process can occur. Concentration polarization and ohmic polarization are most commonly observed in reinforced concrete structures. Concentration polarization occurs when a change in concentration of one of the key factors in the corrosion process, such as moisture or oxygen, limits the rate at which the surface reactions can proceed.

Concentration polarization can occur if the supply of oxygen is impeded. The result is that the formation of rust is impeded because the rust reaction involves the consumption of hydroxide ions. Thus, the diffusion of oxygen influences the rate at which corrosion and rusting occur. The concrete cover is what controls the diffusion of oxygen to the reinforcing steel; consequently, the thickness and quality of the concrete cover is an important factor influencing the rate of corrosion. The water-binder (cement and supplementary cementing materials) ratio is one measure of the quality of the concrete cover. The diffusion of oxygen is impeded at lower water-binder ratios. This can be attributed to a reduction in the permeability of concrete at lower water-binder ratios. Fly ash and silica fume are supplementary cementing materials which can reduce the concrete's permeability.

Concentration polarization can occur when the concrete is saturated. The oxygen must diffuse to the level of the reinforcing steel through the solution in the concrete pores. If the concrete is partially saturated (exposed to wet-dry cycles), the oxygen can partially diffuse as a gas to the level of the reinforcing steel and then dissolve into solution. Oxygen diffusion in a gaseous state is a much faster process; consequently, corrosion occurs faster in partially saturated concrete.

Ohmic polarization occurs when the ionic current flow is slowed down. The ionic current flow is the flow of charged ions between the anode and the cathode. This flow is essential to complete the circuit. This flow can be slowed down by concrete with a high electrical resistance; the result is that the corrosion rate will be decreased. This phenomenon is known as ohmic polarization. Neville

(1996) reports that the resistivity of concrete depends on factors such as: moisture, water-cement ratio, supplementary cementing materials and the amount of ions such as chlorides. Resistivity is measured in units of ohm-m. There is a significant difference between the resistivity of moist concrete (100 ohm-m) and air-dried concrete (10,000 ohm-m). At lower water-cement ratios, the pore structure of concrete is altered such that there are fewer pores and they are less connected. Consequently, the amount of pore water available for conduction is less, so the resistivity of the concrete increases. The resistivity of concrete can be increased 10 times if silica fume or blast furnace slag is added to the concrete mix. The electrical properties of concrete are influenced by the presence of chlorides such as calcium chloride (commonly used as a de-icer); it has been reported that the resistivity of concrete can decrease as much as 15 times.

2.2.5 Formation of Rust

The formation of rust is a consequence of the corrosion process. Concrete defects – cracking, spalling, and delamination – would not occur as frequently if the rusting process did not occur. The corrosion process provides ferrous and hydroxide ions in solution; a number of reactions occur to form common rust. One form of these reactions is as follows:



The first step in the rusting process is the formation of ferrous hydroxide. A subsequent reaction involving oxygen and water forms ferric hydroxide; the last reaction represents the hydration of the ferric hydroxide to form common red rust (Broomfield, 1997). The corrosion products (rust) have a volume that is many times more than the parent steel (Figure 2.3); this volume change results in expansive forces that can cause tensile stresses to develop in concrete which cause cracking or cracks between reinforcing bars (delamination).

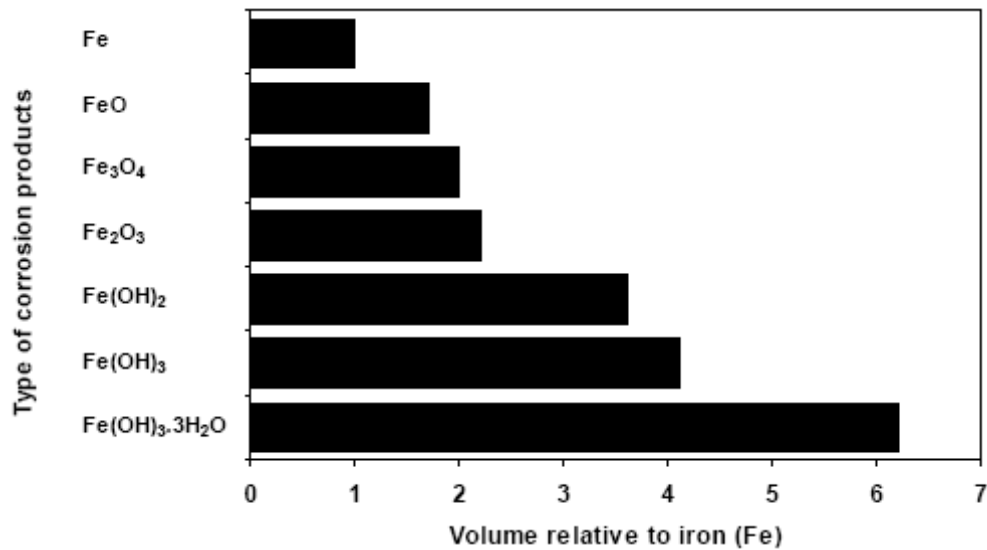


Figure 2.3 Volume of Rust (Liu and Weyers, 1998)

2.2.6 Strength of Corroded Reinforced Concrete

Corrosion of steel reinforcement influences the strength of reinforced concrete members by two main mechanisms: loss of reinforcing steel bond, and loss of reinforcing steel cross section. These mechanisms generally influence the serviceability of a structure; there have been few reported cases of structural failure due to corrosion (Broomfield, 1997). The failure of structures due to the effects of corrosion is rare because corrosion damage can be easily detected and repaired in reinforced concrete structures.

It is the formation of rust which causes cracking of the concrete. The primary factors influencing the time to cracking are: depth of cover, quality of concrete, and the environmental effects (chloride ingress and carbonation). The cracked concrete allows moisture and oxygen to migrate to the reinforcing steel; this will accelerate the corrosion process. The cracked concrete causes a loss of bond between the reinforcing steel and the surrounding concrete. (ACI 222, 2001)

The loss of cross sectional area in reinforcing steel is attributed to a loss of ferrous ions at areas of the reinforcing steel which have become anodic. Reinforcing steel section loss can be uniform over a large area; conversely, corrosion can also be localized due to pitting corrosion which results in much larger section losses.

Research on the effects of corrosion on bond strength has been conducted by many researchers (Auyeng, Balaguru, and Chung, 2000; Fang, Lundgren, Chen, and Zhu, 2004; Craig, 2005). In general, most researchers found that initially (before cracking) with low corrosion (up to 2% mass loss) the bond strength increases and then it decreases at higher degrees of corrosion. Al-Sulaimani et al. (1990) postulated that this increase in bond strength is due to an increased surface roughness from the rust formation. Additionally, Almusallam et al. (1996a) reports that the expansive forces that precede cracking cause a confining effect on the reinforcing steel; this confining effect increases the bond strength. After cracking, the bond strength decreases in reinforced concrete members that lack appropriate confinement. It is suggested that the loss of bond strength can be attributed to three things: a loss of confinement due to concrete cracking, a loss of mechanical anchorage due to corrosion of reinforcing steel ribs, and a loss in friction due to the build-up of corrosion by-products (rust). If confinement, such as stirrups, is provided then there is not as strong a correlation between bond strength degradation and corrosion mass loss level.

Almusallam (2001) studied the effects of corrosion on the mechanical properties of reinforcing steel bars. It was concluded that corrosion does affect the tensile strength of the reinforcing steel, but significant reductions in the ductility and ultimate strain were observed. Figure 2.4 shows the load-elongation behaviour for 6 mm diameter deformed reinforcing steel bar which has corroded to varying degrees (corrosion level is indicated by percentage in the plot).

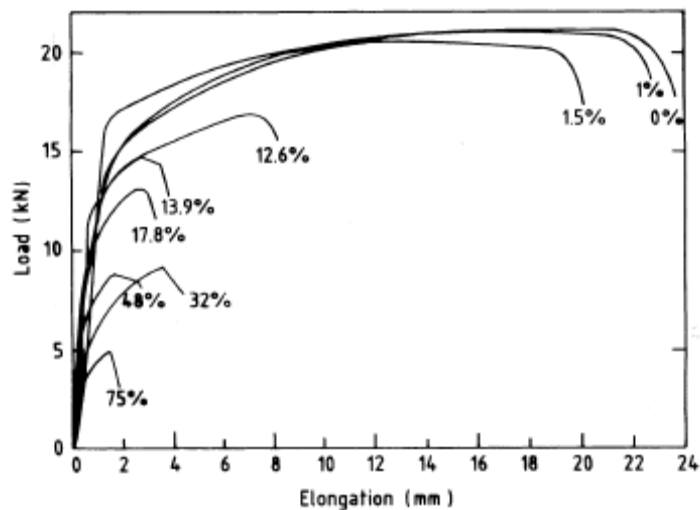


Figure 2.4 Load Elongation Behaviour of Corroded Reinforcing Steel (Almusallam, 2001)

The flexural strength of corroded reinforced concrete members has been studied by a number of researchers. (Almusallam et al., 1996b; Mangat and Elgarf, 1999; Sherwood, 2000; Badawi, 2003; El Maaddawy, 2004; Chung et al., 2008) The strength and ductility of reinforced concrete members is due to the inherent ductility of reinforcing steel in tension. The concrete must transfer the tensile stresses to the reinforcing steel; this stress transfer is achieved through the bond between the concrete and reinforcing steel interface. In general, it is reported that at low levels of corrosion (less than 2% mass loss) there is a minor increase in the ultimate strength of reinforced concrete members. Researchers attribute this to an enhanced bond due to increased friction from the accumulation of rust. It has been shown that a decrease in ultimate strength of reinforced concrete members can be expected when higher levels of corrosion are present. This strength reduction can be attributed to both the loss of cross sectional area of the reinforcing steel and a loss in bond of the reinforcing steel. There is no agreement between the researchers on the influence the two mechanisms (loss of cross section and bond degradation) have on the reduction of ultimate strength in corroded reinforced concrete members. Masoud (2002) showed no significant reduction in the ultimate strength of specimens corroded up to a maximum corrosion level of 12.5% mass loss; it was noted that a reduction in the yield load of the beam was observed with increasing corrosion mass loss levels.

2.2.7 Accelerated Corrosion by Impressed Current

There are two accepted methods to accelerate the corrosion process in the laboratory. The potentiostatic approach maintains a constant voltage potential between the anode and cathode by varying the current. The galvanostatic approach keeps the current constant by varying the voltage potential.

The most acceptable approach is generally the galvanostatic approach because it provides a more reliable way to correlate laboratory results with Faraday's law. Faraday's law relates metal mass loss with corrosion current, so keeping a constant current in laboratory experiments is preferable. In the galvanostatic approach all of the reinforcing steel becomes anodic, and a conductive material is used as a cathode (either embedded in the concrete or placed externally). The placement of the cathode depends on the corrosion setup. A schematic diagram of the corrosion setup typically utilized in the research work at the University of Waterloo is shown in Figure 2.5.

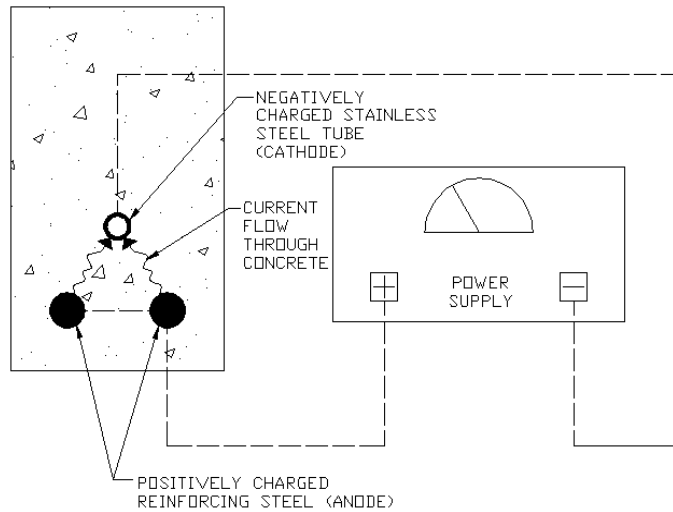


Figure 2.5 Accelerated Corrosion Schematic

The highest rates of corrosion based on field measurements are 10 to 25 $\mu\text{A}/\text{cm}^2$ (FIB Bulletin 10, 2000; Mangat and Elgarf, 1999). These rates are unrealistic because it would take many years to complete a laboratory experiment. Researchers have used current densities up to 10,400 $\mu\text{A}/\text{cm}^2$; an upper limit of 200 $\mu\text{A}/\text{cm}^2$ is suggested so that the crack growth and the strain in the concrete are comparable to field conditions (El Maaddawy and Soudki, 2003). The rate of the corrosion reaction is a function of the current flow to the area where the corrosion reaction is occurring. This rate can be predicted by Faraday's law (Equation 2.5).

$$m = \frac{Ita}{nF}$$

Equation 2.5

m = mass (g)

I = corrosion current (A)

t = time (sec)

a = number of equivalents exchanged (2 for Fe^{2+})

n = atomic weight (55.9 g for Fe^{2+})

F = Faradays Constant (96,500 A-sec)

2.3 Shear in Reinforced Concrete

A flexural failure is ductile in under-reinforced concrete sections; conversely, a shear failure in reinforced concrete is brittle and sudden in nature. There are two primary shear transfer mechanisms in reinforced concrete beams: beam (Bernoulli) action and arch (disturbed) action.

2.3.1 Beam and Arch Action

In general, the load imposed on a structure has to be transferred through a load path(s) to a support. There are two basic methods (beam and arch action) by which shear loads are transferred to the support; the shear transfer method is dependant on the shear-span to effective depth ratio (a/d). The shear span is the distance between the load application point and the support; the effective depth is the depth from the compression face to the centroid of the main reinforcing steel area. In members supporting uniformly distributed loads, arch action will occur when the span to depth ratio is less than 4. Reinforced concrete beams are typically divided into deep and slender beams; deep beams transfer the majority of the shear forces by arch action, and slender beams transfer shear forces primarily by beam action. Furthermore, deep and slender beams are categorized as very short, short, slender and very slender based on the shear-span to depth ratio (Table 2.1) (MacGregor and Bartlett, 2000).

Table 2.1 Beam Shear Classification

Type	Classification	a/d Ratio
Deep	Very Short	$a/d < 1$
Deep	Short	$1 < a/d < 2.5$
Slender	Slender	$2.5 < a/d < 6.5$
Slender	Very Slender	$a/d > 6.5$

Beam action generally occurs in areas that are not near supports or changes in cross section. The shear is transferred through both the concrete and tension in the transverse reinforcement. The concrete carries shear through three primary components: shear in the compression zone, aggregate interlock, and dowel action of the main reinforcement.

Very short and short beams transfer shear through arch action. Very short beams behave as arches because during loading cracks typically form between the load application point and the support; this lessens the beams ability to transfer loads through beam action.

In short beams the load is carried partially by arch action and partially by beam action; thus, the mechanics of this type of shear transfer mechanism are complex. The failure mode in beams with this type of shear span can be due to bond failure, splitting failure, or dowel failure of the main reinforcing steel; in addition, a shear compression failure can occur when the concrete crushes under the load application point.

2.3.2 General Shear Models

There are a number of models used to predict the shear capacity of reinforced concrete members; the four common models are truss analogy, compression field theory, modified compression field theory, and strut-tie models.

2.3.2.1 Truss Analogy

The truss analogy is a very common way to model shear behaviour; in fact, a number of codes are based on this model. Previous versions of the Canadian concrete design standard (CSA A23.3) included shear design equations that were based on a constant 45 degree angle truss model (simplified method). In the current edition of the standard (CSA A23.3-04) shear provisions are based on modified compression field theory. The truss model is considered a lower bound theorem. This theorem assumes the following: a truss system will be satisfactory when all forces are in equilibrium, and when all members in this truss are designed or checked to ensure they are at or below the yield limit. Furthermore, virtually any truss system will work, but some systems will be more efficient because more of the individual members are close to the safe load capacity.

A truss for a simply supported slender beam is composed of top and bottom chords representing the compression in the concrete and the tension in the main reinforcement. Vertical struts represent tension in the shear reinforcement; these vertical struts represent multiple stirrups that would cross a diagonal crack. The final element in a truss model is the diagonals that represent the compressive stress in concrete struts defined by diagonal cracking in the beam. This model neglects the effects of shear in the compression zone, the vertical component of aggregate interlock, and the dowel action of the reinforcement (MacGregor and Bartlett, 2000).

2.3.2.2 Compression Field Theory

Compression field theory is a method that is based on compatibility, equilibrium, and constitutive relationships. After the concrete member has cracked, it is idealized as series of concrete struts bounded by cracks. These concrete struts resist the principle compressive forces. The strength of the concrete is based on a stress-strain formulation for transversely cracked concrete; this formulation takes into account the softening effect that tension has on concrete. The concrete is assumed to have no tensile strength across the cracks; thus, it cannot support the principle tensile force. A modified compression field theory includes the tensile capacity of concrete that occurs from the tension stiffening effect.

2.3.2.3 Strut and Tie Model

Strut and tie models are typically used to design disturbed regions which encompass one member depth from a concentrated load or change in member cross section. The first step is to determine the stress that act on the boundary of the disturbed region. Next, the boundary needs to be divided into subdivisions. The forces on these subdivisions can be computed based on the stresses that act on the boundary. A truss, consisting of concrete compression struts and steel tension ties, can be drawn to transmit force between the boundaries of the disturbed region. The intersection of the compression struts and tension ties are known as nodal zones. It is important to make sure that the struts, ties, and nodal zones can resist the forces imposed on them. Additionally, the concrete struts must fit within the geometric constraints of the beam (MacGregor and Bartlett, 2000).

2.3.3 Deep Beam Shear Models

Shear transfer in short beams cannot be attributed to one mechanism (beam or arch action); it can best be described as a combination of both mechanisms (Figure 2.6). The shear resistance in a concrete beam without web reinforcement is determined from first principles based on the moment capacity (Equation 2.6) (MacGregor and Bartlett, 2000):

$$M = Tjd \qquad \text{Equation 2.6}$$

M = Moment Resistance of Beam (kN·m)

T = tension in the main reinforcement (kN)

j = Ratio of lever arm to effective depth

d = effective depth (m)

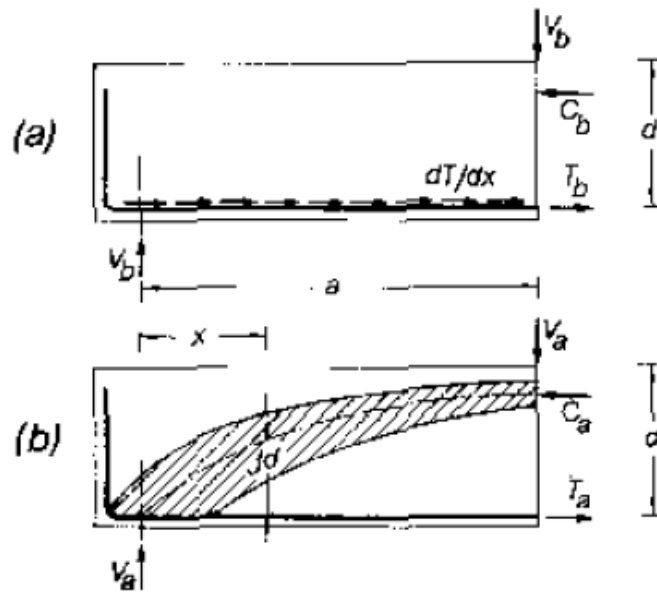


Figure 2.6 Shear Transfer Mechanisms (Russo and Puleri, 1997)

The shear resistance can be determined by (Equation 2.7):

$$\frac{dM}{dx} = V = jd \frac{dT}{dx} + Td \frac{dj}{dx} \quad \text{Equation 2.7}$$

V = Shear Resistance of Beam

x = distance along the beam (m)

The first term in Equation 2.7 represents the beam action due to horizontal shear flow. The second term represents arch action. Arch action will only occur when the shear flow is interrupted by inclined crack.

2.3.3.1 Bažant and Kim Model

Bažant and Kim (1984) developed an expression for the shear resistance considering both beam and arch action:

$$\begin{aligned}
v_{uc} &= v_b + v_a \\
v_b &= 0.83\xi\rho^{1/3} f'_c{}^{1/2} \\
v_a &= 206.9\xi\rho^{5/6} \frac{a}{d}^{-5/2} \\
\xi &= \frac{1}{\sqrt{1 + \frac{d}{25d_a}}}
\end{aligned}$$

Equation 2.8

v_{uc} = mean shear stress

ρ = tensile reinforcement ratio

f'_c = concrete compressive strength

a = shear span

d = effective depth

d_a = maximum aggregate size

It is important to note that in Equation 2.8 both beam and arch action depend on the reinforcement ratio. Also, the beam action depends on the concrete strength, and arch action depends on the shear span to effective depth ratio.

2.3.3.2 Russo and Puleri Model

Russo and Puleri (1997) provide a method to quantify the effectiveness of stirrups based on a 45° variable angle truss model. The shear resistance from the stirrups is typically added to the shear resistance from beam and arch action. However, they argue that simply summing the three basic shear components is not logical. The reason is that the stress in the stirrups will be lower or equal to their yield strength depending on whether arch or beam action is governing. Stirrups have a positive effect when beam action is predominate by increasing the concrete shear transfer mechanisms (dowel action, aggregate interlock etc.). Therefore, they have formulated a “stirrup effectiveness factor” (Equation 2.9):

$$\psi = 1.67 \frac{\sqrt{f'_c}}{\chi}$$

$$\chi = \sqrt{f'_c} + 250 \sqrt{\rho \left(\frac{d}{a}\right)^5}$$

Equation 2.9

ψ = stirrup effectiveness factor

f'_c = concrete compressive strength (MPa)

ρ = tensile reinforcement ratio

a = shear span (mm)

d = effective depth (mm)

χ = Coefficient

The effectiveness factor (Equation 2.9) was developed based on the hypothesis that stirrups are less effective when arch action is dominant and more effective when beam action is dominant. The shear stress expression (Equation 2.10) (partially based on the Bazant and Kim (1984) expression) from Russo and Puleri's (1997) research is:

$$v_u = v_{uc} + v_{si}$$

$$v_{uc} = 0.83 \xi \rho^{1/3} f_c^{1/2} + 206.9 \xi \rho^{5/6} \left(\frac{a}{d}\right)^{-5/2}$$

$$v_{si} = \psi \rho_v f_{yv}$$

$$v_u = 0.83 \xi \chi^3 \sqrt{\rho} + 1.67 \frac{\sqrt{f'_c}}{\chi} \rho_v f_{yv}$$

Equation 2.10

ξ = See Equation 2.8

ρ = tensile reinforcement ratio

f'_c = concrete compressive strength

χ = See Equation 2.9

ρ_v = stirrup reinforcement ratio

f_{yv} = yield strength of stirrup reinforcement

2.3.3.3 Matamoros and Wong Model

Matamoros and Wong (2003) developed an expression based on the contribution from arch and beam action. They used the superposition of a number of strut and tie models to formulate their expression. Figure 2.7 shows the strut and tie models that are utilized.

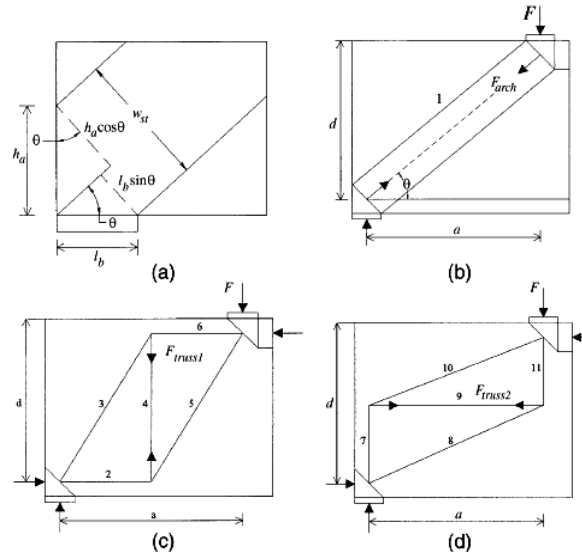


Figure 2.7 Strut and Tie Models (Matamoros and Wong, 2003)

The shear resistance consists of the sum of three components: a direct strut, a vertical tie, and a horizontal tie. Each component is the product of the element strength (determined from strut and tie models b, c, and d in Figure 2.7) and a coefficient:

$$V = C_c S_{strut} + C_{wv} S_{tv} + C_{wh} S_{th}$$

$$V = \frac{0.3}{a/d} f'_c b w_{st} + A_{tv} f_{yv} + 3(1 - a/d) A_{th} f_{yh}$$

Equation 2.11

C_c = corrected factor for force in strut

C_{wh} = correction factor for force in horizontal tie

C_{wv} = correction factor for force in vertical tie

S_{strut} = nominal strength of struts

S_{th} = nominal strength of horizontal tie

S_{tv} = nominal strength of vertical tie

The coefficients (C_c , C_{wv} , and C_{wh} - Equation 2.12) are lower bound expressions based on experimental data (Figure 2.8). It is evident that there is a significant amount of scatter in the coefficients that were calculated based on experimental data.

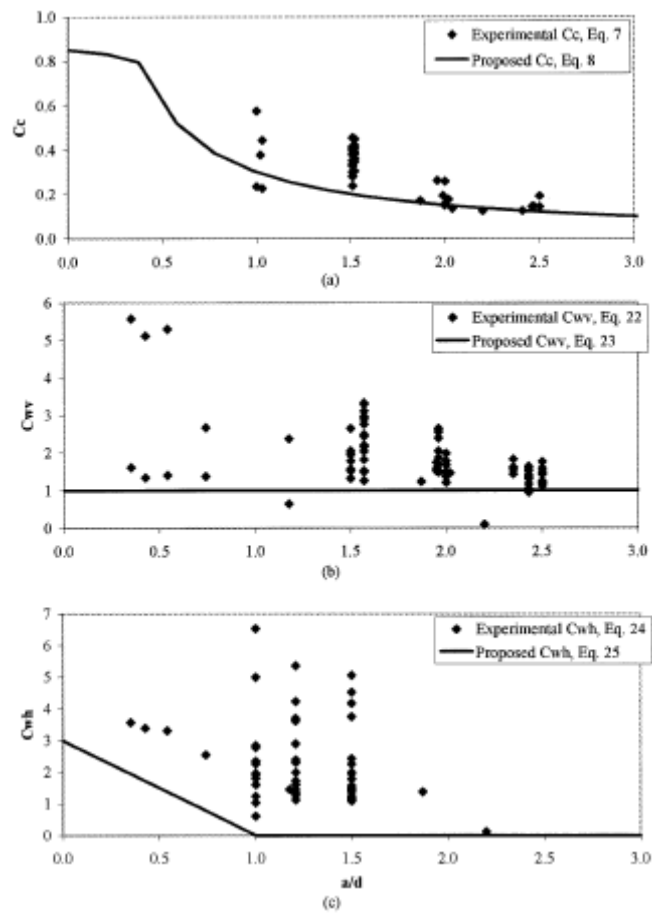


Figure 2.8 Strength Coefficients (Matamoros and Wong, 2003)

$$C_c = \frac{0.3}{a/d} \leq 0.85 \sin \theta$$

$$C_{wv} = 1$$

$$C_{wh} = 3 \left(1 - \frac{a}{d} \right) \geq 0$$

Equation 2.12

θ = angle between the strut and horizontal plane

Substituting Equation 2.12 into Equation 2.11 gives the shear resistance proposed by Matamoros and Wong (2003):

$$V = \frac{0.3}{a/d} f'_c b w_{st} + A_{rv} f_{yv} + 3(1 - a/d) A_{th} f_{yh} \quad \text{Equation 2.13}$$

2.3.3.4 Russo, Venir, and Pauletta Model

Russo, Venir, and Pauletta (2005) developed a formula, based on a strut and tie approach, to predict the shear strength of reinforced concrete beams. Their model included the softening effect experienced by concrete in tension and the effects of web reinforcement. The formula was calibrated with experimental results. The shear strength has contributions from the concrete strut and web reinforcement. The concrete strut contribution (Equation 2.14) is:

$$v_c = c_1 k \chi f'_c \cos \theta \quad \text{Equation 2.14}$$

c_1 = constant from experimental tests

k = nondimensional (with respect to d) depth of compressive zone

χ = interpolating function modifies concrete strength for effects of tension

θ = angle of inclination of the concrete strut

The shear resistance due to web reinforcement (Equation 2.15) is:

$$v_w = q_1 \rho_h f_{yh} \cot \theta + q_2 \frac{a}{d} \rho_v f_{yv} \quad \text{Equation 2.15}$$

q_1 = Reinforcement stress reduction factor, determined from experiments

θ = angle of inclination of the concrete strut

q_2 = Reinforcement stress reduction factor, determined from experiments

The authors hypothesize that the stresses in the web reinforcing are most likely less than the yield strength. In some cases, the vertical stirrups may yield near the centre of the shear span. Therefore, in the above expression the average tensile stress in the web reinforcement is determined by multiplying the yield strength by a factor that is less than unity. The contribution from horizontal reinforcement can be determined as an increase in the compression force that the inclined strut can

support. After calibration with experimental results from research in the literature, Equation 2.16 gives the shear strength:

$$v_n = 0.76 \left(k \chi f'_c \cos \theta + 0.25 \rho_h f_{yh} \cot \theta + 0.35 \frac{a}{d} \rho_v f_{yv} \right) \quad \text{Equation 2.16}$$

k = nondimensional (with respect to d) depth of compressive zone

χ = interpolating function modifies concrete strength for effects of tension

θ = angle of inclination of the concrete strut

Ramin and Matamoros (2006) developed a model that is similar in nature to the previous models that involve the superposition of truss and arch action; in addition, the contribution from friction and compressive zone shear strength are included. The model is described by the following equations:

$$\begin{aligned} V_n &= V_a + V_t + (V_{cz} + V_f) \\ V_a &= k_a R_a \beta_s f'_c \cdot w \cdot b \cdot \sin \theta \\ V_{t,v} &= \rho_{w,v} f_{wy,v} b \cdot jd \cdot \cot \phi \\ V_{t,h} &= \rho_{w,h} f_{wy,h} b \cdot a \cdot \tan^2 \psi \\ V_c = V_{cz} + V_f &= 0.4 \cdot \sqrt[3]{f'_c} bd \left[k + (1-k) \left(1 - \frac{\Delta w}{\Delta w_u} \right) \right] \end{aligned} \quad \text{Equation 2.17}$$

Explanation of the variables is given below.

The expression for arch action includes three coefficients. The coefficient k_a represents the amount of arch action occurring in the beam; it is a transition function (transition from deep to slender beam). The coefficient R_a is required to adjust the amount of arch action that occurs based on the “stress demand” of the compressive arch. Both arch and beam action impose a diagonal compressive stress on the concrete; consequently, the amount of either mechanism that can occur has to be controlled based on the strength of the concrete. The final term β_s defines the effective compressive strength of the concrete.

The contributions from horizontal and vertical reinforcement are derived based on commonly utilized variable angle truss model. The final term ($V_{cs} + V_f$ in Equation 2.17) provides the contribution from the compressive zone strength and friction. The factor k is used to calculate the

depth of the compressive zone (this depth is the product of k and d); it is calculated based on conventional flexure theory. The term Δw_u limits the crack width over which friction is applicable; it is suggested that a reasonable value for this term would be 1.0 mm. The term Δw is the average crack width which is determined from the strain in the longitudinal reinforcement, and the crack spacing and orientation.

2.4 Corrosion of Shear Reinforcement

There are a limited number of studies that have investigated corrosion of shear reinforcement in concrete beams. The results of these studies are presented in this section.

Rodriguez, Ortega, and Casal (1997) studied the effects of corrosion on the strength of reinforced concrete beams. The reinforced concrete beam specimens were 200 mm deep by 150 mm wide by 2300 mm long. The flexural reinforcement consisted of either 2 – 10 mm diameter deformed bars or 4 – 12 mm diameter deformed bars; the compression reinforcement was 2 or 4 – 8 mm diameter deformed bars; and the shear reinforcement was 6 mm diameter deformed bars spaced at 85 mm, 150 mm, or 170 mm. The test variables in this study were the amount of tensile reinforcement, the amount of compression reinforcement, the spacing of shear stirrups, the anchorage condition, and which reinforcing steel elements (just flexural or both flexural and shear) were corroded. The beams were tested in four-point bending with a shear span to height ratio of 4.0. The authors concluded that pitting corrosion of the stirrups influenced the load carrying capacity of the reinforced concrete beams.

Kage, Abe, and Lee (1997) and Sungho, Hanseung, and Taesoo (2007) (republished version of 1997 study) studied the effects of adding carbon fibre reinforced polymer (CFRP) sheets to strengthen beams that had stirrups that were damaged from corrosion. The specimens were 200 mm x 200 mm with a total length of 2000 mm and a shear span of 800 mm. The shear span-height ratio was 4.0. The section was reinforced in the top and bottom with 3 – 13 mm diameter steel bars; the authors did not specifically state whether the bars were deformed or plain. The shear reinforcement was 6 mm diameter steel bars spaced at 100 mm. A schematic section of the beams is provided in Figure 2.9.

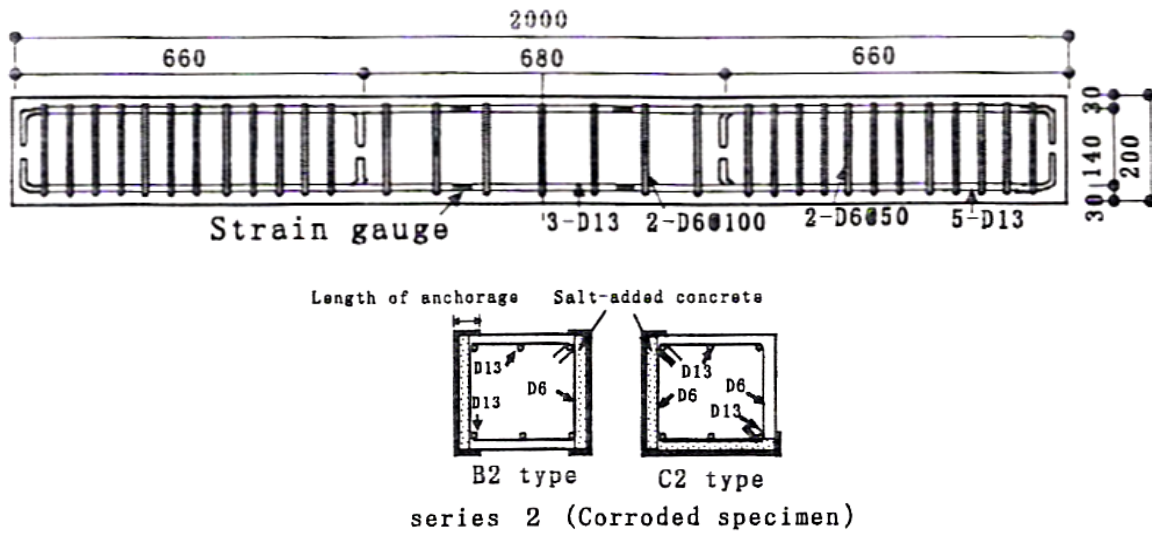


Figure 2.9 Beam Elevation and Cross Section Kage et al. (1997)

A schematic of the test setup is provided in Figure 2.10.



Figure 2.10 Beam Loading and Crack Pattern Kage et al. (1997)

The shear reinforcement was corroded using an impressed current technique. The results indicate that the shear strength of the corroded specimen (SBD3-0) was 20% less than the specimen that was not corroded (SA-1) specimen (Figure 2.11). The authors observed that the stirrups in the corroded specimen fractured. The corroded specimens that were strengthened with CFRP (SBD3-2 and SBD3-23) were stronger than the specimen that was not subjected to accelerated corrosion. The results for the Series C were similar to Series B; the reduction in strength of the corroded specimen (SCD3-0) was attributed to a bond failure and loss of mechanical properties of the reinforcing steel.

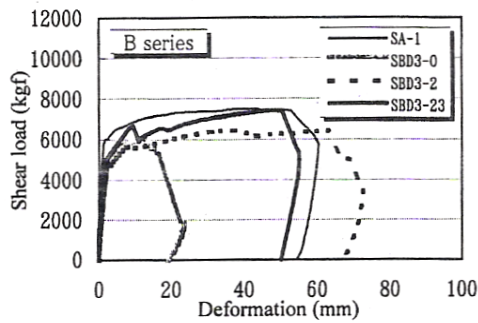


Figure 12 Load-Deformation Relation

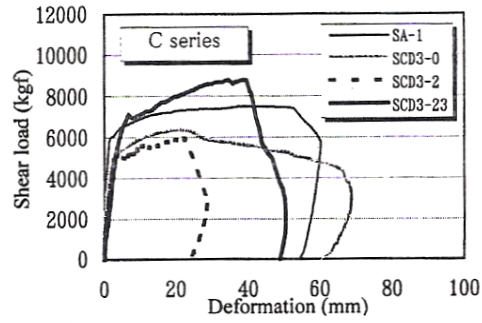


Figure 13 Load-Deformation Relation

Figure 2.11 Load-Deflection Plot Kage et al. (1997)

Regan and Kennedy Reid (2004) conducted tests on reinforced concrete beams where they simulated the effects of pitting corrosion on the anchorage of stirrups; additionally, they investigated the effects of spalling of concrete cover on the bottom of beams. A total of 14 beams were tested: 10 beams were 150 mm by 400 mm and 4 beams were 150 mm by 250 mm. The clear spans of these beams were 2.5 m and 1.5 m resulting in shear span to effective depth ratios ranging from 3.50 to 3.66. The main flexural reinforcement consisted of 4 – 20 or 25 mm diameter deformed bars, and the compression reinforcement was 2 – 20 or 25 mm diameter deformed bars. The plain steel shear reinforcement was placed as follows: 6 mm diameter at 75 mm, 6 mm diameter at 150 mm, or 8 mm diameter at 150 mm. The loss of end anchorage was simulated, in most cases, by using two straight vertical pins. In one case a “U” shaped stirrup was used. A selected beam cross section is depicted in Figure 2.12. The shear strength reduction was 14% to 33% when 65% to 75% of the stirrups lacked end anchorage. The authors concluded that stirrups that lack appropriate anchorage are still effective in adding shear strength to reinforced concrete beams.

Toongoenthong and Maekawa (2005) conducted a study that was similar to the study by Regan and Kennedy Reid (2004). The effect of stirrups that have been fractured was investigated. This could simulate fracture caused by corrosion. The cross sectional dimensions of the reinforced concrete beams were 250 mm by 350 mm with a clear span of 2000 mm. The resulting shear span to depth ratio was 3.2. The compression and tension steel consisted of 4 – 19 mm diameter high strength deformed bars. The stirrups were 6 mm diameter deformed bars spaced at 100 mm; the shear reinforcement was “U” shaped with no reinforcing steel enclosing the bottom portion of the beam. Vinyl tape was used to de-bond 50 mm of the shear reinforcing to study the effect bond has on shear strength. A schematic drawing of the beam configuration is provided in Figure 2.13.

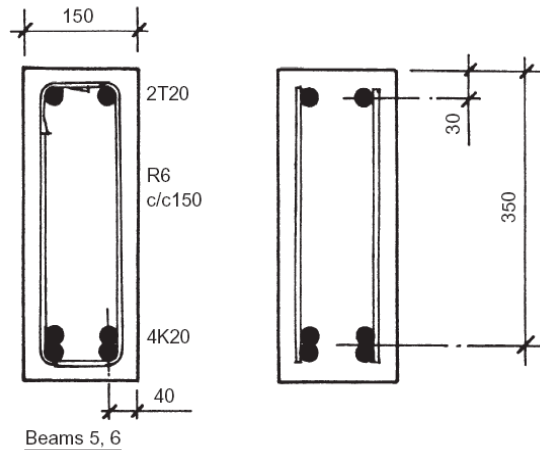


Figure 2.12 Beam Cross Section Regan and Kennedy Reid (2004)

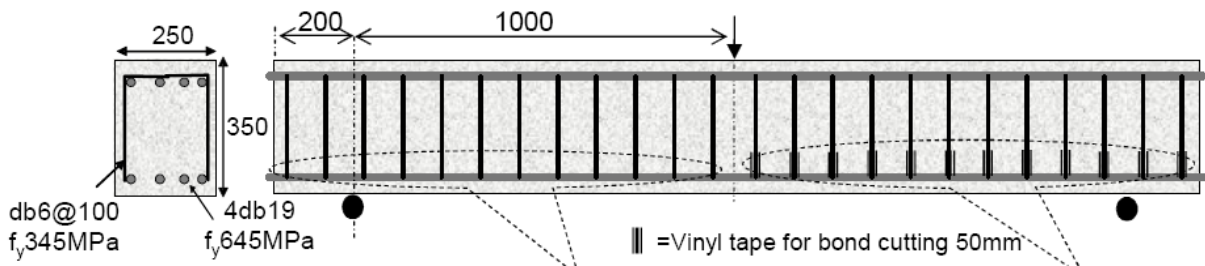


Figure 2.13 Beam Configuration Toongoenthong and Maekawa (2005)

The authors recorded a 37% reduction in shear capacity of the beams with damaged stirrup anchorages. The corresponding load deflection curves are provided in Figure 2.14. A different cracking pattern was observed between the control and the damaged beams. In the undamaged beam, the crack pattern was a series of diagonal cracks. In the damaged beam, flexural cracks were observed initially, and then diagonal cracks began to form. This suggests that a truss mechanism has formed. Finally, localized shear cracks and cracks along the longitudinal steel formed. It is suggested that this type of crack pattern can be attributed to lack of anchorage in the main reinforcement. The authors concluded that the truss mechanism in the damaged beam is less effective in carrying loads; this was confirmed by the fact that the stirrup reinforcement did not yield.

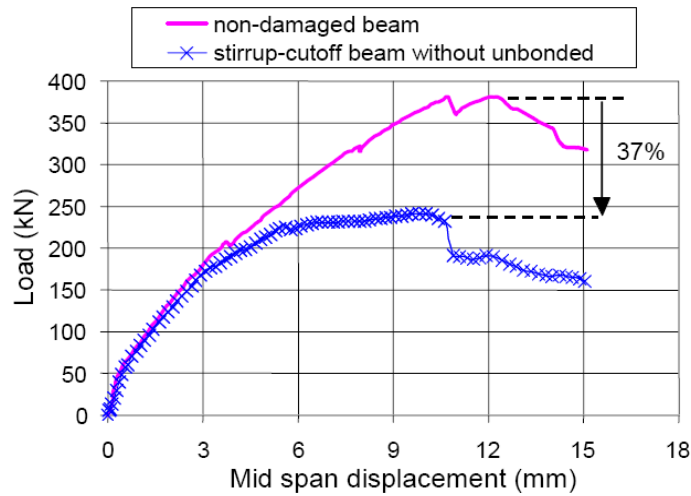


Figure 2.14 Load Deflection Curves Toongoenthong and Maekawa (2005)

Higgins and Farrow (2006) conducted a study designed to investigate the shear capacity of beams where the stirrups were damaged due to the effects of corrosion. In their study, the authors constructed a total of 14 beams: 8 of these beams had a rectangular cross section, 3 beams had a T section configuration, and 3 beams had an inverted T configuration. The beams were 3050 mm in length with a 2440 mm clear span. The rectangular section dimensions are 254 mm by 610 mm. The T section was 610 mm deep with a flange width of 610 mm and a web width of 254 mm. The beams were tested in four-point bending with a shear span to effective depth ratio of 2.04. The main variables studied in this case were the stirrup spacing (203 mm, 254 mm, and 305 mm) and the degree of corrosion (3 levels). The specimens were subjected to accelerated corrosion by impressed current, and then they were visually inspected and assigned grades (based on Oregon Department of Transportation Guidelines for Bridge Inspection) based on the severity of corrosion damage.

The authors categorize the results based on the expected mass loss level (none, light, moderate, or severe) which corresponds to a letter value (A, B, C, or D) in the nomenclature. The results indicate that at all corrosion levels there is a reduction in the shear capacity of the beam as well as a loss in ductility. Figure 2.15 shows the load-deflection plots for rectangular beams with stirrups spaced at 254 mm at different corrosion levels. The corrosion mass loss results vary considerably between different stirrups; the maximum mass loss for the beam with stirrups spaced at 254 mm were 12.7%, 28.9%, and 43.9% for light, moderate, and severe corrosion levels, respectively. Strength losses of 12%, 19%, and 30% relative to the control (un corroded) beam are evident in Figure 2.15. Shear-compression failures for the control and lowest corrosion level beams were observed. In the higher

corrosion level beams failure by stirrup fracture was observed. The stirrup fracture is due to significant localized corrosion and the associated section loss. The maximum strength reductions for the T and inverted T sections were 26% and 42%, respectively. The maximum strength loss occurs when the locations of pitting corrosion match the location of the diagonal crack. The authors concluded that structural performance in shear can be decreased significantly when sequential stirrups have a reduction in cross sectional area.

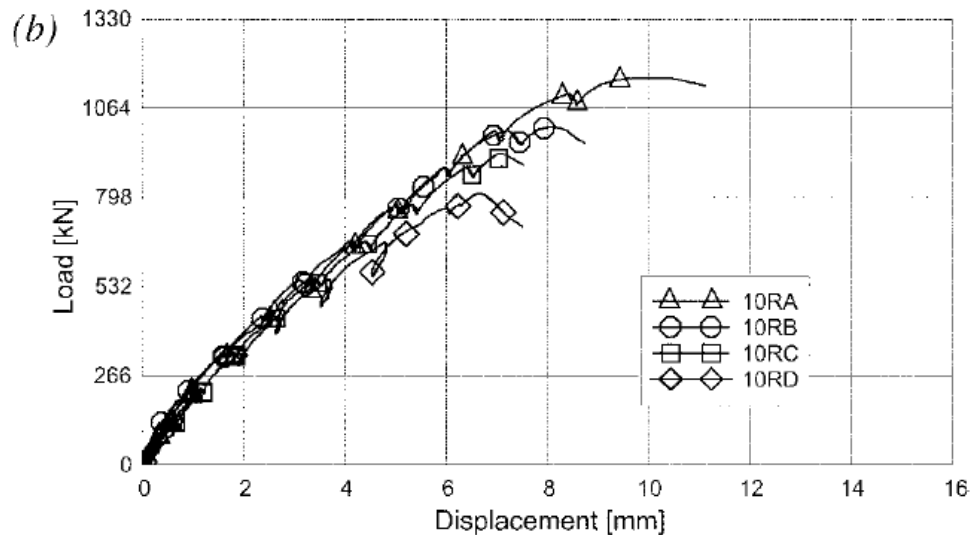


Figure 2.15 Load-Deflection Response Higgins and Farrow (2006)

Val (2007) conducted an analytical study on the reliability of beams where the shear reinforcement was subjected to corrosion. It was concluded that at higher rates of corrosion (greater than $1.0 \mu\text{A}/\text{cm}^2$) general and pitting corrosion influence the mode of failure of reinforced concrete beams. The researcher shows that at a current density of $1.0 \mu\text{A}/\text{cm}^2$ shear failure can become the dominant mode of failure after 25 years. It was concluded that pitting corrosion can be a particularly insidious form of corrosion.

Higgins, Farrow, Potisuk, Miller, Yim, Holcomb, Cramer, Covino, and Bullard (2003) proposed a strut and tie model that includes the effects of corrosion of shear reinforcement in reinforced concrete beams and they compared the model predictions to their experimental results (Higgins and Farrow, 2006). Their model simulated the effects of corrosion by reducing the area of steel reinforcement to account for the mass loss and reducing the width of the reinforced concrete section to account for the effects of cracking and spalling of the concrete cover. The following explains how this was achieved.

The section loss in the shear reinforcement could be accounted for by determining an average value for section loss or by determining the area at the point of maximum section loss for each leg of the stirrup. In the laboratory the average area of corroded stirrups would typically be determined by a gravimetric mass loss (Section 3.9.2) analysis. The gravimetric method is a destructive method which would not be possible for existing structures; the authors suggested the use of digital calipers to determine an average section loss for in service structures.

The effects of corrosion cracking and spalling can be accounted for by a reduction in the width of the concrete section. As the spacing of the stirrups gets smaller the spall wedges interact; thus, a smaller effective beam width must be used. Figure 2.16 provides an example of the cracking pattern that might result from corrosion of stirrups with different spacings.

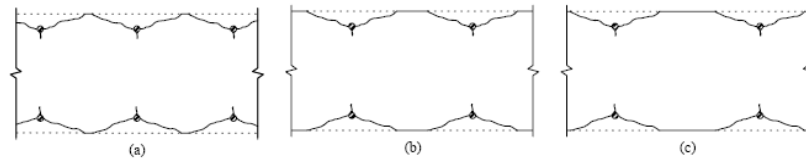


Figure 2.16 Corrosion of Shear Stirrups Concrete Crack Pattern (Higgins et al., 2003)

This effective width is determined based on the depth of cover, the diameter of the reinforcing bar, and the spacing of the reinforcement as given in Equation 2.18.

$$b_{eff} = b - 2(c_v + \phi_v) + \frac{s}{5.5} \quad \text{if } s \leq 5.5c_v$$

$$b_{eff} = b - \frac{5.5}{s}(c_v + \phi_v)^2 \quad \text{if } s > 5.5c_v$$

Equation 2.18

b_{eff} = Effective width of concrete beam

b = Undamaged width of concrete beam

c_v = Concrete cover

ϕ_v = Stirrup Diameter

s = Stirrup spacing

Higgins et al. (2003) noted that a strut and tie model that incorporated the local minimum section loss in the shear reinforcement was more conservative than the same model that incorporated the average section loss. The average ratio of experimental strength to predicted strength was 1.13 with a

coefficient of variation of 0.16 for the strut and tie model incorporating the average section loss. The strut and tie model that includes the local minimum stirrup area has an experimental versus predicted strength ratio of 1.70 with a coefficient of variation of 0.66.

Chapter 3

Experimental Program

3.1 Introduction

The experimental program consists of casting sixteen reinforced concrete beams to study the effects of corrosion of the shear reinforcement on the shear behaviour. This chapter describes the test program, the test specimens, and the test specimen fabrication. The material properties of the concrete and steel will be reported. The setup and procedure used for the accelerated corrosion will be provided. Also, the instrumentation and data acquisition used for the testing will be described.

3.2 Test Program

The program is comprised of 16 reinforced concrete specimens, 125 mm wide x 350 mm deep x 1850 mm long. The test variables studied include: the shear span to effective depth ratio, the presence of shear reinforcement within the shear span, and the degree of corrosion. The corrosion levels correspond to exposure times of 21 days (low), 60 days (medium), and 120 days (high). The test matrix is given in Table 3.1. The specimens are identified as follows: Corrosion Level—a/d Ratio—Reinforcing. Corrosion level is identified as 0 (No Corrosion), L (Low), M (Medium), and H (High); a/d ratio is specified with the actual ratio 1, 1.5, or 2; and reinforcing is either specified as R for reinforced or UR for the three unreinforced specimens. One specimen is identified as a repaired specimen; it will be repaired following a medium to high corrosion level using wet-layup CFRP.

Table 3.1 Test Matrix

Type*	a/d		
	1	1.5	2
No Reinforcement	0-1-UR	0-1.5-UR	0-2-UR
Control	0-1-R	0-1.5-R	0-2-R
Low Corrosion Level	L-1-R	L-1.5-R	L-2-R
Medium Corrosion Level	M-1-R	M-1.5-R	M-2-R
High Corrosion Level	H-1-R	H-1.5-R	H-2-R

* One additional specimen (H-1.5-Repair) will be repaired with CFRP sheets.

3.3 Formwork Fabrication

Formwork was constructed for the concrete specimen fabrication. A schematic drawing of the formwork is provided in Figure 3.1

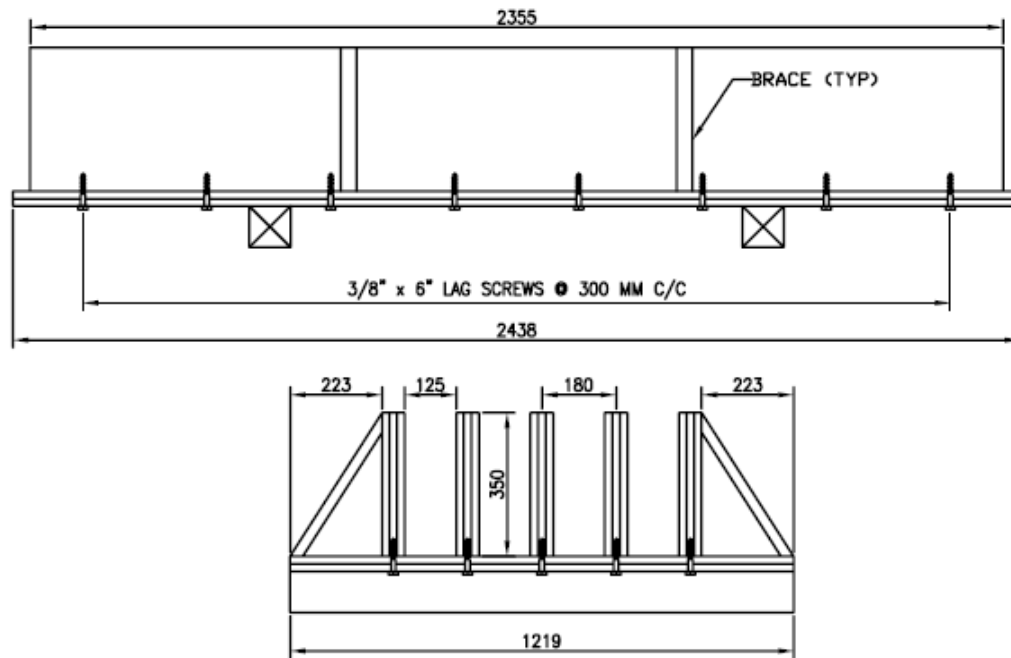


Figure 3.1 Formwork Drawing

The formwork consists of uprights made out of laminated plywood, and a base composed of two layers of 19 mm plywood. The uprights are made of 3 layers of plywood; the outside layers are 19 mm Formply, and the middle layer is 19 mm SPF Plywood. The plywood layers were laminated using Sikadur® -32 Epoxy resin bonding agent. The bonding agent was applied to the inside face of the Formply and one side of the SPF plywood and then these surfaces were laminated together; this process was repeated to adhere the other layer of Formply. Two uprights were constructed in each session. Then, the uprights were cured for a minimum of 8 hours under the pressure of heavy steel sections.



Figure 3.2 Upright Fabrication

The plywood layers were cut oversized by approximately 25 mm; after they were laminated together they were cut to height (350 mm) using a table saw. Then, the uprights were cut to length (2355 mm) using a radial arm saw. The uprights were connected to the base of the formwork using 8 – 3/8” (9.53 mm) diameter x 6” (152.4 mm) long lag screws. The lag screws were installed by drilling a lead hole to accept the threaded portion of the screw and a counterbore hole that was the diameter of the unthreaded portion of the screw. The lead hole was selected to be 15/64” (5.94 mm) and the counterbore hole was 3/8” (9.53 mm). A jig was constructed in order to ensure that the hole that was drilled into the uprights was vertical. A similar jig was used to ensure that the hole drilled into the base material was also vertical. The final step in fabrication was to install the lag screws using a pneumatically operated ratchet; drawings of the drilling jigs are provided in **Error! Reference source not found.** The use of the drilling jig, the installation of the lag screws, and the assembled formwork are depicted in Figure 3.3.



Figure 3.3 Formwork Construction

3.4 Test Specimens

The test specimens were designed to reflect typical deep beam dimensions. Consequently, a beam cross section of 125 mm by 350 mm was selected. Each beam was 1850 mm long with a clear span of 1500 mm. The stirrups were 10M deformed bars with anchorage provided by overlapping the bar ends at the top of the stirrup (Figure 3.7). The stirrups were spaced at 150 mm throughout the beam with a closer stirrup spacing of 50 mm provided at the support and loading points. The main reinforcement in the beam was two 25M deformed bars that were bundled together. This reinforcement was provided with a 180° hook to prevent a pull-out failure. A 22.5 mm cover to the stirrup was selected based on CSA A23.1 minimum requirement of 2.0 for the ratio of cover to nominal bar diameter for an exposure class of C-1. Figure 3.4 provides a drawing of the cross section of the beams.

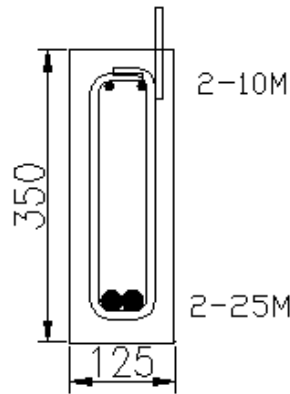


Figure 3.4 Beam Cross Section

Three shear spans (300 mm, 450 mm, and 600 mm) were selected to achieve shear-span to depth ratios of 1, 1.5, and 2; the number of stirrups within these shear spans were 1, 2, or 3 respectively. Three specimens were constructed with no stirrups within the shear span; the results from these tests will be compared with the reinforced (control) beams to determine the effect the stirrups have on the structural capacity of the beams. Figure 3.5 provides a drawing detailing the beam reinforcing and Figure 3.6 of the three different types of beams.

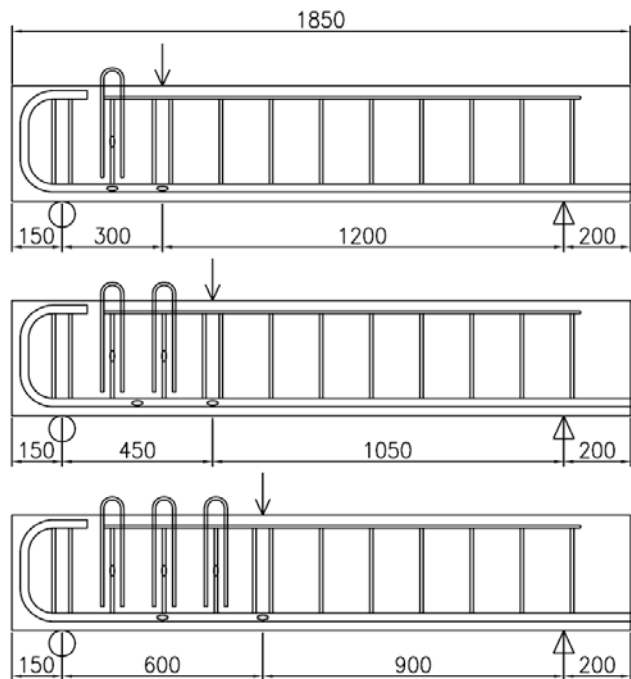


Figure 3.5 Beam Reinforcing

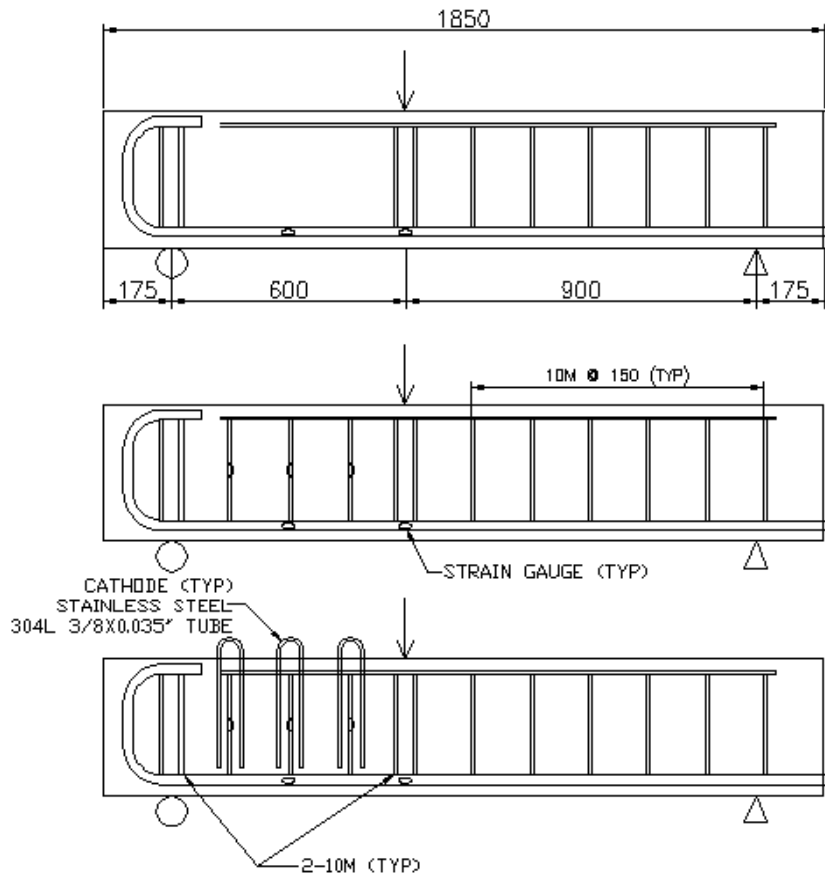


Figure 3.6 Beam Type

The stirrups that were corroded required additional details (Figure 3.7). An electrical connection had to be made between the stirrups and the power supply; to complete the electrical connection a steel bar which extended outside the specimen was welded to the stirrup. The ties used to attach the corrosion stirrups were wrapped in electrical tape to prevent an electrical connection with the main steel reinforcement. Also, the main reinforcement was covered with black electrical tape at the stirrup locations. A multimeter (Figure 3.8) was used to test the continuity between the reinforcement; this reading should be OL (open) which indicates there is no electrical connection.

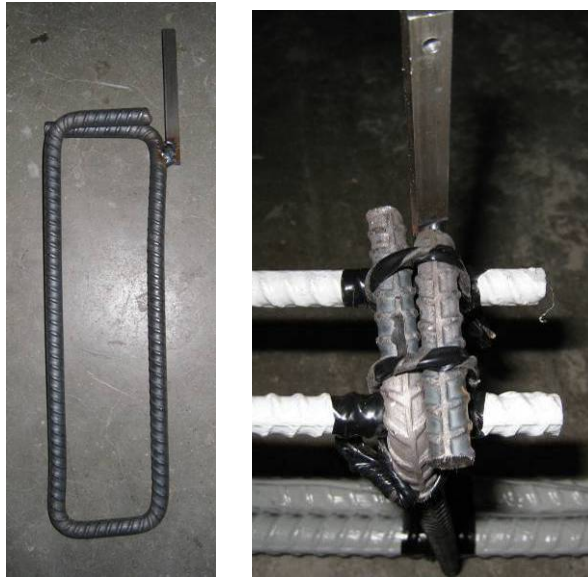


Figure 3.7 Stirrup Electrical Connection



Figure 3.8 Continuity Test

The main and compression reinforcement was epoxy (Devoe Coatings Bar-Rust 235) coated within the shear span to prevent corrosion of these elements. The main reinforcement was extended so that it could lock into the formwork end block. Figure 3.9 shows the three different types (no shear reinforcement, control, and corrosion) of specimens that were constructed; the cages depicted are for the 600 mm shear span.



Figure 3.9 Reinforcing Steel Cages

The accelerated corrosion process requires a cathode for the corrosion process to occur. A 9.5 mm diameter stainless steel tube was bent into a U shape and embedded within the concrete. A self-tapping screw was installed in the top of the cathode prior to the placement of the concrete. The cathodes are shown in Figure 3.10.



Figure 3.10 Stainless Steel Tube Cathode

Dividers were constructed to contain the salted concrete within the region around the corroded stirrup. Salted and un-salted concrete were placed in equal amounts and consolidated with a concrete

vibrator. This process was repeated until the formwork was filled. Figure 3.11 shows the dividers in the formwork and during the concrete placement. The width of the salted zone is 65 mm with a 90 mm unsalted zone between stirrups. This configuration is depicted in Figure 3.12.



Figure 3.11 Concrete Dividers

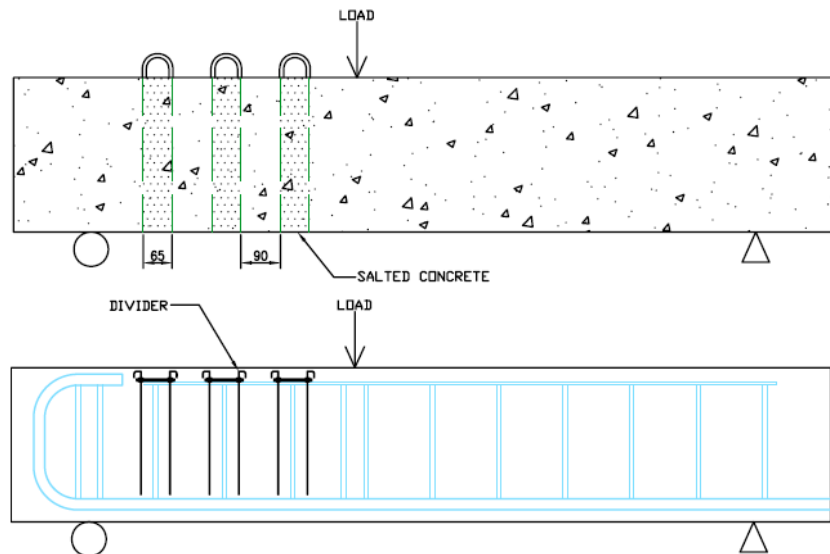


Figure 3.12 Salted Concrete Distribution

3.5 Material Properties

3.5.1 Concrete

The concrete was procured from a local ready-mix concrete supplier. The mix design is provided in Table 3.2. The concrete was batched with Type 10 portland cement; the maximum coarse aggregate size was 10 mm. The concrete was batched at a water-cementing materials ratio of 0.45, and the water-cementing materials ratio was adjusted on site to be 0.55. A measured volume of concrete was removed from the concrete transit mixer truck and salted water was mixed into this concrete in an on-site mixer. The amount of salt added was based on requiring 2.3% chlorides by mass of cement; this amount of salt was used in previous corrosion studies at the University of Waterloo. In addition, water was added to the remaining concrete in the truck, and the operator mixed this water by rotating the drum of the ready mix truck at a rapid rate. The exact mass of the water that was added to the truck was determined using precision scales.

Table 3.2 Concrete Mix Design

Material	Mass (kg/m ³)	
	Unsalted	Salted
Portland Cement	275	275
Slag Cement	70	70
Water	190	190
Fine Aggregate	950	950
Coarse Aggregate	1000	1000
Salt	0	13

The 28 day compressive strength of the concrete was tested using standard concrete cylinders (100 mm diameter x 200 mm long). The compressive strength values are provided in Table 3.3.

Table 3.3 Concrete Compressive Strength

Pour Date	Lot	Test Day	Compressive Strength (MPa)
November 30, 2007	Unsalted	33	40
November 30, 2007	Salted	33	28
December 13, 2007	Unsalted	28	47
December 13, 2007	Salted	28	35

3.5.2 Reinforcing and Stainless Steel

Grade 400R reinforcing steel (10M and 25M) were obtained from a local steel supplier. Three 10M specimens were tested according the specifications provided in ASTM 370-05. The specimens had following average material properties: a yield strength of 414 MPa, a modulus of elasticity of 190 GPa, a ultimate strength of 593 MPa, and a failure strain of 16.0%. The stainless steel used as cathodes was Type 304L with an outside diameter of 9.5 mm and a wall thickness of 0.89 mm.

3.5.3 Carbon Fibre Reinforced Polymer System

The carbon fibre reinforced polymer (CFRP) system was manufactured by SIKA Canada. The system is composed of SIKAWRAP 230C CFRP sheets and SIKADUR 330 epoxy. The epoxy is a two component epoxy composed of a resin and a hardener. The mechanical properties of the CFRP system are provided in Table 3.4.

Table 3.4 Properties of CFRP System

Property	SIKAWRAP 230C	SIKADUR 330	Cured Laminate Properties
Thickness (mm)	0.381	--	--
Tensile Strength (MPa)	3450	30	715
Tensile Modulus (MPa)	230000	--	61012
Elongation (%)	1.5	1.5	1.09

3.6 Accelerated Corrosion

Accelerated corrosion was utilized in order to achieve a significant amount of corrosion in the steel stirrups within a reasonable amount of time. The accelerated corrosion was conducted by impressing a constant current into the concrete beam specimens. This current polarizes the reinforcing steel stirrups with respect to a conductor (cathode). The conductor is either placed within the concrete or externally in a chloride contaminated bath. In this study, the conductor (stainless steel tubes) was placed within the concrete.

Chloride ions are introduced into the system either at the time of casting or by immersing the beam in chloride contaminated water. In this study, chlorides were introduced into the specimens by adding sodium chloride (NaCl) (2.3% by mass of cement) into the concrete mix. The chloride ions have two

purposes; the first is to depassivate the steel so that the corrosion process can occur, and secondly to lower the resistivity of the concrete.

As mentioned, the accelerated corrosion utilized an electrical current to polarize the reinforcing steel. This current is applied with a direct current (DC) power supply (Figure 3.13); the power supply can apply a maximum current of 500 mA with an accuracy of 1%. Researchers have used current densities up to 10, 400 $\mu\text{A}/\text{cm}^2$; an upper limit of 200 $\mu\text{A}/\text{cm}^2$ is suggested so that the crack growth and the strain in the concrete are comparable to field conditions (El-Maaddawy and Soudki, 2003). Based on previous experience it has been determined that Faraday's law under-predicts the mass loss at lower corrosion levels; conversely, it has been shown that at higher corrosion levels Faraday's law over-predicts the mass loss. The current was impressed in two stages: 450 $\mu\text{A}/\text{cm}^2$ for 840 hours and 150 $\mu\text{A}/\text{cm}^2$ for the remainder of the corrosion cycles. Consequently, the power supplies were initially set for 115 mA. The low beams were corroded for 504 hours, and the medium and high beams were corroded for 840 hours. At this point, the power supplies were set at 39 mA; the medium and high beams were corroded for 600 hours and 2040 hours respectively. This two stage corrosion cycle was done in order to achieve significant corrosion induced damage in the concrete. Two power supplies were connected to each set of beams (low, medium, and high levels). The impressed current calculations are provided in Appendix E.

The electrical connections are composed of wires connected to the power supply and reinforcing steel, wires connected to the cathode and reinforcing steel, and wires connected to the cathode and back to the power supply. Figure 3.14 provides a wiring schematic for the corrosion setup. The connections are coated in wax to prevent moisture from getting into the connection.

The corrosion process consumes oxygen and water at the cathode sites. The moisture is provided by a mist nozzle which is connected to a water tap and a pressurized air tap; the result is an extremely fine mist that maintains the humidity. The beams are supported on steel frames. The steel frames were covered with plastic in order to contain the moisture from the mist nozzle.



Figure 3.13 Power Supplies

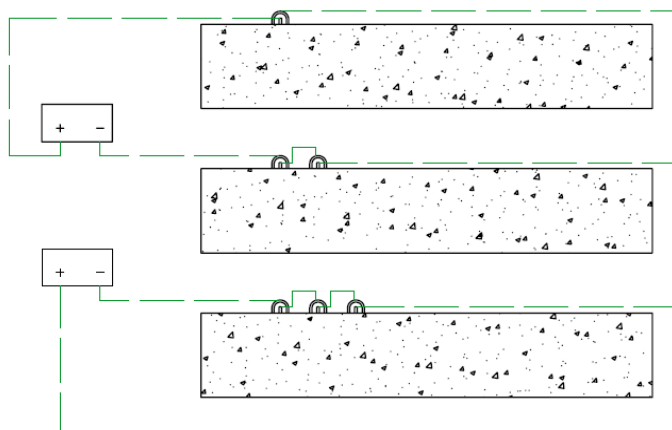


Figure 3.14 Corrosion Wiring Schematic



Figure 3.15 Anode and Cathode Connections

3.7 CFRP Strengthening

The CFRP strengthening procedure is composed of three main steps: surface preparation, application, and curing. The surface was prepared by using a grinder with an abrasive attachment to form a radius to the corners of the specimen. A radius between 20 mm and 35 mm was selected to conform to the existing code requirements (CSA S806-02, CHBDC S6-06). The specimen was left to air dry for 24 hours to ensure that surface moisture evaporated.

The epoxy resin was mixed according to the manufacturer's instructions. The first coat of the epoxy resin was applied to the concrete surface using a roller. The CFRP was then adhered to the surface; in addition, a second coat of resin was impregnated into the fabric using a steel laminating roller. Then a second layer of CFRP was adhered. Finally, a sealer coat of epoxy resin was applied to the outer CFRP layer. The system was left to cure according to the manufacturer's instructions (5 days at 21°C to 25 °C).

3.8 Test Setup and Instrumentation

3.8.1 Test Setup

The test frame utilized for the tests is custom built with a bottom crosshead base; a moveable upper crosshead is mounted on four posts. The test frame supports a servo-hydraulic MTS 244.41 actuator with a 500 kN load capacity and a stroke of 500 mm. The data inputs are controlled by a MTS Testar II controller. The controller can accommodate six channels of data. Four channels were used for strain data and two channels were used for external displacement transducers. The data acquisition and servo-hydraulic control were combined in the 793 multi-purpose testware (MPT) software. The strain gauge bridge completion and excitation were accomplished with a Vishay Instruments 2100 series strain gauge conditioning system. Figure 3.17 shows the test setup used for the experimental program.



Figure 3.16 CFRP Application



Figure 3.17 Test Setup

3.8.2 Support System

The specimen supports were placed on a modular steel beam system that was bolted together to accommodate the three shear spans. The specimens were supported on square 125 mm steel loading plates. The steel loading plates were fabricated with a groove in the middle designed to rest on a

modified structural steel section. The structural steel section was half a wide flange section with a machine surface on the flange. A chamfer was machined into the flange to support the loading plate and allow rotation of the loading plate. The pin connection was provided by clamping the modified structural steel section to the modular beam system. A roller connection was provided by placing steel roller rods under the support system. Figure 3.18 shows the specimen support system.



Figure 3.18 Specimen Support System

Figure 3.19 shows the system utilized at the load point which was composed of four parts. The loading plate was 125 mm square. To ensure a uniform stress distribution the loading plate was potted to the specimen using a gypsum cement product called hydro-stone (manufactured by USG). A spherical seat was placed on top of the loading plate that could shift to a position parallel with the load cell face. This was required because minor construction errors could cause the beam to be not perfectly level. A roller system was placed on top of the spherical seat to transfer the load from the actuator to the specimen. The roller could provide limited lateral displacement.



Figure 3.19 Load Point System

3.8.3 Strain Measurement

Strain gauges (Figure 3.20) were applied to both the longitudinal bars (25M) and the transverse stirrups (10M). The medium and high corrosion level beams only had strain gauges on the main steel because strain gauges installed on the stirrups would be destroyed during the accelerated corrosion phase. Also, strain gauges were applied to the main steel in specimens that did not have transverse reinforcement. The strain gauge locations are shown in Figure 3.6.



Figure 3.20 Strain Gauge Application

The strain gauges were 5 mm long, manufactured by KYOWA Japan; they had a resistance of 120 Ω . The reinforcing steel surface was ground smooth to provide a uniform surface for bonding the strain gauge. The surface was cleaned with an acid cleaner by wet sanding, and then it was neutralized with a conditioner. The steel surface was allowed to dry, and then the strain gauge were applied. Cyanacrolate adhesive was applied to the back of the strain gauge, and then it was adhered under pressure to the steel. A similar procedure was used to apply a terminal. The strain gauge wires were soldered to the terminal, and then a lead wire was also soldered to the same terminal. The final step was to apply coatings of urethane based sealant and wax to protect the strain gauge from the moisture present in the concrete.

3.8.4 Displacement Measurement

Displacement was measured using a direct current (DC) linear variable differential transformer (LVDT). The displacement of the specimen directly under the load point and the diagonal displacement perpendicular to the assumed compressive strut were measured. The LVDT under the load point was supported with a magnetic base and a fixture to keep it vertical. The diagonal LVDT was supported using magnetic mounts attached to steel plates adhered to the surface of the concrete

with LePage® 5-Minute Epoxy. The steel plates were oriented based on an assumed compressive strut; this was done to ensure that the diagonal crack growth was captured. A drawing of the diagonal magnetic mounts is provided in **Error! Reference source not found.** and Figure 3.21 shows the diagonal displacement setup.



Figure 3.21 Diagonal Displacement Setup

3.9 Mass Loss Analysis

3.9.1 Extraction of Reinforcing Steel

The stirrups were extracted from the specimens after the monotonic testing was complete. The concrete surrounding the stirrups was removed using a electric jackhammer. The removal concrete was done in a careful manner to avoid damaging the stirrup with the jackhammer or bending to stirrup; these actions would influence the mass loss results. The extraction of the stirrups is shown in Figure 3.22.



Figure 3.22 Stirrup Extraction

3.9.2 Gravimetric Mass Loss Analysis

Gravimetric mass loss analysis is used to determine the actual mass loss in the reinforcing steel after the beam is loaded to failure. The procedure specified in ASTM G1-03 is used to determine the actual steel mass loss from corrosion. The procedure designated as C.3.5 was selected because it works well at room temperature, the solution is made with two chemicals, and it has a comparatively shorter cleaning time. This procedure specifies that a solution composed of the following should be prepared: 500 mL hydrochloric (HCl) acid, 3.5 g hexamethylene tetramine, and reagent water to make a total volume of 1000 mL. Reinforcing steel coupons that had a length of 250 mm were extracted from both legs of all stirrups; a total of 40 coupons were analyzed. The coupons were immersed in the solution detailed above, and then they were brushed with a wires brush and cleaned with water. The specimens were dried and the mass was recorded. This procedure was repeated until the difference in the recorded mass between each cycle was negligible. The mass from the last cycle was used to determine the corrosion mass loss of each coupon. Photographs of this process are shown in Figure 3.23.



Figure 3.23 Mass Loss Analysis

Chapter 4

Experimental Results and Discussion

4.1 Introduction

The experimental results of this study are presented in this chapter. The focus of this study was to explore the behaviour of the specimens with respect to shear-span to depth ratio and degree of corrosion. A total of 16 reinforced concrete beams were tested monotonically to failure. Ten beams were subjected to accelerated corrosion and the remaining 6 beams were not corroded. To evaluate the feasibility of strengthening beams with corrosion damaged shear reinforcement, one of the corroded beams was repaired using dry lay-up CFRP strips. The corrosion crack width and mass loss results are presented in this chapter. Also, the load-deflection results, load induced crack patterns, failure modes, diagonal deformation, and the load-reinforcing steel strain behaviour are presented in this chapter.

4.2 Accelerated Corrosion Results

4.2.1 Corrosion Crack Widths

The corrosion cracks were primarily vertical at the locations of the vertical shear reinforcement with secondary cracks that were oriented along the horizontal reinforcement. A typical corrosion crack pattern is provided in Figure 4.1. A full set of corrosion crack width drawings are provided in Appendix B.

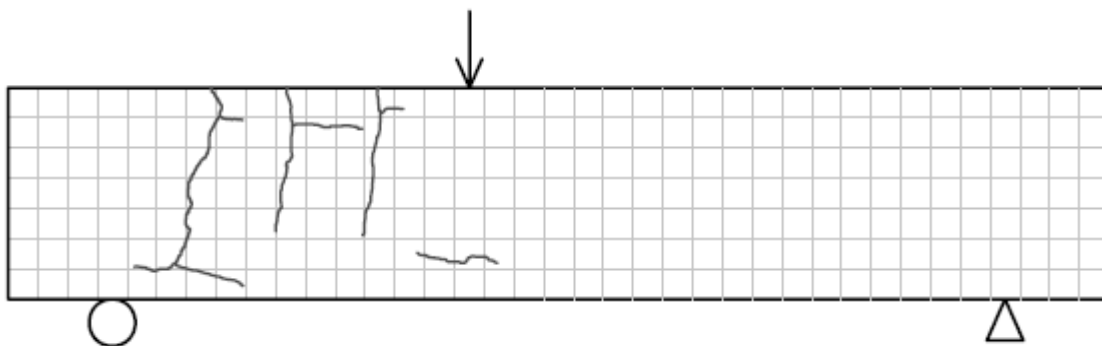


Figure 4.1 Typical Corrosion Crack Pattern

The crack width measurements were taken using a microscope with a magnification of 25 times after the accelerated corrosion phase was completed. The minimum crack width that can be measured is 0.05 mm. Cracks with a width below 0.10 mm were not measured because they were considered to be structurally insignificant. Table 4.1 provides a summary of the maximum and average crack widths for each beam; in addition, the overall average and average maximum crack width for each corrosion level were calculated. The maximum crack width for the low, medium and high level beams was found to be 0.60 mm, 0.90 mm, and 3.00 mm, respectively.

Table 4.1 Corrosion Crack Widths

Specimen Name	Maximum Crack Width (mm)	Average (mm)	Corrosion Level Average (mm)	Corrosion Level Average Maximum (mm)
L-1.0-R	0.45	0.30		
L-1.5-R	0.45	0.30	0.30	0.50
L-2.0-R	0.60	0.30		
M-1.0-R	0.90	0.50		
M-1.5-R	0.45	0.30	0.40	0.65
M-2.0-R	0.60	0.35		
H-1.0-R	1.50	0.90		
H-1.5-R	3.00	1.00	0.80	2.40
H-2.0-R	2.60	0.60		
H-1.5-Repair	1.00	0.45	0.45	0.45

4.2.2 Reinforcing Steel Mass Loss

The actual mass loss of the reinforcing steel can deviate significantly compared to the theoretical mass loss calculated from Faraday’s law. Consequently, a chemical cleaning procedure conforming to ASTM G1-03 was performed on reinforcing steel coupon specimens. The coupon specimens were extracted using an electric jackhammer to remove the surrounding concrete. Care was taken to avoid damaging or bending the shear reinforcement with the electric jackhammer. Each leg of the shear reinforcement was cut into specimens 200 mm long. The shear reinforcement that was ground to allow for the strain gauge application was cut into two pieces.

Figure 4.2 shows the variation in the mass loss of the shear reinforcement. The white and black bars represent the right and left legs of the stirrups looking in the shear-span of the beam. The variation between adjacent white and black bars represents the variation in the mass loss of the

stirrups within one specimen. The figure shows that corrosion is relatively uniform over each individual stirrup. There is a significant variation in mass loss when comparing individual stirrups within the same beam. This variation is most pronounced in specimens M-1.5-R, H(M)-1.5-R, H(M)-1.5-Repair.

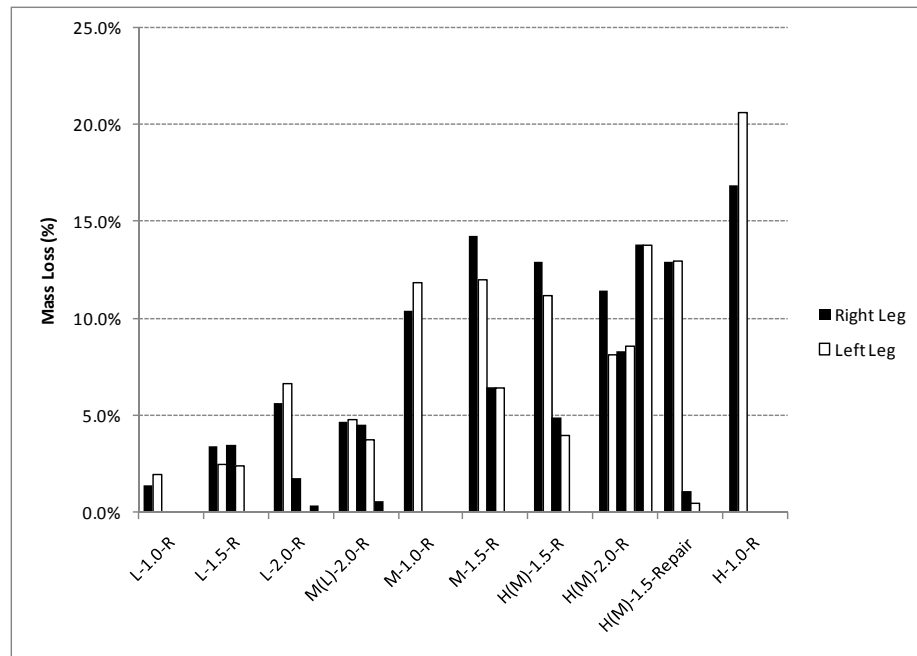


Figure 4.2 Mass Loss Variation

The mass loss for each beam specimen is determined based on the average mass loss for the shear reinforcement in the specimen. This data is presented in Table 4.2. The specimens were re-categorized based on the measured mass loss results. The nomenclature has been modified as follows: specimen H-1.5-R is renamed specimen H (M)-1.5-R indicating the actual mass loss level is medium. Table 4.3 shows the re-categorized testing matrix. The average mass loss for each corrosion level is 2.5% for low, 10.0% for medium, and 18.7% for high.

Table 4.2 Mass Loss Results

Theoretical Corrosion Level	a/d		
	1	1.5	2
Low	1.7%	2.8%	2.5%
Medium	11.1%	9.8%	2.9%
High	18.7%	8.2%	10.7%
Repair	8.1%		

Table 4.3 Re-categorized Test Matrix

Theoretical Corrosion Level	a/d		
	1	1.5	2
Low	L-1.0-R	L-1.5-R	L-2.0-R
Medium	M-1.0-R	M-1.5-R	M(L)-2.0-R
High	H-1.0-R	H(M)-1.5-R	H(M)-2.0-R
		H(M)-1.5- Repair	

4.3 Monotonic Test Results

This section will provide details on the cracking load, load deflection behaviour, crack patterns, modes of failure, and reinforcing steel strain behaviour. The specimens are grouped and presented according to shear-span to depth ratio; consequently, three beam series are presented ($a/d = 1.0, 1.5,$ and 2.0). In order to compare the results of specimens with different concrete compressive strengths, the measured load applied at any load level during the response for each specimen was normalized to a concrete strength of 35 MPa based on Equation 4.1. The concrete strength was determined from the cylinder strength determined at the time of testing (provided in Appendix C).

$$P_{NORM} = P_{MEASURED} \sqrt{\frac{35 \text{ MPa}}{f'_c}} \quad \text{Equation 4.1}$$

P_{NORM} = Normalized load (kN)

$P_{MEASURED}$ = Measured load (kN)

f'_c = Concrete compressive strength (MPa)

4.3.1 Experimental Results – a/d = 1.0

All beams were tested to failure except specimen 0-1.0-R. Specimen 0-1.0-R reached the capacity of the loading equipment, so the test was stopped. The load-deflection behaviour for beams with a shear-span to depth ratio of 1.0 is presented in Figure 4.3.

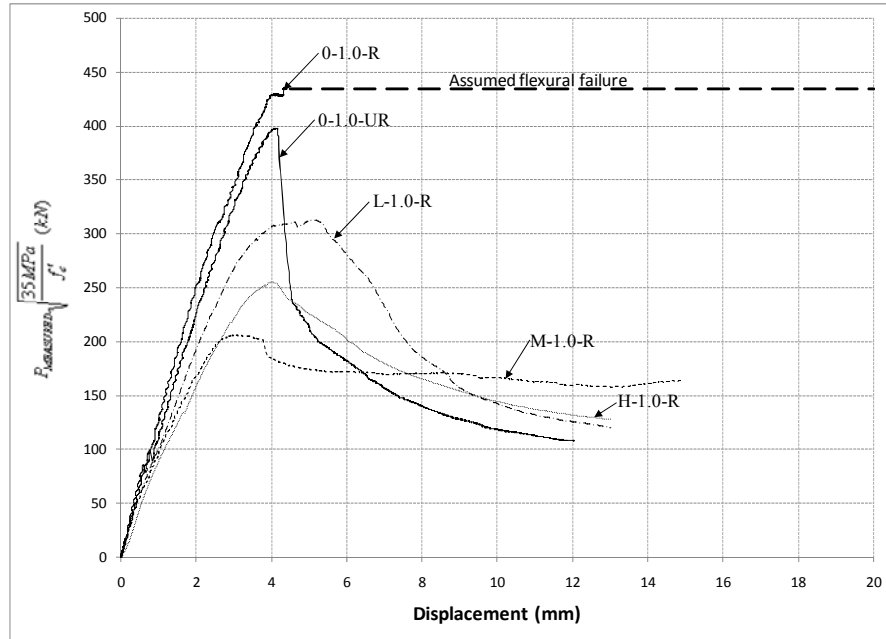


Figure 4.3 Load-Deflection Behaviour a/d =1.0

Table 4.4 presents the measured and normalized diagonal cracking and ultimate loads. Table 4.4 also presents the vertical deflection corresponding to the load when diagonal cracks formed and the deflection at ultimate load. The vertical deflection was measured at the load point.

Table 4.4 Load-Deflection Behaviour Summary a/d = 1.0

Specimen	Measured Load			Normalized Load		Deflection	
	Concrete Strength (MPa)	Diagonal Cracking (kN)	Ultimate (kN)	Diagonal Cracking (kN)	Ultimate (kN)	Diagonal Cracking (mm)	Ultimate (mm)
0-1.0-UR	35.7	100	401	99	397	0.84	4.16
0-1.0-R	41.3	105	473	97	435	0.76	4.31
L-1.0-R	45.4	62	356	54	313	0.46	5.19
M-1.0-R	40.5	64	221	60	205	0.53	3.06
H-1.0-R	43	87	283	78	255	0.87	3.99

4.3.1.1 Cracking Load

The cracking loads for the specimens are tabulated in Table 4.4. The diagonal cracking load is determined from the diagonal displacement data. The value that corresponds to 0.1 mm of diagonal deformation is selected to be the cracking load. The crack width value of 0.1 mm was selected because this is roughly the level at which cracks can be seen by the naked eye.

The diagonal cracking loads for the corroded specimens are less than the diagonal cracking load for the control specimen. This can be explained by the fact that the load induced cracks tend to propagate along the same path as the corrosion induced cracks. The corrosion cracking reduces the stiffness of the cross section; this will be reflected by an increase in the diagonal deformation which is used to determine the cracking load.

4.3.1.2 Stiffness and Ductility

Table 4.5 shows the stiffness for each specimen. The stiffness is calculated from the slope of the load-deflection curve. The pre-cracking stiffness is calculated based on the deflection at a load of 15 kN and the deflection at the diagonal cracking load. The post-cracking stiffness is determined from the deflection at the diagonal cracking load and the deflection at a load close to the ultimate load. It is evident that the corrosion cracking in the corroded specimens (L-1.0-R, M-1.0-R, and H-1.0-R) causes a reduction in stiffness of the specimen. The stiffness degradation is more pronounced in the corroded specimens with an average reduction of 30%. The reduction in stiffness observed in the corroded specimens can be attributed to the corrosion cracking.

Table 4.5 Stiffness a/d = 1.0

Specimen	Pre-Diagonal Cracking	Post-Diagonal Cracking	Stiffness Degradation
	Stiffness (kN/mm) K_1	Stiffness (kN/mm) K_2	$\frac{K_1 - K_2}{K_1}$
0-1.0-UR	116	103	11%
0-1.0-R	123	114	7%
L-1.0-R	114	86	25%
M-1.0-R	111	75	32%
H-1.0-R	99	66	33%

4.3.1.3 Ultimate Shear Strength

The ultimate shear strength (Equation 4.2) of the specimens was determined using statics from the normalized ultimate load. The ultimate shear force is normalized with respect to concrete strength in order to provide an accurate relative comparison of the behaviour of the specimens.

$$V = \frac{1200 \text{ mm}}{1500 \text{ mm}} P_{NORM} \quad \text{Equation 4.2}$$

V = Ultimate Shear Force (kN)

P_{NORM} = Ultimate Normalized Load (kN)

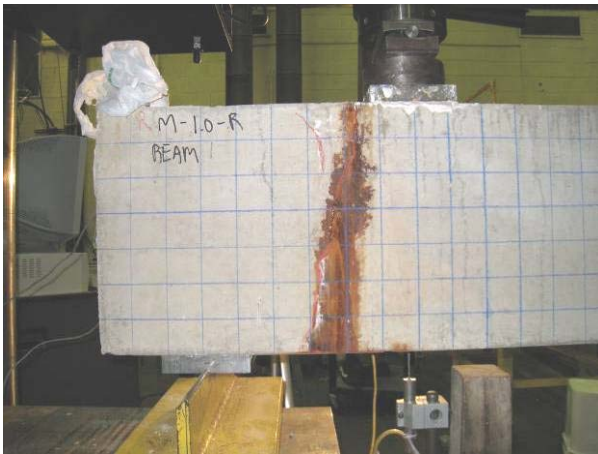
A significant degradation in the ultimate shear strength of the corroded specimens was observed when compared with specimens 0-1.0-UR (no steel stirrups) and 0-1.0-R (reinforced). Table 4.6 provides a quantitative measure of the shear strength reduction in this series of specimens. If corrosion cracking has no effect on the behaviour than a logical assessment of the situation would conclude that corroding the shear reinforcement to a degree where it is no longer effective would result in a strength reduction similar to specimen to 0-1.0-UR (w/o shear reinforcement). The corroded specimens experienced strength reductions that are in excess of what was observed in the specimen without shear reinforcement. This suggests that the corrosion cracks that result from corroding the shear reinforcement significantly affect the shear strength of the specimens.

The primary shear resisting mechanism in deep beams is achieved by a compression strut. If the compression strut is transferring the load efficiently then long, continuous cracks will be evident. What was observed in the corroded specimens is isolated cracks that follow the vertical corrosion crack. This results in a less direct load path from the load point to the support; consequently, the ultimate strength is reduced.

Specimen M-1.0-R exhibited the least strength in this group. It should be noted that the shear reinforcement in this specimen shifted during the concrete placement; this results in an inclined corrosion crack (Figure 4.4). This diagonal corrosion crack coincides closely with the compressive strut; if the compressive strut is weakened through longitudinal cracks along the axis of the strut then the strength of the specimen would be reduced. This observation suggests that inclined reinforcement that is corroded is a more critical case than corroded vertical shear reinforcement.

Table 4.6 Strength Reduction a/d = 1.0

Specimen	Average Mass Loss (%)	Normalized Shear Strength (kN)	Percentage Difference
0-1.0-UR	--	318	9%
0-1.0-R	--	348	--
L-1.0-R	1.7%	250	28%
M-1.0-R	11.1%	164	53%
H-1.0-R	18.7%	204	41%



Specimen M-1.0-R



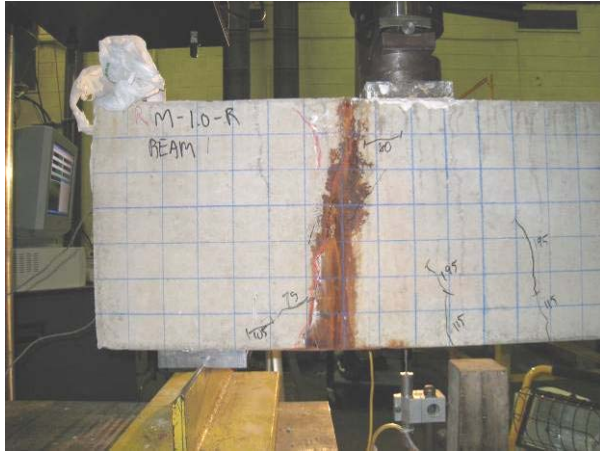
Specimen H-1.0-R

Figure 4.4 Inclined Corrosion Crack in Specimen M-1.0-R

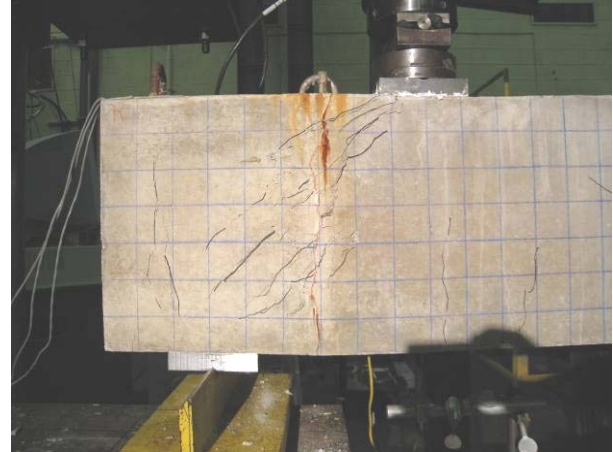
4.3.1.4 Crack Patterns and Modes of Failure

Typically in this series, flexural cracks formed first in the long span of the specimens. The flexure cracks were spaced at approximately 150 mm apart which is the spacing of the stirrups in the long span. Diagonal crack formation was observed in the shear span after the flexural cracks became apparent. In specimens M-1.5-R and H-1.0-R, load induced cracking was in isolated regions; some of the cracking may have coincided with the vertical corrosion cracks. This observation is supported by the fact that the compressive strut in this region is oriented at a very steep angle. In specimen 0-1.0-R (control) specimen and specimen L-1.0-R the diagonal cracks were continuous from the loading point to the support region. Figure 4.5 shows the diagonal crack patterns in specimens L-1.0-R and M-1.0-R. In specimen 0-1.0-R diagonal cracks were evident in the long span; whereas, in the corroded

specimen very few diagonal cracks were observed. This is because the control beam reached significantly higher loads than the corroded specimens.



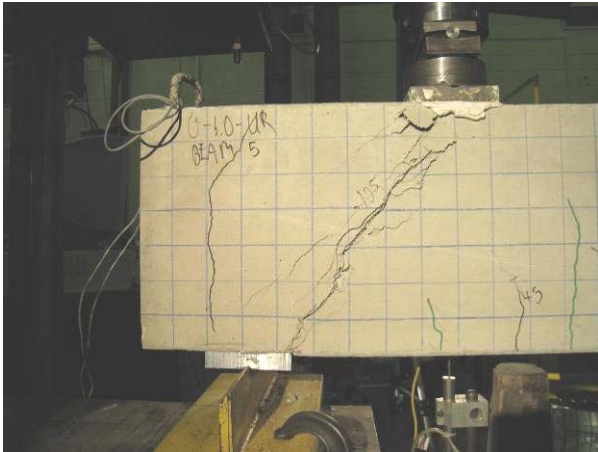
Specimen M-1.0-R
Isolated Cracks



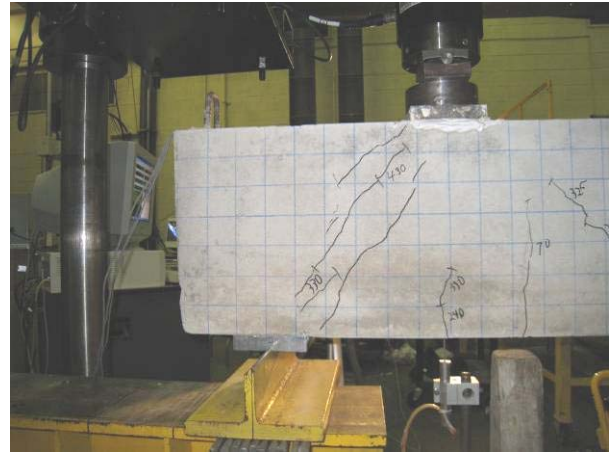
Specimen L-1.0-R
Continuous Cracks

Figure 4.5 Isolated and Continuous Cracks in Specimens M-1.0-R and L-1.0-R

Figure 4.6 shows a view of the shear span after the specimens failed. The corroded specimens failed in a diagonal crushing mode and specimen 0-1.0-UR failed in a diagonal splitting mode. Specimen 0-1.0-R (control) was not tested to failure because the capacity of the loading equipment was reached. The typical sequence of events over the loading history of the corroded specimens was: flexural crack formation, diagonal shear crack formation, yielding of the shear reinforcement, crushing of the compressive strut, and vertical crack formation at the anchorage point. Figure 4.7 shows a vertical crack that was observed at the edge of the corrosion damaged zone; this is most likely the extent of a delamination zone.



O-1.0-UR (Diagonal Splitting)



O-1.0-R (Failure not reached – Crack Pattern at a normalized load level of 435 kN)



L-1.0-R (Diagonal Crushing)



M-1.0-R (Diagonal Crushing)



H-1.0-R (Diagonal Crushing)

Figure 4.6 Failure Crack Patterns $a/d = 1.0$

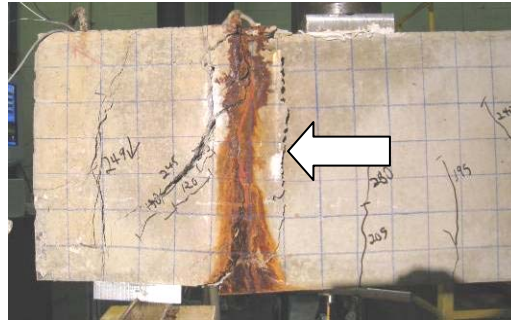


Figure 4.7 Crack Pattern in Specimen H-1.0-R

4.3.1.5 Diagonal Displacement

The diagonal deformation response shown in Figure 4.8 provides information about two important characteristics of the specimens: the cracking load and the diagonal stiffness. The diagonal stiffness for the control (0-1.0-R) was not measured because the displacement transducer did not function. The first diagonal cracks in the corroded specimens occurred at approximately 50% of the load that the diagonal crack was observed at in specimen 0-1.0-R.

The diagonal stiffness response is compared with the overall load-deformation behaviour to see if there are any important differences. The stiffest response was from specimen 0-1.0-UR.; a reduction in stiffness is observed when the first diagonal crack occurred. Specimens L-1.0-R and M-1.0-R have similar stiffness; specimen H-1.0-R shows a stiffer response than the other two corroded specimens. This is contradictory to the overall response of the corroded specimens which reveals that specimen H-1.0-R has the least stiff response. This contradiction suggests that more deformation (cracking) must be occurring outside the assumed compressive strut. This supports the hypothesis that compressive stresses are being transferred to the support through inefficient compression load paths.

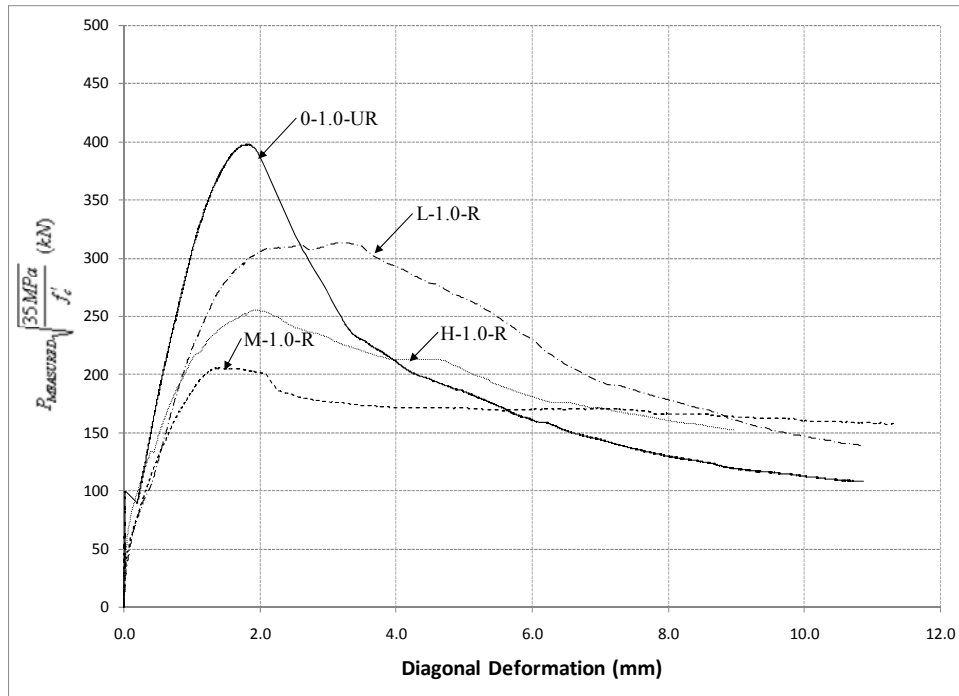


Figure 4.8 Diagonal Displacement Behaviour $a/d = 1.0$

4.3.1.6 Reinforcing Steel Strain Behaviour

Table 4.7 gives the strains in the reinforcing steel (stirrups, longitudinal bars) at the ultimate state. The yield strain for the shear reinforcement determined from tensile testing (Appendix C) is 2300 microstrain. The yield strain for the longitudinal reinforcement is also taken as 2300 microstrain. A strain gauge was placed on the stirrup within the shear span. Also, strain gauges were placed on the longitudinal reinforcement at the loading point and the middle of the shear span. The strain gauge failure for the corroded specimens is most likely due to corrosion occurring under the strain gauge.

The stirrup in specimen 0-1.0-R yielded and the stirrup in specimen L-1.0-R was approaching the yield point when the strain gauge failed. Figure 4.9 shows the strain in the shear reinforcement for specimen 0-1.0-R. The strain in the shear reinforcement starts to increase at an applied load of 85 kN. This corresponds to the point when the stirrups become effective in restraining crack growth. The strain behaviour (provided in Appendix D) for specimen L-1.0-R is similar to specimen 0-1.0-R.

Table 4.7 Strain in Reinforcing Steel at Ultimate Load $a/d = 1.0$

Specimen	Shear Reinforcement	Longitudinal Reinforcement	
	Stirrup 1 ($\mu\epsilon$)	Load Point ($\mu\epsilon$)	Middle of Shear Span ($\mu\epsilon$)
0-1.0-UR		1912	1901
0-1.0-R	2462	2182	3862
L-1.0-R	1940*	1690	1491
M-1.0-R		1196	1616
H-1.0-R		X	506

* Strain gauge failed prior to ultimate load

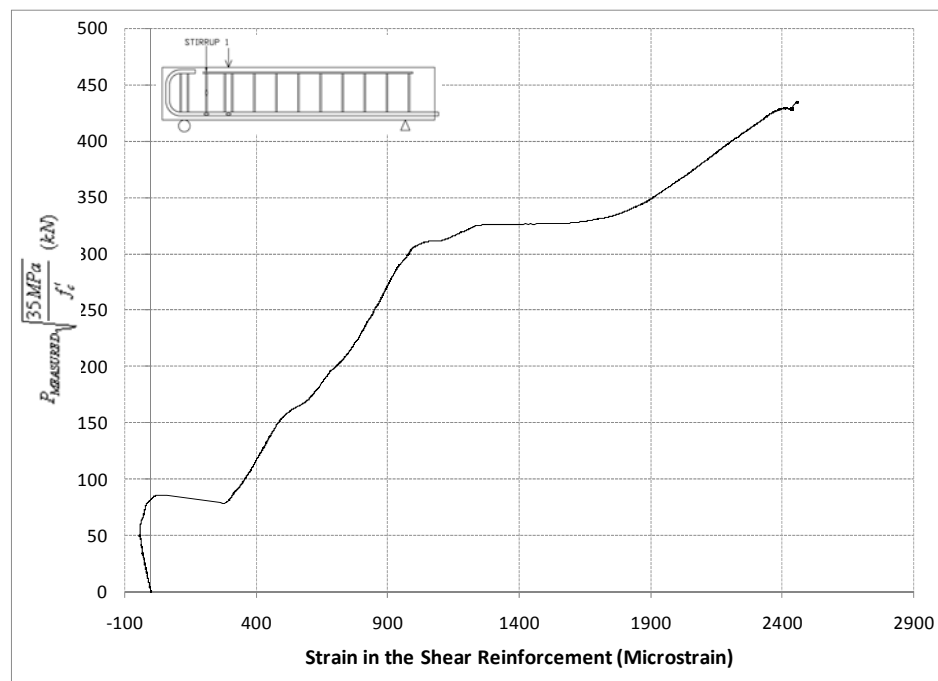


Figure 4.9 Strain Behaviour of the Shear Reinforcement in Specimen 0-1.0-R

The strain behaviour in the longitudinal reinforcement for specimens 0-1.0-R and L-1.0-R is provided in Figure 4.10 and Figure 4.11, respectively. The strain behaviour of specimens 0-1.0-UR and M-1.0-R (provided in Appendix D) is similar to the behaviour shown in Figure 4.10. It is evident that in specimen 0-1.0-R the strain in the longitudinal reinforcement at the load point is larger than the strain at the middle of the shear span prior to the formation of diagonal cracks. This behaviour is the same as what would be predicted by conventional beam theory. As the diagonal cracks propagate, the strain values at the load point and at the middle of the shear span become similar. This behaviour, known as tied arch action, occurs when the diagonal cracks propagate from the load point to the

reaction point (forming a compression strut) (MacGregor and Bartlett, 2000). The strain values in specimen L-1.0-R deviate after the applied load reaches 30 kN. The point at which the strains deviate corresponds to the initiation of flexural cracks (flexural cracks were visible at 45 kN for this specimen). The strain values tend to decrease with higher corrosion because the ultimate load decreases with respect to the degree of corrosion.

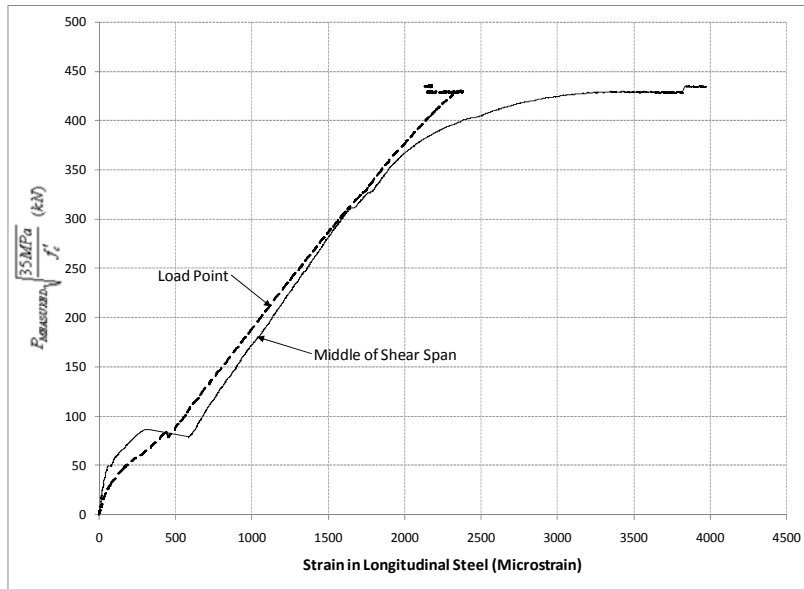


Figure 4.10 Strain Behaviour Longitudinal Reinforcement in Specimen 0-1.0-R

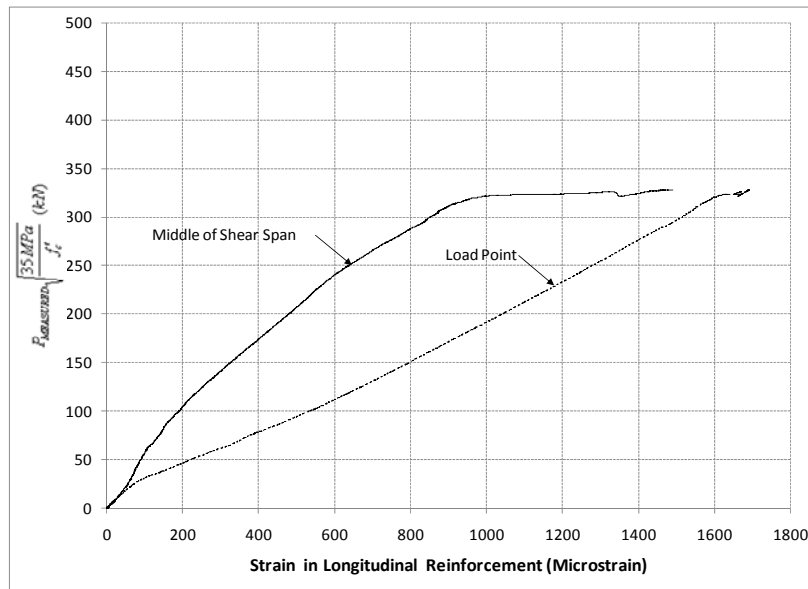


Figure 4.11 Strain Behaviour Longitudinal Reinforcement in Specimen L-1.0-R

4.3.2 Experimental Results – a/d = 1.5

This section focuses on the test results of beams with a shear-span to depth ratio of 1.5. All specimens in this series were tested to failure.

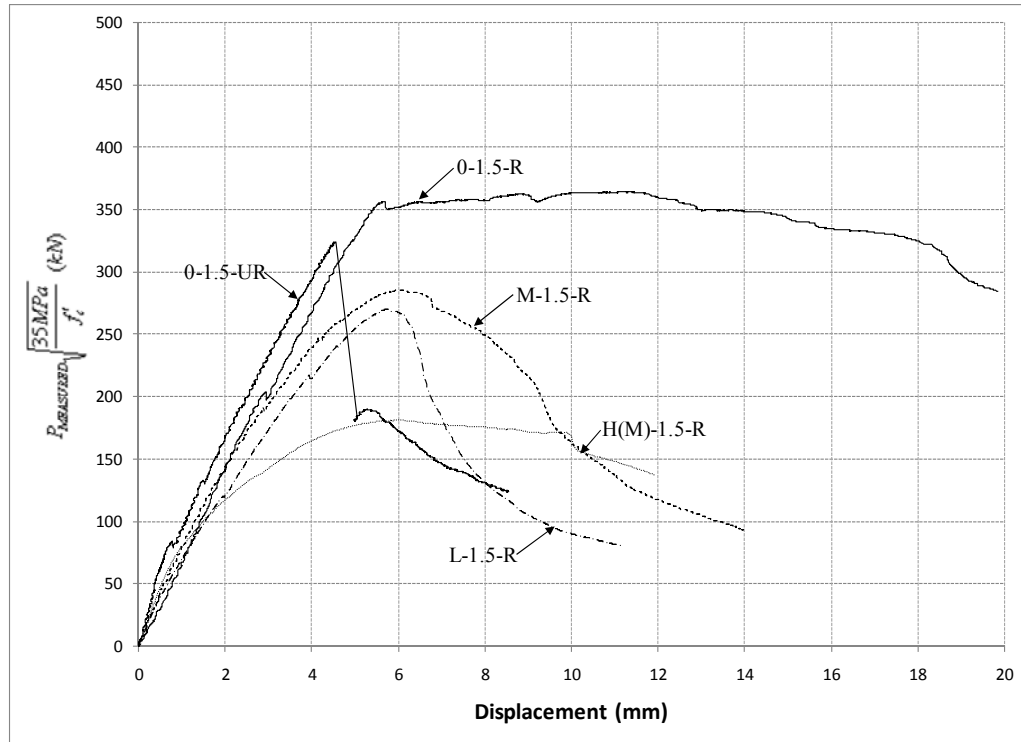


Figure 4.12 Load-Deflection Behaviour a/d = 1.5

Table 4.8 presents the concrete strength, measured cracking and ultimate loads, normalized cracking and ultimate loads according to Equation 4.1, and the deflection at diagonal cracking and the ultimate stage.

Table 4.8 Load-Deflection Behaviour Summary a/d = 1.5

Specimen	Measured Load			Normalized Load		Deflection	
	Concrete Strength (MPa)	Diagonal Cracking (kN)	Ultimate (kN)	Diagonal Cracking (kN)	Ultimate (kN)	Diagonal Cracking (kN)	Ultimate (mm)
0-1.5-UR	41.3	90	352	83	324	0.85	4.54
0-1.5-R	41.3	49	396	45	365	0.70	11.21
L-1.5-R	45.4	78	308	68	270	1.50	5.72
M-1.5-R	40.5	78	307	73	285	0.88	6.00
H(M)-1.5-R	43	95	201	86	181	1.13	6.07

4.3.2.1 Cracking Load

The cracking loads for each beam are presented in Table 4.8. The analysis of this data is similar to what is presented for beams with a shear-span to depth ratio of 1.0 (Section 4.3.1). The diagonal cracking load increases with the degree of corrosion for specimens with a shear-span to depth ratio of 1.5. This behaviour is different from specimens with a shear-span to depth ratio of 1.0 where a reduction in the shear cracking load was observed. Specimens with a shear-span to depth ratio of 1.5 have more corrosion cracks because two stirrups were corroded compared with one stirrup in specimens with a shear-span to depth ratio of 1.0. It is likely that there are stronger load paths outside of the zone that diagonal deformation was measured. This would result in a larger load to cause a diagonal deformation of 0.1 mm which could explain the increase in shear cracking load shown in Table 4.8.

4.3.2.2 Stiffness and Ductility

Table 4.9 presents the stiffness for the specimens in this series. The stiffness was calculated using the same formulations that were described for the previous series. Specimen 0-1.5-R was inadvertently dropped before testing which caused some cracking within the specimen; this affected the pre-diagonal cracking stiffness. The stiffness degradation in the corroded specimens is similar to what was observed for specimens with a shear-span to depth ratio of 1.0. Specimen H(M)-1.5-R has the largest stiffness degradation of 60% compared to all the other corroded specimens. The average stiffness degradation in the corroded specimens is 38%.

Table 4.9 Stiffness a/d = 1.5

Specimen	Pre-Diagonal Cracking	Post-Diagonal Cracking	Stiffness Degradation
	Stiffness (kN/mm) K_1	Stiffness (kN/mm) K_2	$\frac{K_1 - K_2}{K_1}$
0-1.5-UR	91	68	25%
0-1.5-R	64	64	0%
L-1.5-R	63	50	21%
M-1.5-R	83	55	33%
H(M)-1.5-R	71	29	60%

4.3.2.3 Ultimate Shear Strength

The shear strength of the specimens is calculated from the normalized load based on statics with Equation 4.3. In this series, the corroded specimens were not as strong as the control specimen. Table 4.10 presents the strength reduction experienced by the corroded specimens compared to the control (0-1.5-R) specimen. The reduction experienced by specimens L-1.5-R and M-1.5-R are similar; in fact, specimen L-1.5-R experienced a slightly larger strength reduction which is somewhat counter-intuitive. This phenomenon can be rationalized by the fact that the average crack width for both specimens is 0.3 mm (Table 4.1). In addition, specimen L-1.5-R had corrosion cracks which were diagonal in a direction that is closer to the inclination of the assumed compressive strut. These diagonal corrosion cracks tend to weaken the compression strut; this is a similar behaviour to what was observed for specimen M-1.0-R.

$$V = \frac{1050 \text{ mm}}{1500 \text{ mm}} P_{NORM} \quad \text{Equation 4.3}$$

V = Ultimate Shear Force (kN)

P_{NORM} = Ultimate Normalized Load (kN)

Table 4.10 Strength Reduction $a/d = 1.5$

Specimen	Average Mass Loss (%)	Normalized Shear Strength (kN)	Percentage Difference
0-1.5-UR	--	227	11%
0-1.5-R	--	255	--
L-1.5-R	2.8%	189	26%
M-1.5-R	9.8%	200	22%
H(M)-1.5-R	8.2%	127	50%

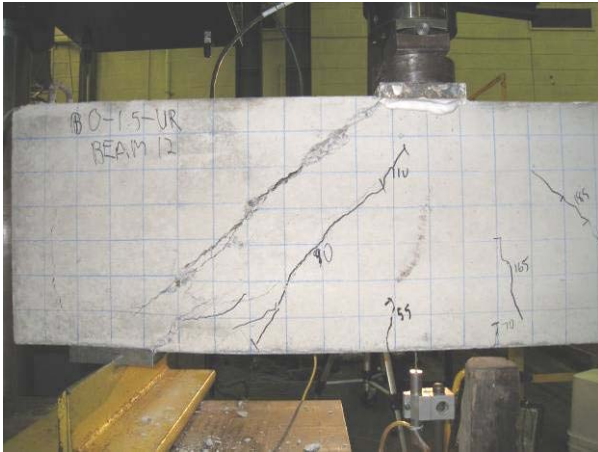
In this series of beams, the corrosion cracks appear to have the most significant influence on the strength of the specimens. The section loss in the reinforcing steel is not as significant. The reasoning behind providing shear reinforcement in disturbed regions is to provide a slightly more ductile behaviour. This is achieved by restraining growth of shear cracks. The effect of shear reinforcement in disturbed regions is best illustrated by comparing the load-deflection behaviour of specimen 0-1.5-R (with shear reinforcement) with specimen 0-1.5-UR (no shear reinforcement). This overall load-deflection behaviour is provided in Figure 4.12. The specimen without shear reinforcement failed very suddenly. Specimens with corroded stirrups (L-1.5-R, M-1.5-R, H(M)-1.5-

R) exhibited a significant reduction in ductility in comparison to the control specimen (0-1.5-R). However, even when the shear reinforcement was corroded there was sufficient reinforcement to provide limited ductility and warning of impending failure.

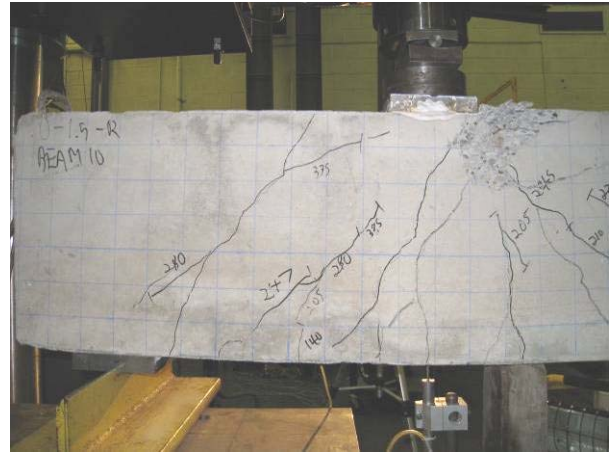
4.3.2.4 Crack Patterns and Modes of Failure

The flexural cracks formed in a pattern that was similar compared to specimens with a shear-span to depth ratio of 1.0. After the formation of flexure cracks, diagonal cracks formed in the shear span. The diagonal cracks in the corroded specimens formed in random locations. The crack propagation was typically interrupted by the vertical corrosion cracks, but the diagonal cracks eventually propagated through the cracks. In addition, diagonal cracks became visible in the long span of the beams at higher load levels. In the control beam, the diagonal cracks in the short span were significantly longer at lower load levels when compared with the corroded specimens because the load supported by the control specimen was larger compared to the corroded specimens.

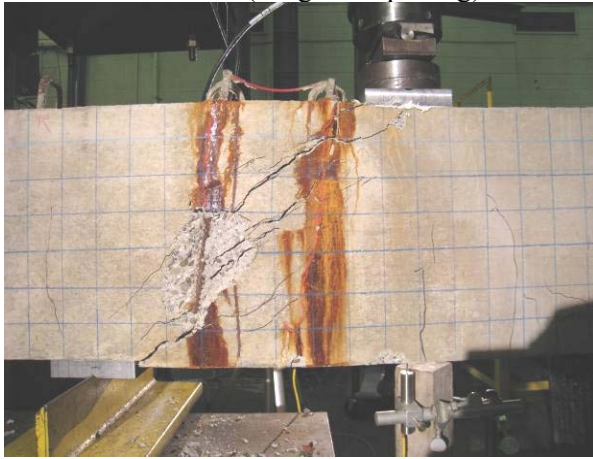
There were three failure modes identified in this series of beams: flexural failure, diagonal crushing, and diagonal splitting. Figure 4.13 shows the shear –span after the specimen failed. The corroded specimens all failed due to diagonal crushing of the compression strut. The control specimen failed in flexure, and the un-reinforced specimen failed in diagonal splitting. The sequence of events leading up to the failure of the corroded specimens was the same as what was observed for specimens with a shear-span to depth ratio of 1.0. The control beam behaved as a typical under-reinforced beam in flexure; the main reinforcement yielded before the concrete crushed adjacent to the loading plate in the long span. The corrosion of the shear reinforcement weakened the corroded beams sufficiently to cause a shear failure.



O-1.5-UR (Diagonal Splitting)



O-1.5-R (Flexural)



L-1.5-R (Diagonal Crushing)



M-1.5-R (Diagonal Crushing)



H(M)-1.5-R (Diagonal Crushing)

Figure 4.13 Failure Crack Patterns $a/d = 1.5$

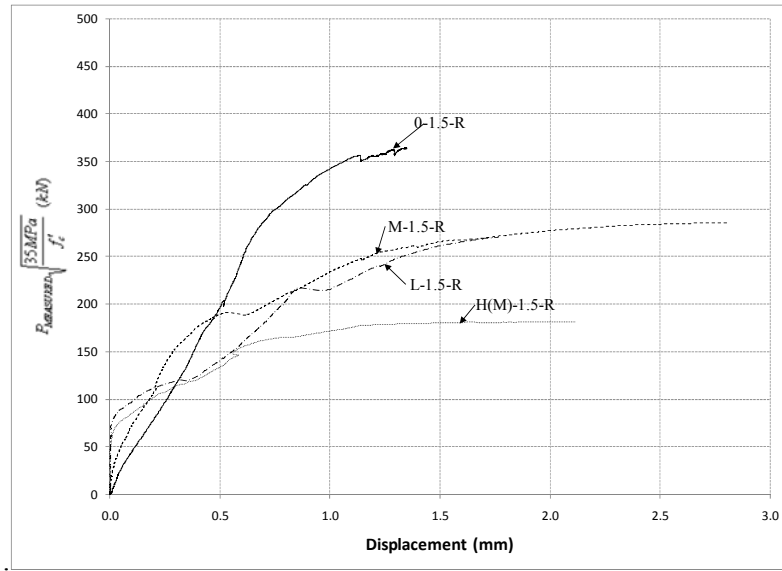


Figure 4.14 Diagonal Displacement Behaviour $a/d = 1.5$

The diagonal displacement for specimen 0-1.5-UR (Figure 4.15) is significantly different than the other specimens in this series. The most significant difference is the sudden jump in crack width when the beam fails. This reflects the sudden nature of the shear failure in beams without shear reinforcement. The diagonal displacement increased 3 mm almost instantaneously at the point of failure. A negative displacement before diagonal cracking is shown for this specimen; this displacement is minimal compared to the overall displacement so it could be considered noise within the test setup.

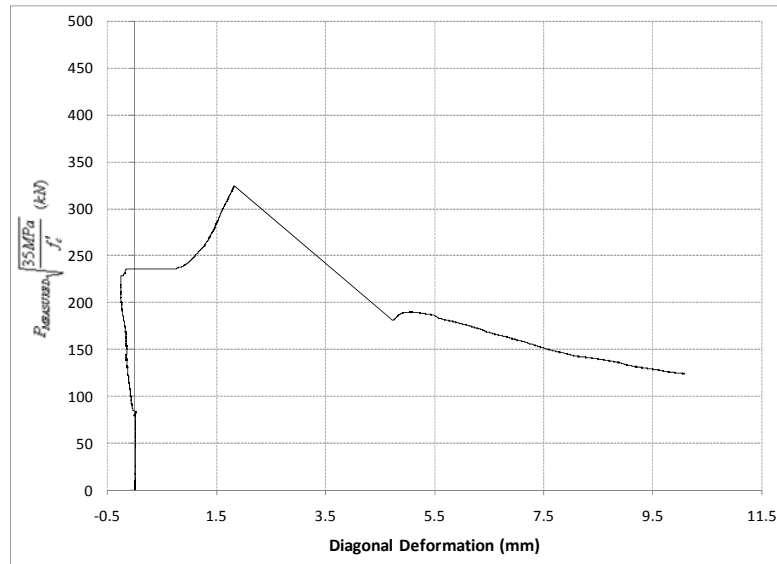


Figure 4.15 Diagonal Displacement Behaviour for Specimen 0-1.5-UR

4.3.2.5 Reinforcing Steel Strain Behaviour

The maximum reinforcing steel strain values are presented in Table 4.11. The strain gauges were placed on the shear reinforcement for specimens 0-1.5-R and L-1.5-R; the stirrups are numbered starting with stirrup 1 adjacent to the support. In addition, strain gauges were placed on the main reinforcement at the load point and the middle of the shear span. An “X” indicates that data from the strain gauge were not measured. For specimen 0-1.5-R the data acquisition channel recording the strains failed.

The stirrup located adjacent to the support had a strain that exceeded the yield strain in both the control and the low level corrosion specimen. The main reinforcement and stirrup 2 did not yield before the specimens failed. Typically, the strain in the main reinforcing steel increased approximately linearly until failure. Figure 4.16 shows this behaviour for specimen L-1.5-R. The strains diverged when the load increased above 65 kN. This divergence can be attributed to the onset of flexural cracking which started to propagate near the load point. The strain in the main reinforcement for specimens M-1.5-R and 0-1.5-R exhibited a similar behaviour compared to what is depicted for specimen L-1.5-R.

Table 4.11 Strain in Reinforcing Steel at Ultimate Load $a/d = 1.5$

Specimen	Shear Reinforcement		Longitudinal Reinforcement	
	Stirrup 1 ($\mu\epsilon$)	Stirrup 2 ($\mu\epsilon$)	Load Point ($\mu\epsilon$)	Middle of Shear Span ($\mu\epsilon$)
0-1.5-UR			1839	1894
0-1.5-R	2503	1682	2218*	X
L-1.5-R	2509	2104	1906	1612
M-1.5-R			1893	X
H(M)-1.5-R			X	X

* Strain reading at onset of failure

The strain in the stirrups does not show as discernable a trend as in the main steel; this behaviour for specimen L-1.5-R is shown in Figure 4.17. The strain in the shear reinforcement began to increase after the specimen cracked. For specimen L-1.5-R, the strains began increasing at 75 kN and 150 kN for stirrups 1 and 2, respectively. This corresponds to the point when the stirrups become effective in restraining crack growth. The strain data shows that the stirrups yielded close to the ultimate stage.

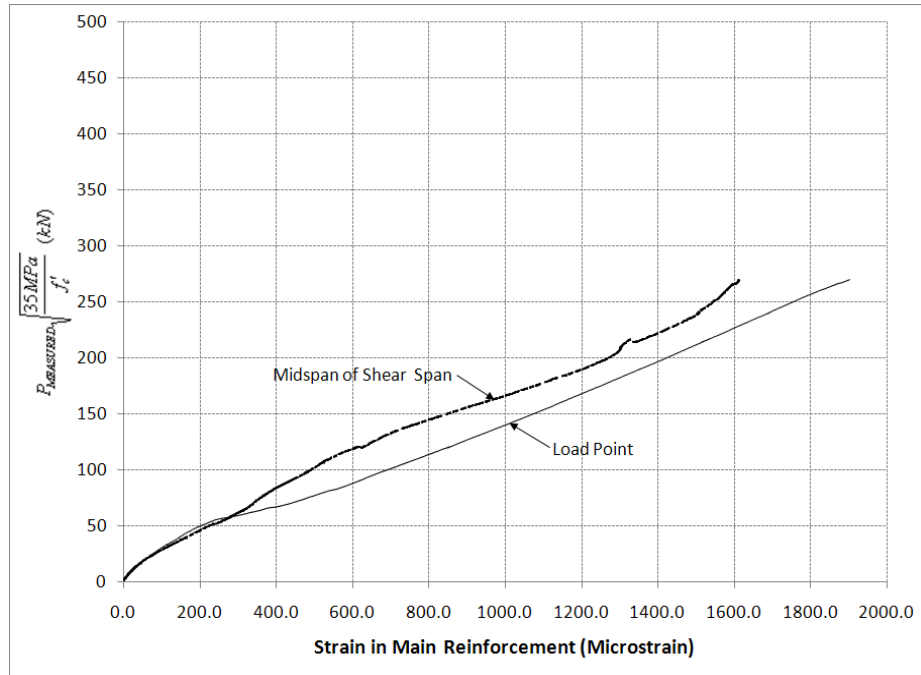


Figure 4.16 Strain Behaviour in the Main Reinforcement Specimen L-1.5-R

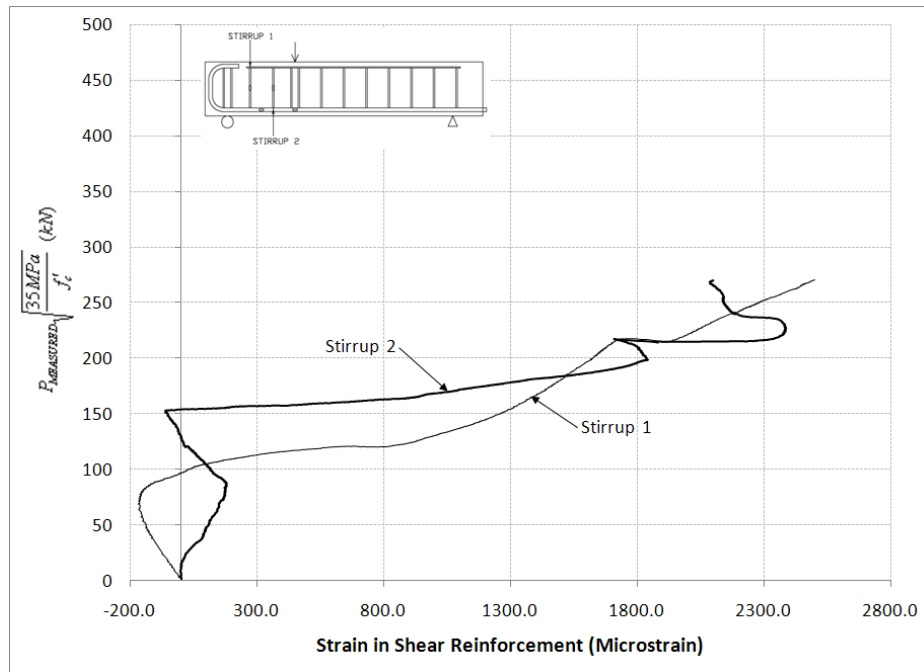


Figure 4.17 Strain Behaviour of the Shear Reinforcement Specimen L-1.5-R

The strain in the stirrups for specimen 0-1.5-R (control) is shown in Figure 4.18. The load-strain response was non-linear from the beginning of the test due to the presence of initial cracks that occurred during the handling of the specimen. Strains at stirrup 1 were consistently higher than those measured at stirrup 2 as shown in Figure 4.18. Stirrup 1 was the only stirrup to exhibit yielding at the ultimate state.

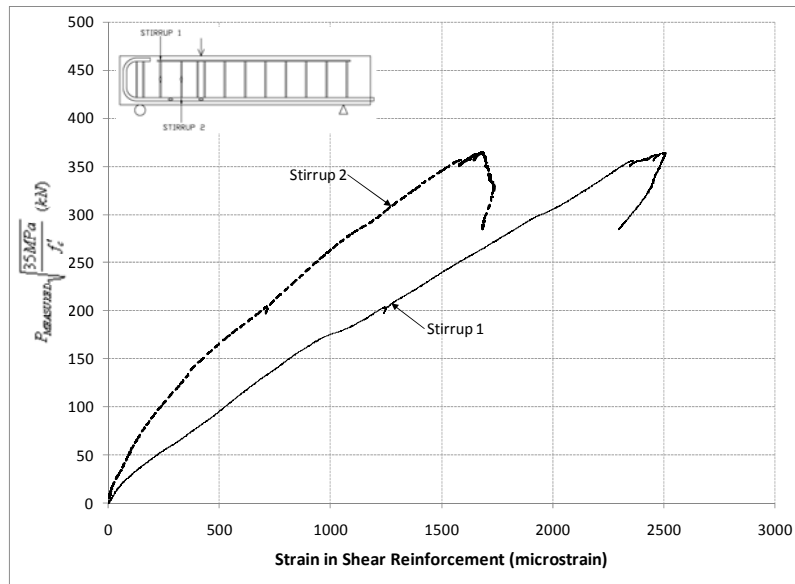


Figure 4.18 Strain Behaviour in the Shear Reinforcement Specimen 0-1.5-R

4.3.3 Experimental Results – $a/d = 2.0$

The specimens in this series of beams were all tested to failure. This series of specimens is closer to the shear-span to depth ratio limit of 2.5 for slender beam behaviour. Figure 4.19 shows the normalized load-deflection behaviour for the specimens in this series.

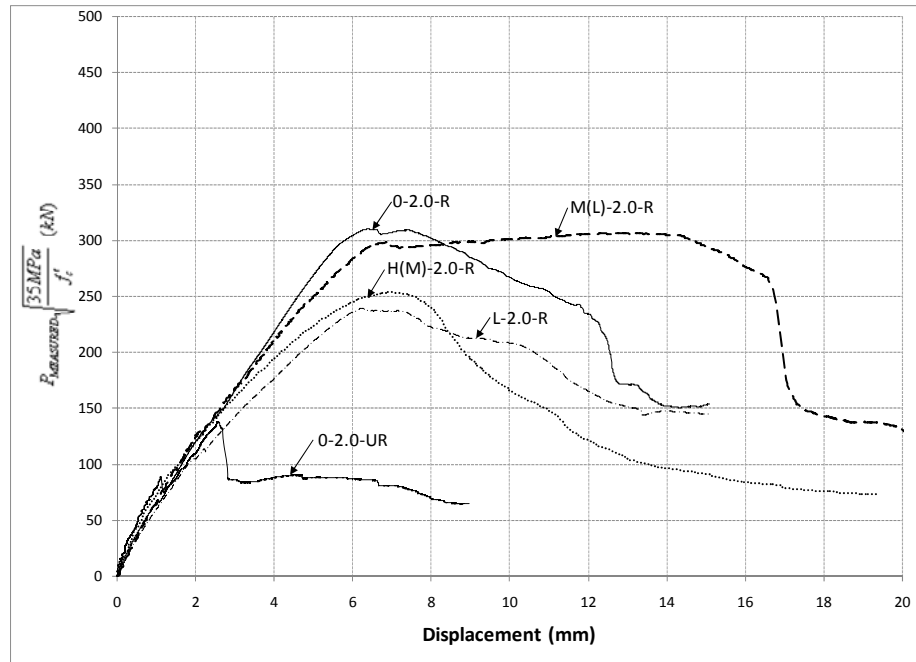


Figure 4.19 Load-Deflection Behaviour $a/d = 2.0$

Table 4.12 presents a summary of the important load-deflection characteristics at cracking and ultimate stages.

Table 4.12 Load-Deflection Behaviour Summary $a/d = 2.0$

Specimen	Measured Load			Normalized Load		Deflection	
	Concrete Strength (MPa)	Diagonal Cracking (kN)	Ultimate (kN)	Diagonal Cracking (kN)	Ultimate (kN)	Diagonal Cracking (kN)	Ultimate (mm)
0-2.0-UR	41.3	95	150	87	138	1.13	2.58
0-2.0-R	41.3	80	337	74	310	1.21	6.42
L-2.0-R	45.4	114	273	100	240	1.82	6.21
M(L)-2.0-R	40.5	144	330	134	307	2.26	12.79
H(M)-2.0-R	43	158	282	143	254	2.57	7.01

4.3.3.1 Cracking Load

Table 4.12 presents the cracking loads for the specimens in this series. The diagonal cracking load for specimen 0-2.0-R is based on the observed crack formation on the side of the specimen without

the displacement transducer; the corresponding cracking load is significantly less than what would correspond to 0.1 mm of measured diagonal deformation. The shear cracking loads for the corroded specimens are all higher than the control specimen. This behaviour is similar to what is observed for specimens with a shear-span to depth ratio of 1.5. Specimens with shear-span to depth ratios of 1.5 and 2.0 have 2 and 3 corroded stirrups within the shear-span. More stirrups within the shear span results in more cracking.

4.3.3.2 Stiffness and Ductility

Table 4.13 presents the pre-diagonal cracking and post-diagonal cracking stiffness of the specimens. The difference in stiffness between the corroded specimens and the control before diagonal cracking is negligible. The un-reinforced specimen exhibits the stiffest response before diagonal crack propagation. There is stiffness degradation evident in the corroded specimens compared to the control specimen after diagonal cracking occurs. The average stiffness degradation for the corroded specimens is 35%. Specimen 0-2.0-UR experienced a very sudden reduction in stiffness after the onset of diagonal cracking with a stiffness degradation of 49%.

Table 4.13 Stiffness a/d = 2.0

Specimen	Pre-Diagonal Cracking	Post-Diagonal Cracking	Stiffness Degradation
	Stiffness (kN/mm) K_1	Stiffness (kN/mm) K_2	$\frac{K_1 - K_2}{K_1}$
0-2.0-UR	69	35	49%
0-2.0-R	56	51	8%
L-2.0-R	53	34	36%
M(L)-2.0-R	58	41	30%
H(M)-2.0-R	53	33	38%

4.3.3.3 Ultimate Shear Strength

The strength reductions evident in the corrosion and un-reinforced specimens with respect to the control specimen are presented in Table 4.14. Equation 4.4 was to calculate the shear strength of the specimens using statics and the normalized load.

$$V = \frac{900 \text{ mm}}{1500 \text{ mm}} P_{NORM} \quad \text{Equation 4.4}$$

V = Ultimate Shear Force (kN)

P_{NORM} = Ultimate Normalized Load (kN)

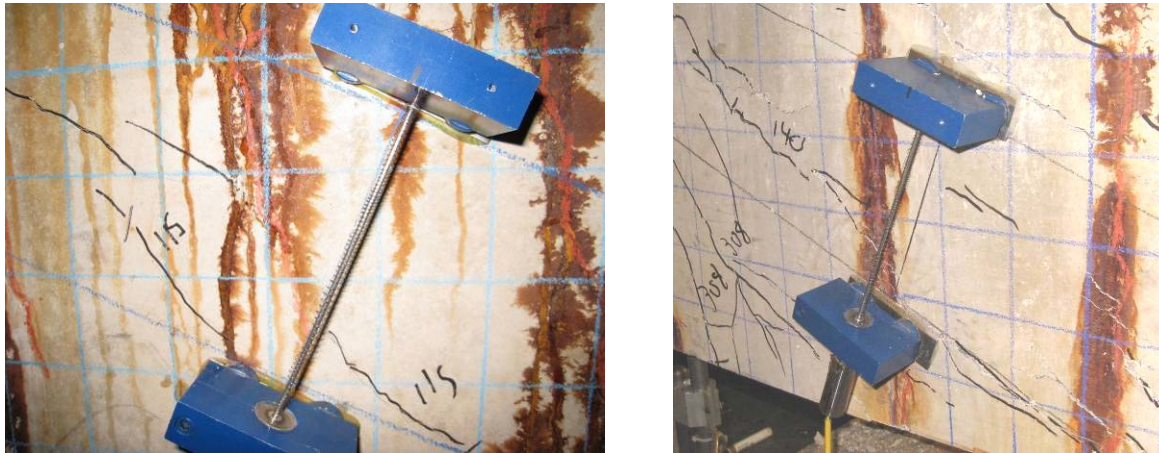
Table 4.14 Strength Reduction $a/d = 2.0$

Specimen	Average Mass Loss (%)	Normalized Shear Strength (kN)	Percentage Difference
0-2.0-UR	--	83	56%
0-2.0-R	--	186	--
L-2.0-R	2.5%	144	23%
M(L)-2.0-R	2.9%	184	1%
H(M)-2.0-R	10.7%	153	18%

The un-reinforced specimen had a strength reduction of 56% compared to the control specimen. This reduction is significantly larger than the strength reductions from specimens 0-1.0-UR (9% strength reduction) and 0-1.5-UR (11% strength reduction). Disturbed regions resist shear by a combination of arch and beam action, but the primary shear resisting mechanism is arch action. The beam action becomes more prevalent in specimens with larger shear-span to depth ratios. Shear reinforcement is required for beam action to develop. Consequently, since no shear reinforcement was provide in specimen 0-2.0-UR and the shear-span to depth ratio is larger than in specimens 0-1.0-UR and 0-1.5-UR it is expected that the percentage difference would be larger.

Specimen L-2.0-R had a strength reduction of 23%; whereas, specimen M(L)-2.0-R had a minimal strength reduction. Specimens L-2.0-R and M(L)-2.0-R had similar average crack widths of 0.3 mm and 0.35 mm, respectively. The average mass loss that was measured for these specimens was 2.5% for L-2.0-R and 2.9% for L(M)-2.0-R. These average crack width and average mass loss are indicators of the degree of corrosion, so it was expected that the strength reduction in these specimens would be similar. This was not the case possibly because the shear reinforcement in specimen L-2.0-R shifted during the casting procedure such that it was more closely aligned with the diagonal compressive strut. There are two reasons this could cause a more significant strength reduction. Firstly, the diagonal shear reinforcement would not be as effective in supporting the tensile stress and restraining crack growth. This is evident by the fact that the load-deflection behaviour for specimen M(L)-2.0-R is more ductile than for specimen L-2.0-R. The second reason for this strength reduction is because the corrosion cracks that formed in specimen L-2.0-R were aligned more closely with the compressive strut. This crack formation would weaken the compressive strut. Figure 4.20 shows the

load induced cracks in specimen L-2.0-R aligning with the corrosion cracks. This is important because it shows that the diagonal corrosion cracks influence the compressive load paths.



Specimen L-2.0-R

M(L)-2.0-R

Figure 4.20 Crack Pattern in Specimens L-2.0-R and M(L)-2.0-R

4.3.3.4 Crack Patterns and Modes of Failure

The first cracks that were apparent in this series of beams were flexure cracks in the long span of the specimens. Similar to the other specimens, the flexure cracks were spaced at approximately 150 mm. The propagation of the flexure cracks was minor in comparison to the diagonal cracks which propagated throughout the depth of the beam. The diagonal cracks are indicative of disturbed regions; the long span in this series of specimens is composed almost entirely of disturbed regions. The diagonal cracks typically formed after the formation of diagonal shear cracks in the shear span of the beam.

In the corroded specimens, the crack propagation was similar to the observed behaviour in the other specimen series. The load induced cracks were initially interrupted at the vertical corrosion cracks and then began to propagate through the vertical cracks. If the corrosion crack was diagonal (from misalignment of the shear reinforcement) then the load induced cracks followed the alignment of the corrosion cracks.

Diagonal splitting, shear-compression, and diagonal crushing were the observed failure modes for the specimens in this series. Photos of the failed specimens are presented in Figure 4.22. The failure of specimen 0-2.0-UR was a sudden un-restrained growth in the size of the main diagonal crack.

Specimens 0-2.0-R, L-2.0-R, M(L)-2.0-R, and H(M)-2.0-R failed in shear-compression. Evidence of the shear-compression failure is provided by the horizontal cracks that formed in the compression zone of the shear-span. A similar horizontal crack in the compression zone was not as evident in specimen H(M)-2.0-R because the failure mode is diagonal crushing.

4.3.3.5 Diagonal Displacement

Figure 4.21 shows the diagonal deformation of the specimens with respect to the normalized load. The overall diagonal deformation response shows that the corroded specimens are not as stiff as the control (0-2.0-R) specimen. The plot shows that specimen H(M)-2.0-R has a stiffer response than specimen M(L)-2.0-R in some instances. This can be attributed to the fact that specimen H(M)-2.0-R had many corrosion induced cracks and there were significant areas of delaminated concrete. This type of deterioration prevents compressive stresses from being transferred to the support exclusively through the assumed strut. The compressive stresses must take alternative load paths which would not be captured by the displacement transducer; hence, the overall stiffer response. Secondly, the surface delamination would prevent cracking from being visible on the surface. The consequence of this is that the displacement transducer would not be able to measure the crack growth. Specimen 0-2.0-UR shows a sudden crack growth of approximately 0.25 mm. This is the nature of a shear failure in a specimen where shear reinforcement has not been provided.

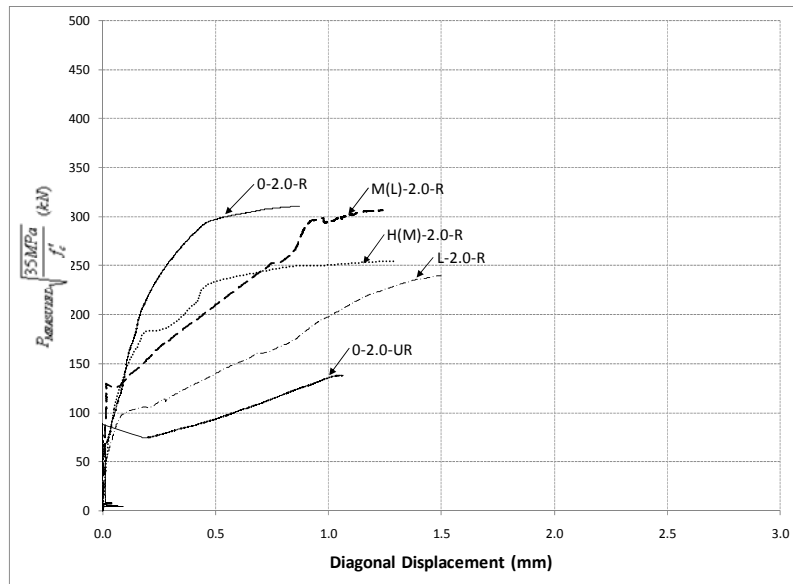
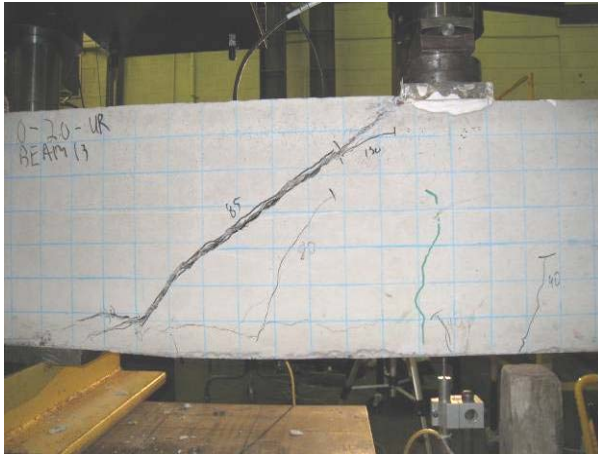
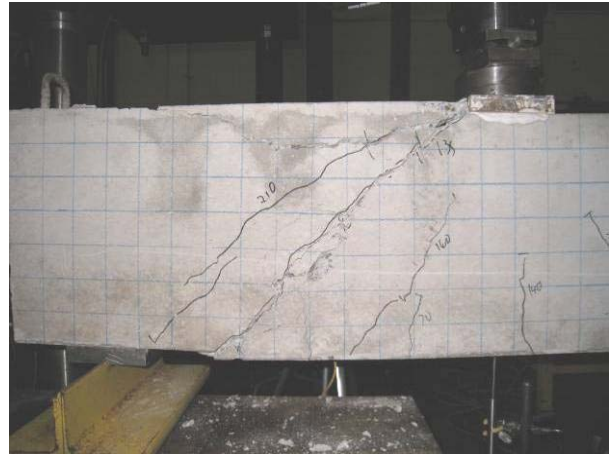


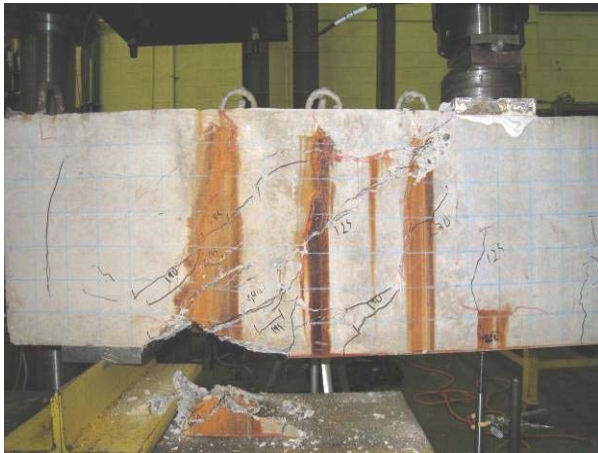
Figure 4.21 Diagonal Displacement $a/d = 2.0$



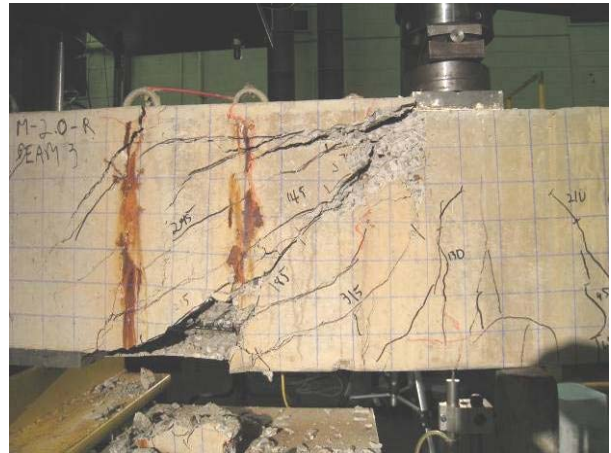
O-2.0-UR (Diagonal Splitting)



O-2.0-R (Shear Compression)



L-2.0-R (Shear Compression)



M(L)- 2.0-R (Shear Compression)



H(M)- 2.0-R (Diagonal Crushing)

Figure 4.22 Failure Crack Patterns $a/d = 2.0$

4.3.3.6 Reinforcing Steel Strain Behaviour

The strains in the reinforcing steel at the ultimate stage are provided in Table 4.15. Figure 4.23 shows the behaviour of the shear reinforcement for specimen 0-2.0-R. In specimen 0-2.0-R, the strain in stirrups 2 (middle of shear span) and 3 (adjacent to load point) began to increase at an applied load of 30 kN, and strain in stirrup 1 (adjacent to support) started to increase at 75 kN. The largest strain value at ultimate load corresponded to stirrup 2; this stirrup was located in the middle of the shear span. The strain behaviour in the shear reinforcement provided in specimen L-2.0-R was significantly different. The strain in the stirrups in specimen L-2.0-R began to increase at a total applied load of 110 kN, and the strain at the ultimate load were both very similar at 1180 Microstrain. The stirrups in specimen L-2.0-R shifted during the casting process thus causing the stirrups to be less effective in resisting the crack growth; this would account for the increased load when the stirrups became effective (110 kN) and the lower strain at ultimate load.

Table 4.15 Strain in Reinforcing Steel at Ultimate Load $a/d = 2.0$

Specimen	Shear Reinforcement			Longitudinal Reinforcement	
	Stirrup 1 ($\mu\epsilon$)	Stirrup 2 ($\mu\epsilon$)	Stirrup 3 ($\mu\epsilon$)	Load Point ($\mu\epsilon$)	Middle of Shear Span ($\mu\epsilon$)
0-2.0-UR				889	1089
0-2.0-R	1997	3030*	1280	3142	2245
L-2.0-R	1180	1173	X	X	1800
M(L)-2.0-R				3129†	X
H(M)-2.0-R				X	1484

* Strain reading at onset of failure

† Strain gauge failed before failure

The strain in the main reinforcing steel was measured at the load point and the middle of the shear span. In specimen 0-2.0-R, the strain gauges indicated that the reinforcing steel yielded at the ultimate stage. Whereas, in the corroded specimens the strain measurements indicate that the steel did not yield at the ultimate stage owing to the fact that the corroded specimens were weaker than the control specimen. Plots of the strain behaviour of the main reinforcement are provided in Appendix D.

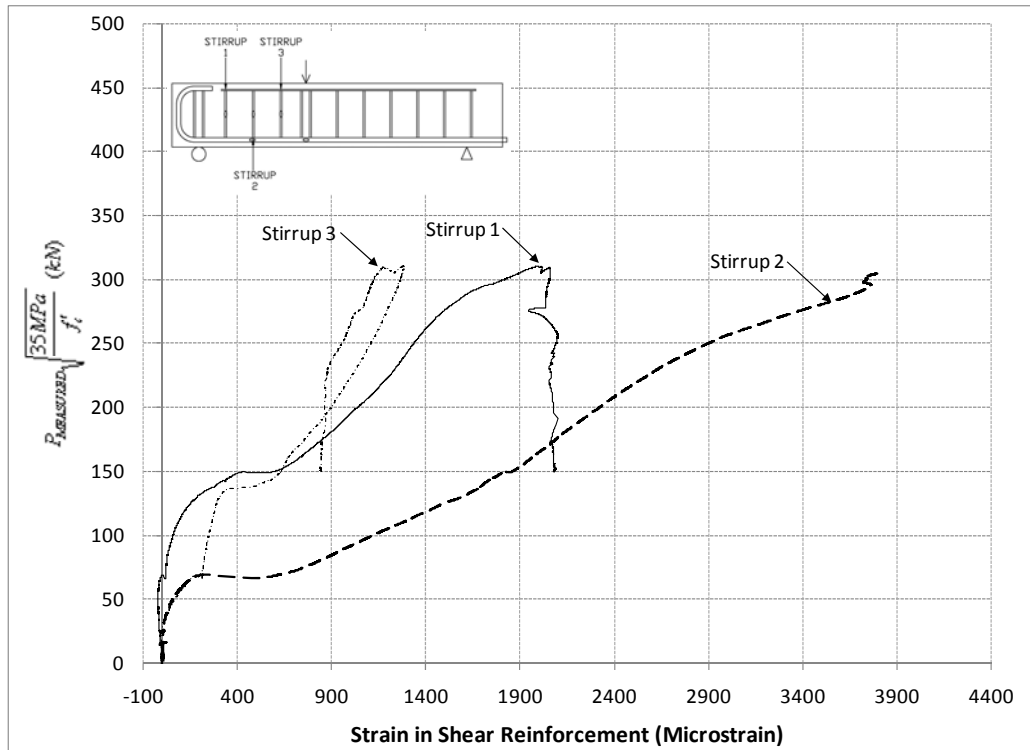


Figure 4.23 Strain in Shear Reinforcement Specimen 0-2.0-R

4.4 Feasibility of CFRP Repair

Specimen H(M)-1.5-Repair was strengthened using a CFRP dry lay-up technique (Section 3.7). This section will evaluate the feasibility of utilizing a CFRP strengthening system to repair disturbed regions with corrosion damaged shear reinforcement. The average corrosion crack width was 0.45 mm and the average mass loss was 8.1%. Corrosion crack width is an important factor in the behaviour of the specimens with corrosion damaged shear reinforcement. An average crack width of 0.45 mm is similar to the measured average crack width for medium level corrosion of 0.40 mm. Consequently, a comparison between the specimens M-1.5-R and H(M)-1.5-Repair is carried out in the following section.

Figure 4.24 presents the load-deflection of specimen H(M)-1.5-Repair along with the other specimens with a shear-span to depth ratio of 1.5. The stiffness response before failure is bi-linear. The first portion of the response corresponds to the point when the flexural cracks became apparent. It is evident that the strengthened specimen exhibits a much stiffer response compared to the other corroded specimens. The normalized ultimate load was 314 kN and the normalized shear strength

was 220 kN. This corresponds to a strength improvement 20 kN or 16% with respect to the shear strength of specimen M-1.5-R.

The cracking pattern in specimen H(M)-1.5-Repair was similar to specimen M-1.5-R. The observed normalized diagonal shear cracking load was 194 kN. The CFRP system prevents the entire diagonal crack pattern from being visible; consequently, the estimate of diagonal shear cracking is based on a diagonal deformation of 0.1 mm. The most impressive improvement in specimen H(M)-1.5-Repair was the diagonal shear cracking load of 194 kN compared to a diagonal cracking load for specimen M-1.5-R of 78kN.

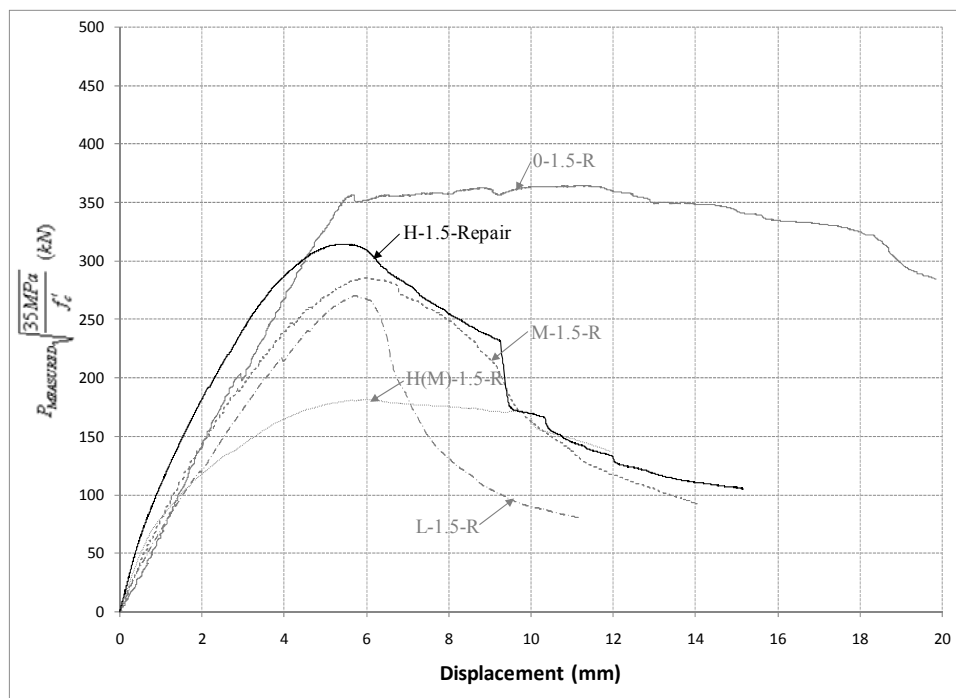


Figure 4.24 Load-Deflection Behaviour of H-1.5-Repair

The failure mode of specimen H(M)-1.5-Repair is difficult to determine due to the presence of the CFRP wrapping. However, the crushing in the compression zone makes it plausible to expect the mode of failure to be shear compression. This crushing in the compression zone was confirmed during the removal of the shear reinforcement for mass loss analysis. The sequence of events that preceded this failure were: minor flexural cracking, diagonal crack formation in the long span, diagonal crack formation in the shear span, vertical cracks at the anchorage, rupture of the CFRP at the anchorage, and horizontal cracks in the compression zone. Figure 4.25 provides a view of the

final cracking pattern. The most significant drop in load shown in Figure 4.24 for specimen H-1.5- Repair corresponds to the rupture of the CFRP.

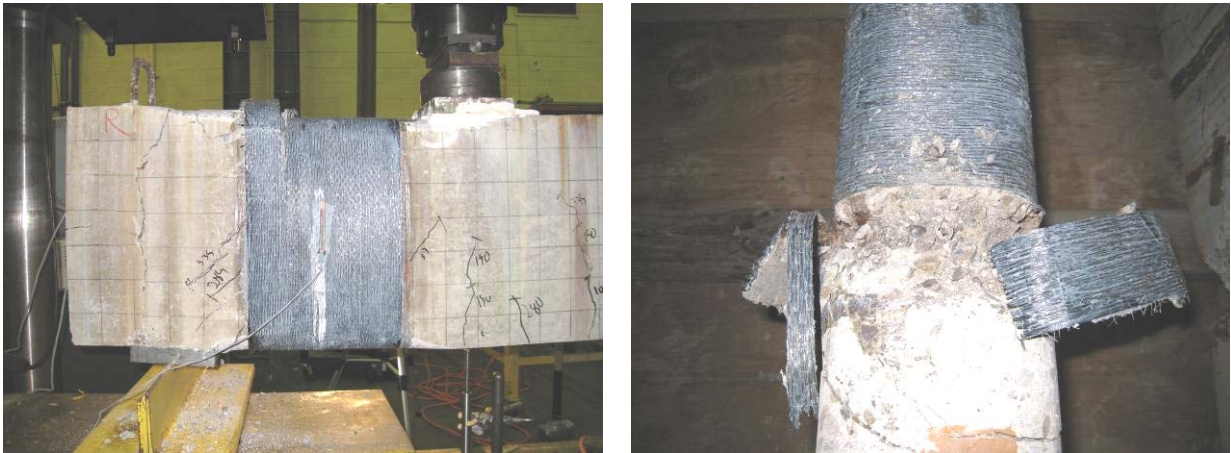


Figure 4.25 Crack Pattern at Failure and Crushing under CFRP Specimen H-1.5-Repair

The transverse strain in the CFRP was measured utilizing a strain gauge with a 60 mm gauge length. Figure 4.26 shows the strain behaviour of the CFRP. The CFRP began to resist significant strains when diagonal cracks became apparent in the shear span; the total applied load at this point was 215 kN. The strain at failure was approximately 2000 microstrain, and the strain at the point when the CFRP ruptured was 3265 microstrain or 0.33%. The ultimate strain for the CFRP sheets is 1.09%. The CFRP ruptured after the specimen reached its ultimate load, so it can be concluded that the CFRP was fully effective at confining the section. Figure 4.27 shows the strain behaviour of the longitudinal reinforcement. The maximum strain in the reinforcing steel at the load point was 2545 Microstrain.

The results indicate that repairing disturbed regions in reinforced concrete beams with corrosion damaged shear reinforcement utilizing a CFRP dry lay-up technique is feasible. The improvement in diagonal cracking load was significant at 2.5 times higher than the companion specimen. The ultimate strength improvement was 16% over the companion specimen with a similar corrosion level. To put this in perspective, the ISIS Canada Design Manual (2008) gives the shear strength contribution of the CFRP to be 90 kN; this is based on the formulation for slender beams. The manual does not provide recommendations for the shear strength from CFRP in disturbed regions, so this calculation can be considered an approximation. The strain value used in the calculation was 4000 microstrain which is significantly larger than the strain measured in the CFRP (2545

microstrain) at the ultimate stage. The most impressive improvement was in the stiffness of the repaired specimen. More research is required prior to making conclusive recommendations on using this system.

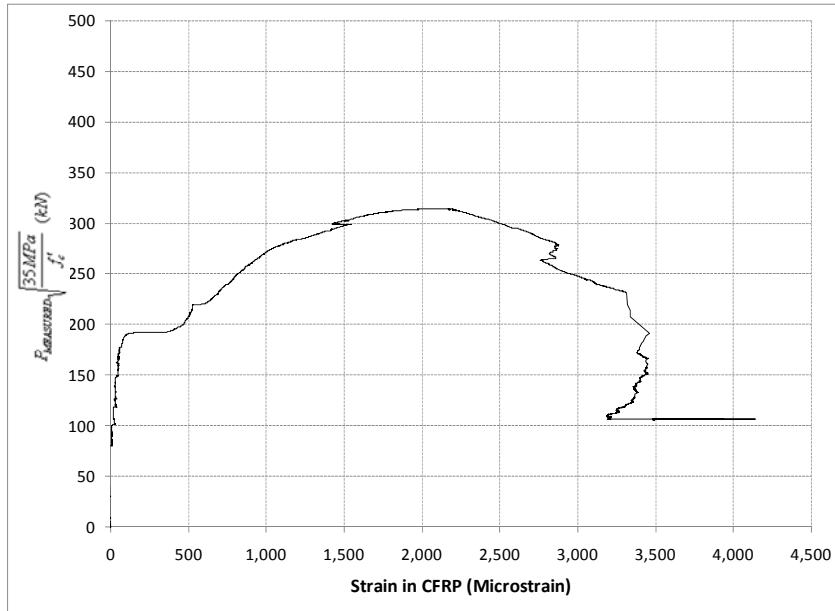


Figure 4.26 Strain Behaviour of CFRP

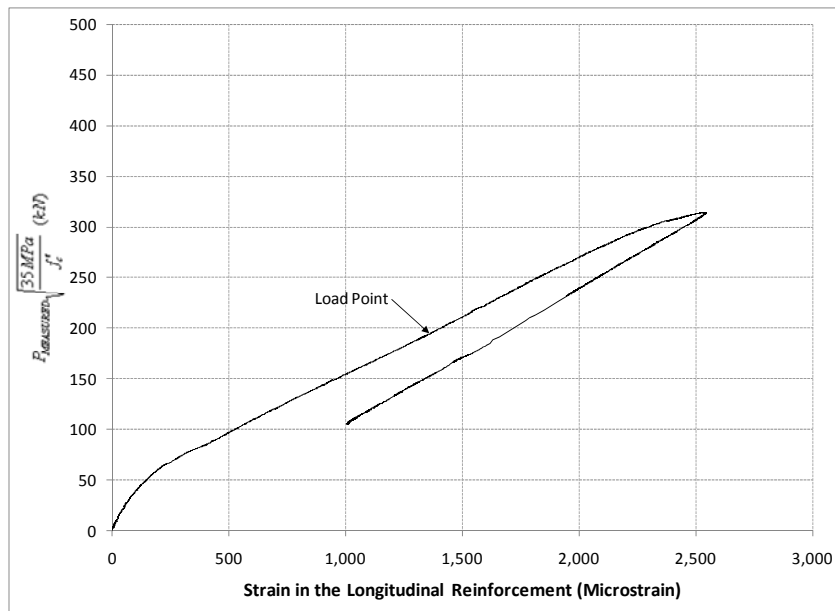


Figure 4.27 Strain Behaviour of the Reinforcing Steel Specimen H-1.5-Repair

4.5 Summary

The focus of this work is on the effect of the degree of corrosion and shear-span to depth ratio on the shear behaviour of disturbed regions in reinforced concrete beams. This section provides overall comparisons with respect to the parameters investigated. Diagonal cracking load, shear strength, deflection at failure, and stiffness were assessed with respect to the study parameters.

4.5.1 Un-corroded Specimens

4.5.1.1 Diagonal Cracking Load

Figure 4.28 presents the diagonal cracking data for the un-corroded control (with shear reinforcement) and un-reinforced specimens. It is clear that the control specimens (0-1.0-R, 0-1.5-R, and 0-2.0-R) formed diagonal cracks at lower loads than the companion un-reinforced specimens. The control specimens initially formed cracks that were shorter compared to the un-reinforced specimens. The diagonal cracks that were formed in the un-reinforced specimen propagated suddenly over the entire depth of the section.

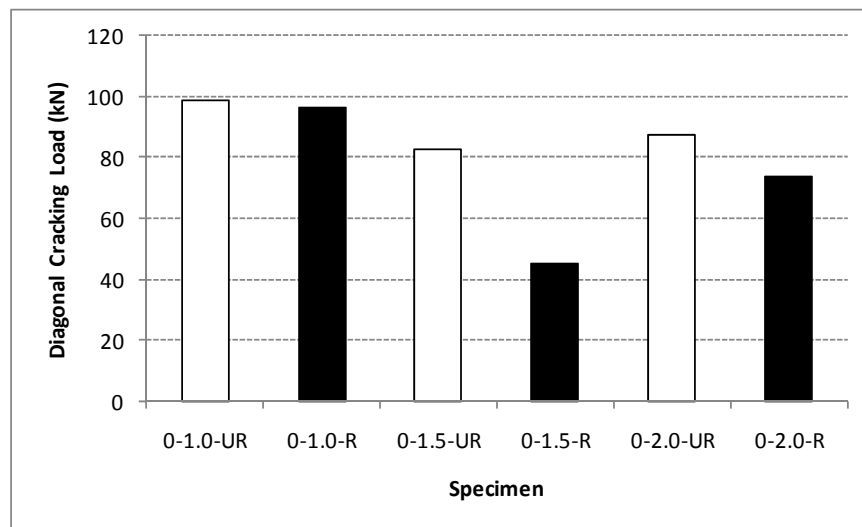


Figure 4.28 Diagonal Cracking Load for Control and Un-reinforced Specimens

4.5.1.2 Ultimate Shear Strength

Figure 4.29 shows the ultimate shear strength of the control and un-reinforced specimens. The control (reinforced specimens) failed at higher ultimate loads than the un-reinforced specimens. This

difference in ultimate load is indicative of the effect of shear reinforcement. This increase in shear strength is most pronounced in specimen 0-2.0-R because the relative contribution of beam action is more pronounced in specimens with higher shear-span to depth ratios. The development of beam action is dependant on the provision of shear reinforcement.

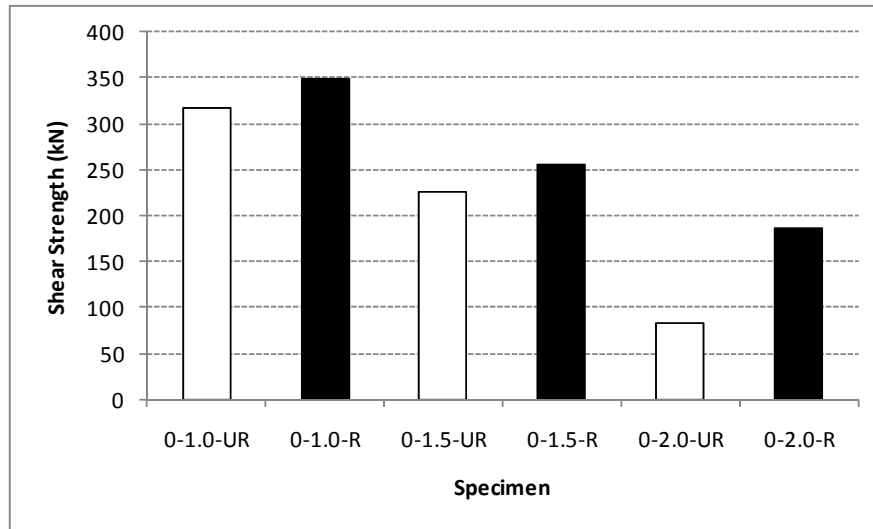


Figure 4.29 Ultimate Shear Strength of Control and Un-reinforced Specimens

4.5.1.3 Deflection at Failure

Figure 4.30 shows the deflection at failure for the control and un-reinforced specimens. The deflection at failure for specimens 0-1.0-UR, 0-1.0-R, and 0-1.5-UR is similar. Specimen 0-1.5-R experienced a much larger deflection at failure because it failed in a ductile flexural mode. The deflection at failure for specimen 0-2.0-UR is the lowest compared to the other specimens due to the fact that it failed at a low ultimate load.

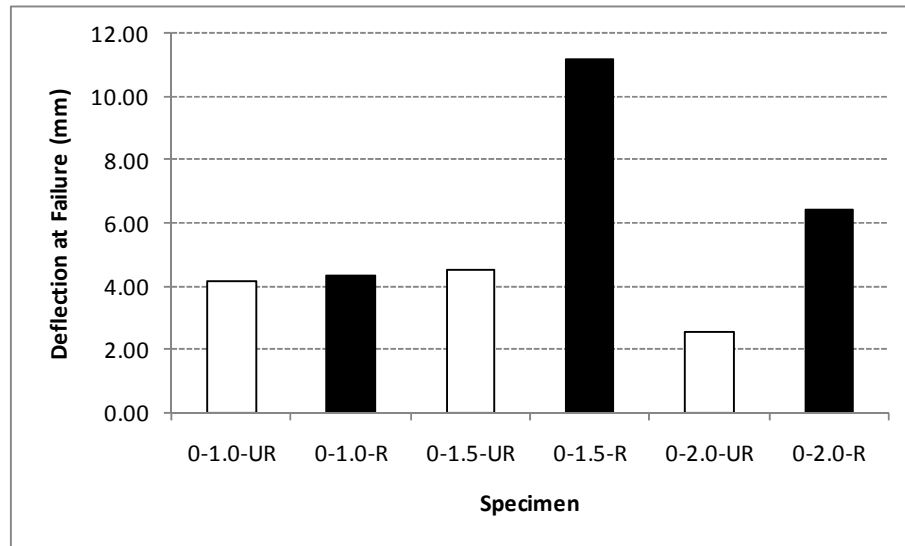


Figure 4.30 Deflection at Failure of Control and Un-reinforced Specimens

4.5.2 Corroded Specimens

The following section summarizes the effects of corrosion of shear reinforcement with respect to the parameters that were studied. The control and un-reinforced specimens are also considered for comparison.

4.5.2.1 Diagonal Cracking Load

Figure 4.31 shows the effect of degree of corrosion on the normalized diagonal cracking load. The effects of corrosion have been expressed in two ways: percentage mass loss in the shear reinforcement and average corrosion crack width. It is evident that there is no distinct trend between the diagonal cracking load and corrosion mass loss or crack widths. Specimens with a shear-span to depth ratio of 1.0 formed diagonal cracks at lower loads compared to the other series of specimens. This trend is also evident for specimens with a shear-span to depth ratio of 2.0 which formed cracks at the highest loads. This is a logical trend because the shear force in the specimens with a shear-span to depth ratio of 2.0 is comparatively less than the other specimens at the same load level. This means that higher overall loads would be required to reach the tensile strength of the concrete and cause cracking.

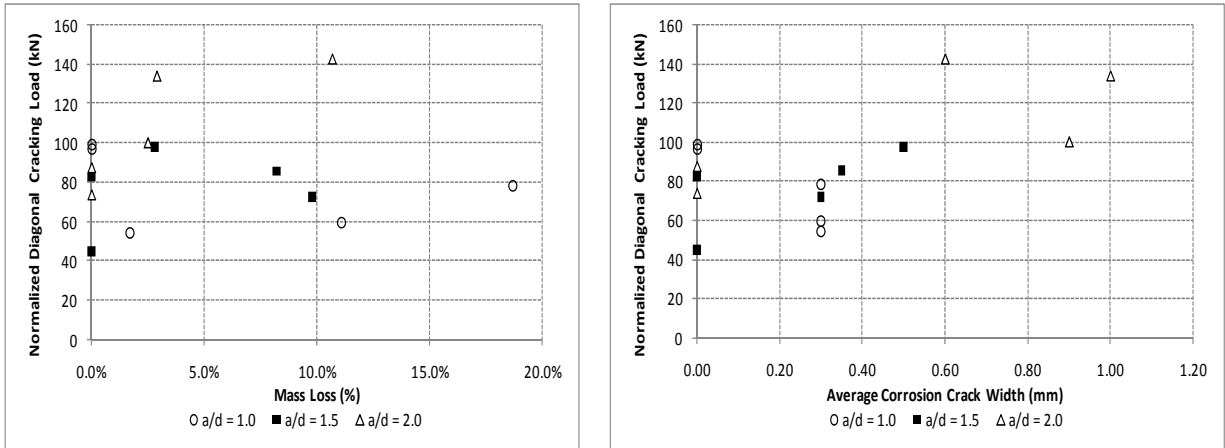


Figure 4.31 Diagonal Cracking Load versus Degree of Corrosion

Figure 4.32 illustrates the relationship between normalized diagonal cracking load and shear-span to depth ratio. The diagonal cracking loads for the corroded specimens are less than the control for the series with a shear-span to depth ratio of 1.0. Conversely, the diagonal cracking loads for the corroded specimens are higher for the series with shear-span to depth ratios of 1.5 and 2.0. This can be explained by the difference in corrosion cracking these series. The specimens with shear-span to depth ratios of 1.5 and 2.0 have 2 and 3 stirrups within the shear span. Consequently, more vertical corrosion induced cracks are present in these specimens; this allows the load induced cracks to follow the same path as the corrosion induced cracks. This means that the specimens would support larger loads before the diagonal cracks become apparent.

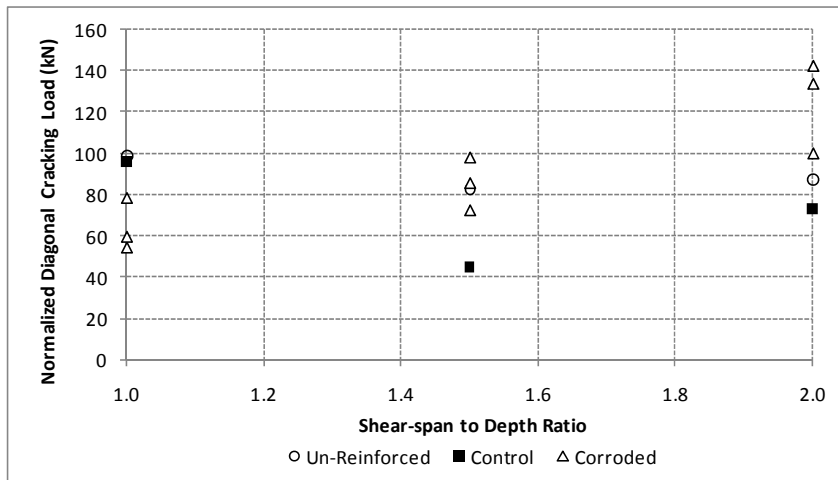


Figure 4.32 Diagonal Cracking Load versus Shear-span to Depth Ratio

4.5.2.2 Ultimate Shear Strength

Figure 4.33 shows a comparison of the shear strength of the specimens with degree of corrosion. In general, the ultimate shear strength drops as degree of corrosion (mass loss, crack width) increases.

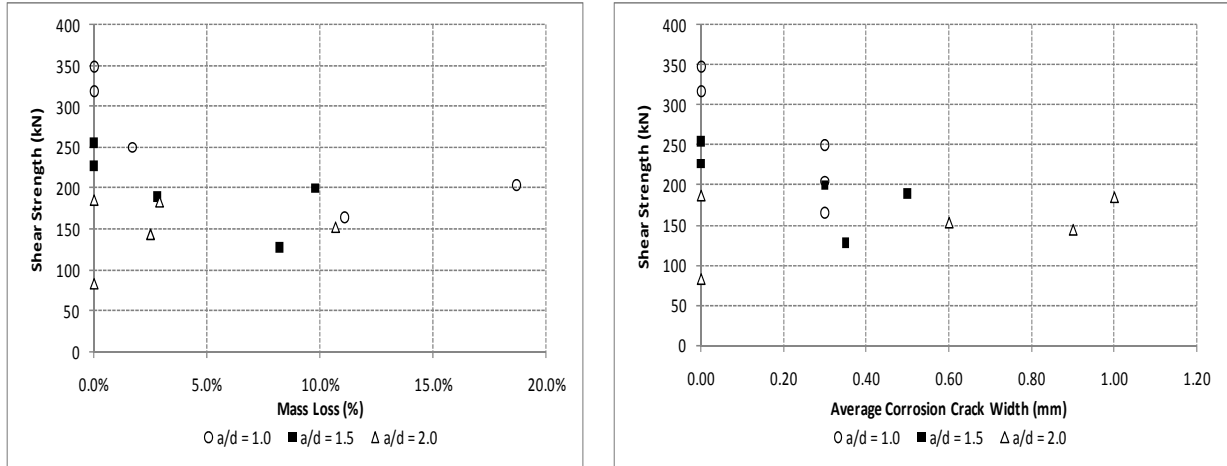


Figure 4.33 Shear Strength Vs. Degree of Corrosion

Figure 4.34 shows the relationship between shear strength and shear-span to depth ratio. It is obvious that the shear strength of the specimens decreases with respect to shear-span ratio. This relationship has been well documented for disturbed regions. It is also evident that the corroded specimens were not as strong as the control specimens. The variation in the shear strength of the specimens that were corroded is less in the specimens with a shear-span to depth ratio of 2.0 compared to the other corroded specimens. This could be attributed to the ability of the specimen with a shear-span to depth ratio of 2.0 to redistribute forces into the long span due to the fact that the load transfer mechanisms in both the shear-span and long span are similar. Both spans are composed of disturbed regions; whereas, in the specimens with smaller shear-span to depth ratios a portion of the long span could be considered slender.

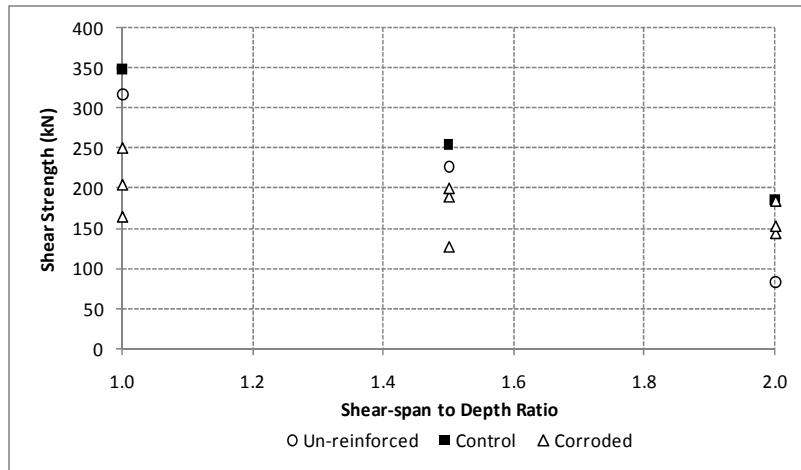


Figure 4.34 Shear Strength Vs. Shear-span to Depth Ratio

4.5.2.3 Deflection at Failure

Figure 4.35 shows the deflection at failure plotted against degree of corrosion. The deflection at failure remained relatively constant at approximately 6 mm for most corroded specimens. Specimen M(L)-2.0-R had the highest deflection at failure of 12.8 mm. There was significant ductility in this specimen which was not observed in the other specimens in this series. The load-deflection response for this specimen reached the ultimate stage at a similar deflection (6 mm) as the other specimens. Specimens M-1.0-R and H-1.0-R had deflections at failure that were comparatively less than the other corroded specimens. These specimens had a stiffer response compared to the other corroded specimens. The corroded specimens with a shear-span to depth ratio of 1.0 had a stiffness that was 1.7 and 2.1 times more than specimens with shear-span to depth ratios of 1.5 and 2.0.

Figure 4.36 shows a comparison of deflection at failure with shear-span to depth ratio. It is evident that the deflection at failure increases with shear-span to depth ratio. Specimen 0-2.0-UR is contradictory to this trend, but it failed in a sudden manner due to the fact that shear reinforcement was not provided in this specimen. Specimen 0-1.5-R had a higher deflection compared to the other specimens because it failed in a flexural failure mode which is ductile. As noted above, specimen M(L)-2.0-R failed in a more ductile failure mode which caused the deflection at failure to be higher than the other specimens.

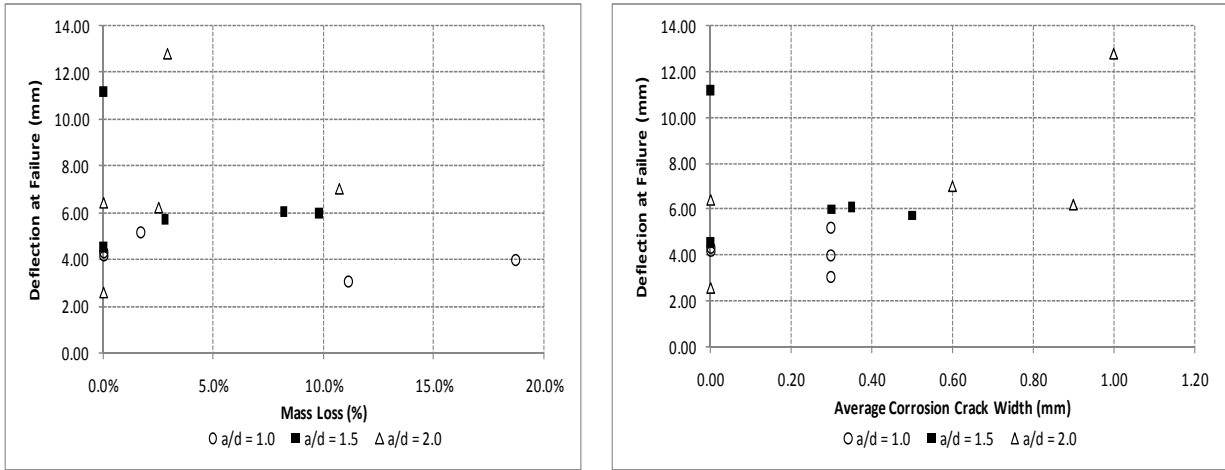


Figure 4.35 Deflection at Failure Vs. Degree of Corrosion

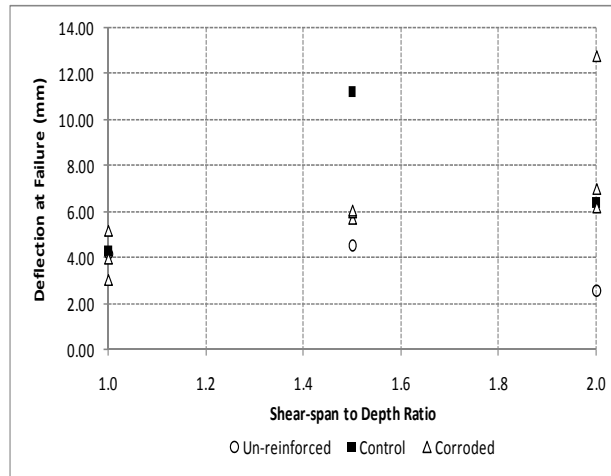


Figure 4.36 Deflection at Failure Vs. Shear-span to Depth Ratio

Chapter 5

Strut and Tie Modeling

5.1 Introduction

Strut and tie models are used to design disturbed regions which encompass the depth of the element along the axis of the member from a concentrated load, change in member cross section, or support. Deep beams are typically defined as beams with a shear span less than 2 times the height of the beam or a beam with a clear span that is less than 4 times the height of the beam (ACI Committee 318, 2005). Deep beams are entirely composed of disturbed regions; slender beams, on the other hand, contain both disturbed and Bernoulli regions. The strain distribution in disturbed regions is non-linear; thus, plane sections will not remain plane under bending. The assumption of plane sections remaining plane can be applied to Bernoulli regions.

Strut and tie models can be used to represent the physical system of forces within a deep beam. The stresses that are imposed on the boundary of a disturbed region must be supported by a truss system. This truss consists of concrete compression struts, steel tension ties, and confined nodal regions (joints). The strength of these components are defined by code imposed limits for design purposes.

This chapter will provide details about the strut and tie approach that will be used to investigate the strength of the beams from the experimental program (Chapter 3). The effects of corrosion of shear reinforcement will be incorporated into the proposed strut and tie models in Chapter 6.

5.2 Design Codes

A review of strut and tie model provisions provided in Canadian, American, and European codes is provided in this section. The strength provisions in various reinforced concrete codes for strut and tie models are similar in nature; however, the major difference is in how the strength of the compressive struts is calculated.

5.2.1 CSA A23.3-04

The CSA code specifies that the area of a compressive strut is determined from both the available concrete area (struts can not overlap) and the anchorage conditions at the end of struts. The concrete

compressive strength (Equation 5.1) is limited based on the tensile strain perpendicular to the compression strut:

$$f_{cu} = \frac{f'_c}{0.8 + 170\varepsilon_1} \leq 0.85f'_c \quad \text{Equation 5.1}$$

f_{cu} = Compressive strength of strut

f'_c = Concrete compressive strength

ε_1 = Tensile strain perpendicular

The tensile strain perpendicular to the strut can be calculated based on the following transformation (Equation 5.2). The tensile strain in the adjoining tie is typically assumed to be the yield strain of the reinforcing steel because the reinforcing steel tension tie would be designed to be at or near the yield stress.

$$\varepsilon_1 = \varepsilon_s + (\varepsilon_s + 0.002) \cot^2 \theta_s \quad \text{Equation 5.2}$$

θ_s = The smallest angle between the strut and adjoining tie

ε_s = Tensile strain in adjoining tie

The relationships outlined above can be graphically shown as function of the crushing strength of a compressive strut and the angle between the strut and the adjoining tie (Figure 5.1).

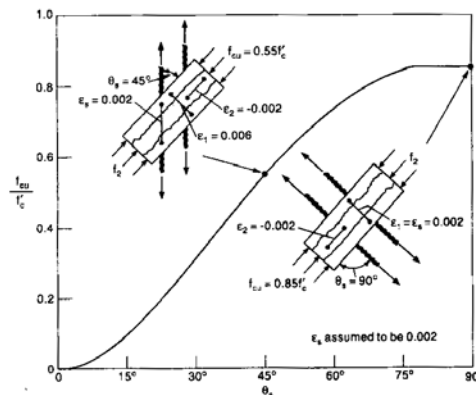


Figure 5.1 Crushing Strength of Concrete Strut (CSA A23.3-04, 2006)

The strength of the reinforcing steel ties is determined based on the area of reinforcing steel and the yield strength of the reinforcing steel. The strength of the nodal regions is determined based on stress conditions; the code provides the following limits:

- (a) $0.85\phi_s f'_c$ in node regions bounded by struts and bearing areas;
- (b) $0.75\phi_s f'_c$ in node regions anchoring a tie in only one direction; and
- (c) $0.65\phi_s f'_c$ in node regions anchoring ties in more than one direction.

5.2.2 ACI 318-05

The ACI code specifies that the width of the strut is the smallest dimension perpendicular to the axis of the strut, w_s , and the thickness of the strut is the thickness of the member, b . The width of the strut (w_s) is determined based on the dimensions of the bearing plates and the depth of the nodes. The area of the strut (Equation 5.3) is calculated as follows:

$$A_{cs} = w_s b \quad \text{Equation 5.3}$$

The effective compressive strength (Equation 5.4) of the strut is defined as follows:

$$f_{ce} = 0.85 \beta_s f'_c \quad \text{Equation 5.4}$$

f'_c = Compressive strength of the concrete

$\beta_s = 1.0$ for a strut of uniform cross-sectional area over its length

= 0.75 for bottle shaped struts with reinforcement satisfying code requirements

= 0.60λ for bottle shaped struts without reinforcement satisfying code requirements ($\lambda = 1.0$ for normal weight concrete, 0.85 for sand-light weight concrete, and 0.75 for light weight concrete)

= 0.40 for struts in tension members, or the tension flanges of members

= 0.60 for all other cases

The reinforcement requirements for bottle shaped struts are:

$$\sum \frac{A_{si}}{b_s s_i} \sin \alpha_i \geq 0.003 \quad \text{Equation 5.5}$$

A_{si} = Total area of surface reinforcement

b_s = Width of the section

s_i = i-th layer of reinforcement (eg. horizontal or vertical)

α_i = Angle between i-th layer and strut

The strength of a tie (F_{nt}) is based on the amount and strength of the reinforcement (Equation 5.6):

$$F_{nt} = A_{ts} f_y + A_{tp} (f_{se} + \Delta f_p) \quad \text{Equation 5.6}$$

F_{nt} = Nominal strength of the tie

A_{ts} = Area of nonprestressed reinforcement in the tie

f_y = Yield strength of steel reinforcement

A_{tp} = Area of prestressing steel in the tie

f_{se} = Effective stress in prestressing steel

Δf_p = Increase in stress in prestressing steel due to factored loads (suggested values – 60, 000 psi for bonded prestressed reinforcement, or 10, 000 psi for unbonded prestressed reinforcement)

The strength of the nodal zones is given by (Equation 5.7):

$$F_{nz} = f_{ce} A_{nz} \quad \text{Equation 5.7}$$

F_{nz} = Nominal compression strength of a nodal zone

f_{ce} = Effective compression strength in the nodal zone

A_{nz} = Area of a face of a nodal zone or a section through a nodal zone

The effective compression strength of the nodal zone (f_{ce}) is given by (Equation 5.8):

$$f_{ce} = 0.85 \beta_n f'_c \quad \text{Equation 5.8}$$

$\beta_n = 1.0$ in nodal zones bounded by struts or bearing areas, or both

$\beta_n = 0.80$ in nodal zones anchoring one tie

$\beta_n = 0.6$ in nodal zones anchoring two or more ties

5.2.3 CEB-FIP Model Code 1990

The strength of steel in tension (Equation 5.9) is specified as:

$$f_{ytd} = \frac{f_{ytk}}{\gamma_s} \quad \text{Equation 5.9}$$

f_{ytd} = Design value of yield strength in tension

f_{ytk} = Characteristic value of yield strength in tension

γ_s = Safety factor

The CEB-FIP Model code specifies two methods for calculating the strength of compression struts. The first method involves using a parabolic-rectangular stress-strain diagram (as seen in Figure 5.2). This formulation (Equation 5.10) is for un-cracked compression zones.

$$\sigma_{cd} = 0.85f_{cd} \left[2 \left(\frac{\varepsilon_c}{\varepsilon_{c1}} \right) - \left(\frac{\varepsilon_c}{\varepsilon_{c1}} \right)^2 \right] \quad \text{for } \varepsilon_c < \varepsilon_{c1}$$

$$\sigma_{cd} = 0.85f_{cd} \quad \text{for } \varepsilon_{c1} \leq \varepsilon_c \leq \varepsilon_{cu}$$

$$\sigma_{cd} = 0.00 \quad \text{for } \varepsilon_{cu} < \varepsilon_c$$

σ_{cd} = Design concrete compression strength in strut

f_{cd} = Design value for concrete cylinder strength

ε_c , ε_{c1} , ε_{cu} = Shown in Figure 5.2. For axial compression $\varepsilon_{cu} = 0.002$

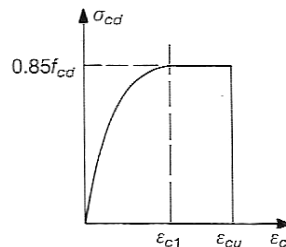


Figure 5.2 Parabola-Rectangle Stress-Strain Diagram (CEB-FIP, 1990)

The second method (Equation 5.11) for determining the strength of compression zones uses a uniform stress; the strength of the compression zone is affected by cracking. The strength of nodes is categorized based on whether the main tension reinforcement is anchored within the node. The strength of pure compression nodes for uncracked concrete (f_{cd1}) and the strength for nodes anchoring tension ties for cracked concrete (f_{cd2}) are based on Equation 5.11.

$$f_{cd1} = 0.85 \left[1 - \frac{f_{ck}}{250} \right] f_{cd}$$

$$f_{cd2} = 0.6 \left[1 - \frac{f_{ck}}{250} \right] f_{cd}$$

Equation 5.11

f_{cd1} = Compressive strength in uncracked zones

f_{cd2} = Compressive strength in cracked zones

f_{ck} = Characteristic compressive strength (cylinder)

f_{cd} = Design value for concrete strength (cylinder)

A schematic diagram of the compressive strength of concrete subjected to transverse tension is provided in Figure 5.3.

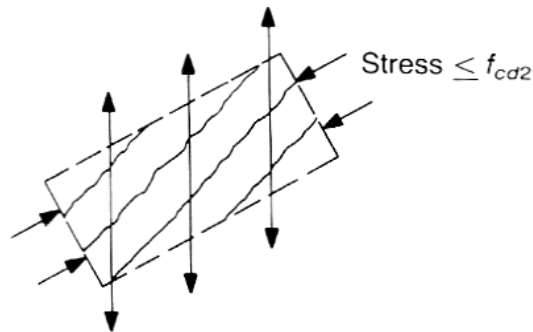


Figure 5.3 Schematic of Stress from Uniform Stress Method (CEB-FIP, 1990)

5.3 Strut and Tie Model Evaluation

The objective of the current study is to investigate the effect of corrosion of shear reinforcement in disturbed regions of reinforced concrete members. Therefore, it is necessary to develop a strut and tie model to predict the strength of disturbed regions. One of the key considerations in the model development is that the tension in the stirrups should be explicitly considered.

Three options for strut and tie models were evaluated. Model 1 is composed of a direct strut from the load point to the support. Models 2 and 3 are composed of a direct strut and a truss mechanism. The truss mechanism utilizes a tension tie representing the tension in the shear reinforcement; indirect struts are anchored at the top and bottom of this tie. The indirect struts frame into the nodes at the load point and the support. Model 3 reduces the tension in the shear reinforcement tie with an effectiveness factor from literature. In order to allow direct comparison between the three models, the strength reduction factors for the concrete struts were kept the same in all models, and the material resistance factors were taken as equal to unity. CEB-FIP (1999) suggests that the strength for struts (Equation 5.12) can be taken as:

$$f_{ytd} = 0.6f'_c \quad \text{Equation 5.12}$$

The strength of the nodes was selected based on CSA A23.3-04 code requirements:

$0.85 f'_c$ in node regions bounded by struts and bearing areas; and

$0.75 f'_c$ in node regions anchoring a tie in only one direction.

The accuracy of the three models was validated by comparing the strength output from the models against published test results of experimental work (Clark, 1951; de Paiva and Siess, 1965; Kong and Robins, 1970; Smith and Vantsiotis, 1982; Tan, Kong, Teng, and Guan, 1995; Tan, Teng, Kong, and Lu, 1997; Tan, Kong, Teng and Weng, 1997; Shin, Lee, Moon, and Ghosh, 1999; Yun, 2000; Oh and Shin, 2001; Aguilar, Matamoros, Parra-Montesinos, Ramirez, and Wight, 2002; Higgins and Farrow, 2006). A total of 95 data sets were input into the models, and the predicted results were plotted versus the experimental load. The test specimens chosen from the literature were all deep beams; the failure mode of the test specimens was shear or a combination of shear-flexure. The other selection criteria included providing information on the bearing plates, a shear-span to depth ratio of 1 to 2.5, vertical shear reinforcement in the shear span, and no horizontal skin reinforcement. A summary of the dimensions and structural characteristics of the data sets is provided in Table 5.1. A table showing important structural characteristics and the results from the strut and tie models (for all data sets) is provided in Appendix F.

Table 5.1 Data Sets Summary

Researcher	Width (mm)	Height (mm)	Effective Depth (mm)	Concrete Strength (MPa)	Flexural Reinf. Ratio (%)	Shear Reinf. Ratio (%)	a/d Ratio
Shin, Lee, Moon, and Ghosh (1999)	125	250	215	52 & 73	3.77%	0.25% to 1.81%	1.5 to 2.5
Tan, Kong, Teng, and Guan (1995)	110	500	463	41 to 51	2.58%	0.48%	1.1 to 2.2
Clark (1951)	152 & 203	381 & 457	314 & 391	14 to 48	1.63% to 3.42%	0.34% to 1.22%	1.2 to 2.4
Tan, Teng, Kong, and Lu (1997)	110	500	443 & 448	68 to 72	2.00% & 2.58%	0.48%	1.1 to 2.3
Higgins and Farrow (2006)	254	610	521	29 to 33	1.90%	0.33% to 0.55%	2.0
Yun (2000)	203	508	417	43	2.72%	0.52%	2.2
Aguliar et al. (2002)	305	914	800	28	1.25%	0.31%	1.1
Tan, Kong, Teng, and Weng (1997)	110	500	443	78	2.58%	1.43%	1.1 & 1.7
Oh and Shin (2001)	120	560	500	51 & 74	1.29%	0.13%	1.3
Kong and Robins (1970)	76	254	216	20	1.73%	0.85%	1.2
de Paiva and Siess (1965)	76	229	203	20 & 34	1.67% & 2.58%	1.09% & 1.31%	1.0
Smith and Vansiotis (1982)	102	356	305	16 to 22	1.94%	0.18% to 1.25%	1.2 & 1.5

5.3.1 Model 1 – Direct Strut Mechanism

This model consists of a direct strut from the loading point to the support, and a tension tie that is supported by the main tension reinforcement. The long span of the tested beams was modeled with a typical sectional model from CSA A23.3-04. A typical model is provided in Figure 5.4.

The length of the base of the node at the support is based on the length of the bearing plate and the height is double the depth from the soffit of the beam to the centroid of the main reinforcement. The length of the base of the node at the load point is based on the bearing plate and the height is based on the depth of the compression block from flexural analysis.

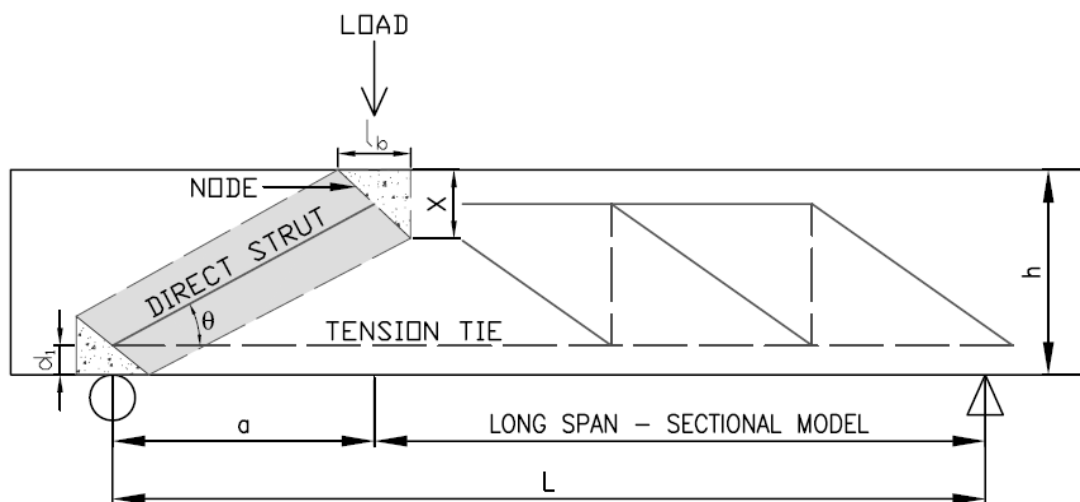


Figure 5.4 Direct Strut Mechanism

A flowchart detailing the algorithm for model 1 is provided in Figure 5.5. The decision checks are shown as diamonds in the flowchart. There are three engineering checks that have to be evaluated. The first decision is required to determine the area of the direct strut; this area is determined based on the smallest node. The second decision is to check the top and bottom nodes based on the appropriate stress limits. The third decision is to check that the main tension tie can support the applied load.

Figure 5.6 shows that the direct strut model predictions for the experimental data set in Table 5.1 were conservative. The average ratio of experimental load to predicted load was 1.56 with a coefficient of variation of 38%. For excellent correlation, the ratio of experimental to predicted load should be close to 1.00.

Legend

x = Depth of the stress block from flexure theory (mm)

a = Shear span (mm)

l_b = Length of the bearing plate (mm)

h = Height of the beam (mm)

L = Length of the beam (mm)

d_1 = Height of the centroid of the main reinforcing steel (mm)

V = Shear force in the shear span (kN)

T = Tension in the main reinforcement (kN)

R = Reaction for the long span support (kN)

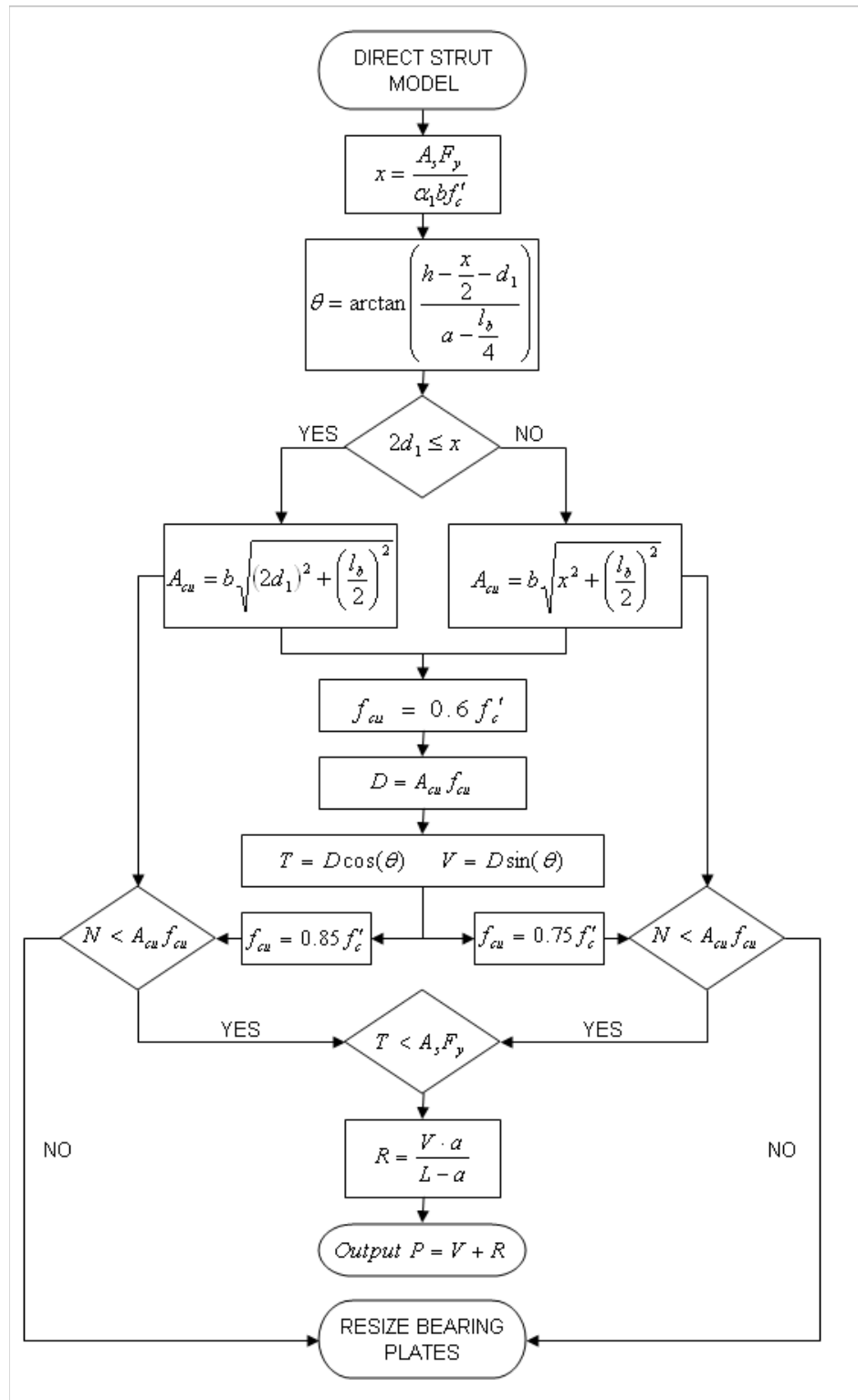


Figure 5.5 Direct Strut Model Algorithm

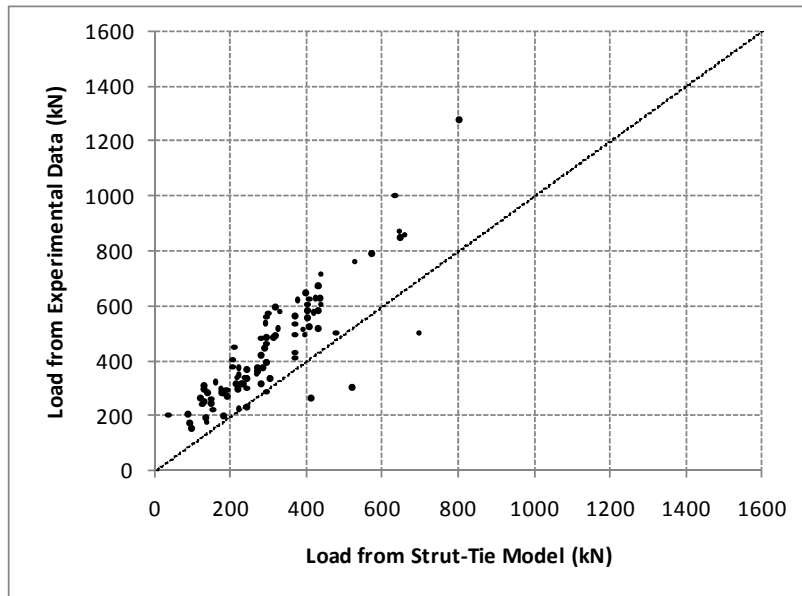


Figure 5.6 Direct Strut Model Validation

5.3.2 Model 2 – Direct and Indirect Strut Mechanism

CEB-FIP (1999) recommends utilizing a strut and tie model composed of direct and indirect struts. This model is based on two mechanisms. The direct strut mechanism utilizes a concrete strut from the loading point to the support with the tension forces resisted by the main reinforcement. In addition, the truss mechanism is composed of indirect strut from the load and support points to the bottom and top of the stirrup tie. This model is desirable because it captures the contribution of the stirrups in the overall shear resistance of the beam. Figure 5.7 provides a schematic diagram of the FIB model. The underlying assumption in the model is that stirrups within a certain region contribute to the vertical tie force. This region is defined by Equation 5.13.

$$a_w = 0.85a - \frac{z}{4} \tag{Equation 5.13}$$

a_w = Length over which stirrups are effective (mm)

a = Shear span (mm)

z = The flexural lever arm (mm)

The area of the stirrups that are within the region defined by Equation 5.13 is used to determine the force in the vertical tie (assuming the stirrups have yielded). This assumption allows the

determination the forces in the struts and ties. In addition, it is assumed that the node at the intersections between the indirect struts and the vertical tie will not fail.

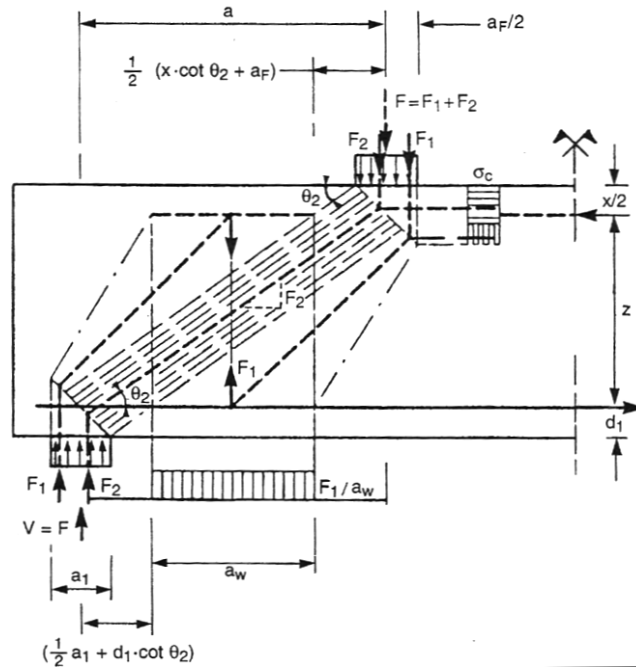


Figure 5.7 Direct and Indirect Strut and Tie Model (CEB-FIP, 1999)

Figure 5.8 shows the application of the direct and indirect strut and tie model to the beams in the present study. The angles that the struts form with the horizontal or vertical (θ and θ_2) are shown in Figure 5.8.

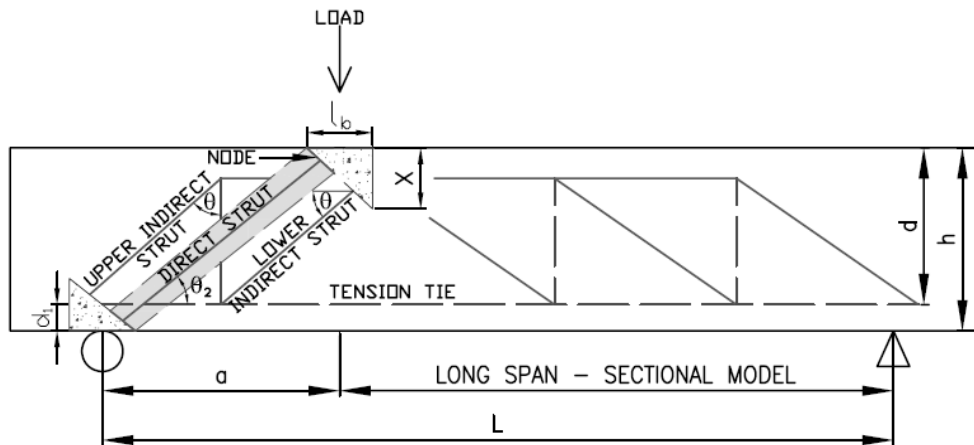


Figure 5.8 Direct and Indirect Strut Mechanism

An algorithm was developed to solve the truss system and determine the load the beam can support. The algorithm was developed to determine the angle at which the indirect struts are oriented with respect to the horizontal; initially, this value is unknown. A number of variables (angles α , β , θ) were defined in order to solve this problem; these variables are shown in Figure 5.9.

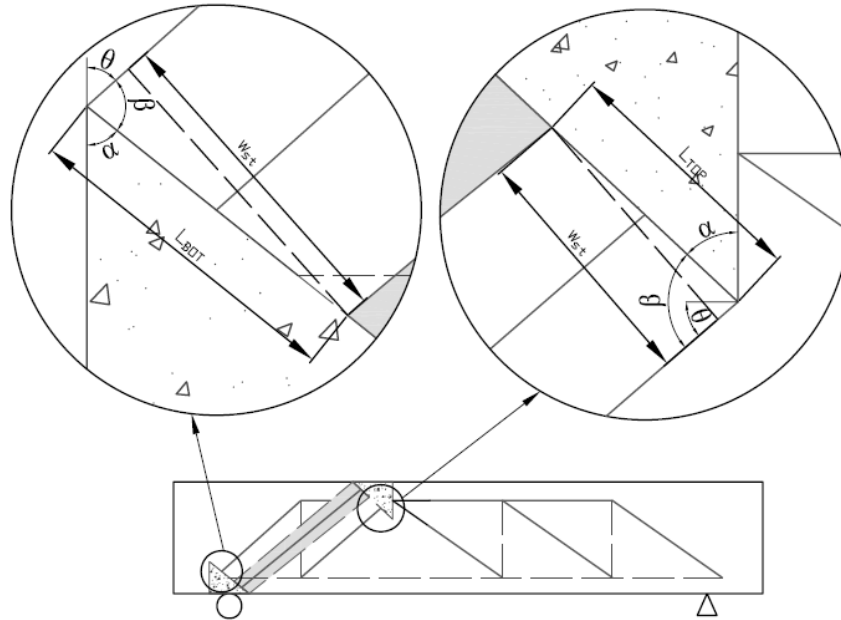


Figure 5.9 Angles at Node-Strut Connections

The solution algorithm for model 2 is presented in Figure 5.10. A key element of the solution is to determine the orientation angle of the indirect struts. The algorithm used to determine indirect strut orientation is provided in Figure 5.11.

An iterative procedure is used to determine the orientation angle of the indirect struts (Figure 5.11). The first step is to assume an orientation angle of the lower indirect strut; then the force in the lower indirect strut is determined from statics and the required width of the strut is determined. The angle at which the strut frames into the node can be determined. A new value for the lower indirect strut orientation angle is determined and compared with the assumed value. This procedure is repeated until an acceptable level of accuracy is obtained. A similar procedure is used to find the orientation angle of the upper strut. The next step is to determine the strength of the compression strut. Finally, the nodes and the tension reinforcement are checked to ensure that they can support the imposed load that is determined from this analysis.

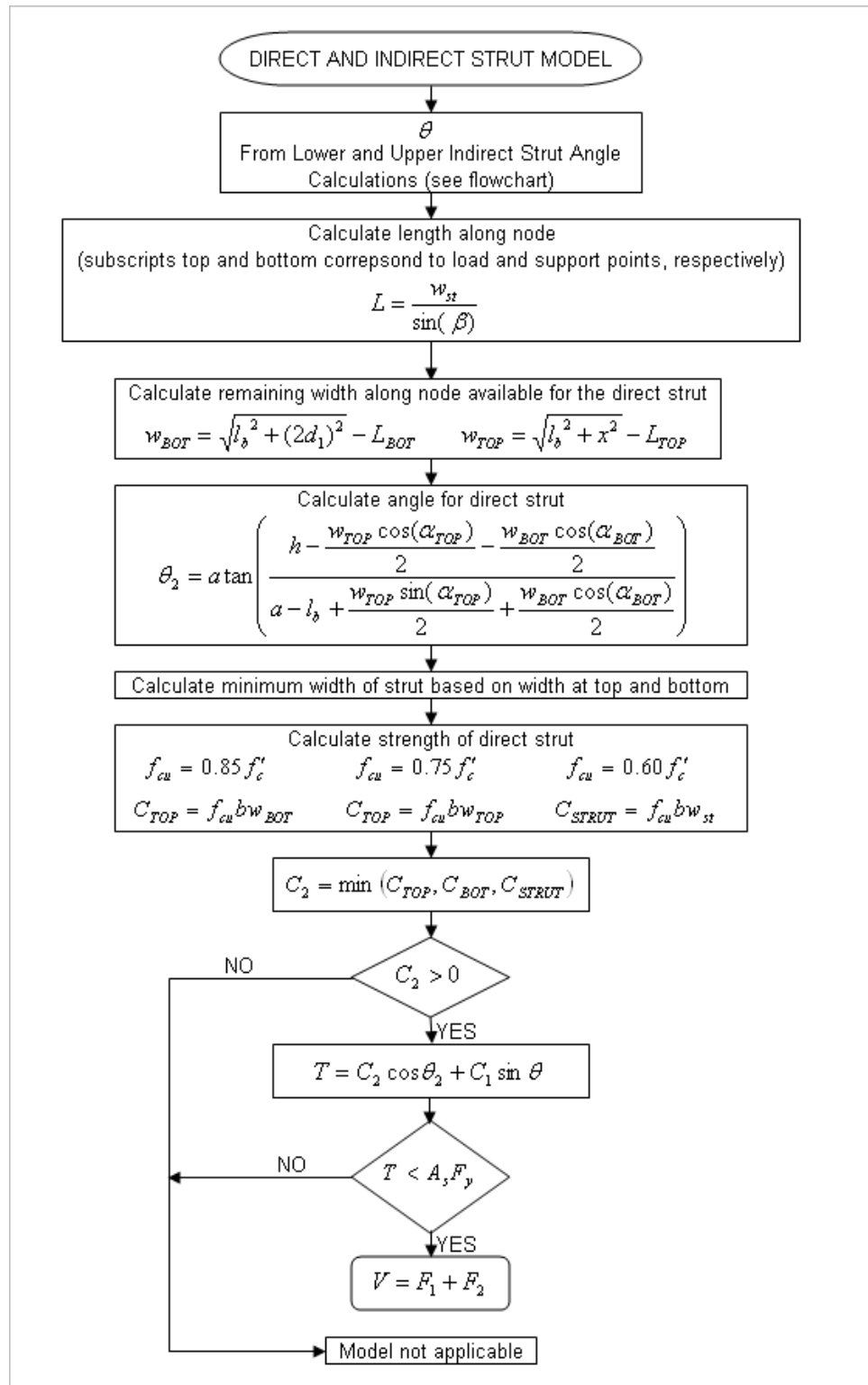


Figure 5.10 Direct and Indirect Model Algorithm

- Legend**
- x = Depth of the stress block from flexure theory (mm)
 - a = Shear span (mm)
 - l_b = Length of the bearing plate (mm)
 - d = Effective depth of beam (mm)
 - L = Length of the beam (mm)
 - w_{st} = Width of indirect strut (mm)
 - F_1 = Force in the stirrups (tension tie) (kN)
 - C_1 = Compression force in indirect strut (kN)
 - β = Angle strut frames into node with respect to diagonal face of node (degrees)
 - α = Angle diagonal face of node makes with respect to vertical (degrees)
 - θ = Orientation angle of indirect strut (degrees)

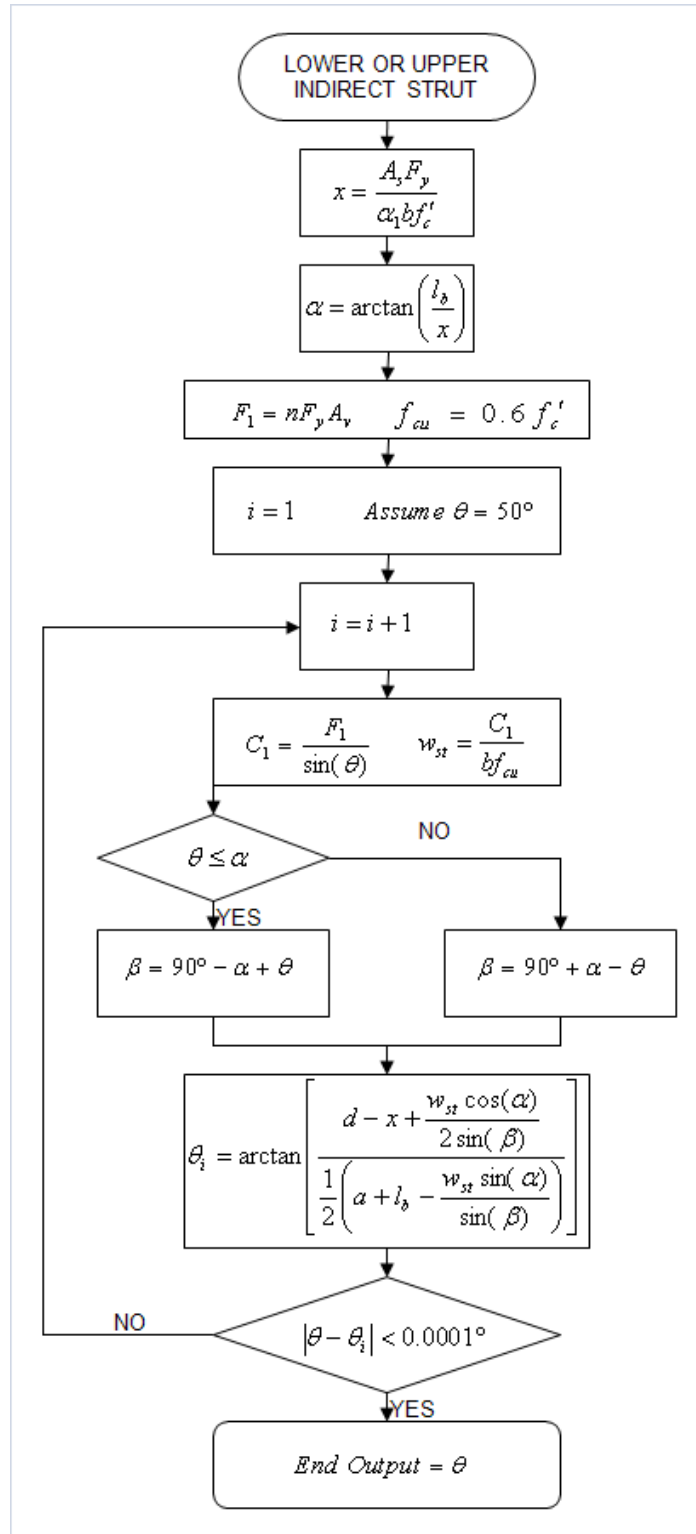


Figure 5.11 Calculation Algorithm for Lower or Upper Strut

Figure 5.12 shows a plot of the predicted values versus measured data set (Table 5.1). The correlation was better than model 1, but it is evident that model 2 (direct and indirect strut model) is slightly un-conservative. The average ratio of experimental load to predicted load was 0.98 with a coefficient of variation of 21%.

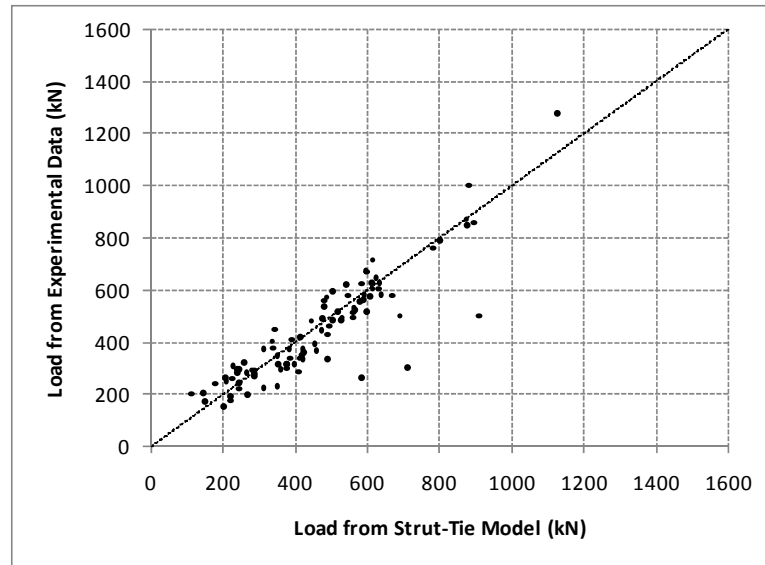


Figure 5.12 Direct and Indirect Strut Model Validation

5.3.3 Model 3 – Direct and Indirect Strut Mechanism with Effectiveness Factor

Model 2 assumes that the stirrups yield in calculating the force in the vertical tie; this might not be necessarily true. The stress in the stirrups could be reduced by using the effectiveness factor as proposed by Russo and Puleri (1997). Equation 5.14 gives the stirrup effectiveness factor.

$$\psi = 1.67 \frac{\sqrt{f'_c}}{\chi}$$

$$\chi = \sqrt{f'_c} + 250 \sqrt{\rho \left(\frac{d}{a} \right)^5}$$

Equation 5.14

ψ = Stirrup effectiveness factor

f'_c = Concrete compressive strength (MPa)

ρ = Tensile reinforcement ratio

a = Shear span (mm)

d = Effective depth (mm)

χ = Coefficient

Model 3 follows the same calculation procedure as model 2 (Figure 5.10). The only difference is that the force in the vertical tie is reduced by the effectiveness factor (Equation 5.14) to reflect that the stress in the stirrups is below the yield stress.

$$F_1 = n\psi F_y A_v \quad \text{Equation 5.15}$$

Figure 5.13 shows the experimental values collected from the literature (Table 5.1) versus the predicted strengths. This model produces values that are more conservative in comparison to the Model 2. The average ratio of experimental load to predicted load was 1.09 with a coefficient of variation of 24%. Sample calculations for the direct and indirect strut and tie model with effectiveness factor are provided for selected specimens in Appendix G.

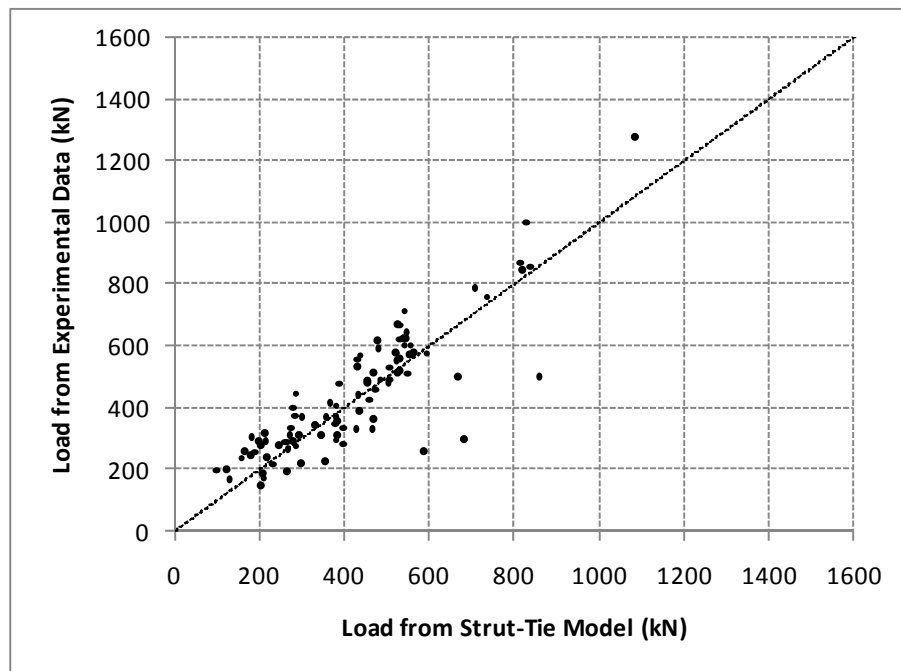


Figure 5.13 Direct and Indirect Strut (with Effectiveness Factor) Model Validation

5.3.4 Discussion

Model 3 was the most effective at predicting the strength of the test data in the published literature with a ratio of experimental to predicted values of 1.09. The important parameters for shear strength in deep beams are concrete strength, shear span to depth ratio, shear reinforcement ratio, and flexural reinforcement ratio. The ratio of experimental to predicted strength was plotted versus these different parameters to examine the sensitivity of the models to these parameters.

Figure 5.14 shows a plot of experimental to predicted strength (STM) ratio versus beam shear-span to depth (a/d) ratio. As the shear-span to depth ratio increases, models 2 and 3 become less conservative. The stirrup effectiveness factor gives values that suggest that at shear-span to depth ratios closer to 1.0 the stirrups are significantly less effective than at shear-span to depth ratios closer to 2.5. In fact, the effectiveness factor is approximately 1.0 at shear-span to depth ratios close to 2.5. A shear span to depth ratio of 2.5 represents the transition point between deep and slender beam action. This means that the effectiveness factor has no effect at higher shear-span to depth ratios; conversely, at lower shear span to depth ratios model 3 will give more conservative predictions.

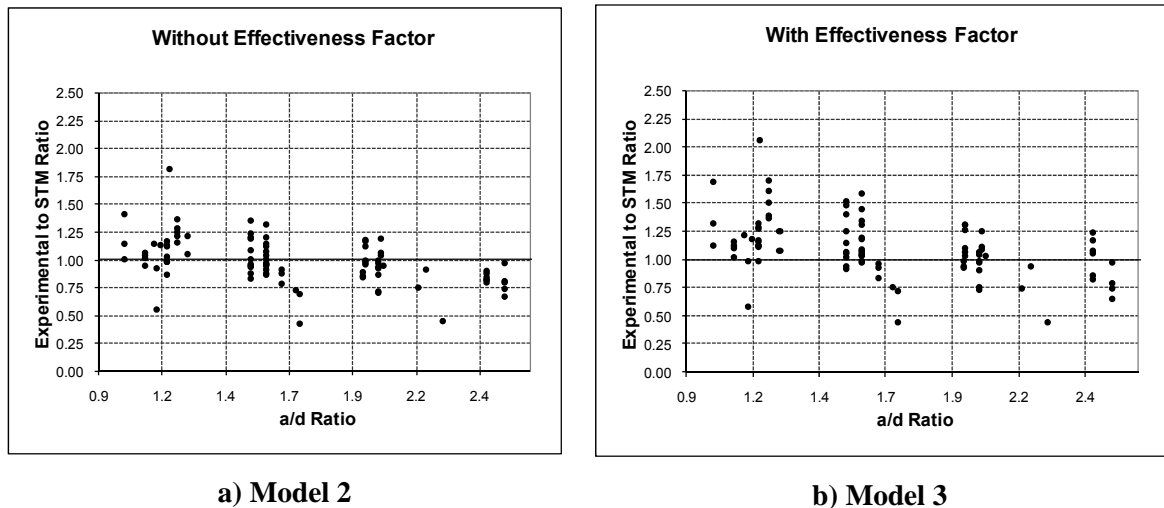


Figure 5.14 Comparison of Models 2 and 3 with Shear-span to Depth ratio

Rogowsky and MacGregor (1986) recommend that the struts form an angle between 25° and 65° with respect to the horizontal axis of the member. The specimens with shear-span to depth ratios close to 2.5 have struts that form angles that are close to the lower limit of 25° ; this may also explain the trend shown in Figure 5.14.

In summary, the effectiveness factor has little effect on beams with shear-span to depth ratios closer to 2.5 which explains why the same trend exists in models 2 and 3. At higher shear-span to depth ratios the predictions are less conservative because of the transition point between deep and slender beam action at 2.5 and the concrete struts forming angles of about 25° at shear-span to depth ratios of 2.5.

Figure 5.15 shows a plot of the experimental to predicted strength ratios versus concrete strength using models 2 and 3. The observed trend is that at higher concrete strengths the model predictions are less conservative. It is evident (especially in Figure 5.15b) that generally the specimens with a shear-span to depth ratio less than 2.0 produce more conservative values compared to the specimens with a shear-span to depth ratio between 2.0 and 2.5. This would indicate that the observed trend may not necessarily be related to concrete strength. Therefore, it is important for the designer to ensure that the strut angles are within acceptable limits (25° to 65°) in order to ensure that conservative shear strength values are predicted.

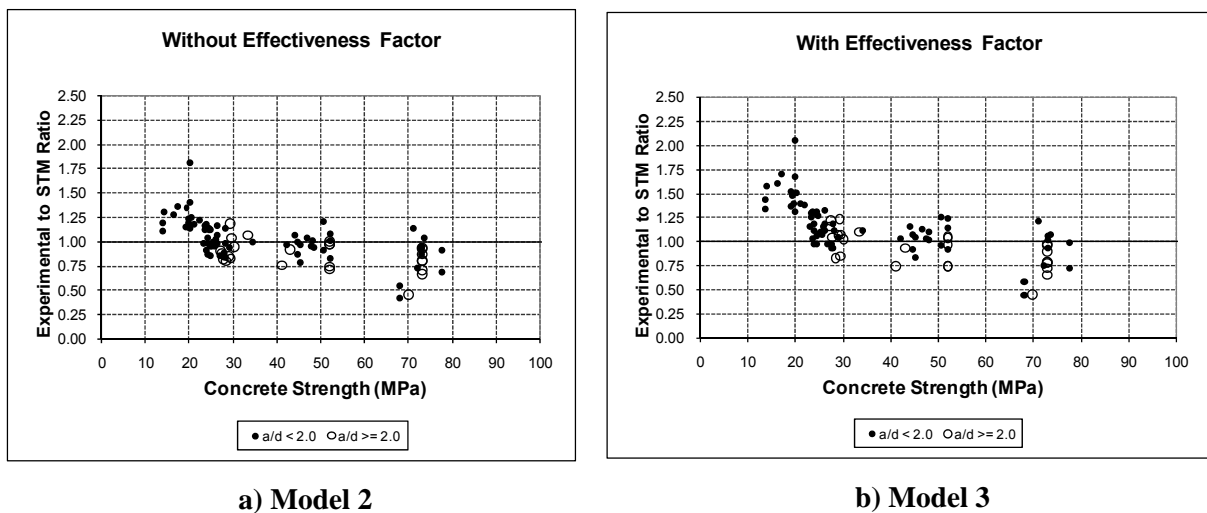
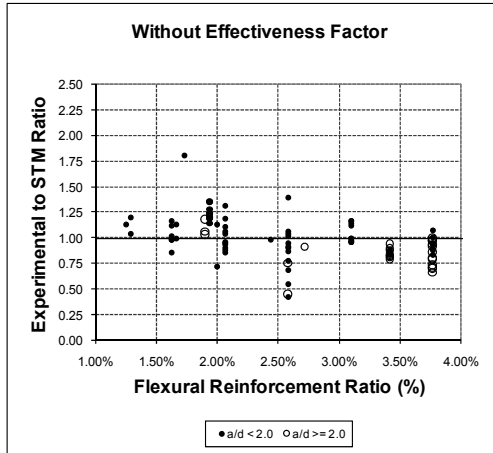


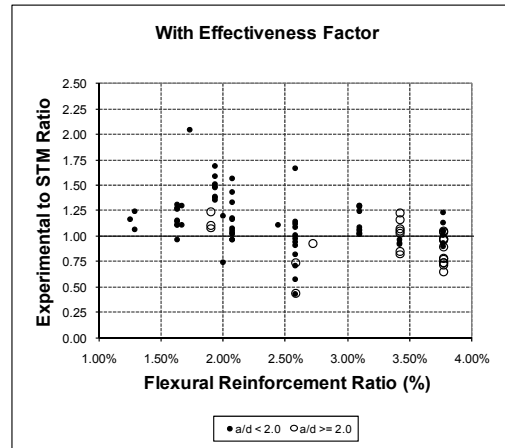
Figure 5.15 Comparison of Models 2 and 3 with Concrete Strength

There is no clear trend exhibited when the experimental to predicted strength ratio is plotted against flexural reinforcement ratio (Figure 5.16). Similarly, there are scattered results when the experimental to predicted strength ratios are plotted versus the shear reinforcement ratio (Figure 5.17). It is important to note that a model limitation exists with respect to shear reinforcement ratio explained in the following. In some cases the force the stirrups can resist would require an indirect strut width that would be larger than the width of the node that it frames into. This would mean that

no direct strut could be formed; in practice, the model produces a negative value for the strength of the direct strut. The data sets that would produce this situation have not been included in the comparison.

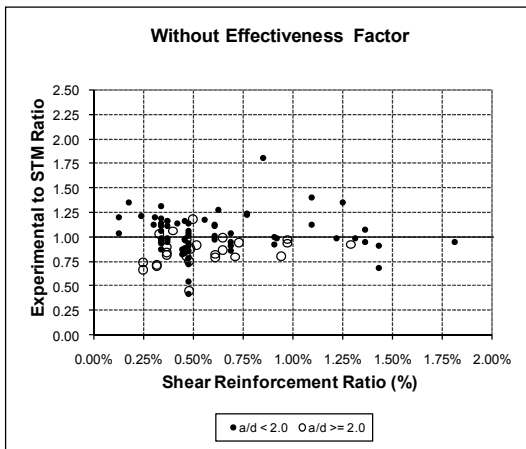


a) Model 2

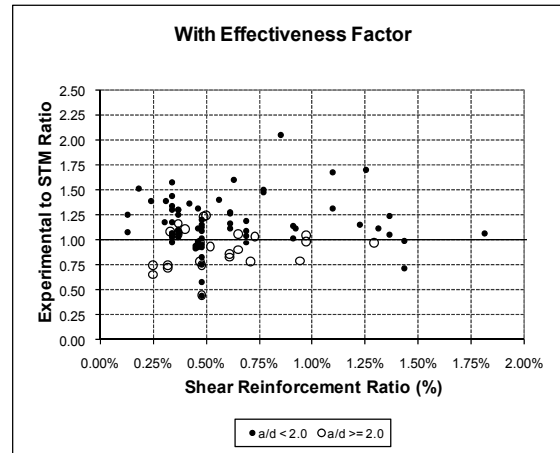


b) Model 3

Figure 5.16 Comparison of Models 2 and 3 with Flexural Reinforcement Ratio



a) Model 2



b) Model 3

Figure 5.17 Comparison of Models 2 and 3 with Shear Reinforcement Ratio

Chapter 6

Effect of Corrosion in Strut and Tie Modelling

6.1 Introduction

This section presents the development of a model capable of predicting the strength of disturbed regions with corroded shear reinforcement. The model is based on the “direct and indirect” strut and tie model developed in Chapter 4. The effects of corrosion on the shear strength are included by considering the mass loss in the steel reinforcement, an effective concrete compressive strength, and an effective cross section width (effect of cracking).

6.2 Proposed Model

The proposed model has been developed utilizing the experimental results. It was shown in Chapter 4 that the corrosion cracking influences the overall strength of disturbed regions in beams with corrosion damaged shear reinforcement. In Chapter 5 it was shown that a model utilizing both a direct and indirect strut with a stirrup effectiveness factor is the best model to predict the shear strength of an un-corroded reinforced concrete member. Consequently, this model will be expanded to include the effects of corrosion.

The corrosion crack width is incorporated into the direct and indirect strut model in two ways. First, the section loss in the reinforcing steel is determined based on the mass loss model. Second, the effective concrete strength of the compression strut is modified based on a reduction model. Also, the recommended model includes a reduction in the cross section width. A flowchart showing the steps required to modify the inputs for the direct and indirect strut and tie model (with effectiveness factor) is provided in Figure 6.1. The model presented in this section is based solely on the corrosion crack width. From a practical perspective, this is what would be available to practicing engineers to assess the strength of a corrosion damaged structure. The following sections describe the development of the model that is presented in Figure 6.1.

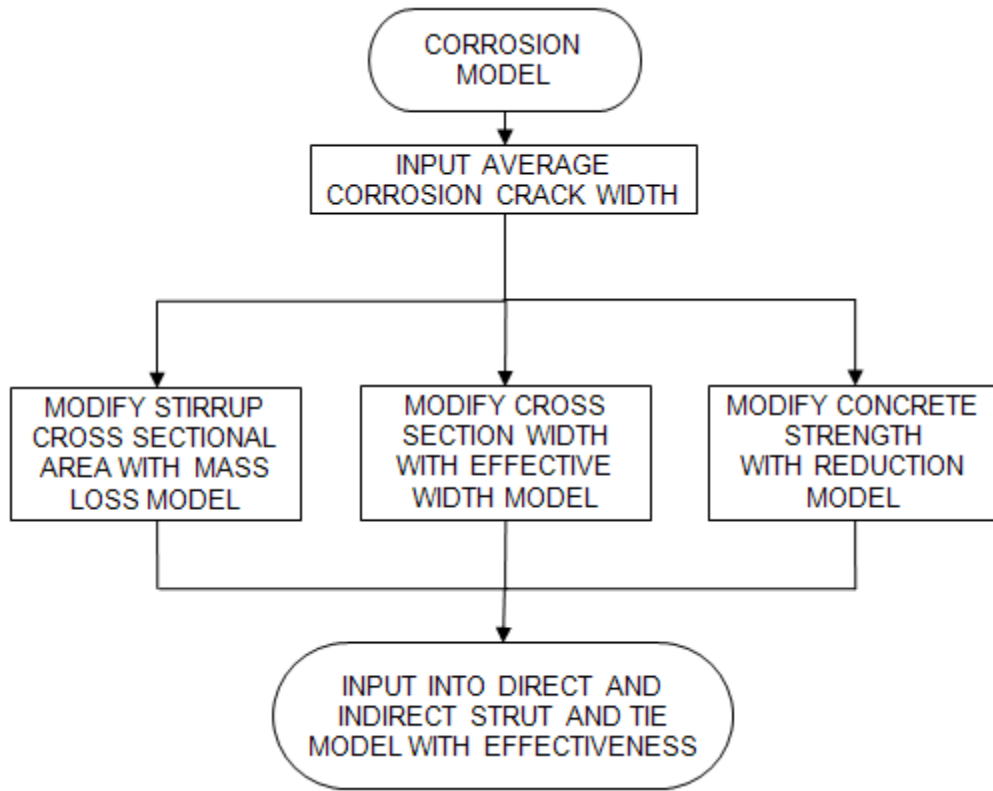


Figure 6.1 Corrosion Model Flowchart

6.2.1 Mass Loss Model

Vidal, Castel, and Francois (2003) developed a model (Equation 6.1) that correlates the mass loss in the reinforcement with corrosion crack width. The model has two parts: the first step is to determine the section loss that will initiate cracking in the concrete and the second step is to determine the actual mass loss based on a known crack width.

$$\Delta A_{s,o} = A_s \left[1 - \left[1 - \frac{\alpha}{d_b} \left(7.53 - 9.32 \frac{c}{d_b} \right) 10^{-3} \right]^2 \right]$$

$$\Delta A_s = \frac{w}{K} + \Delta A_{s,o}$$

Equation 6.1

A_s = Sound steel cross section (mm²)

$\Delta A_{s,o}$ = Local steel cross-section loss necessary for crack initiation (mm²)

ΔA_s = Reinforcing steel cross section loss (mm²)

d_b = Corroding bar diameter (mm)

c = Concrete cover (mm)

α = Pit concentration factor (mm) ($\alpha = 2$ for homogenous corrosion; $4 < \alpha < 8$ for localized corrosion)

w = Crack width (mm)

K = Regression factor (0.0575 mm^{-1})

Table 6.1 presents the reinforcing steel section loss with respect to crack width for two different pit concentration factors. This analysis shows that at higher pit concentration factors the overall mass loss is higher. This suggests that lower pit concentration factors should be used for uniform corrosion. When pitting corrosion is evident, a higher pit concentration factor should be used.

Table 6.1 Section Loss from Mass Loss Model

Crack Width (mm)	Minimum Section Loss (%) ($\alpha = 2$ mm)	Maximum Section Loss (%) ($\alpha = 8$ mm)
0.2	4.4%	7.1%
0.4	7.9%	10.6%
0.6	11.4%	14.1%
0.8	14.8%	17.6%
1.0	18.3%	21.1%
1.2	21.8%	24.5%

Figure 6.2 shows the average corrosion crack width versus mass loss measured after the specimens were tested to failure along with the predictions from the Vidal, Castel, and Francois (2003) model (shown as a dashed line). It is apparent that there is a significant amount of scatter in the results. The use of the model is justifiable because the study conducted by Vidal, Castel, and Francois (2003) was done under realistic conditions. The reinforced concrete specimens were subjected to a dead load, and the corrosion occurred naturally over a period of 12 years. The model provides the designer with a rough estimate of the mass loss. It is important to note that the mass loss in the shear reinforcement is not the primary strength determining factor in the shear behaviour of disturbed regions with corrosion damaged shear reinforcement.

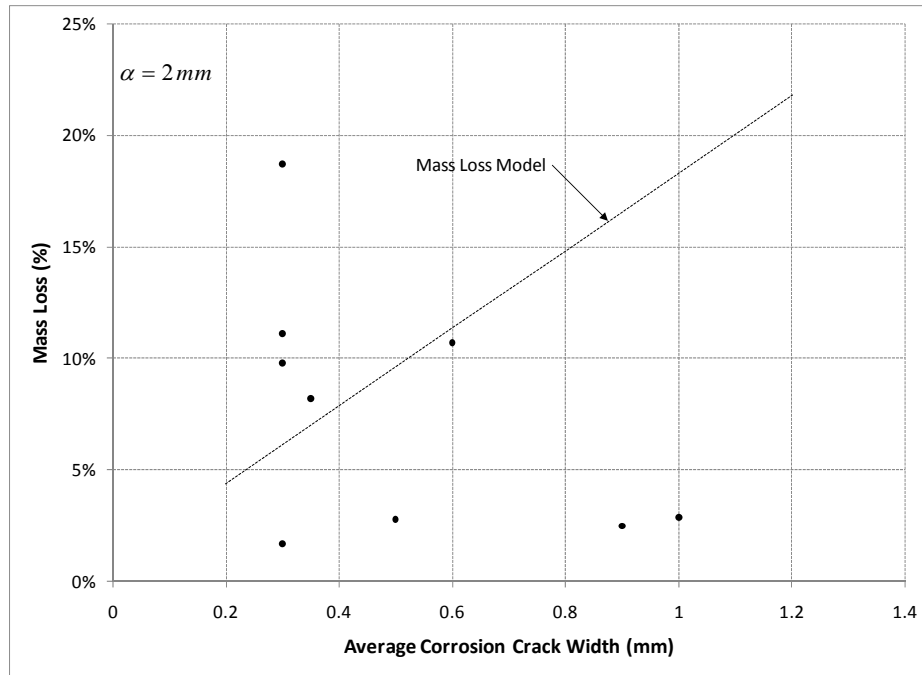


Figure 6.2 Average Corrosion Crack Width versus Mass Loss

6.2.2 Effective Concrete Strength

The effective concrete strength is required to determine the shear strength of the reinforced concrete beams. The effective concrete strength was calculated twice based on model 1 (direct strut and tie model) and model 3 (direct/indirect strut and tie model) from Chapter 5.

The first step in determining the effective concrete strength from model 1 is to determine the cross sectional area of the direct compression strut based on the nodal dimensions. The shear strength of the section is based on the vertical component of the force in the compression strut; thus, a trigonometric relationship is provided in the denominator of the effective concrete expression. The experimental shear strength has not been normalized as was done in Chapter 4. Figure 6.3 shows the direct strut and tie model from Chapter 5.

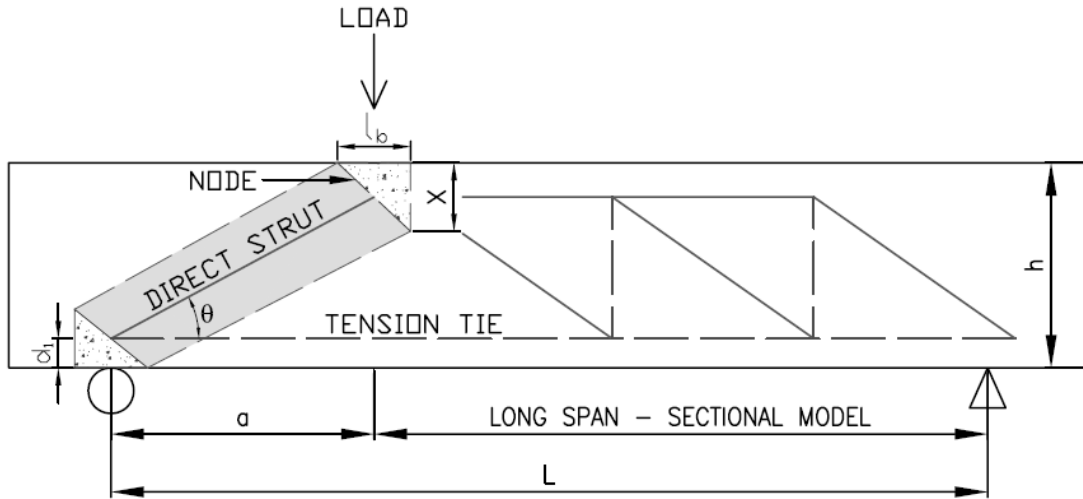


Figure 6.3 Direct Strut and Tie Model

The effective concrete strength is defined as follows (Equation 6.2):

$$A_{cu} = b\sqrt{(l_b)^2 + (2d_1)^2} \quad \text{Equation 6.2}$$

$$f_{cu_eff} = \frac{V_{exp}}{A_{cu} \sin(\theta)}$$

b = Width of the cross section (mm)

l_b = Length of the bearing plate (mm)

d_1 = Height of the centroid of the main reinforcing steel (mm)

A_{cu} = Cross sectional area of compressive strut (mm²)

V_{exp} = Shear force in the shear span (N)

θ = Orientation angle of compressive strut (rad)

f_{cu_eff} = Effective compressive strength (MPa)

Model 1 provides one equation for effective concrete strength; whereas, model 3 utilizes three struts which is more complex. Consequently, a single expression cannot be determined. Equation 6.4 provides the formulation that was used in the spreadsheet to determine the effective concrete strength from model 3.

$$f_{cu_eff} = \frac{V_{exp} - F_1}{bw_{st}} \quad \text{Equation 6.3}$$

F_1 = Force in the stirrups (tension tie) (kN)

w_{st} = Width of the direct strut (mm)

The effective concrete strengths for the corroded specimens obtained using models 1 and 3 are presented in Table 6.2. The effective concrete strength data can be plotted against the average corrosion crack width to determine what relationship best describes the behaviour of corrosion damaged concrete.

Table 6.2 Effective Concrete Strength from Measured Shear Strength

Specimen Name	Average Crack Width (mm)	V_{exp} (kN)	θ	f_{cu_eff} Model 1 (MPa)	f_{cu_eff} Model 3 (MPa)
L-1.0-R	0.30	285	0.749	20.9	15.1
L-1.5-R	0.30	216	0.538	21.1	10.1
L-2.0-R	0.3	164	0.414	20.3	-3.1
M-1.0-R	0.50	177	0.749	13.0	8.7
M-1.5-R	0.30	215	0.538	21.0	10.0
M-2.0-R	0.35	198	0.414	24.6	3.2
H-1.0-R	0.90	227	0.749	16.7	11.6
H-1.5-R	1.00	141	0.538	13.7	5.2
H-2.0-R	0.60	169	0.414	21.0	-0.2

6.2.3 Linear Reduction Model

The results that are shown in Table 6.2 are plotted in Figure 6.4 to see what relationship exists. The negative effective strength values that were determined from model 3 are omitted from the figure. It is clear that no mathematical relationship can be derived using model 3. Furthermore, model 3 gives negative effective concrete strength values for specimens L-2.0-R and H-2.0-R. Model 1 provides effective concrete strength values that decrease linearly with respect to corrosion crack width. Consequently, model 1 is used to develop a linear reduction expression which is provided in Equation 6.4. The model relates the effective concrete strength to corrosion crack width and the reduced compressive strength due to corrosion of a typical compressive strut.

$$f_{cu_corr} = 0.6f'_c - 11w_c \geq 13MPa \quad \text{Equation 6.4}$$

f'_c = Concrete compressive strength (MPa)

f_{cu_corr} = Concrete strut compressive strength modified for corrosion (MPa)

w_c = Average corrosion crack width (mm)

The predicted results of the effective concrete strength from the linear reduction equation (dashed line) are plotted versus corrosion crack width in Figure 6.4. The concrete strength input into the linear reduction model was the average value for the corroded specimens from the experimental program. The figure also includes the data obtained from the measured shear strength (Table 6.2). One data point (Specimen M-1.0-R) was significantly un-conservative (fell significantly below the curve); this specimen was removed in order to determine the linear reduction model. The model was determined based on a “best fit” curve. The coefficient of determination (R²) was 0.69. The coefficient determined from the “best fit” analysis was 11.12 MPa/mm; this value was rounded down to simplify the expression. The concrete that is confined by the shear reinforcement is still effective at resisting compressive forces; consequently, some residual strength can be expected even in the most severely corroded specimens. The magnitude of this residual strength was determined from the experimental results. The lowest effective concrete strength from model 1 was 13.0 MPa. As a result, a lower limit of 13 MPa is recommended.

6.3 Effective Width Model

The corrosion of the shear reinforcement causes cracking, delamination, and spalling. These deteriorations contribute to making the cross section less effective in resisting imposed loads. Consequently, an effective concrete width is proposed in this section. Higgins et al. (2003) proposed an effective section width model based on the concrete cover thickness, stirrup diameter, and stirrup spacing. They suggested that when the stirrups were spaced closer together more interaction between corrosion cracks occurred. Furthermore, they postulated that this interaction can cause an increase in the severity of the spalling. They attempted to reflect this with their formulation which is provided in Chapter 2.

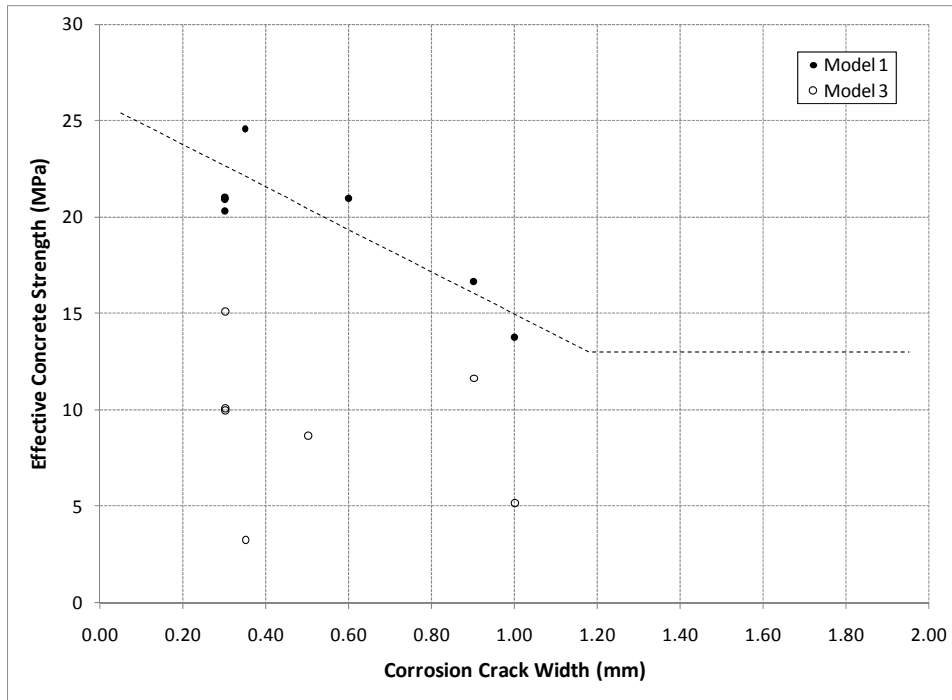


Figure 6.4 Linear Reduction Model

The concrete deterioration in the form of spalling and delamination, due to corrosion, affects the concrete cover in reinforced concrete beams. The concrete confined by the shear reinforcement remains undisturbed and can effectively resist load. A simple and conservative way to consider the effects of corrosion on the concrete section at the ultimate stage would be to reduce the section width based on the concrete cover; this step is justifiable because delamination was observed in specimen H(M)-2.0-R. Equation 6.5 provides the proposed effective width formulation.

$$b_{eff} = b - 2c \quad \text{Equation 6.5}$$

b_{eff} = Effective width (mm)

b = Section width (mm)

c = Concrete cover (mm)

6.4 Model Evaluation

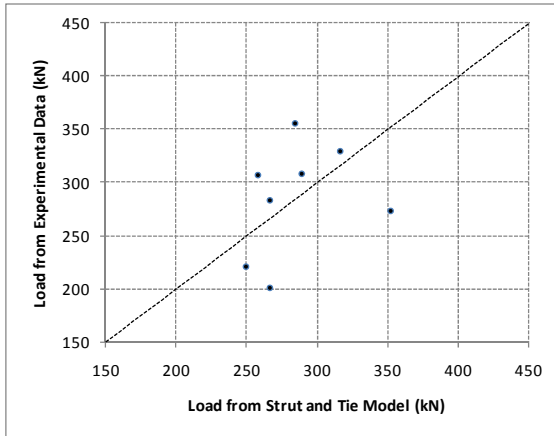
Two different combinations of the proposed models were evaluated against the model proposed by Higgins et al. (2003). The first combination utilizes the mass loss and linear reduction models (Model 1). The second combination incorporates the mass loss, linear reduction, and effective width

models (Model 2). The indirect and direct strut model with the effectiveness factor will be used because it gives the most accurate predictions for un-corroded specimens.

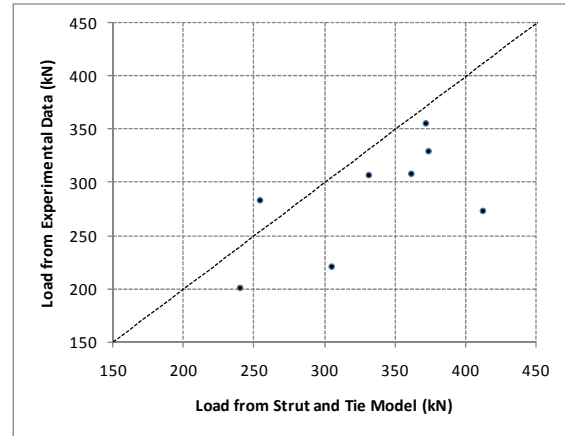
The section loss in the specimens is incorporated into the strut and tie model by reducing the strength of the vertical tension tie using the mass loss model. It should be noted that the observed performance of the shear reinforcement in the experimental study was not degraded due to the section loss in the reinforcing steel. The main function of the shear reinforcement in disturbed regions is to provide limited ductility; this function was accomplished even in the most severely corroded specimens. Nevertheless, the section loss is incorporated into the model. The area of shear reinforcement is reduced based on the change in reinforcing steel area (ΔA_s) determined from the mass loss model based on the input average corrosion crack width.

Specimen H-2.0-R was removed from this analysis because the direct and indirect strut and tie model is not valid for this specimen. The concrete compressive struts encompass the entire width of the nodes; consequently, the direct strut mechanism cannot be evaluated as part of the model.

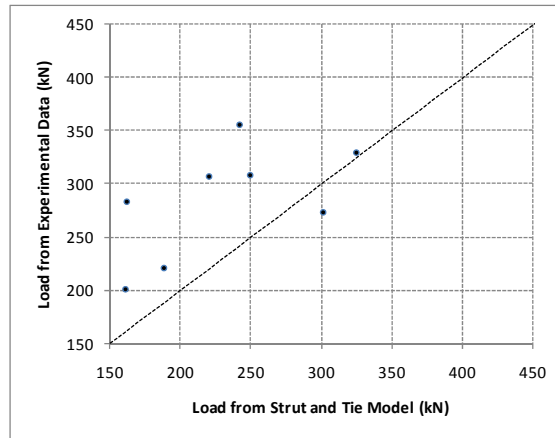
Figure 6.5 provides a comparison of the results of the Higgins et al. and the proposed models with respect to the experimental results. The Higgins et al. model gave un-conservative results for 3 out of 8 specimens; the average ratio of experimental to predicted strength was 1.02 with a coefficient of variation of 16%. Model 1 provided primarily un-conservative predictions (7 out of 8 specimens). The average ratio of experimental to predicted strength was 0.87, and the coefficient of variation was 16%. Model 2 provided the best predictions with un-conservative results for 1 out of 8 specimens. The average ratio of experimental to predicted strength was 1.27 with a coefficient of variation of 21%; a summary of the results from model 2 is provided in Table 6.3.



Higgins et al. Model



Mass Loss + Linear Reduction Models (Model 1)



Mass Loss + Linear Reduction + Effective Width Models (Model 2)

Figure 6.5 Model Comparison

Table 6.3 Model 2 Results

Specimen	Experimental Ultimate Load (kN)	Predicted Ultimate Load (kN)	Ratio of Experimental to Predicted Load
L-1.0-R	356	242	1.47
L-1.5-R	308	250	1.23
L-2.0-R	273	301	0.91
M-1.0-R	221	188	1.18
M-1.5-R	307	220	1.40
M(L)-2.0-R	330	325	1.02
H-1.0-R	283	162	1.75
H(M)-1.5-R	201	161	1.25

The experimental testing (Chapter 4) showed that there is a significant amount of variability in the ultimate strength of disturbed regions with corroded shear reinforcement. This variability was due to factors such as the inclination of the shear reinforcement, the severity of the concrete deterioration, and the number of corroded stirrups. It is desirable to have a model that has an additional level of conservatism beyond what is provided by material resistance and load safety factors to account for this variability. It is recommended that model 2 be utilized to predict the strength of disturbed regions with corroded shear reinforcement because it has an average experimental to predicted strength ratio of 1.27.

6.5 Application of Model

The corrosion model presented in this chapter is applied to the direct and indirect strut and tie model presented in Chapter 5 by modifying three inputs as follows:

1. Determine ΔA_s , as a function of average corrosion crack width, from the mass loss model and input into the strut and tie model as follows: $A_v = 2(A_s - \Delta A_s)$.
2. The effective compressive strength of the strut (f_{cu}) is modified using the linear reduction model as follows: $f_{cu} = 0.6f'_c - 11w_c \geq 13MPa$.
3. The width of the section is modified for the effects of spalling and delamination as follows:

$$b_{eff} = b - 2c .$$

The application of the model is illustrated through a case study presented in Appendix I.

6.6 Discussion

A well developed method of predicting shear strength is through the use of compression field theory. This theory calculates the shear strength of a member by idealizing it as a series of concrete struts which resist principle compressive forces. The strength of the struts is based on a stress-strain formulation for cracked concrete. It is this stress strain formulation that could be modified for the effects of corrosion cracking. Future work could focus on testing specimens with corroded reinforcing steel similar to those that were tested to develop the compression field theory approach to account for the effects of corrosion.

The accelerated corrosion phase of the experimental testing did not simulate the dead load that would be experienced by an in-situ structure. This type of load tends to cause cracking in a

reinforced concrete member. If these cracks were oriented in the same direction as the reinforcing steel then they could allow moisture and oxygen to penetrate to the level of the reinforcing steel which would cause corrosion. These load induced cracks would cause larger cracks widths than what would occur from corrosion alone. The model would predict a conservative estimate of the shear strength because the overall crack width would be larger. A design engineer would have to keep this point in mind when assessing the strength of a structure.

Chapter 7

Conclusions and Recommendations

7.1 Introduction

In this study, a total of 16 reinforced concrete beam specimens were monotonically tested. Ten of the specimens were subjected to accelerated corrosion prior to being loaded to failure. In addition, a strut and tie model was developed and compared with experimental results from other researchers. A corrosion model was formulated and incorporated into the strut and tie model to predict the strength of the specimens from the experimental program. This chapter summarizes the important findings and conclusions drawn from the experimental program and the theoretical modelling. The main objectives of the study were to:

- Quantify the effect of corrosion of shear reinforcement on reinforced concrete beams with different shear-span to depth ratios.
- Evaluate the feasibility of utilizing CFRP fabric to restore the strength of beams with corroded shear reinforcement.
- Develop a model that quantifies the shear strength of reinforced concrete deep beams with corroded shear reinforcement

7.2 Conclusions

7.2.1 Accelerated Corrosion

- The mass loss results based on a specimen autopsy after testing indicate that corrosion occurred uniformly over both legs of the shear reinforcement.
- There was a significant variation in the mass loss of the stirrups in specimens with 2 or 3 stirrups. This variation was most pronounced in specimens M-1.5-R, H(M)-1.5-R, and H(M)-1.5-Repair. The difference in average mass between the stirrups in these specimens was 6.7%, 7.6%, and 12.2%.
- There was evidence of corrosion cracking in all specimens and delamination of the cover concrete was detected in the more severely corroded specimens. The average crack width was 0.30 mm, 0.40 mm, and 0.80 mm in the low, medium, and high specimens respectively.

7.2.2 Effect of Corrosion

- In specimens with shear-span to depth ratios of 1.5 and 2.0 the corrosion damage delayed the onset of diagonal shear cracking compared to specimens with a shear-span to depth ratio of 1.0. In specimens with a shear-span to depth ratios of 1.5 and 2.0 there was more corrosion induced cracking because 2 and 3 stirrups were corroded. This causes the compressive load to be transferred through stronger load paths which exist outside of the assumed compressive strut. Consequently, diagonal cracking occurred at higher load levels compared to the control specimens.
- Degradation in the beam stiffness was observed in the corroded specimens compared to the control specimens because the corrosion induced cracking significantly affects the compressive strength of the concrete strut. The average stiffness degradation (comparison of post diagonal cracking stiffness to pre diagonal cracking stiffness) was 5% in the control specimens; whereas, the average stiffness degradation in the corroded specimens was 34%. Specimen H(M)-1.5-R had the largest stiffness degradation of 60%.
- A strength reduction was measured in most corroded specimens. The corrosion induced cracking appears to cause a reduction in the strength of the concrete which negatively affects the shear transfer mechanism. Specimens with a low degree of corrosion had a consistent strength reduction with the exception of specimen M(L)-2.0-R; the average strength reduction compared to the control specimens was found to be 26% (excluding specimen M(L)-2.0-R). Specimen M(L)-2.0-R had a strength reduction of 1%. In the medium specimens, the strength reduction varied considerably with a maximum strength reduction of 53% in specimen M-1.0-R and minimum of 18% in specimen H(M)-2.0-R. The only high corrosion level specimen (H-1.0-R) had a strength reduction of 41%.
- A critical case occurred when the shear reinforcement was inclined and/or has shifting during casting to be more aligned with the angle of load induced diagonal cracking.
- Corrosion cracking influenced the load induced cracking in two ways:
 - Vertical corrosion cracks interrupt load induced crack propagation at low load levels.
 - Load induced cracks “follow” the path of diagonal corrosion cracks.
- The strain behaviour of the corroded shear reinforcement shows that the stirrups remain effective in resisting load until failure.

- A reduction in strain in the main reinforcement is observed in the corroded specimens at the point of failure compared to the control specimens because of the reduction in shear strength observed in the corroded specimens.

7.2.3 Effect of the presence of shear reinforcement

- The shear reinforcement provides limited ductility to the specimens; specimens without shear reinforcement fail in a very sudden manner.
- This limited ductility is provided by restricting the growth of diagonal shear cracks. In the un-reinforced specimens a sudden widening of the diagonal shear cracks was observed.
- The reduction in stiffness (comparing pre diagonal cracking versus post diagonal cracking) was most significant in specimen 0-2.0-UR with a stiffness reduction of 51%.
- The shear reinforcement has an effect on the ultimate shear strength of disturbed regions in reinforced concrete beams.
- Specimens 0-1.0-UR and 0-1.5-UR (with no shear reinforcement) had a strength reduction of 9% and 11% compared to their respective specimens with shear reinforcement. Specimen 0-2.0-UR had a strength reduction of 55% relative to the control (reinforced) specimen.

7.2.4 Effect of Shear-span to Depth Ratio

- A similar trend with respect to stiffness is observed in the corroded specimens with an average pre-diagonal cracking stiffness for specimens with shear-span to depth ratios of 1.0, 1.5, and 2.0 of 108 kN/mm, 72 kN/mm, and 55 kN/mm, respectively.
- The stiffness degradation (comparing pre to post diagonal cracking stiffness) in the control specimens was 7%, 0%, and 9% for the specimens with shear-span to depth ratios of 1.0, 1.5, and 2.0, respectively.
- In the corroded specimens the average stiffness degradation of 30%, 38%, and 34% for the specimens with shear-span to depth ratios of 1.0, 1.5, and 2.0.
- The shear strength of the specimens decreased with respect to increasing shear-span to depth ratio. Specimens 0-1.0-R, 0-1.5-R, and 0-2.0-R had normalized shear strengths of 435 kN (assumed failure load), 365 kN, and 310 kN, respectively.

7.2.5 CFRP Repair

- The strength improvement observed in specimen H(M)-1.5-Repair was 16% compared to specimen M-1.5-R. The specimen did not fail in a flexural mode as was observed in the control specimen for this series. This could be attributed to the fact that the corrosion cracks were not injected with epoxy prior to CFRP repair.
- There was a significant increase in stiffness in the repaired specimen compared to the un-strengthened specimens with a shear-span to depth ratio of 1.5.
- The load at which diagonal cracking occurred in the repaired beam was increased 2.5 times compared to specimen M-1.5-R which had a similar degree of corrosion.

7.2.6 Strut and Tie Modelling

- A more accurate prediction of the shear strength of disturbed regions in reinforced concrete beams can be obtained if the shear reinforcement is considered in a strut and tie model by utilizing the direct and indirect strut and tie mode.
- The model prediction can also be improved if the effectiveness of the shear reinforcement is considered in the calculation. When the shear-span to depth ratio is smaller the direct and indirect struts coincide; indicating that the stirrups are less effective at resisting force. Conversely, the direct and indirect struts do not coincide when the shear-span to depth ratio is larger, so the shear reinforcement is more effective because it must transfer more force.

7.2.7 Effect of Corrosion in Strut and Tie Modelling

- The effect of corrosion can be incorporated into strut and tie modelling in three ways:
 - A reduction in the cross sectional area of the shear reinforcement as a function of average crack width.
 - A reduction in the concrete compressive strength based on the average corrosion crack width.
 - A reduction in the width of the cross section.
- It is clear that a model that incorporates these three elements best predicts the shear strength of disturbed regions with corrosion damaged shear reinforcement.

7.3 Recommendations

This section presents recommendations for future work as it pertains to specimen fabrication, accelerated corrosion, and monotonic testing.

7.3.1 Specimen Fabrication

The specimens were fabricated with bars hooked into a 180° hook designed to prevent an anchorage (shear-tension) failure. The anchorage provided in the specimens was successful in preventing this type of failure. In future studies it is recommended that a standard 90° hook and confinement details (3 stirrups) as recommended in CSA A23.3-04 be provided. Utilizing a 90° hook would allow for easier construction of the reinforcing steel cages. It is also recommended that the reinforcing steel supplier bend the stirrups and the main steel; this is more efficient because the reinforcing steel supplier has an automated process (the reinforcing steel for the current study was bent manually in the engineering machine shop).

Additional water was added to the concrete batch of 1 m³ supplied by the batch plant to produce the unsalted and salted concrete. The strength of the concrete used in this study varied considerably between the salted and unsalted concrete, and between the two different batches. There are two ways to mitigate the concrete strength problems. The local concrete producer suggested that a minimum order of concrete should be 2 m³ to ensure that the mix proportions are correct. Also, the researcher should work closely with the concrete producer to ensure that the concrete truck driver does not add water after initial batching. The mix design can also be verified from the batching ticket provided by the concrete supplier; if there are inaccuracies, the amount of water added to the truck can be adjusted on site. In addition, further investigation into the effect of salt on the strength gain of the concrete should be conducted.

7.3.2 Accelerated Corrosion

The shear reinforcement was successfully corroded, but after analysing the results from the mass loss analysis it is apparent that the technique could be improved. There were significant variations in the mass loss of stirrups that should have had the same theoretical mass loss. It is recommended that future studies explore this problem through small-scale experiments to corrode specimens with 3 or more stirrups for a 3 to 4 month period of time. The bars that were utilized as anodes were heavily corroded in some cases; consequently, if they were stainless steel this corrosion could be limited.

7.3.3 Monotonic Testing

One of the most important aspects of shear in reinforced concrete is the shear-span to depth ratio. This study focused on specimens with a shear- span to depth ratio less than 2.0; the type of load transfer mechanism within these beams is completely different than beams with larger shear-span to depth ratios. It is recommended that future studies incorporate slender beams; the corrosion setup (with recommended modifications) used for the current study would be appropriate.

A typical method of performing shear tests for deep beams is with four-point loading. It is recommended that future studies incorporate this type of loading. There were two reasons why this loading configuration was not used in the current study: the corrosion of stirrups needed to be localized to one span and the span that was not corroded would have to be strengthened to ensure that failure occurred within the corroded span. This problem could be overcome by incorporating more stirrups in the un-corroded span. FRP could also be utilized as external strengthening. It is important to consider the overall strength of the specimens in the design of the experiment.

In some cases the corrosion environment (constant moisture) caused the strain gauges on the reinforcing steel to fail. This is a problem that needs to be addressed for future studies. The strain gauges should be installed to ensure that they are not exposed to rust build-up on the surface of the reinforcing steel.

7.3.4 Repair Methods

One typical method of repairing structures with cracked concrete is to inject epoxy into the cracks. This helps to prevent moisture ingress which is an important contributor to the corrosion process, and epoxy injection can structurally repair the cracked concrete. It is recommended that this method of repair be investigated. The feasibility of utilizing CFRP to repair corrosion damaged disturbed regions was investigated with one specimen. Further research is necessary to determine the optimal repair procedure that utilizes epoxy injection and CFRP repair.

Bibliography

- ACI Committee 318 (2005). Building Code Requirements for Structural Concrete. Farmington Hills, Michigan: American Concrete Institute.
- ACI Committee 222. (2001) Protection of Metals in Concrete against Corrosion (ACI 222-01). Farmington Hills, Michigan: American Concrete Institute.
- Aguilar, G., Matamoros, A. B., Parra-Montesinos, G. J., Ramirez, J.A., and Wight, J.K. (2002). Experimental evaluation of design procedures for shear strength of deep reinforced concrete beams. *ACI Structural Journal*, 99(4), 539-548.
- Almusallam, A.A. et al. (1996a). Effect of reinforcement corrosion on bond strength. *Construction and Building Materials*, 10(2), 123-129.
- Almusallam, A.A. et al. (1996b). Effect of reinforcement corrosion on flexural behavior of concrete slabs. *Journal of Materials in Civil Engineering*, 8(3), 123-127.
- Almusallam, A. A. (2001). Effect of degree of corrosion on the properties of reinforcing steel bars. *Construction and Building Materials*. 15(8), 361-368.
- Al-Sulaimani, G. J. et al. (1990) Influence of Corrosion and Cracking on Bond Behavior and Strength of Reinforced Concrete Members. *ACI Structural Journal*. 87(2). 220-231.
- Auyeng, Y., Balaguru. P., and Chung, L. (2000). Bond behavior of corroded reinforcement bars. *ACI Materials Journal*, 97(2), 214-221.
- Badawi, M. A. (2003). Flexural response of uniform and shear-span corroded RC beams repaired with CFRP laminates. MASC Thesis, University of Waterloo, Waterloo, Ontario, Canada.
- Bazant, Z.P. and Kim, J.K. (1984). Size Effect in Shear Failure of Longitudinally Reinforced Concrete Beams. *ACI Structural Journal*, 81(5), 456-468.
- Broomfield, J. P. (1997). Corrosion of steel in concrete. New York: Taylor & Francis.

- Chung, L., Najm, H., and Balaguru, P. (2008). Flexural behavior of concrete slabs with corroded bars. *Cement and Concrete Composites*, 30(8), 184-193.
- CEB-FIP. (1990). *Model code 1990 – Design Code*. London, England: Thomas Telford Services Ltd.
- CEB-FIP. (1999). *Practical Design of Structural Concrete*. London, England: SETO.
- Clark, A. P. (1951). Diagonal tension in reinforced concrete beams. *ACI Journal*, 48(2), 145–156.
- Craig, B.C. (2002). *Confining effects of FRP laminates on corroded concrete members*. MASC Thesis, University of Waterloo, Waterloo, Ontario, Canada.
- CSA A23.3-04. (2006). *CSA A23.3-04 Design of Concrete Structures Standard*. Ottawa, Ontario: Cement Association of Canada.
- El-Maaddawy, T. and Soudki, K. (2003). Effectiveness of impressed current technique to simulate corrosion of steel reinforcement in concrete. *ASCE Materials Journal*, 15(1), 41-47.
- El-Maaddawy, T. A. Z. (2004). *Performance of corrosion-damaged reinforced concrete beams repaired with CFRP laminates*. PhD Thesis, University of Waterloo, Waterloo, Ontario, Canada.
- Fang, C., Lundgren, K., Chen, L., and Zhu, C. (2004). Corrosion influence on bond in reinforced concrete. *Cement and Concrete Research*, 34(11), 2159-2167.
- FHWA. (2002). *Corrosion costs and preventative strategies in the United States*. Publication No. FHWA-RD-01-156. Retrieved August 3, 2008 from the World Wide Web: http://events.nace.org/publicaffairs/images_cocorr/ccsupp.pdf
- FIB Bulletin 10. (2000). *Bond of Reinforcement in Concrete (FIB 10)*. Federation Internationale du Beton, Lausanne, Switzerland.
- Fraczek, J. (1987). *A Review of Electrochemical Principles as Applied to Corrosion of Steel in a Concrete or Grout Environment*. ACI SP-102, *Corrosion, concrete and Chlorides – Steel in Concrete: Causes and Restraints*. Farmington Hills, Michigan: American Concrete Institute.
- Higgins, C. and Farrow, W. C. (2006). Tests of reinforced concrete beams with corrosion damaged stirrups. *ACI Structural Journal*, 103(1), 133-141.

- Higgins, C., Farrow, W.C., Potisuk, T., Miller, T.H., Yim, S.C., Holocomb, G.R., Cramer, S.D., Covino, B.S., and Bullard, S.J. (2003). Shear Capacity Assessment of Corrosion Damaged Reinforced Concrete Beams. Oregon Department of Transportation. Retrieved March 31, 2008 from the World Wide Web:
http://www.oregon.gov/ODOT/TD/TP_RES/docs/Reports/ShearCapacity.pdf and
http://www.oregon.gov/ODOT/TD/TP_RES/docs/Reports/shear_capacity_app.pdf
- ISIS Canada. (2008). FRP Rehabilitation of Reinforced Concrete Structures. Winnipeg, Manitoba: ISIS Canada.
- Jones, D.A. (1996) Principles and prevention of corrosion. New Jersey: Prentice Hall
- Kage, T., Abe, M., and Lee, H. (1997). Effect of CFRP sheets on shear strengthening of RC beams damaged by corrosion of stirrup. Proceedings: Non-Metallic (FRP) Reinforcement for Concrete Structures, Third International Symposium, 443-450.
- Kong, F. and Robins, P. J. (1970). Web reinforcement effects on deep beams. ACI Journal. Title No. 67-73. 1010-1018.
- Liu, Y. and Weyers, R. (1998). Modeling the time-to-corrosion cracking in chloride contaminated reinforced concrete structures. ACI Materials Journal, 95(6), 675-681.
- MacGregor, J.G. and Bartlett, F.M. (2000) Reinforced Concrete Mechanics and Design. Toronto, Ontario: Pearson Education Canada Inc.
- Magnat, P.S. and Elgarf, M. S. (1999). Flexural strength of concrete beams with corroding reinforcement. ACI Structural Journal, 96(1), 149-159.
- Masoud, S. G. (2002). Behaviour of corroded reinforced concrete beams repaired with FRP sheets under monotonic and fatigue loads. PhD Thesis, University of Waterloo, Waterloo, Ontario, Canada.
- Matamoros, A. B. and Wong, K. H. (2003). Design of Simply Supported Deep Beams Using Strut-and-Tie Models. ACI Structural Journal, 100(6), 704-712.
- Neville, A. M. (1996). Properties of concrete. New York: John Wiley and Sons.

- Oh, J. and Shin, S. (2001). Shear strength of reinforced high-strength concrete deep beams. *ACI Structural Journal*, 98(2), 164-173.
- de Paiva, H. A. R. and Siess, C. P. (1965). Strength and behaviour of deep beams in shear. *Journal of the Structural Division – Proceedings of the American Society of Civil Engineers*, ST 5, 19-41.
- Ramin, M. and Matamoros, A. B. (2006). Shear Strength of Reinforced Concrete Members Subjected to Montonic Loads. *ACI Structural Journal*, 103(1), 83-92.
- Regan, P.E. and Kennedy Reid, I. L. (2004). Shear strength of RC beams with defective stirrup anchorages. *Magazine of Concrete Research*, 56(3), 159-166.
- Rodriguez, J., Ortega, L., and Casal, J. (1997). Load carrying capacity of concrete structures with corroded reinforcement. *Construction and Building Materials*, 11(4), 239-248.
- Rogowsky, D.M. and MacGregor, J.G. (1986 August). Design of Reinforced Concrete Deep Beams. *Concrete International*, 49-58.
- Russo, G. and Puleri, G. (1997). Stirrup Effectiveness in Reinforced Concrete Beams under Flexure and Shear. *ACI Structural Journal*, 94(3), 227-238.
- Russo, G., Venir R. and Pauletta M. (2005). Reinforced Concrete Deep Beams – Shear Strength Model and Design Formula. *ACI Structural Journal*, 102(3), 429-437.
- Schiesl, P. and Raupach, M. (1997). Laboratory Studies and Calculations on the Influence of Crack Width on Chloride-Induced Corrosion of Steel in Concrete. *ACI Materials Journal*, 94(1), 56-62.
- Sherwood, E. G. (2000). Behaviour of corroded reinforced concrete beams strengthened with CFRP laminates. MASC Thesis, University of Waterloo, Waterloo, Ontario, Canada.
- Shin, S., Lee, K., Moon, J., and Ghosh, S. K. (1999). Shear strength of reinforced high-strength concrete beams with shear span-to-depth ratios between 1.5 and 2.5. *ACI Structural Journal*, 96(4), 549–556.
- Smith, K.N. and Vantsiotis, A.S. (1982). Shear strength of deep beams. *ACI Structural Journal*, 79(22), 201-213.

Sungho, T., Hanseung, L., and Taesoo, K. (2007). Shear retrofitting effect of RC beams damaged by corrosion of stirrup strengthened with CFS. *Key Engineering Materials*, 348-349, 441-444.

Tan, K., Kong, F., Teng, S. and Guan, L. (1995). High-strength concrete deep beams with effective span and shear span variations. *ACI Structural Journal*, 92(4), 395–405.

Tan, K., Kong, F., Teng, S. and Weng, L. (1997). Effect of web reinforcement on high-strength concrete deep beams. *ACI Structural Journal*, 94(5), 572-582.

Tan, K., Teng, S., Kong, F. and Lu, H. (1997). Main tension steel in high strength concrete deep and short beams. *ACI Structural Journal*, 94(6), 752-768.

Toongoenthong, K. and Maekawa, K. (2005). Multi-mechanical approach to structural performance assessment of corroded RC members in Shear. *Journal of Advanced Concrete Technology*, 3(1), 107-122.

Val, D. V. (2007). Deterioration of strength of RC beams due to corrosion and its influence on beam reliability. *Journal of Structural Engineering*, 133(9), 1297-1306.

Vidal, T., Castel A. and François, R. (2003). Analyzing crack width to predict corrosion in reinforced concrete. *Cement and Concrete Research*, 34(1), 165-174.

Yun, Y. M. (2000). Nonlinear Strut-Tie Model Approach for Structural Concrete. *ACI Structural Journal*, 97(4), 581-590.

Appendix A

Drawings

List of Drawings

Drawing 1 – Beam Reinforcement

Drawing 2 – Beam Layout

Drawing 3 – Concrete Formwork

Drawing 4 – Reinforcement Bending Schedule

Drawing 5 – Corrosion Wiring Schematic

Drawing 6 – Typical Salted Concrete Distribution

Drawing 7 – Concrete Dividers

Drawing 8 – Drilling Jig – Uprights

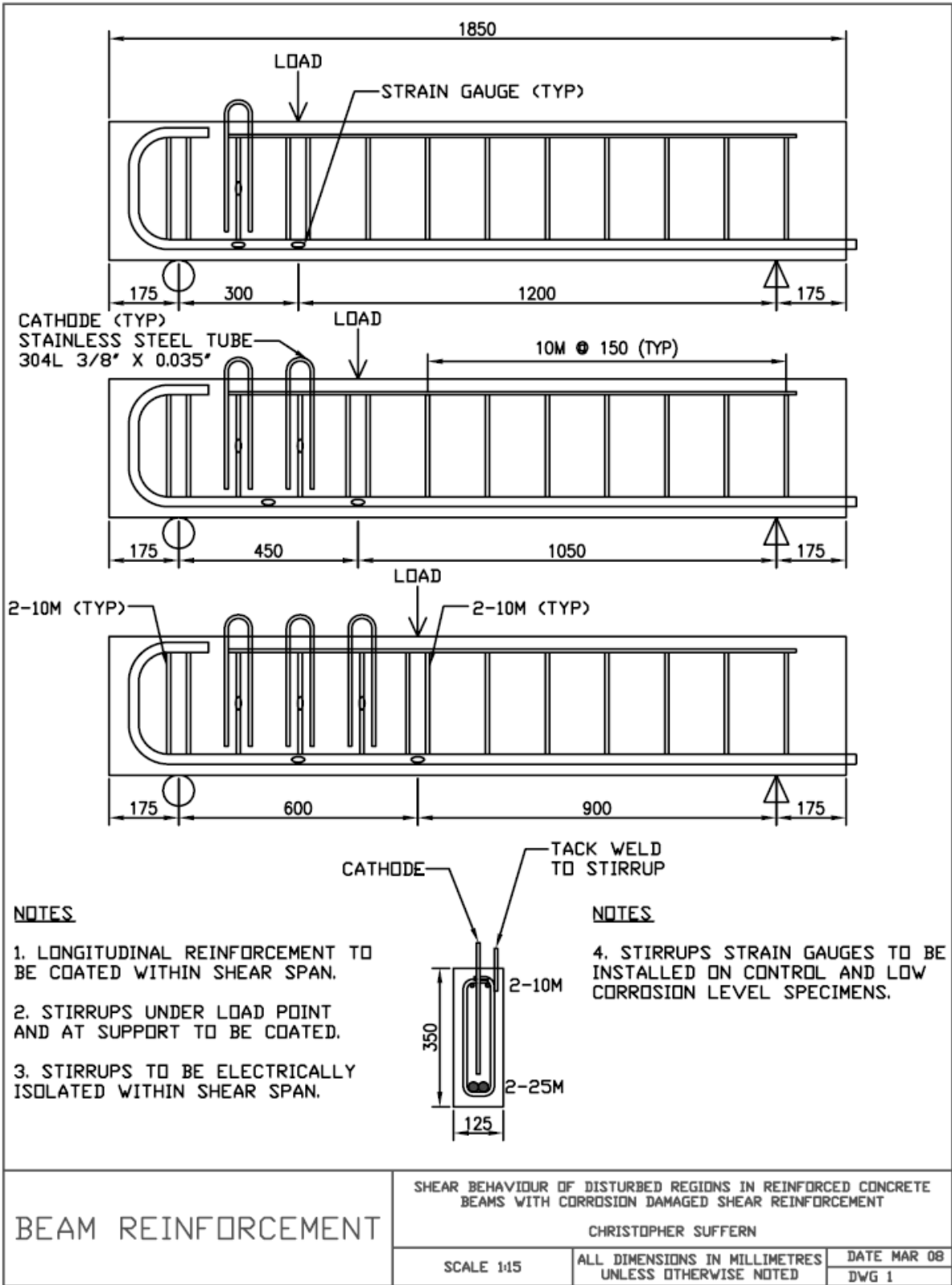
Drawing 9 – Drilling Jig – Base

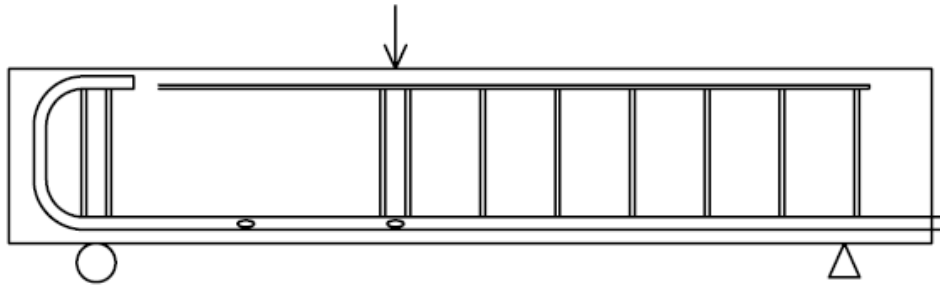
Drawing 10 – Test Setup Elevations

Drawing 11 – Test Setup Sections

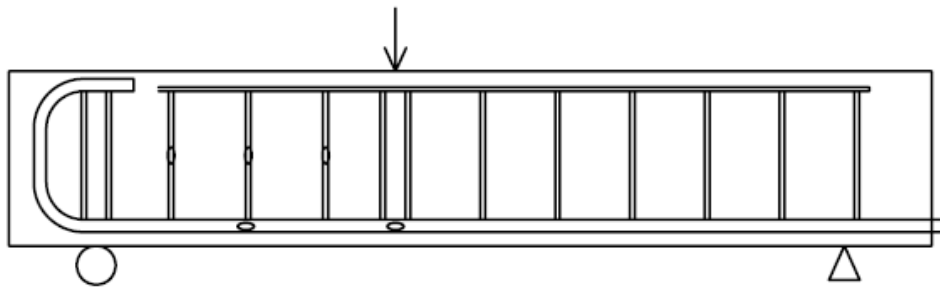
Drawing 12 - Supports

Drawing 13 – Diagonal Displacement Mount

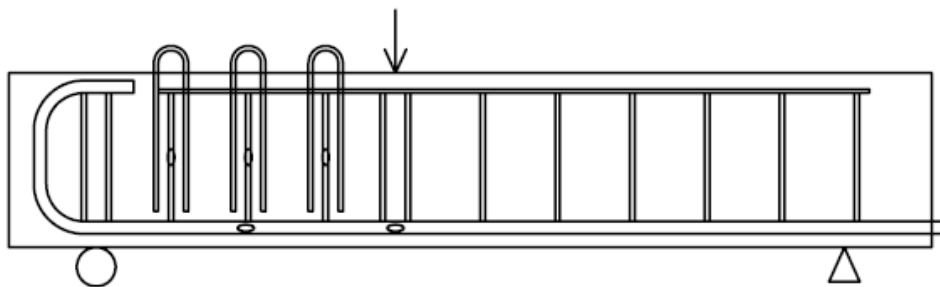




NON-REINFORCED BEAM



CONTROL BEAM



CORROSION BEAM

BEAM TYPE DETAILS

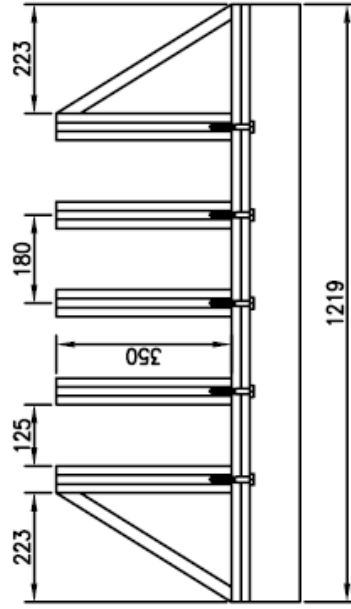
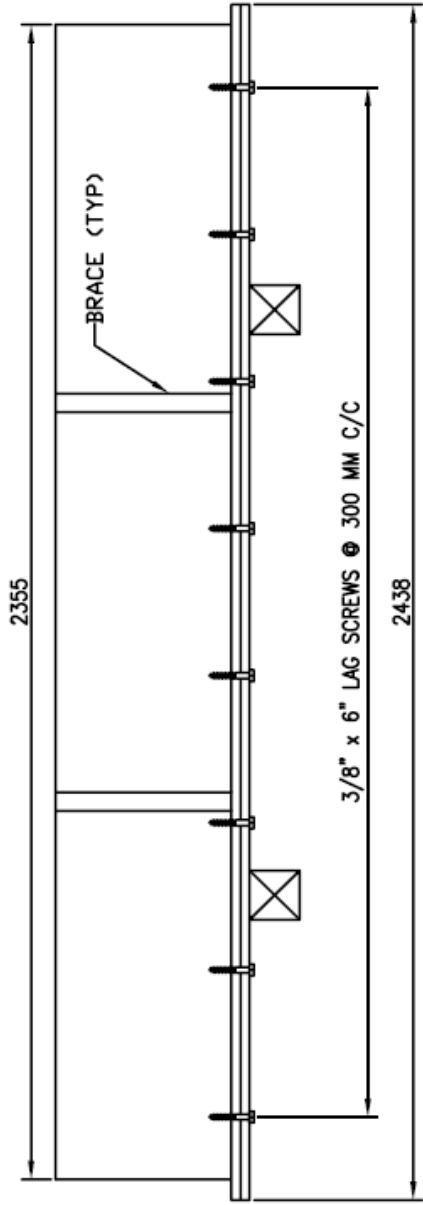
SHEAR BEHAVIOUR OF DISTURBED REGIONS IN REINFORCED CONCRETE BEAMS WITH CORROSION DAMAGED SHEAR REINFORCEMENT

CHRISTOPHER SUFFERN

SCALE 1:15

ALL DIMENSIONS IN MILLIMETRES UNLESS OTHERWISE NOTED

DATE MAR 08
DWG 2



CONCRETE FORMWORK

SHEAR BEHAVIOUR OF DISTURBED REGIONS IN REINFORCED CONCRETE BEAMS WITH CORROSION DAMAGED SHEAR REINFORCEMENT

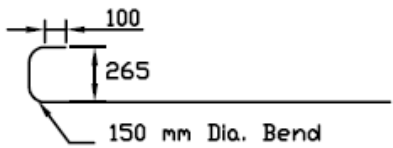
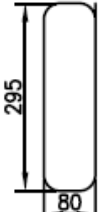
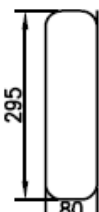
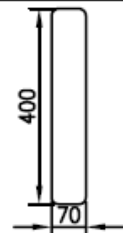
CHRISTOPHER SUFFERN

SCALE 1:15

ALL DIMENSIONS IN MILLIMETRES UNLESS OTHERWISE NOTED

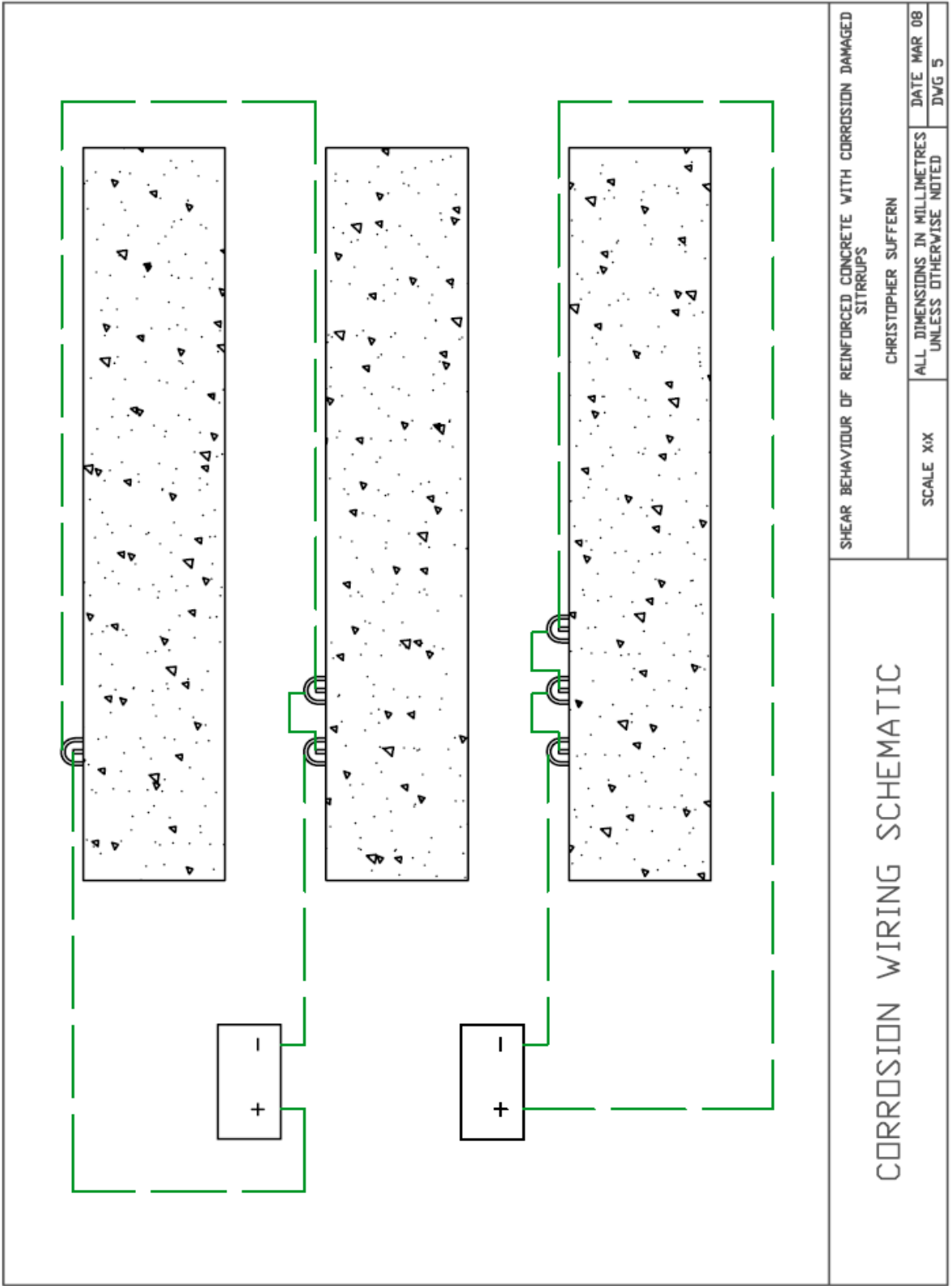
DATE MAR 08

DWG 3

REINFORCEMENT BENDING SCHEDULE			
ITEM	NUMBER	LENGTH	DETAILS
MAIN REINF	32	2235 MM	
STIRRUPS	176	730 MM	
STIRRUPS CORROSION	26	730 MM	
HOOK	32	1010 MM	

NOTE: ALL DIMENSIONS ARE OUTSIDE TO OUTSIDE

REINFORCEMENT BENDING SCHEDULE	SHEAR BEHAVIOUR OF REINFORCED CONCRETE WITH CORROSION DAMAGED STIRRUPS		
	CHRISTOPHER SUFFERN		
SCALE X:1	ALL DIMENSIONS IN MILLIMETRES UNLESS OTHERWISE NOTED	DATE MAR 08	DWG 4



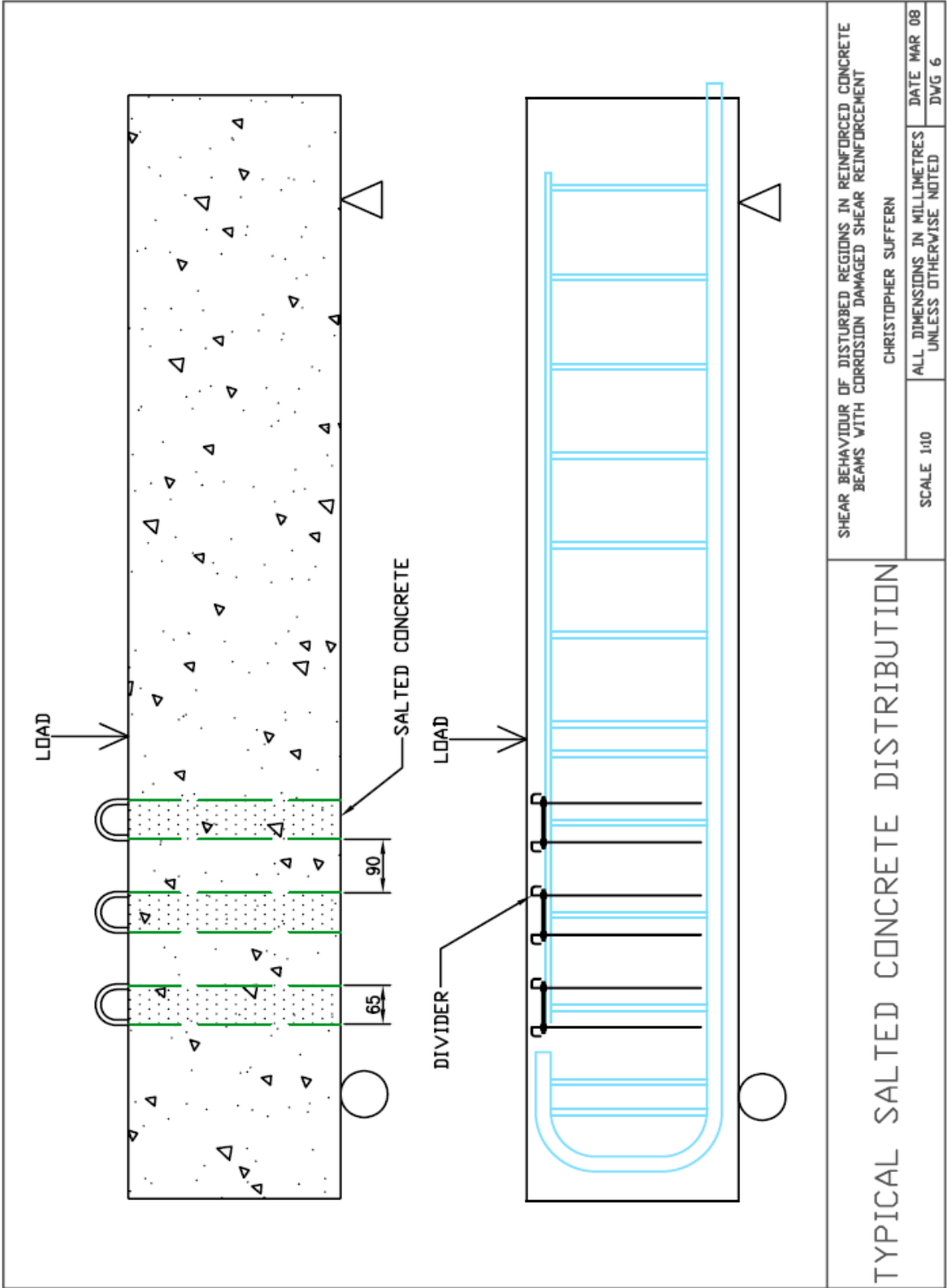
CORROSION WIRING SCHEMATIC

SHEAR BEHAVIOUR OF REINFORCED CONCRETE WITH CORROSION DAMAGED STIRRUPS

CHRISTOPHER SUFFERN

SCALE XIX
 ALL DIMENSIONS IN MILLIMETRES
 UNLESS OTHERWISE NOTED

DATE MAR 08
 DWG 5



SHEAR BEHAVIOUR OF DISTURBED REGIONS IN REINFORCED CONCRETE BEAMS WITH CORROSION DAMAGED SHEAR REINFORCEMENT

CHRISTOPHER SUFFERN

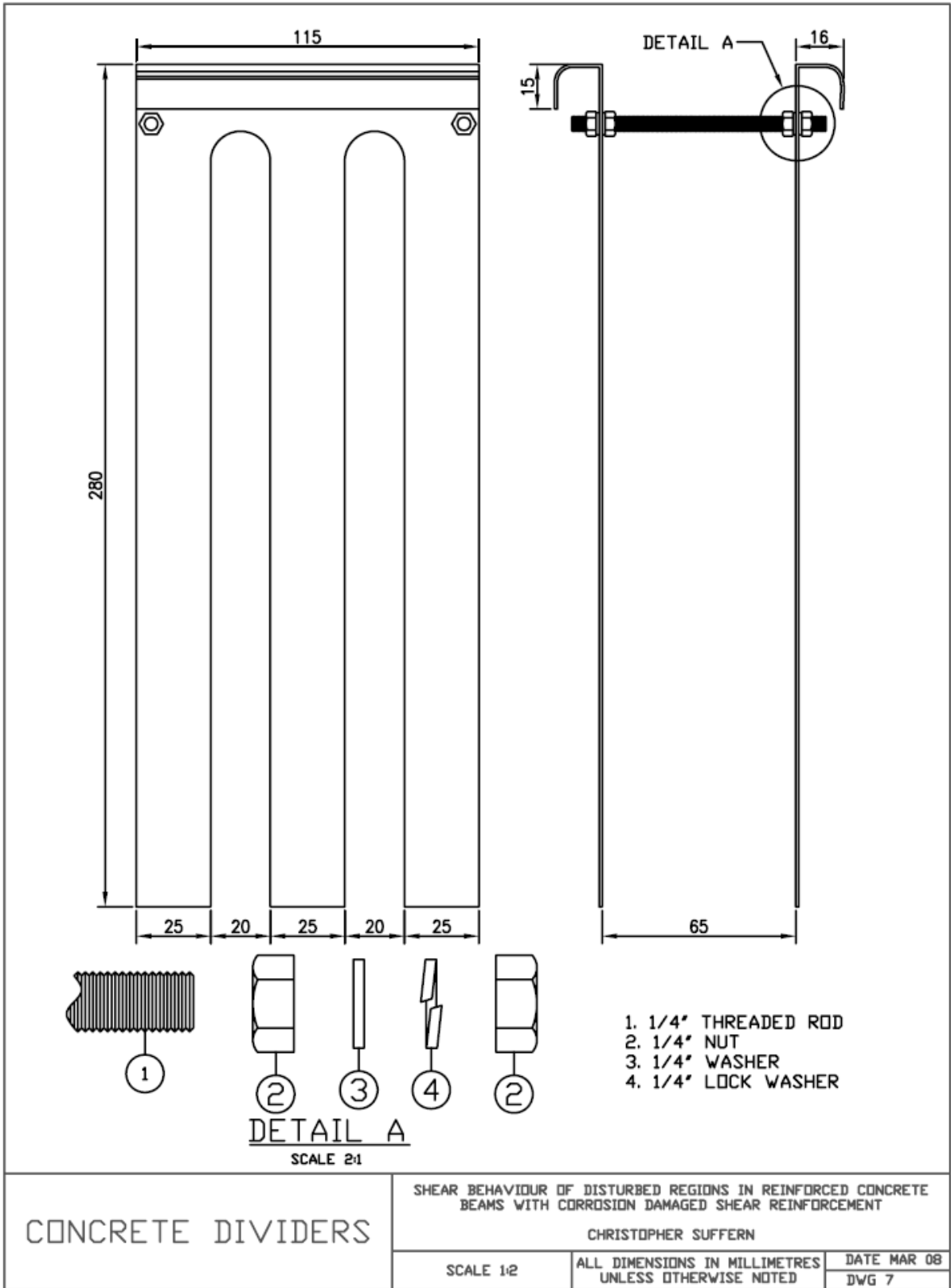
SCALE 1:10

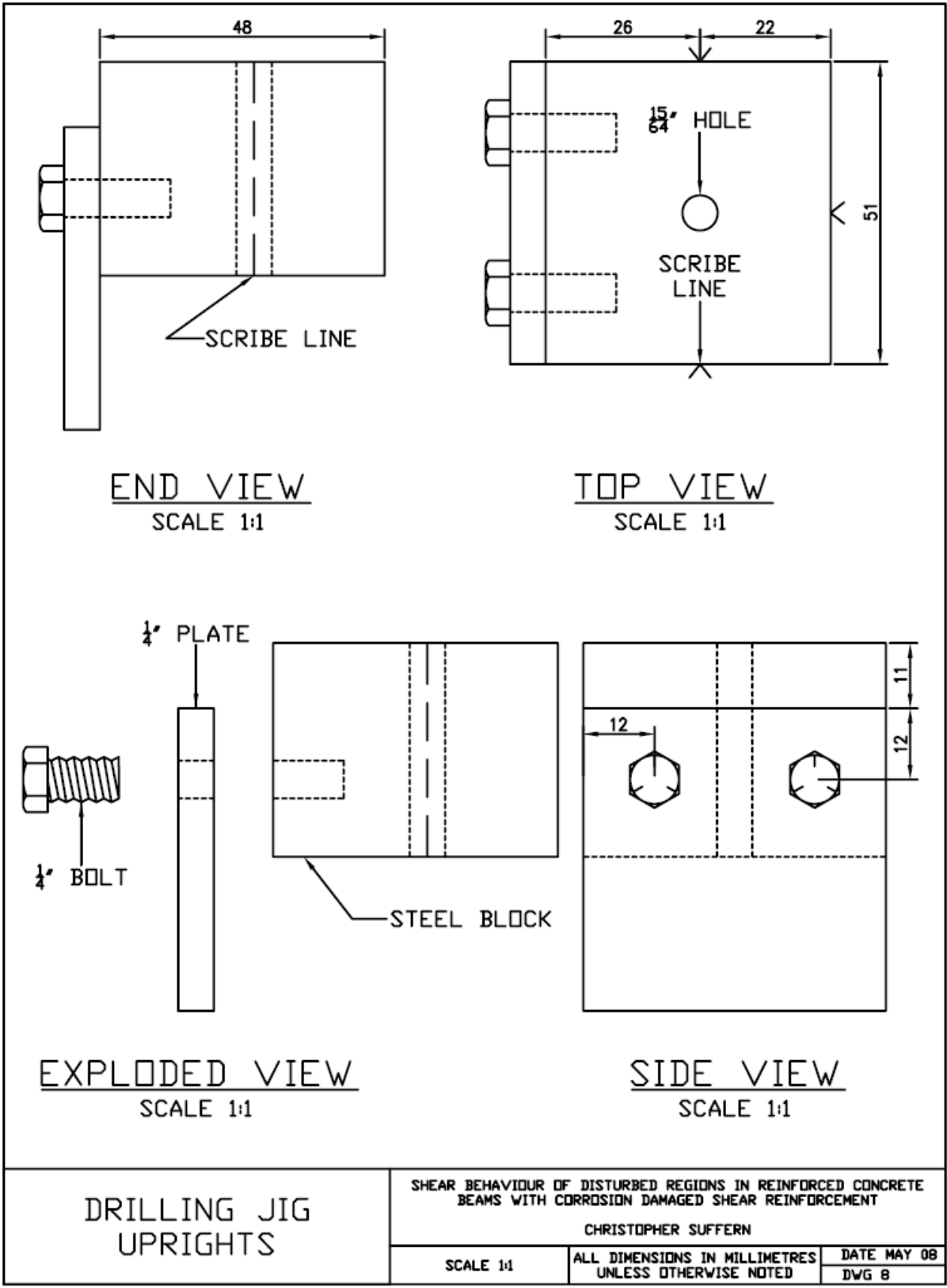
ALL DIMENSIONS IN MILLIMETRES UNLESS OTHERWISE NOTED

DATE MAR 08

DWG 6

TYPICAL SALTED CONCRETE DISTRIBUTION





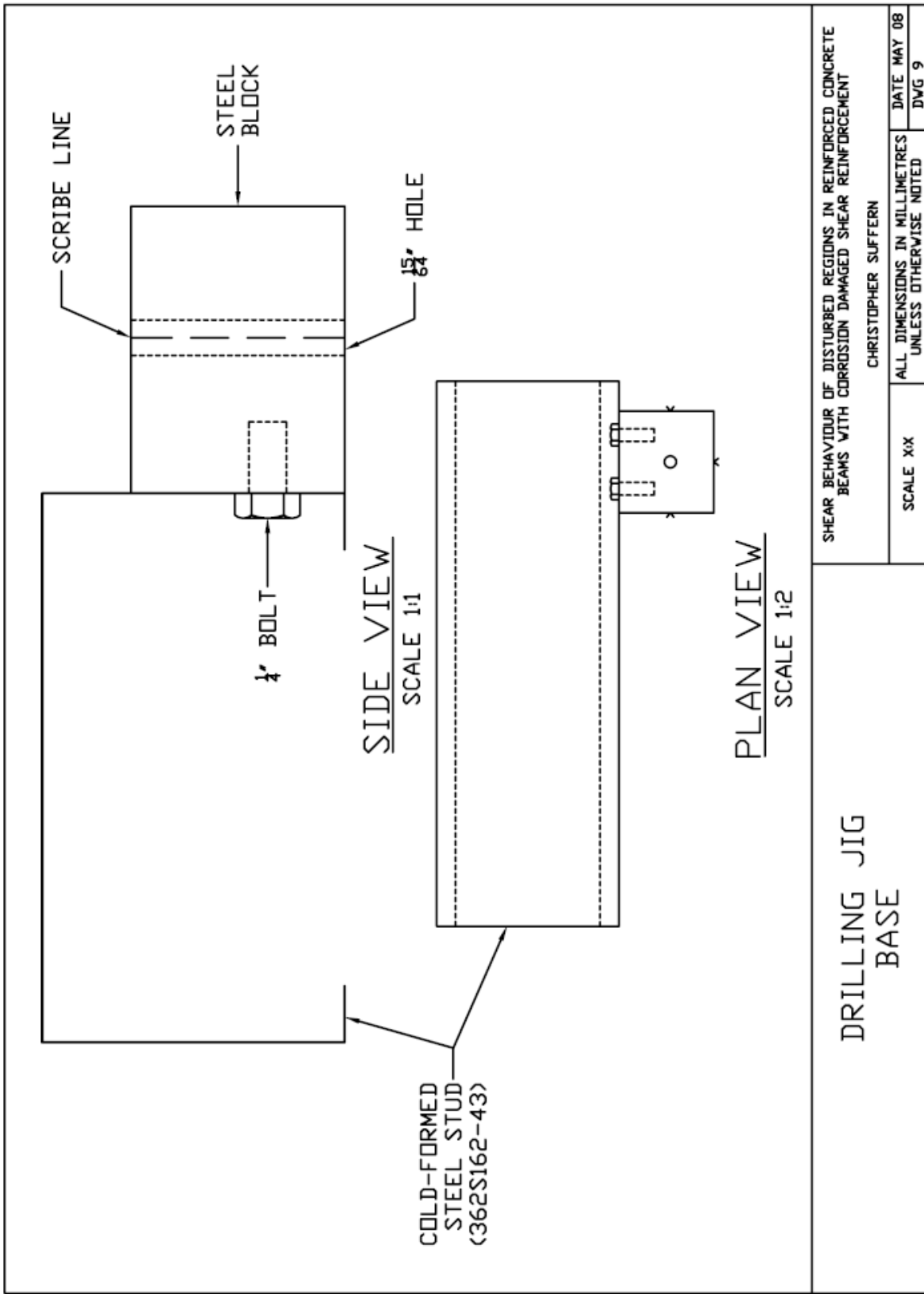
DRILLING JIG
UPRIGHTS

SHEAR BEHAVIOUR OF DISTURBED REGIONS IN REINFORCED CONCRETE
BEAMS WITH CORROSION DAMAGED SHEAR REINFORCEMENT
CHRISTOPHER SUFFERN

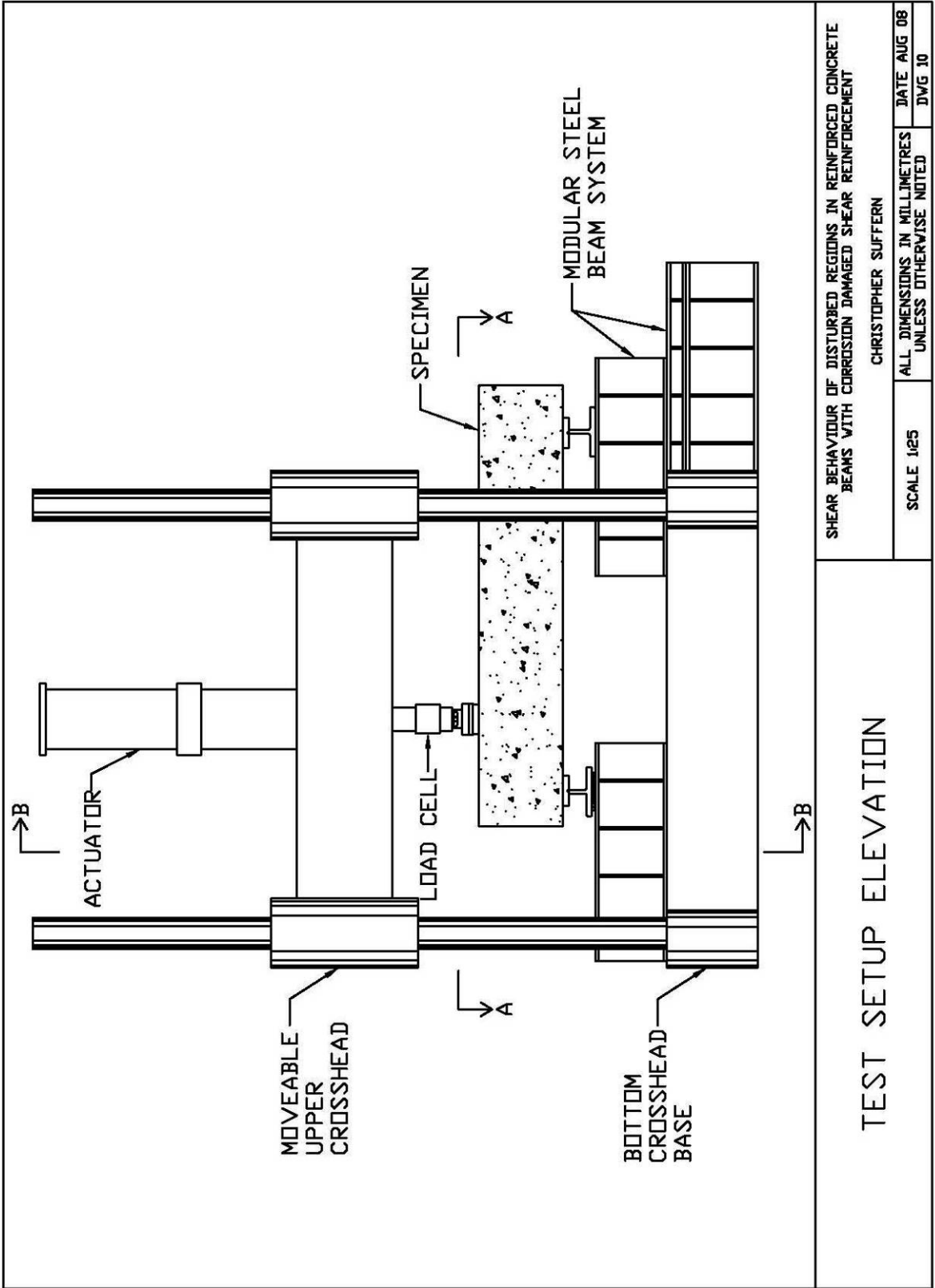
SCALE 1:1

ALL DIMENSIONS IN MILLIMETRES
UNLESS OTHERWISE NOTED

DATE MAY 08
DWG 8



DRILLING JIG BASE		SHEAR BEHAVIOUR OF DISTURBED REGIONS IN REINFORCED CONCRETE BEAMS WITH CORROSION DAMAGED SHEAR REINFORCEMENT	
		CHRISTOPHER SUFFERN	
SCALE XIX	ALL DIMENSIONS IN MILLIMETRES UNLESS OTHERWISE NOTED	DATE MAY 08	DWG 9



SHEAR BEHAVIOUR OF DISTURBED REGIONS IN REINFORCED CONCRETE BEAMS WITH CORROSION DAMAGED SHEAR REINFORCEMENT

CHRISTOPHER SUFFERN

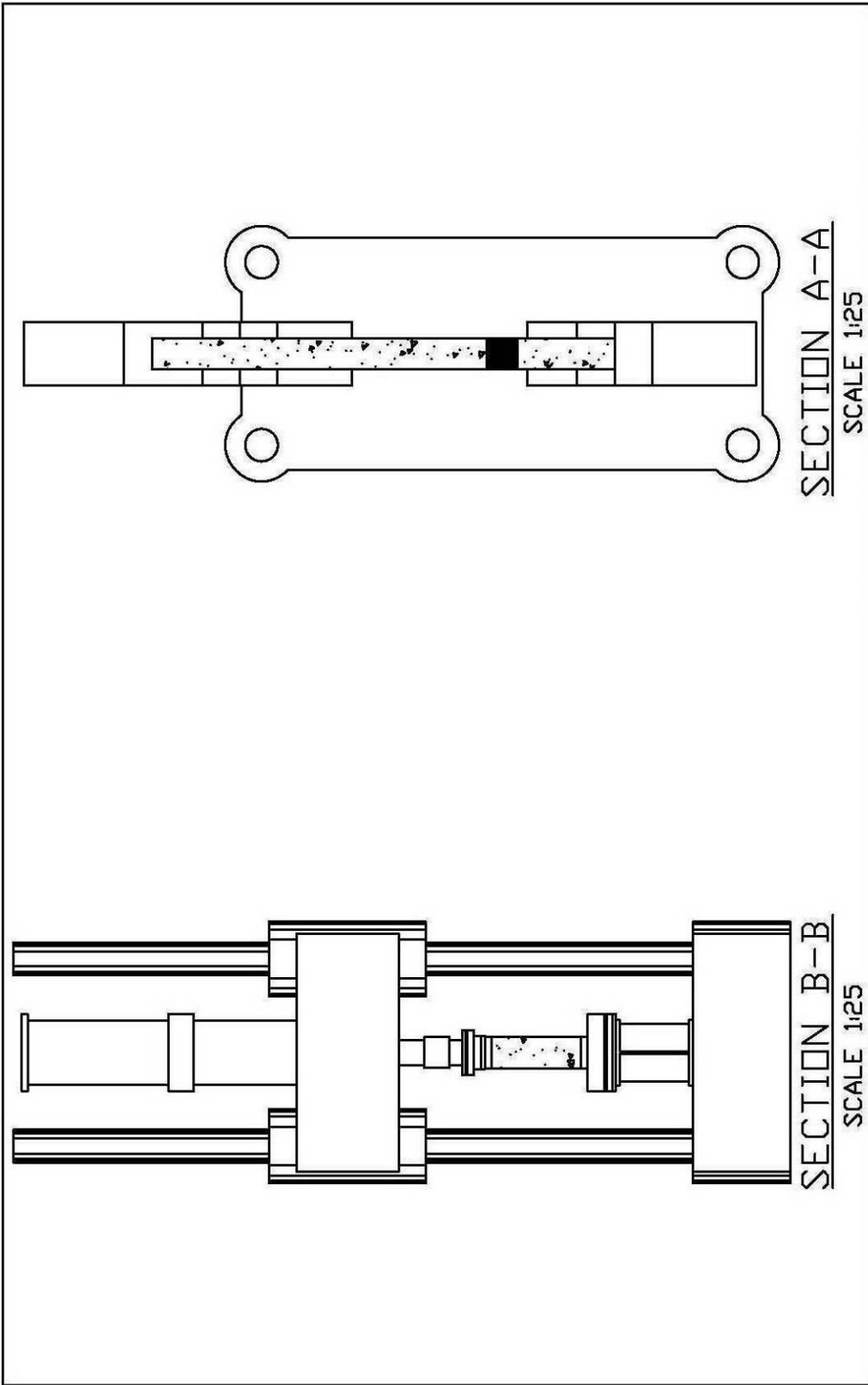
SCALE 1:25

ALL DIMENSIONS IN MILLIMETRES UNLESS OTHERWISE NOTED

DATE AUG 08

DWG 10

TEST SETUP ELEVATION



SHEAR BEHAVIOUR OF DISTURBED REGIONS IN REINFORCED CONCRETE
BEAMS WITH CORROSION DAMAGED SHEAR REINFORCEMENT

CHRISTOPHER SUFFERN

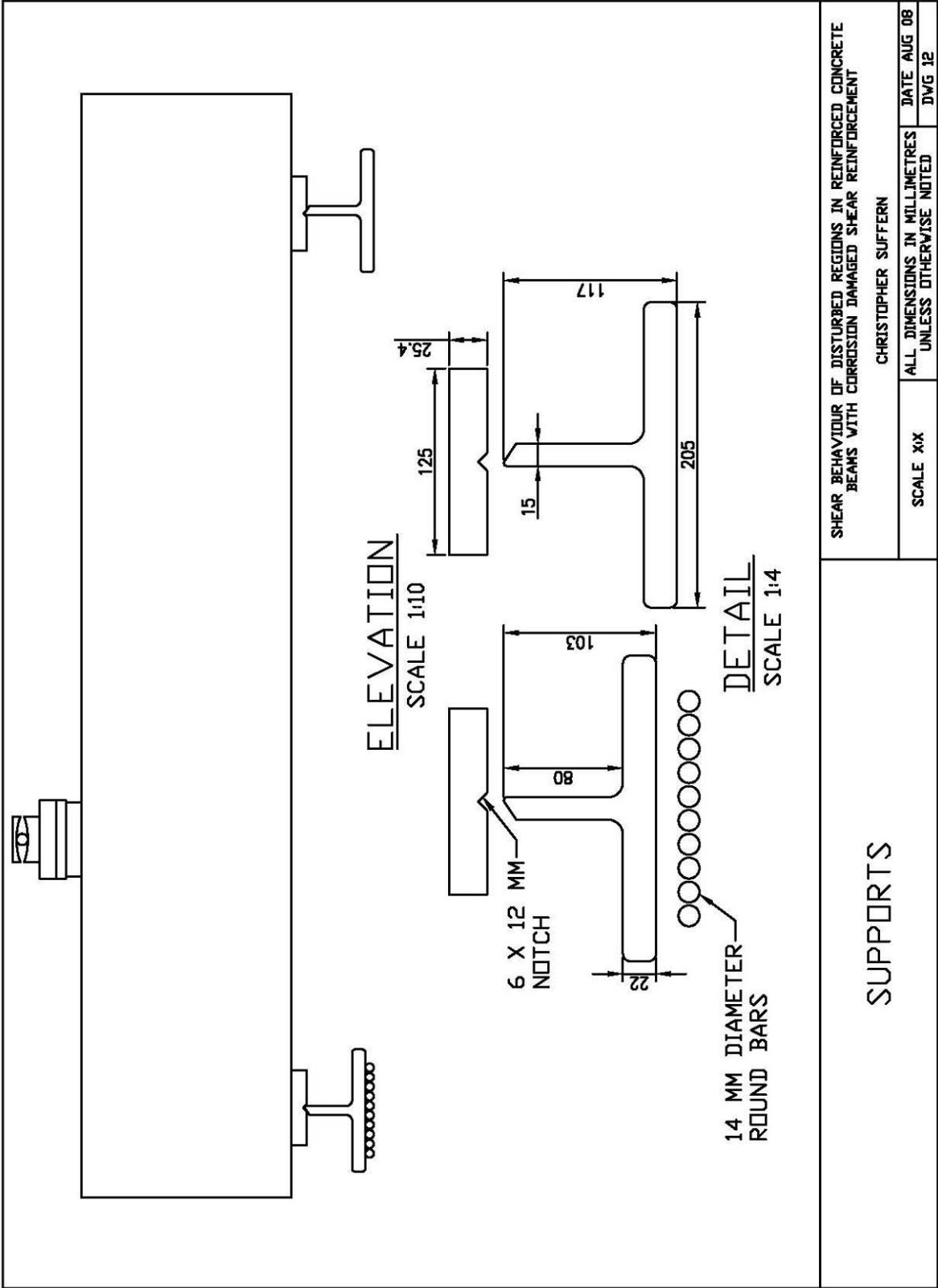
SCALE 1:25

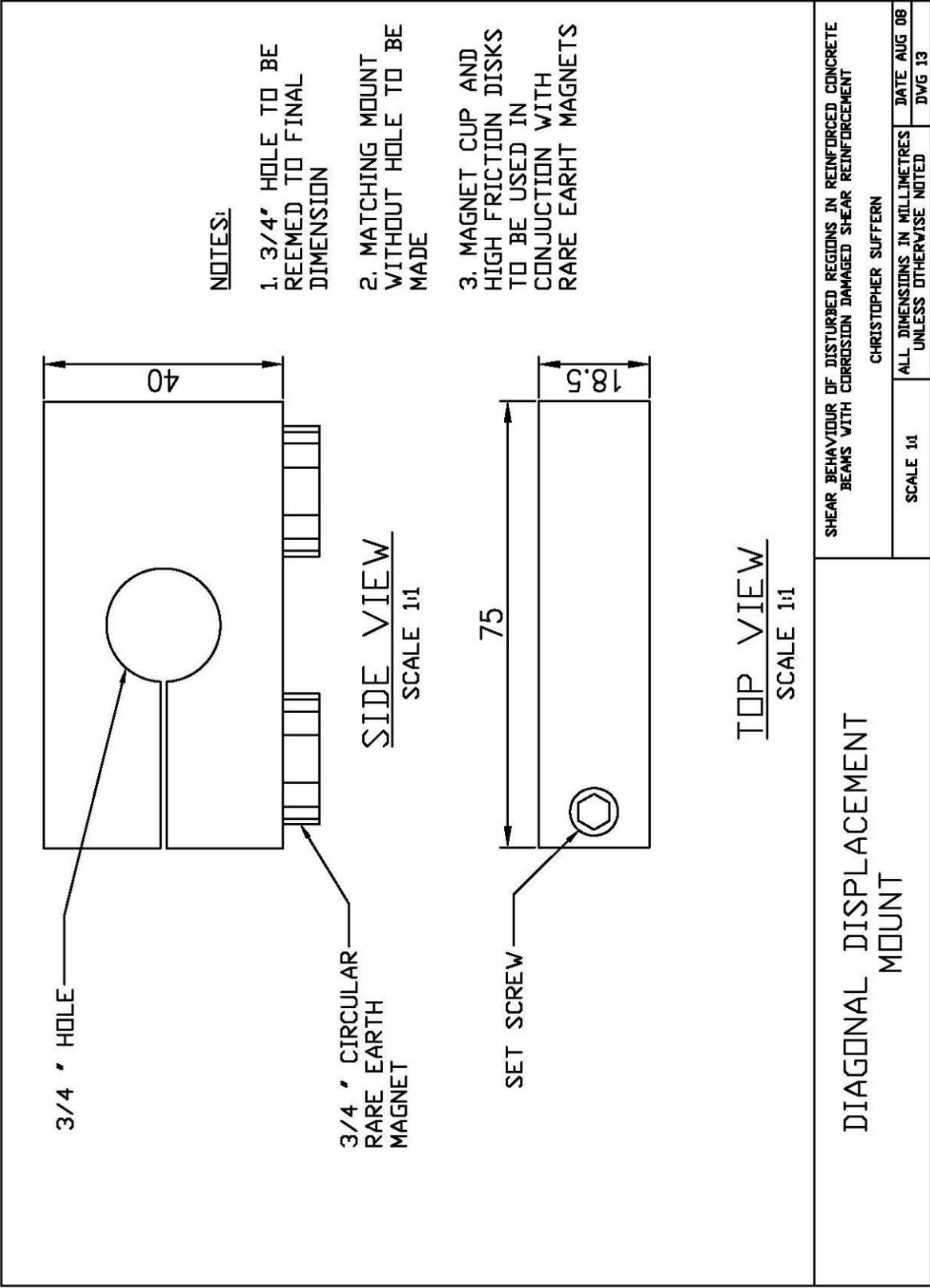
ALL DIMENSIONS IN MILLIMETRES
UNLESS OTHERWISE NOTED

DATE AUG 08

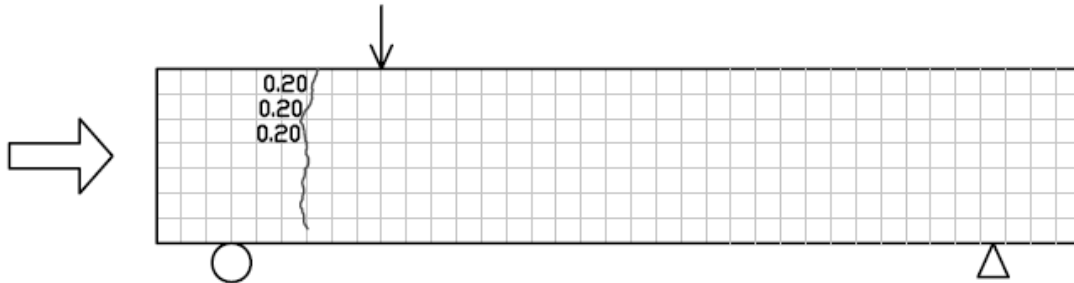
DWG 11

TEST SETUP SECTIONS



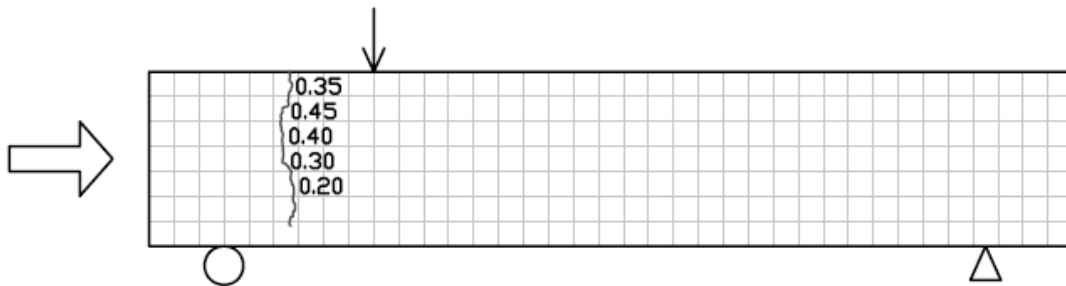


Appendix B
Crack Width Drawings



RIGHT SIDE VIEW

CRACK WIDTH MEASUREMENTS SHOWN ON DRAWING CORRESPOND TO POINT WHERE CRACK CROSSES HORIZONTAL GRIDLINE (BELOW VALUE SHOWN ON DRAWING). IF NO VALUE IS GIVEN THEN CRACK WIDTH IS LESS THAN 0.1 MM.



LEFT SIDE VIEW

CORROSION CRACK
PATTERN
L-1.0-R

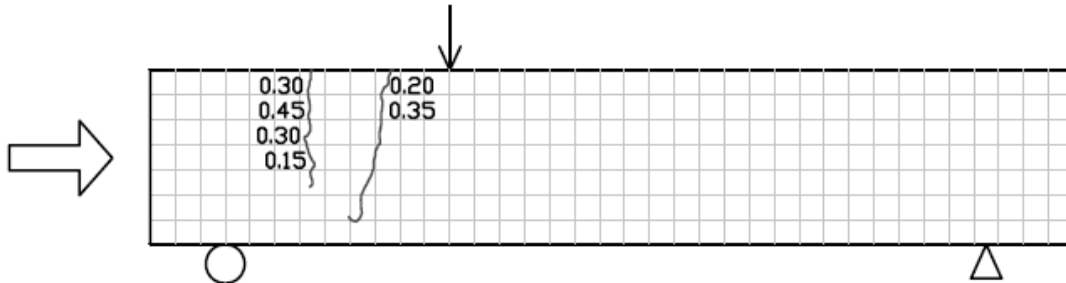
SHEAR BEHAVIOUR OF DISTURBED REGIONS IN REINFORCED CONCRETE
BEAMS WITH CORROSION DAMAGED SHEAR REINFORCEMENT

CHRISTOPHER SUFFERN

SCALE 1:15

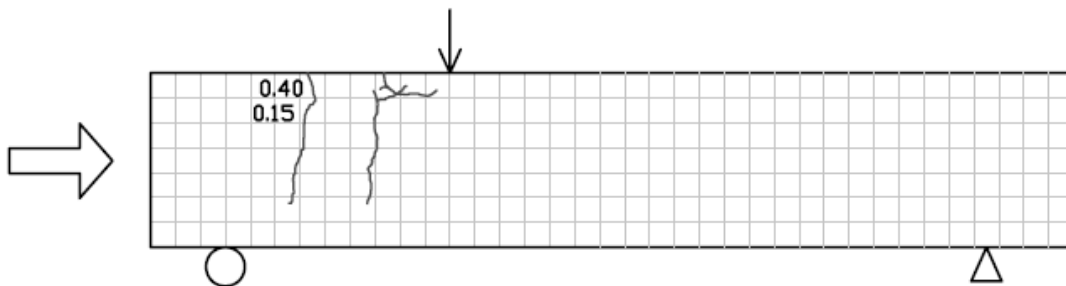
ALL DIMENSIONS IN MILLIMETRES
UNLESS OTHERWISE NOTED

DATE APR 08
DWG 1



RIGHT SIDE VIEW

CRACK WIDTH MEASUREMENTS SHOWN ON DRAWING CORRESPOND TO POINT WHERE CRACK CROSSES HORIZONTAL GRIDLINE (BELOW VALUE SHOWN ON DRAWING). IF NO VALUE IS GIVEN THEN CRACK WIDTH IS LESS THAN 0.1 MM.



LEFT SIDE VIEW

CORROSION CRACK
PATTERN
L-1.5-R

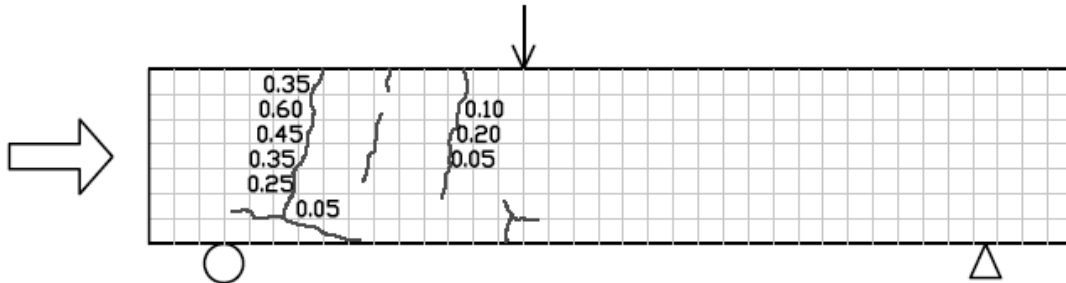
SHEAR BEHAVIOUR OF DISTURBED REGIONS IN REINFORCED CONCRETE
BEAMS WITH CORROSION DAMAGED SHEAR REINFORCEMENT

CHRISTOPHER SUFFERN

SCALE 1:15

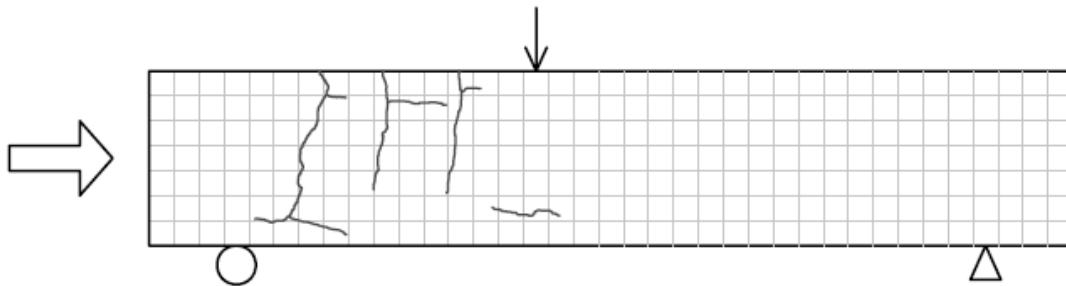
ALL DIMENSIONS IN MILLIMETRES
UNLESS OTHERWISE NOTED

DATE APR 08
DWG 2



RIGHT SIDE VIEW

CRACK WIDTH MEASUREMENTS SHOWN ON DRAWING CORRESPOND TO POINT WHERE CRACK CROSSES HORIZONTAL GRIDLINE (BELOW VALUE SHOWN ON DRAWING). IF NO VALUE IS GIVEN THEN CRACK WIDTH IS LESS THAN 0.1 MM.



LEFT SIDE VIEW

CORROSION CRACK
PATTERN
L-2.0-R

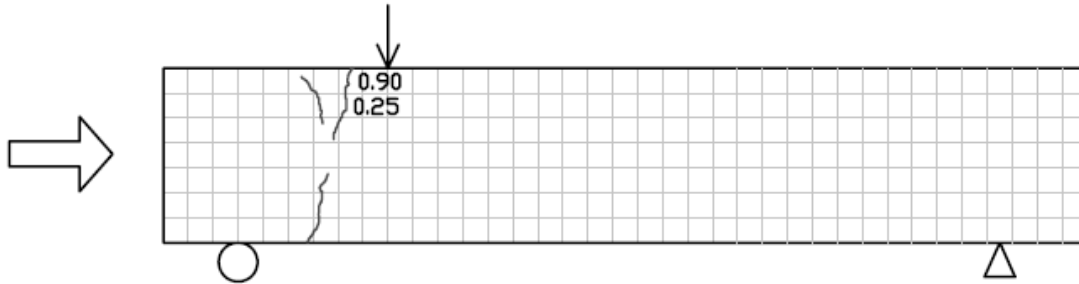
SHEAR BEHAVIOUR OF DISTURBED REGIONS IN REINFORCED CONCRETE
BEAMS WITH CORROSION DAMAGED SHEAR REINFORCEMENT

CHRISTOPHER SUFFERN

SCALE 1:15

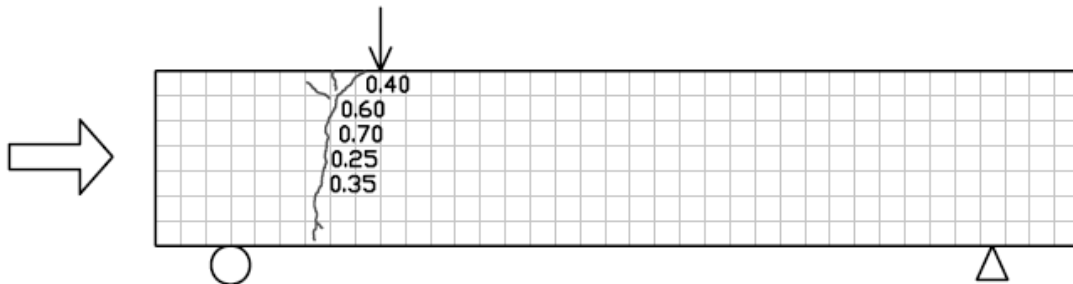
ALL DIMENSIONS IN MILLIMETRES
UNLESS OTHERWISE NOTED

DATE APR 08
DWG 3



RIGHT SIDE VIEW

CRACK WIDTH MEASUREMENTS SHOWN ON DRAWING CORRESPOND TO POINT WHERE CRACK CROSSES HORIZONTAL GRIDLINE (BELOW VALUE SHOWN ON DRAWING). IF NO VALUE IS GIVEN THEN CRACK WIDTH IS LESS THAN 0.1 MM.



LEFT SIDE VIEW

CORROSION CRACK
PATTERN
M-1.0-R

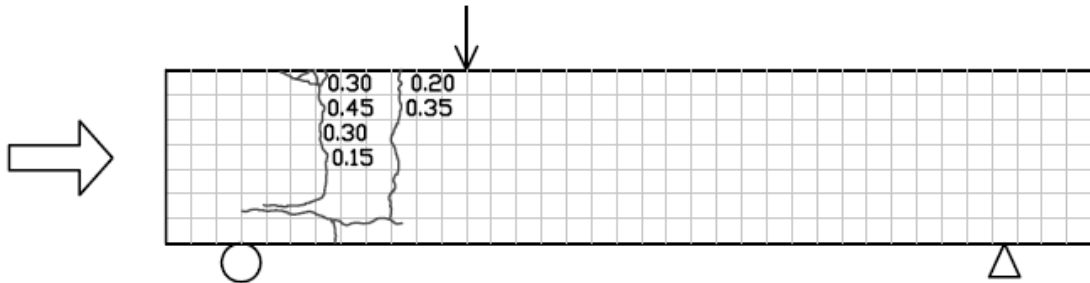
SHEAR BEHAVIOUR OF DISTURBED REGIONS IN REINFORCED CONCRETE
BEAMS WITH CORROSION DAMAGED SHEAR REINFORCEMENT

CHRISTOPHER SUFFERN

SCALE 1:15

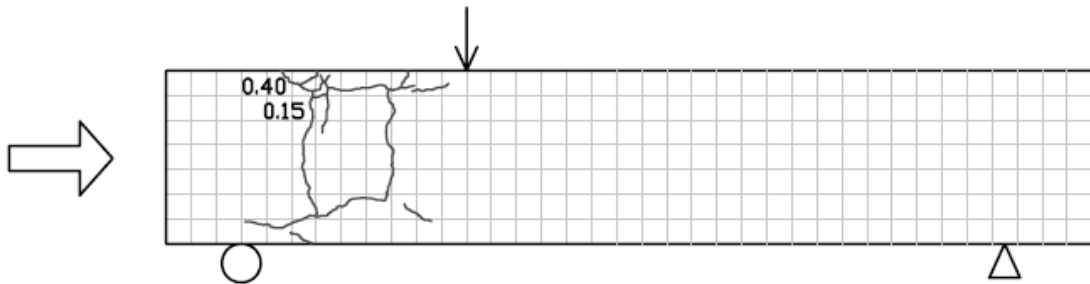
ALL DIMENSIONS IN MILLIMETRES
UNLESS OTHERWISE NOTED

DATE APR 08
DWG 4



RIGHT SIDE VIEW

CRACK WIDTH MEASUREMENTS SHOWN ON DRAWING CORRESPOND TO POINT WHERE CRACK CROSSES HORIZONTAL GRIDLINE (BELOW VALUE SHOWN ON DRAWING). IF NO VALUE IS GIVEN THEN CRACK WIDTH IS LESS THAN 0.1 MM.



LEFT SIDE VIEW

CORROSION CRACK
PATTERN
M-1.5-R

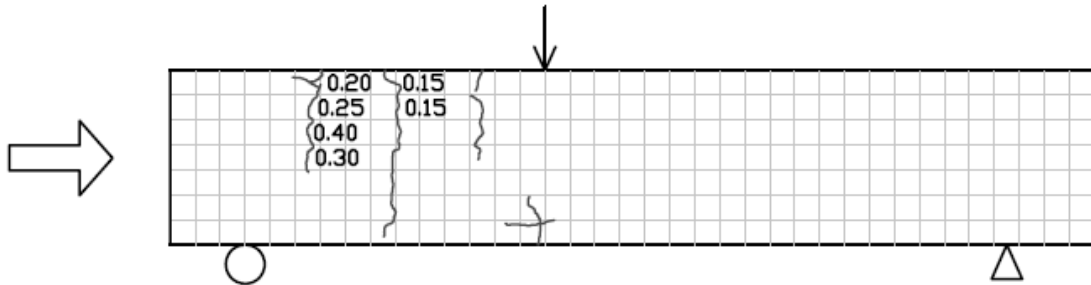
SHEAR BEHAVIOUR OF DISTURBED REGIONS IN REINFORCED CONCRETE
BEAMS WITH CORROSION DAMAGED SHEAR REINFORCEMENT

CHRISTOPHER SUFFERN

SCALE 1:15

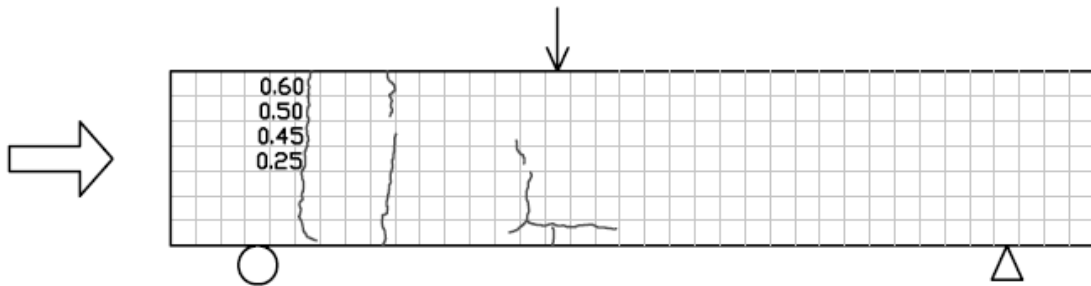
ALL DIMENSIONS IN MILLIMETRES
UNLESS OTHERWISE NOTED

DATE APR 08
DWG 5



RIGHT SIDE VIEW

CRACK WIDTH MEASUREMENTS SHOWN ON DRAWING CORRESPOND TO POINT WHERE CRACK CROSSES HORIZONTAL GRIDLINE (BELOW VALUE SHOWN ON DRAWING). IF NO VALUE IS GIVEN THEN CRACK WIDTH IS LESS THAN 0.1 MM.



LEFT SIDE VIEW

CORROSION CRACK
PATTERN
M(L)-2.0-R

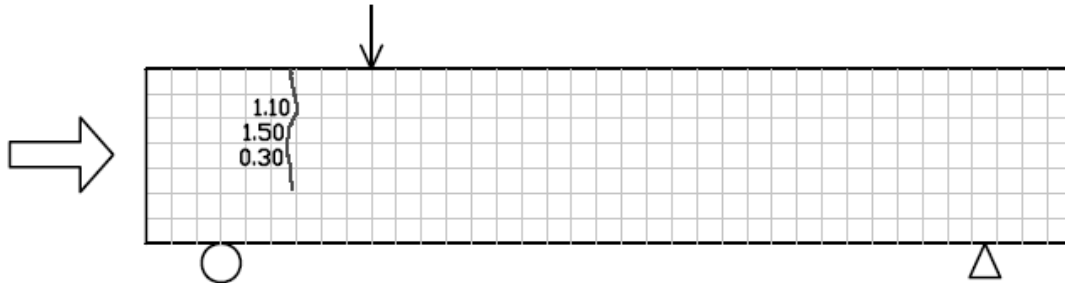
SHEAR BEHAVIOUR OF DISTURBED REGIONS IN REINFORCED CONCRETE
BEAMS WITH CORROSION DAMAGED SHEAR REINFORCEMENT

CHRISTOPHER SUFFERN

SCALE 1:15

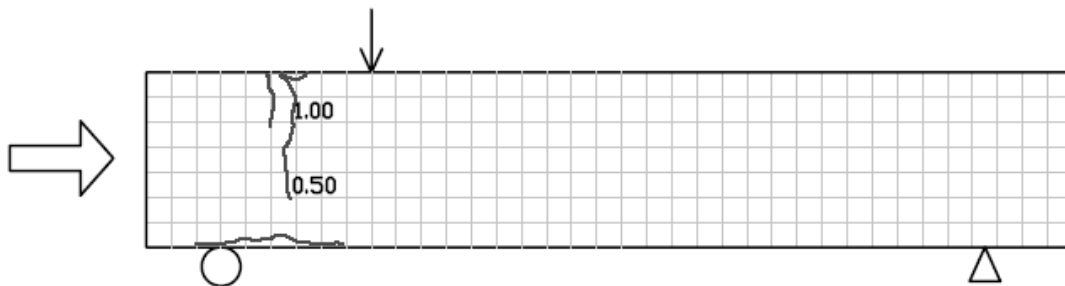
ALL DIMENSIONS IN MILLIMETRES
UNLESS OTHERWISE NOTED

DATE APR 08
DWG 6



RIGHT SIDE VIEW

CRACK WIDTH MEASUREMENTS SHOWN ON DRAWING CORRESPOND TO POINT WHERE CRACK CROSSES HORIZONTAL GRIDLINE (BELOW VALUE SHOWN ON DRAWING). IF NO VALUE IS GIVEN THEN CRACK WIDTH IS LESS THAN 0.1 MM.



LEFT SIDE VIEW

CORROSION CRACK
PATTERN
H-1.0-R

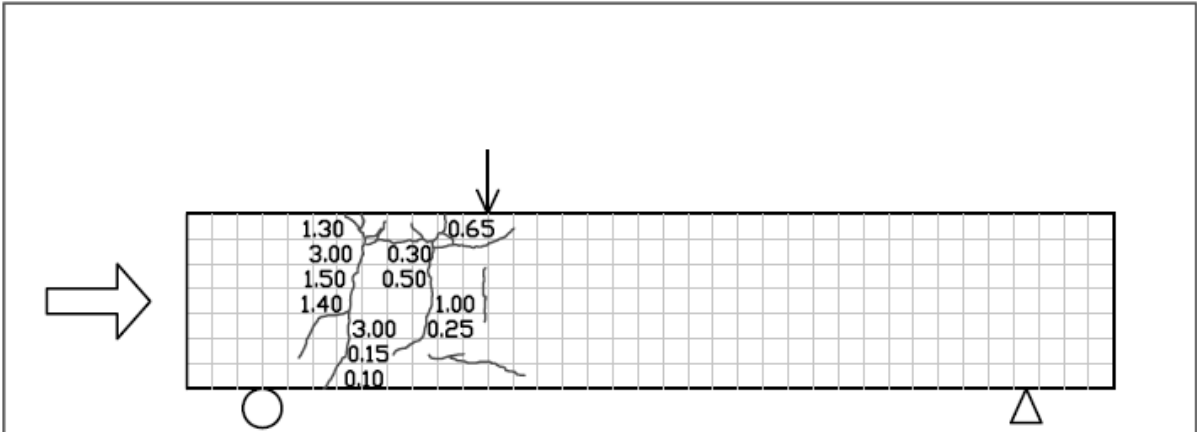
SHEAR BEHAVIOUR OF DISTURBED REGIONS IN REINFORCED CONCRETE
BEAMS WITH CORROSION DAMAGED SHEAR REINFORCEMENT

CHRISTOPHER SUFFERN

SCALE 1:15

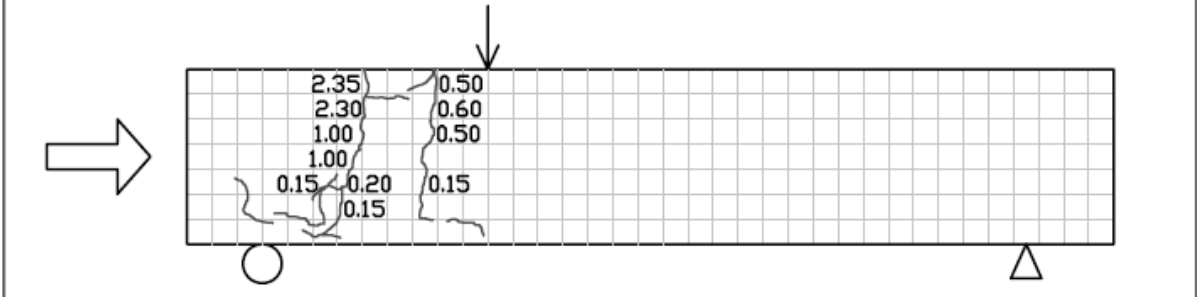
ALL DIMENSIONS IN MILLIMETRES
UNLESS OTHERWISE NOTED

DATE JUL 08
DWG 7



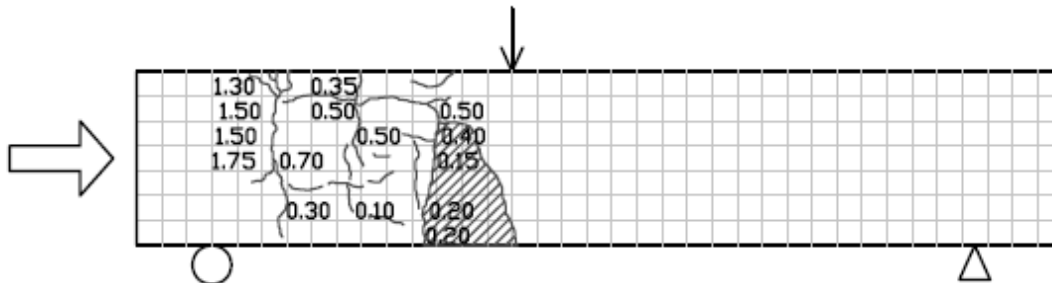
RIGHT SIDE VIEW

CRACK WIDTH MEASUREMENTS SHOWN ON DRAWING CORRESPOND TO POINT WHERE CRACK CROSSES HORIZONTAL GRIDLINE (BELOW VALUE SHOWN ON DRAWING). IF NO VALUE IS GIVEN THEN CRACK WIDTH IS LESS THAN 0.1 MM.



LEFT SIDE VIEW

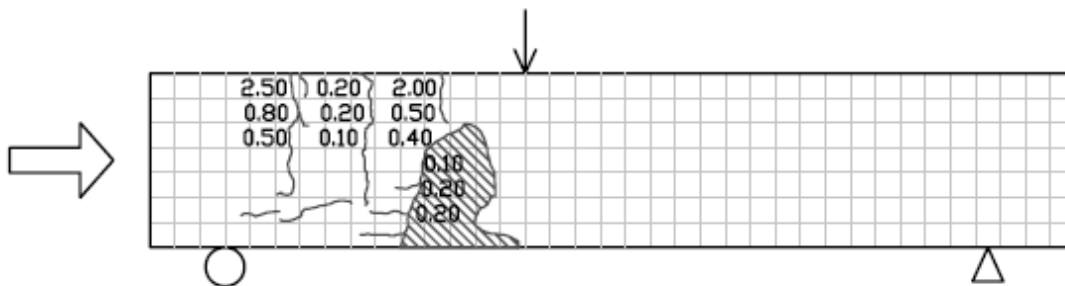
CORROSION CRACK PATTERN H(M)-1.5-R	SHEAR BEHAVIOUR OF DISTURBED REGIONS IN REINFORCED CONCRETE BEAMS WITH CORROSION DAMAGED SHEAR REINFORCEMENT		
	CHRISTOPHER SUFFERN		
SCALE 1:15	ALL DIMENSIONS IN MILLIMETRES UNLESS OTHERWISE NOTED	DATE JUL 08	DWG 8



RIGHT SIDE VIEW

CRACK WIDTH MEASUREMENTS SHOWN ON DRAWING CORRESPOND TO POINT WHERE CRACK CROSSES HORIZONTAL GRIDLINE (BELOW VALUE SHOWN ON DRAWING). IF NO VALUE IS GIVEN THEN CRACK WIDTH IS LESS THAN 0.1 MM.

▨ DELAMINATION



LEFT SIDE VIEW

CORROSION CRACK
PATTERN
H(M)-2.0-R

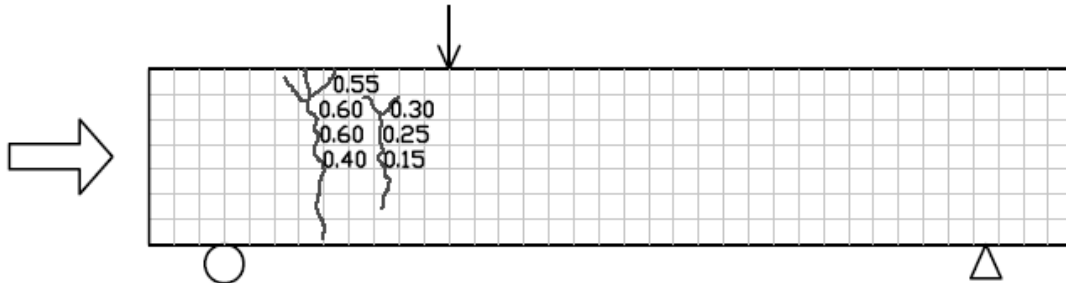
SHEAR BEHAVIOUR OF DISTURBED REGIONS IN REINFORCED CONCRETE
BEAMS WITH CORROSION DAMAGED SHEAR REINFORCEMENT

CHRISTOPHER SUFFERN

SCALE 1/15

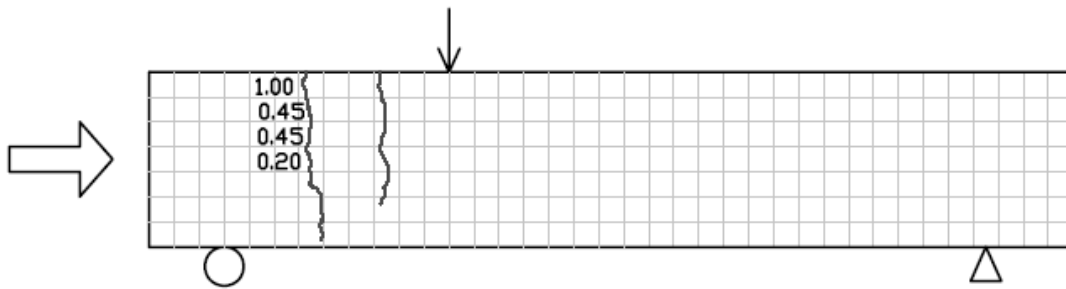
ALL DIMENSIONS IN MILLIMETRES
UNLESS OTHERWISE NOTED

DATE AUG 08
DWG 9



RIGHT SIDE VIEW

CRACK WIDTH MEASUREMENTS SHOWN ON DRAWING CORRESPOND TO POINT WHERE CRACK CROSSES HORIZONTAL GRIDLINE (BELOW VALUE SHOWN ON DRAWING). IF NO VALUE IS GIVEN THEN CRACK WIDTH IS LESS THAN 0.1 MM.



LEFT SIDE VIEW

CORROSION CRACK
PATTERN
H(M)-1.5-Repair

SHEAR BEHAVIOUR OF DISTURBED REGIONS IN REINFORCED CONCRETE BEAMS WITH CORROSION DAMAGED SHEAR REINFORCMENT

CHRISTOPHER SUFFERN

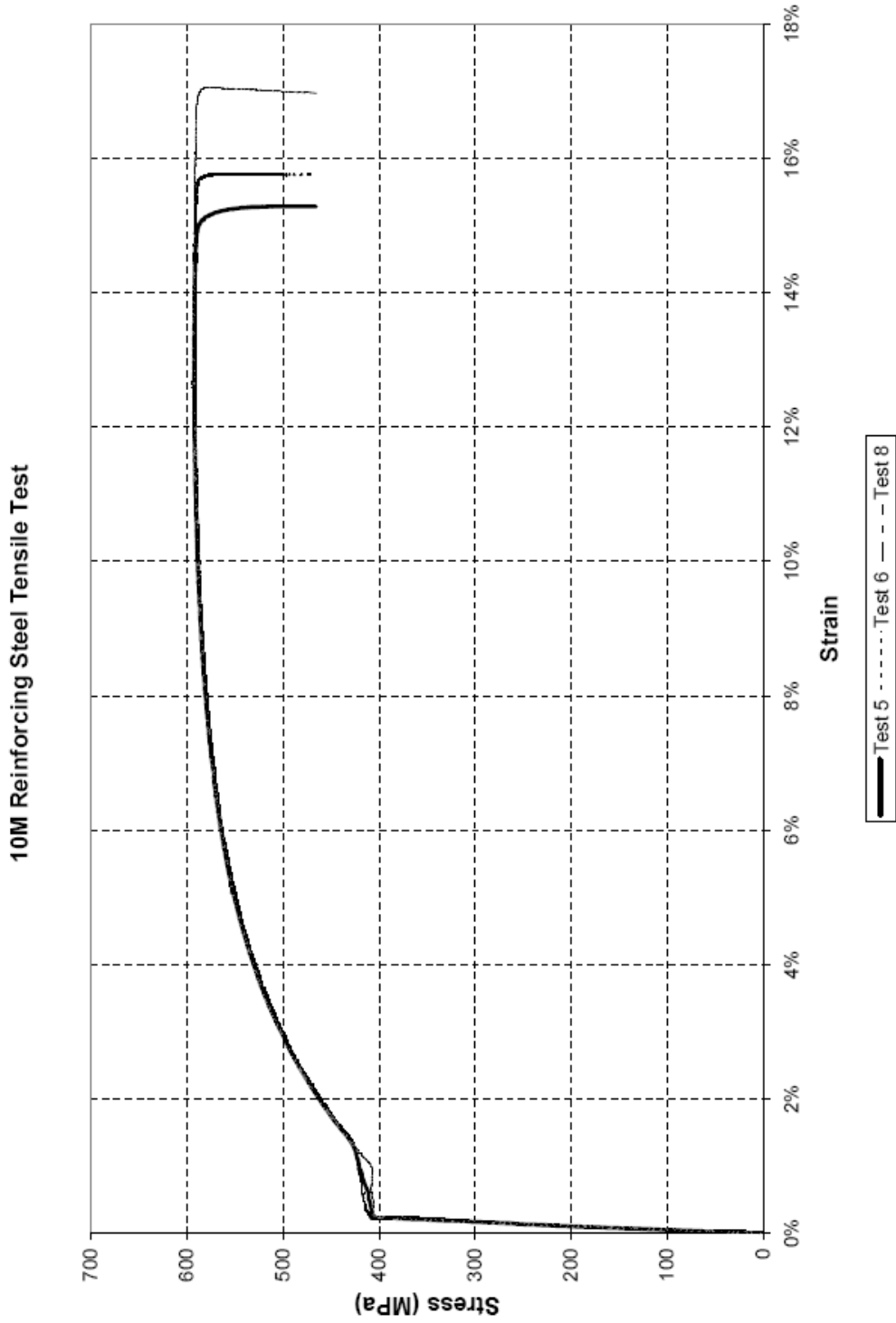
SCALE 1:15

ALL DIMENSIONS IN MILLIMETRES
UNLESS OTHERWISE NOTED

DATE AUG 08
DWG 10

Appendix C

Material Tests and Mass Loss Analysis



Concrete Cylinder Data

Cast Date	Cylinder Number	Specimen	Lot	Diameter				Average (mm)	Length (mm)	Weight (g)	Density (kg/m3)	Test Date	Day	Load (kN)	Strength (MPa)
				Top (mm)	Middle (mm)	Bottom (mm)	Length (mm)								
30-Nov	1	28 Day Test	Salt	102.86	102.23	101.32	102.1	202.59	3944.7	2377	2-Jan-08	33	233	28.4	
30-Nov	2	28 Day Test	Salt	102.03	101.81	101.29	101.7	200.65	3893.1	2388	2-Jan-08	33	220	27.0	
30-Nov	3	28 Day Test	No Salt	101.73	101.53	101.44	101.6	195.78	3772.1	2378	2-Jan-08	33	319	39.4	
30-Nov	4	28 Day Test	No Salt	102.44	102.09	101.42	102.0	194.73	3748.2	2356	2-Jan-08	33	327	40.0	
30-Nov	5	28 Day Test	Salt	101.86	101.85	101.24	101.7	200.98	3887.3	2383	4-Jan-08	35	234	28.8	
30-Nov	6	Medium	Salt	101.24	101.67	101.97	101.6	199.24	3868.4	2394	2-Jul-08	215	261	32.2	
30-Nov	7	28 Day Test	No Salt	101.25	101.36	101.47	101.4	194.63	3743.7	2384	3-Jan-08	34	327	40.6	
30-Nov	9	Medium	Salt	101.35	101.73	102.31	101.8	199.88	3876.7	2383	4-Jul-08	217	269	33.1	
30-Nov	10	High	Salt	101.35	101.68	102.18	101.7	201.22	3920.2	2397	24-Jun-08	207	283	34.8	
30-Nov	11	0-1.0-UR	No Salt	101.91	101.63	101.16	101.6	199.34	3838.4	2377	5-Jul-08	218	288	35.6	
30-Nov	12	0-1.0-UR	No Salt	101.5	101.66	102.21	101.8	198.4	3842	2380	5-Jul-08	218	291	35.7	
30-Nov	14	High	Salt	101.27	101.88	102.34	101.8	201.06	3841.7	2346	24-Jun-08	207	293	36.0	
30-Nov	15	0-1.0-UR	No Salt	101.36	101.94	102.07	101.8	194.9	3777.6	2382	5-Jul-08	218	291	35.7	
30-Nov	16	0-1.0-UR	No Salt	101.46	101.93	102.56	102.0	195.71	3778.4	2363	24-Jun-08	207	287	35.1	
30-Nov	24	High	No Salt	101.59	101.37	101.27	101.4	196.89	3829.1	2408	24-Jun-08	207	430	53.2	
30-Nov	25	High	No Salt	101.08	101.48	102.05	101.5	197.45	3791.2	2371	24-Jun-08	207	463	56.0	
13-Dec	26	28 Day Test	Salt	101.2	101.83	101.76	101.6	203.17	3939.1	2392	10-Jan-08	28	277	34.2	
13-Dec	27	28 Day Test	Salt	101.25	101.51	101.88	101.5	201.42	3908.2	2396	10-Jan-08	28	274	33.9	
13-Dec	28	28 Day Test	Salt	101.21	101.69	102.25	101.7	200.07	3871.7	2381	10-Jan-08	28	289	35.5	
13-Dec	29	28 Day Test	No Salt	101.71	101.53	101.6	101.6	200.81	3956.8	2430	10-Jan-08	28	393	48.5	
13-Dec	30	28 Day Test	No Salt	101.72	101.31	101.1	101.4	199.08	3874.7	2411	10-Jan-08	28	364	45.1	
13-Dec	31	28 Day Test	No Salt	101.85	101.93	101.7	101.8	198.52	3894.4	2409	10-Jan-08	28	386	47.4	
13-Dec	32	Low	No Salt	101.37	101.52	101.48	101.5	199.37	3958.6	2456	25-Jun-08	195	435	53.9	
13-Dec	33	Low	No Salt	101.27	101.48	101.23	101.3	199.57	3939.2	2448	25-Jun-08	195	424	52.6	
13-Dec	34	Low	Salt	101.36	101.56	101.84	101.6	199.05	3887	2409	25-Jun-08	195	311	38.4	
13-Dec	35	Low	Salt	101.41	101.51	101.91	101.6	199.7	3886.2	2400	25-Jun-08	195	314	38.7	
13-Dec	36	Low	No Salt	101.41	101.73	101.93	101.7	199.68	3944.1	2432	25-Jun-08	195	420	51.7	
13-Dec	40	Low	Salt	101.21	101.65	101.86	101.6	197.45	3845.3	2403	25-Jun-08	195	300	37.1	
13-Dec	49	Control	No Salt	101.35	101.42	101.57	101.4	199.83	3881.8	2403	5-Jul-08	205	316	39.1	
13-Dec	50	Control	No Salt	101.38	101.56	101.34	101.4	197.88	3864.4	2417	5-Jul-08	205	338	41.8	
13-Dec	51	Control	No Salt	101.34	101.36	100.8	101.2	200.16	3891	2418	5-Jul-08	205	346	43.1	

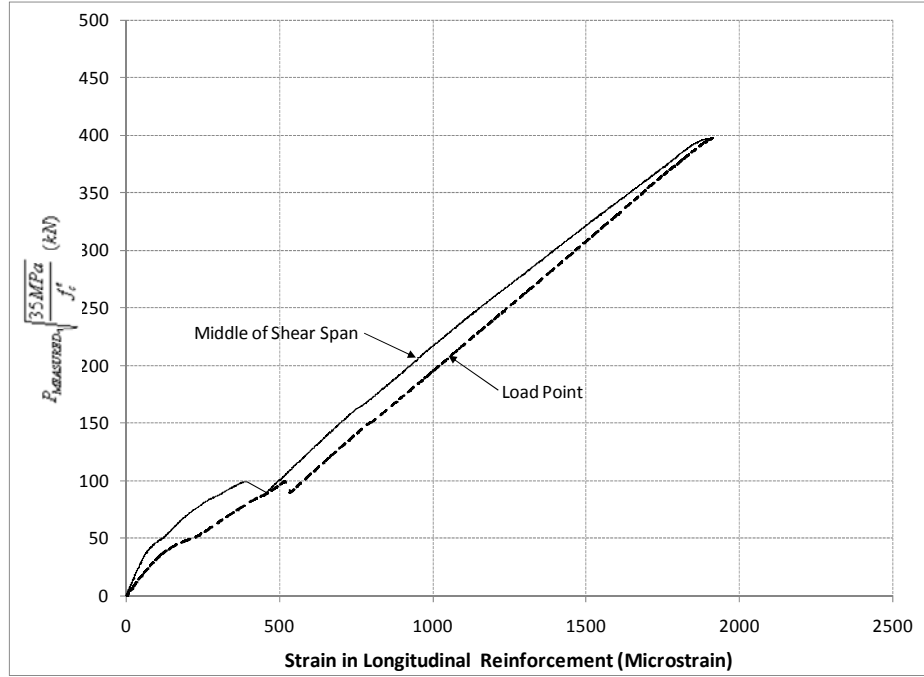
Mass Loss Results

	Stirrup 1		Stirrup 2		Stirrup 3	
Specimen	Right Leg	Left Leg	Right Leg	Left Leg	Right Leg	Left Leg
L-1.0-R	1%	2%				
L-1.5-R	3%	2%	3%	2%		
L-2.0-R	6%	7%	2%	0%	0%	0%
M(L)-2.0-R	5%	5%	5%	4%	1%	0%
M-1.0-R	10%	12%				
M-1.5-R	14%	12%	6%	6%		
H(M)-1.5-R	13%	11%	5%	4%		
H(M)-2.0-R	11%	8%	8%	9%	14%	14%
H(M)-1.5-Repair	13%	13%	1%	0%		
H-1.0-R	17%	21%				

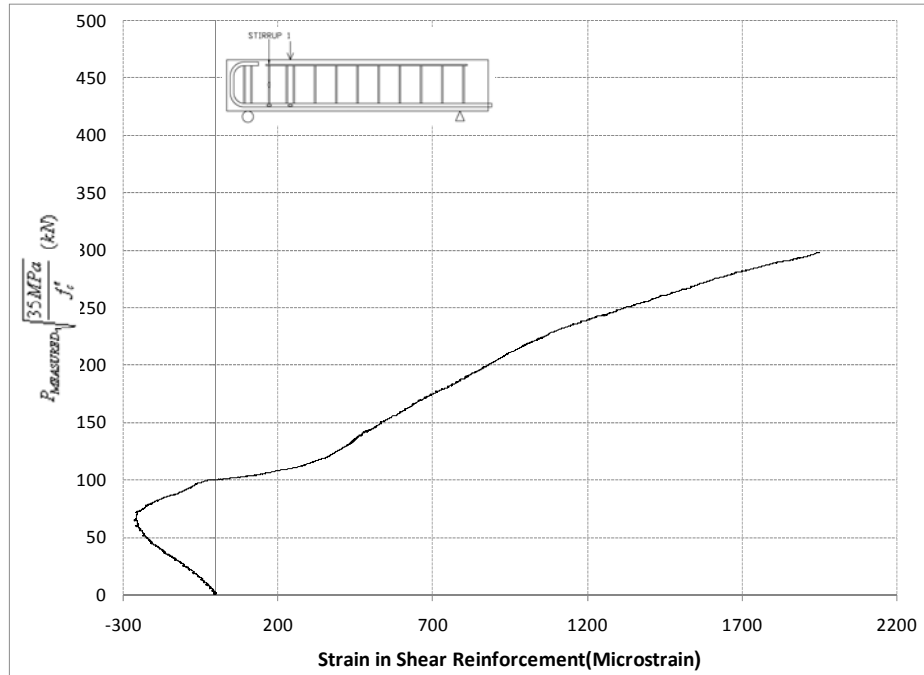
Appendix D

Specimen Strain Data

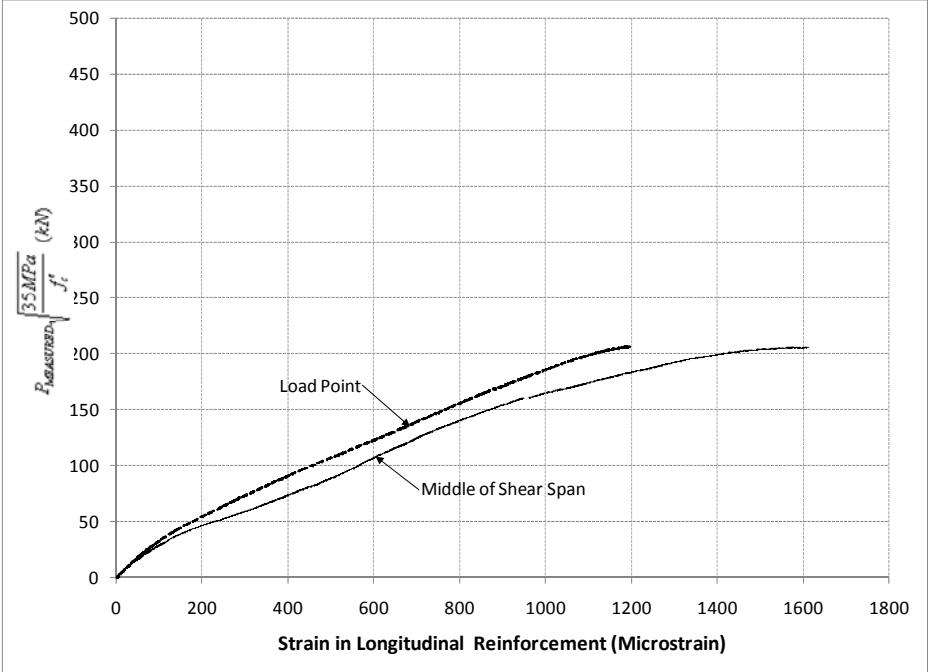
Specimen 0-1.0-UR



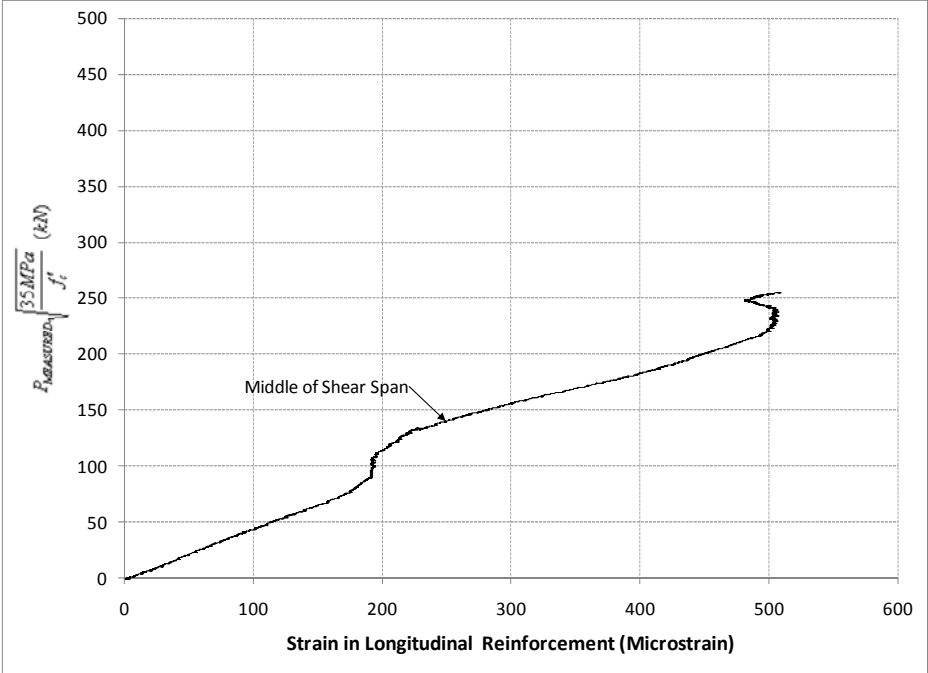
Specimen L-1.0-R



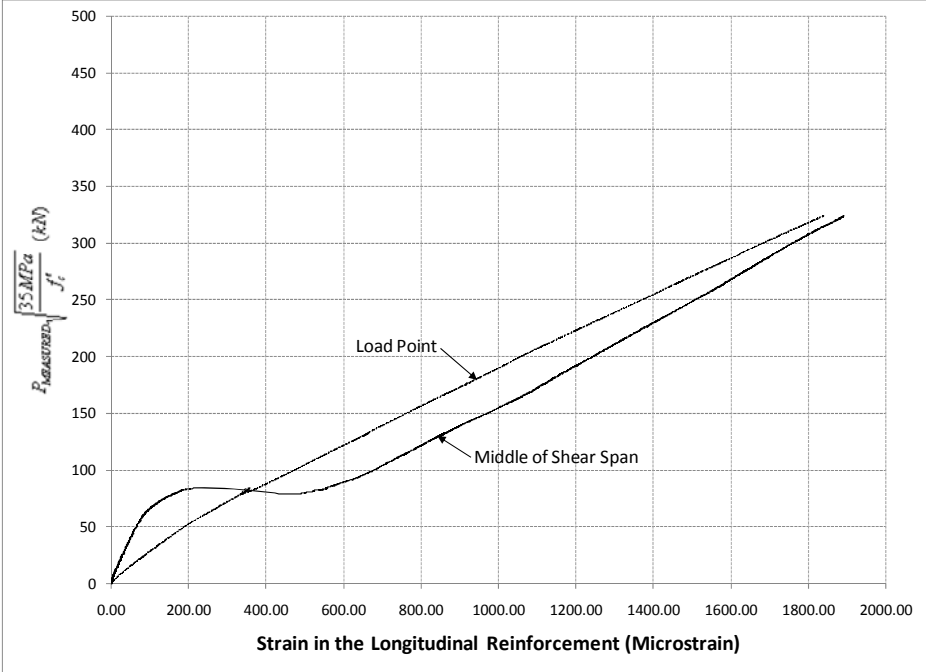
Specimen M-1.0-R



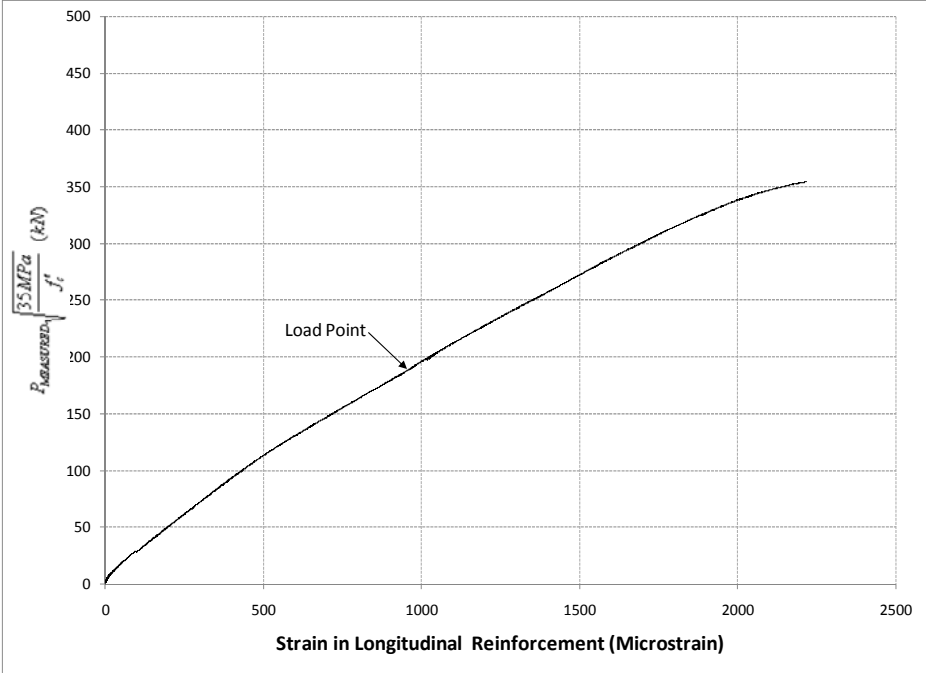
Specimen H-1.0-R



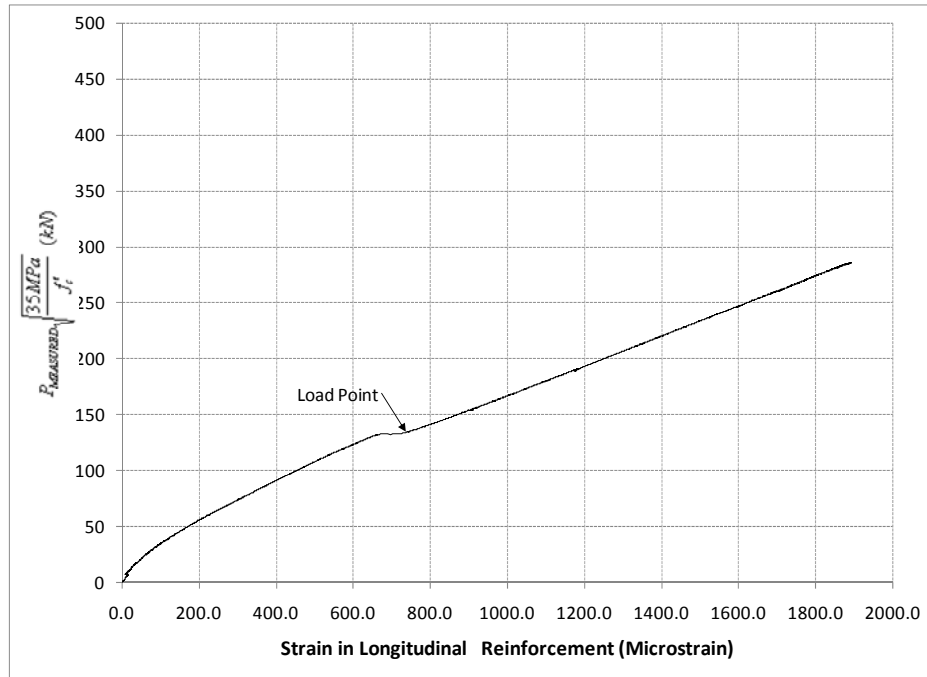
Specimen 0-1.5-UR



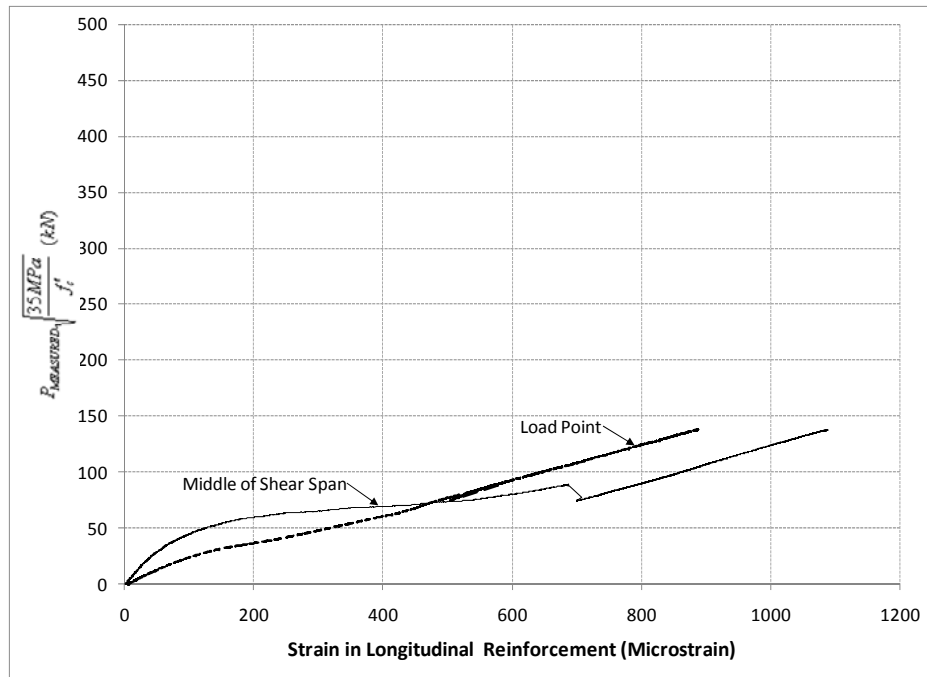
Specimen 0-1.5-R



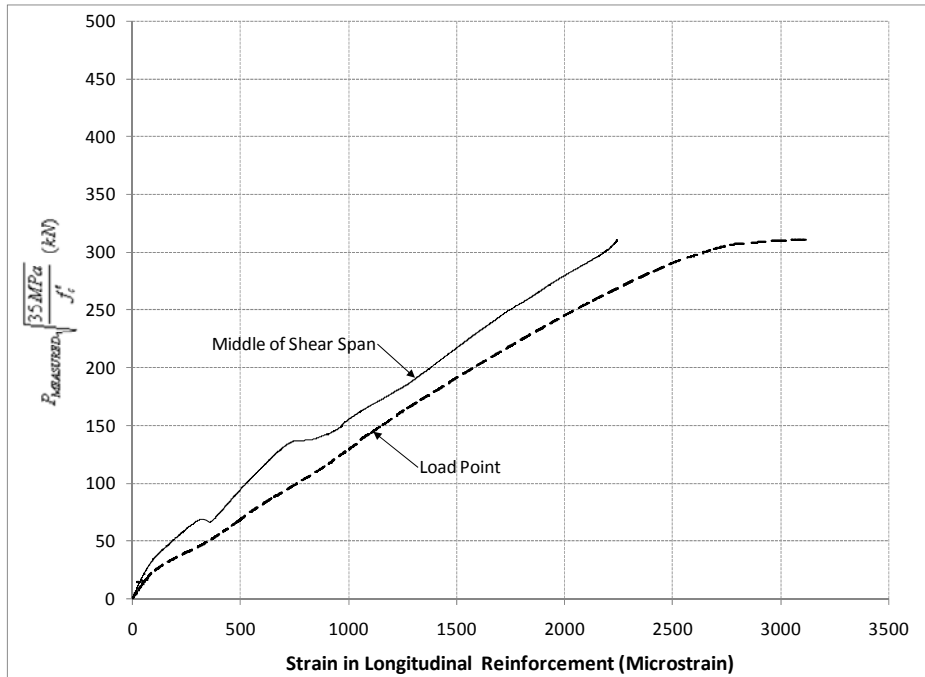
Specimen M-1.5-R



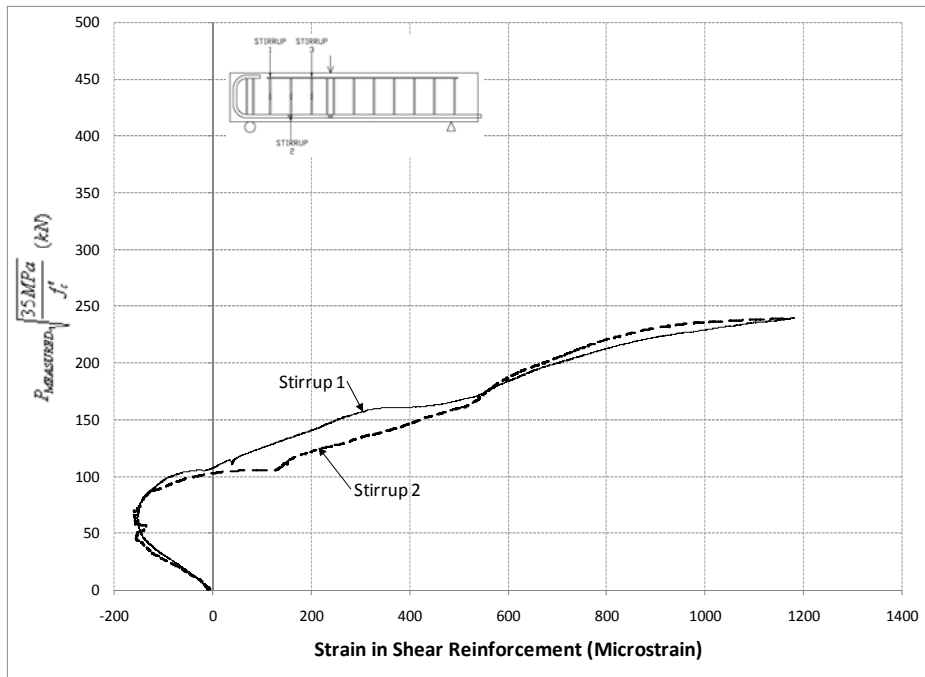
Specimen 0-2.0-UR



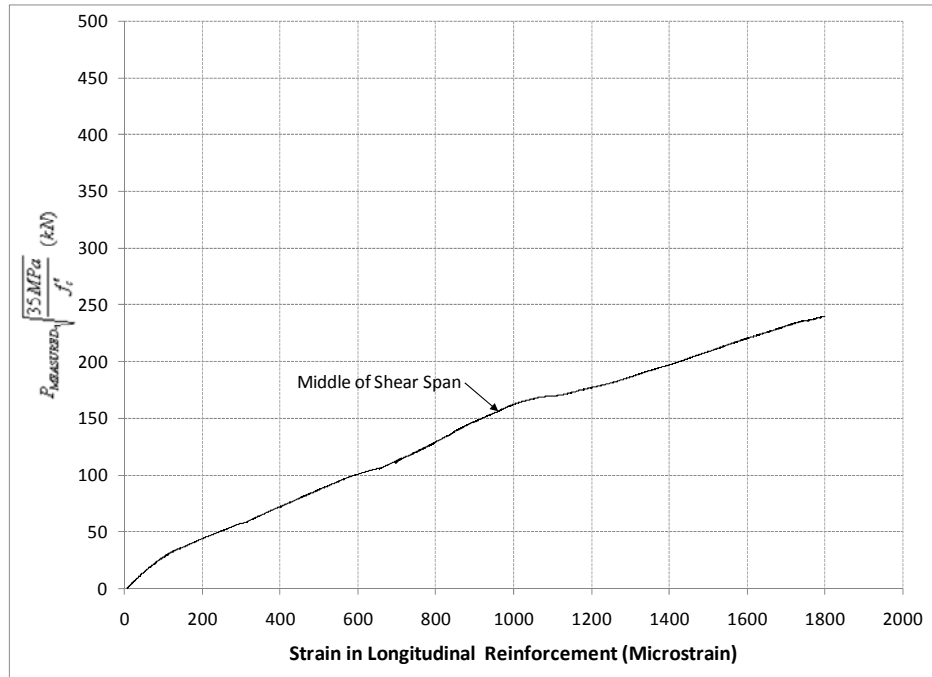
Specimen 0-2.0-R



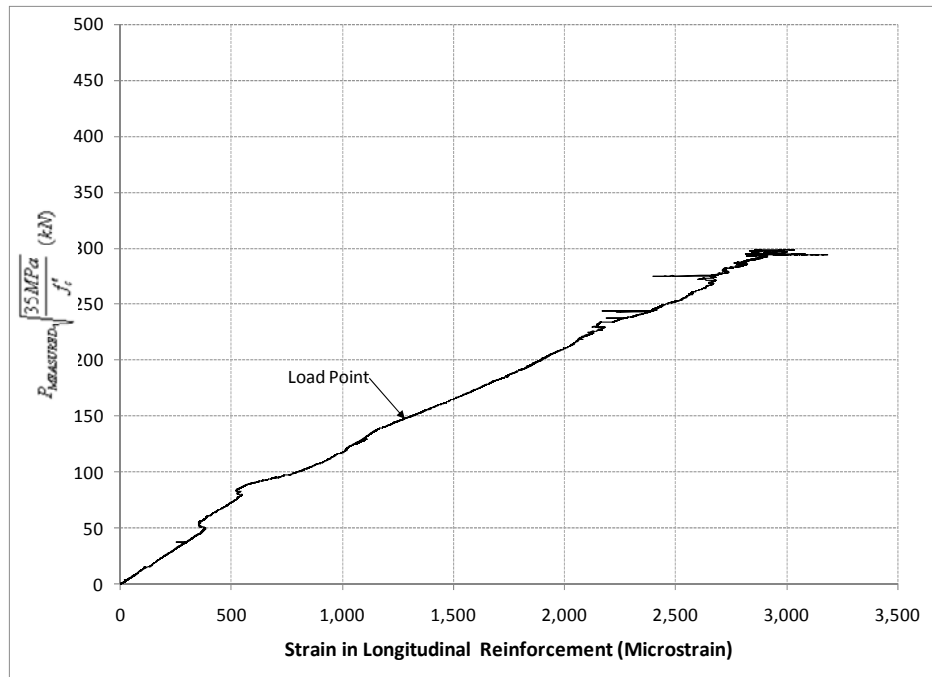
Specimen L-2.0-R



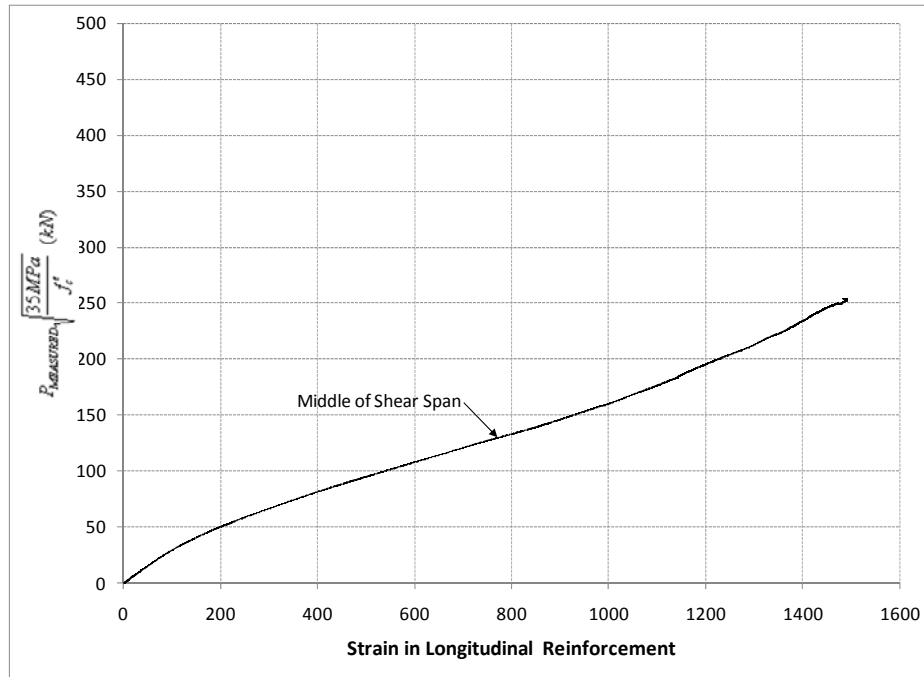
Specimen L-2.0-R



Specimen M(L)-2.0-R



Specimen H(M)-2.0-R



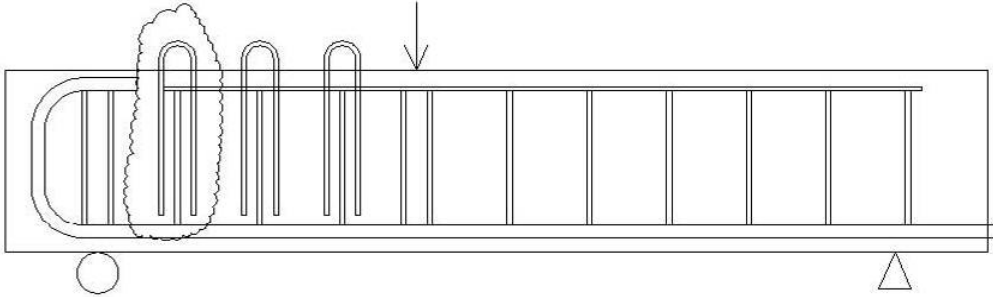
Appendix E

Calculations

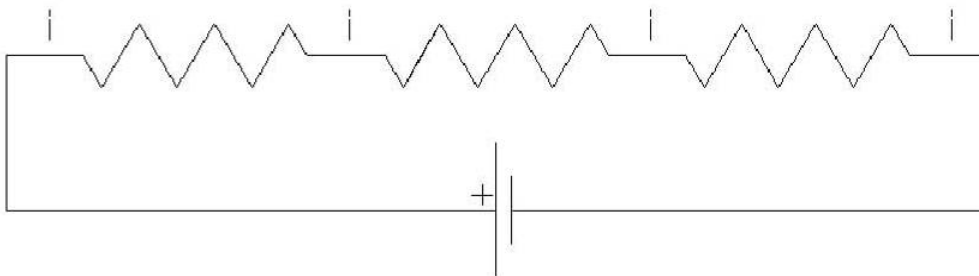
Current Density and Mass Loss Calculation

1. Theory

The applied current is calculated based on basic circuit theory.



The beam shown above can be represented as the following circuit:



Since the current is the same in all branches the current calculation will be based on one cathode-anode combination (shown in bubble above).

2. Properties

Bar Diameter: $d_b := 11.3\text{mm}$ Bar Length: $L := 730\text{mm}$ Steel Density: $\gamma := 7.86 \frac{\text{g}}{\text{cm}^3}$

$A_s := 100\text{mm}^2$

3. Surface Area and Volume Calculation

$P := \pi \cdot d_b$ $P = 35.5\text{mm}$ Surface Area: $A_{\text{surface}} := P \cdot L$ $A_{\text{surface}} = 259.15\text{cm}^2$

$V := A_s \cdot L$ $V = 73\text{cm}^3$ mass := $V \cdot \gamma$ mass = 573.78 g

4. First Stage Current Calculation

Assumed Current Density: $i := 445 \frac{\mu\text{A}}{\text{cm}^2}$ Power Supply Current Setting: $I_1 := i \cdot A_{\text{surface}}$

$I_1 = 115\text{mA}$

5. Second Stage Current Calculation

Assumed Current Density: $i := 150 \frac{\mu\text{A}}{\text{cm}^2}$ Power Supply Current Setting: $I_2 := i \cdot A_{\text{surface}}$

$$I_2 = 39 \text{ mA}$$

6. Mass Loss Calculation - Low Beams

$t := 21 \text{ day}$ $a := 55.9 \text{ g}$ $F := 96500 \text{ A}\cdot\text{s}$ $n := 2$

$$m := \frac{I_1 \cdot t \cdot a}{n \cdot F} \quad m = 60.604 \text{ g} \quad \text{MassLoss} := \frac{m}{\text{mass}} \quad \boxed{\text{MassLoss} = 10.6\%}$$

7. Mass Loss Calculation - Medium Beams

Stage 1

$t_1 := 840 \text{ hr}$ $a := 55.9 \text{ g}$ $F := 96500 \text{ A}\cdot\text{s}$ $n := 2$

$$m_1 := \frac{I_1 \cdot t_1 \cdot a}{n \cdot F} \quad m_1 = 101.006 \text{ g}$$

Stage 2

$t_2 := 600 \text{ hr}$ $a := 55.9 \text{ g}$ $F := 96500 \text{ A}\cdot\text{s}$ $n := 2$

$$m_2 := \frac{I_2 \cdot t_2 \cdot a}{n \cdot F} \quad m_2 = 24.319 \text{ g}$$

Total Mass Loss: $m := m_1 + m_2$ $\text{MassLoss} := \frac{m}{\text{mass}}$ $\boxed{\text{MassLoss} = 21.8\%}$

8. Mass Loss Calculation - High Beams

Stage 1

$t_1 := 840 \text{ hr}$ $a := 55.9 \text{ g}$ $F := 96500 \text{ A}\cdot\text{s}$ $n := 2$

$$m_1 := \frac{I_1 \cdot t_1 \cdot a}{n \cdot F} \quad m_1 = 101.006 \text{ g}$$

Stage 2

$t_2 := 2040 \text{ hr}$ $a := 55.9 \text{ g}$ $F := 96500 \text{ A}\cdot\text{s}$ $n := 2$

$$m_2 := \frac{I_2 \cdot t_2 \cdot a}{n \cdot F} \quad m_2 = 82.686 \text{ g}$$

Total Mass Loss: $m := m_1 + m_2$ $\text{MassLoss} := \frac{m}{\text{mass}}$ $\boxed{\text{MassLoss} = 32\%}$

Appendix F
Strut and Tie Model Validation

Num	Authors	Specimen	Width (mm)	Height (mm)	Effective Depth (mm)	Clear Span (mm)	Shear Span (mm)	Concrete Strength (MPa)	Shear Reinforcement Ratio (%)	Flexural Reinforcement Ratio	In / d ratio	a/d ratio
1	Shin, Lee, Moon, and Ghosh	MHB1.5-25	125	250	215	645	322.5	52.0	0.45%	3.77%	3.0	1.5
2	Shin, Lee, Moon, and Ghosh	MHB1.5-50	125	250	215	645	323	52	0.91%	3.77%	3	1.5
3	Shin, Lee, Moon, and Ghosh	MHB1.5-75	125	250	215	645	323	52	1.36%	3.77%	3	1.5
4	Shin, Lee, Moon, and Ghosh	MHB2.0-25	125	250	215	860	430	52	0.32%	3.77%	4	2.0
5	Shin, Lee, Moon, and Ghosh	MHB2.0-50	125	250	215	860	430	52	0.65%	3.77%	4	2.0
6	Shin, Lee, Moon, and Ghosh	MHB2.0-75	125	250	215	860	430	52	0.97%	3.77%	4	2.0
7	Shin, Lee, Moon, and Ghosh	MHB2.5-25	125	250	215	1075	538	52	0.25%	3.77%	5	2.5
8	Shin, Lee, Moon, and Ghosh	MHB2.5-50	125	250	215	1075	538	52	0.47%	3.77%	5	2.5
9	Shin, Lee, Moon, and Ghosh	HB1.5-25	125	250	215	645	323	73	0.45%	3.77%	3	1.5
10	Shin, Lee, Moon, and Ghosh	HB1.5-50	125	250	215	645	323	73	0.91%	3.77%	3	1.5
11	Shin, Lee, Moon, and Ghosh	HB1.5-75	125	250	215	645	323	73	1.36%	3.77%	3	1.5
12	Shin, Lee, Moon, and Ghosh	HB1.5-100	125	250	215	645	323	73	1.81%	3.77%	3	1.5
13	Shin, Lee, Moon, and Ghosh	HB2.0-25	125	250	215	860	430	73	0.32%	3.77%	4	2.0
14	Shin, Lee, Moon, and Ghosh	HB2.0-50	125	250	215	860	430	73	0.65%	3.77%	4	2.0
15	Shin, Lee, Moon, and Ghosh	HB2.0-75	125	250	215	860	430	73	0.97%	3.77%	4	2.0
16	Shin, Lee, Moon, and Ghosh	HB2.0-100	125	250	215	860	430	73	1.29%	3.77%	4	2.0
17	Shin, Lee, Moon, and Ghosh	HB2.5-25	125	250	215	1075	538	73	0.25%	3.77%	5	2.5
18	Shin, Lee, Moon, and Ghosh	HB2.5-50	125	250	215	1075	538	73	0.47%	3.77%	5	2.5
19	Shin, Lee, Moon, and Ghosh	HB2.5-75	125	250	215	1075	538	73	0.71%	3.77%	5	2.5
20	Shin, Lee, Moon, and Ghosh	HB2.5-100	125	250	215	1075	538	73	0.94%	3.77%	5	2.5
21	Tan, Kong, Teng, and Guan	D-1.08-2.15	110	500	463	1000	500	48	0.48%	2.58%	2	1.1
22	Tan, Kong, Teng, and Guan	D-1.08-3.23	110	500	463	1500	500	44	0.48%	2.58%	3	1.1
23	Tan, Kong, Teng, and Guan	D-1.08-4.30	110	500	463	2000	500	47	0.48%	2.58%	4	1.1
24	Tan, Kong, Teng, and Guan	D-1.08-5.38	110	500	463	2500	500	48	0.48%	2.58%	5	1.1
25	Tan, Kong, Teng, and Guan	E-1.62-3.23	110	500	463	1500	750	51	0.48%	2.58%	3	1.6
26	Tan, Kong, Teng, and Guan	E-1.62-4.30	110	500	463	2000	750	45	0.48%	2.58%	4	1.6
27	Tan, Kong, Teng, and Guan	E-1.62-5.38	110	500	463	2500	750	45	0.48%	2.58%	5	1.6
28	Tan, Kong, Teng, and Guan	F-2.16-4.30	110	500	463	2000	1000	41	0.48%	2.58%	4	2.2
29	Clark	B1-1	203	457	391	1829	762	23	0.37%	3.10%	5	1.9
30	Clark	B1-2	203	457	391	1829	762	25	0.37%	3.10%	5	1.9
31	Clark	B1-3	203	457	391	1829	762	24	0.37%	3.10%	5	1.9
32	Clark	B1-4	203	457	391	1829	762	23	0.37%	3.10%	5	1.9
33	Clark	B1-5	203	457	391	1829	762	25	0.37%	3.10%	5	1.9
34	Clark	B6-1	203	457	391	1829	762	42	0.37%	3.10%	5	1.9
35	Clark	C1-1	203	457	391	1829	610	26	0.34%	2.07%	5	1.6
36	Clark	C1-2	203	457	391	1829	610	26	0.34%	2.07%	5	1.6
37	Clark	C1-3	203	457	391	1829	610	24	0.34%	2.07%	5	1.6
38	Clark	C1-4	203	457	391	1829	610	29	0.34%	2.07%	5	1.6
39	Clark	C2-1	203	457	391	1829	610	24	0.69%	2.07%	5	1.6
40	Clark	C2-2	203	457	391	1829	610	25	0.69%	2.07%	5	1.6
41	Clark	C2-3	203	457	391	1829	610	24	0.69%	2.07%	5	1.6
42	Clark	C2-4	203	457	391	1829	610	27	0.69%	2.07%	5	1.6
43	Clark	C3-1	203	457	391	1829	610	14	0.34%	2.07%	5	1.6

Num	Authors	Specimen	Width (mm)	Height (mm)	Effective Depth (mm)	Clear Span (mm)	Shear Span (mm)	Concrete Strength (MPa)	Shear Reinforcement Ratio (%)	Flexural Reinforcement Ratio	In / d ratio	a/d ratio
44	Clark	C3-2	203	457	391	1829	610	14	0.34%	2.07%	5	1.6
45	Clark	C3-3	203	457	391	1829	610	14	0.34%	2.07%	5	1.6
46	Clark	C4-1	203	457	391	1829	610	24	0.34%	3.10%	5	1.6
47	Clark	C6-2	203	457	391	1829	610	45	0.34%	3.10%	5	1.6
48	Clark	C6-3	203	457	391	1829	610	45	0.34%	3.10%	5	1.6
49	Clark	C6-4	203	457	391	1829	610	48	0.34%	3.10%	5	1.6
50	Clark	D1-1	203	457	391	1829	457	26	0.46%	1.63%	5	1.2
51	Clark	D1-2	203	457	391	1829	457	26	0.46%	1.63%	5	1.2
52	Clark	D1-3	203	457	391	1829	457	25	0.46%	1.63%	5	1.2
53	Clark	D2-1	203	457	391	1829	457	24	0.61%	1.63%	5	1.2
54	Clark	D2-2	203	457	391	1829	457	26	0.61%	1.63%	5	1.2
55	Clark	D2-3	203	457	391	1829	457	25	0.61%	1.63%	5	1.2
56	Clark	D2-4	203	457	391	1829	457	24	0.61%	1.63%	5	1.2
57	Clark	D3-1	203	457	391	1829	457	28	0.92%	2.44%	5	1.2
58	Clark	D4-1	203	457	391	1829	457	23	1.22%	1.63%	5	1.2
59	Clark	D1-6	152	381	314	2438	610	28	0.46%	3.42%	8	1.9
60	Clark	D1-7	152	381	314	2438	610	28	0.46%	3.42%	8	1.9
61	Clark	D1-8	152	381	314	2438	610	28	0.46%	3.42%	8	1.9
62	Clark	E1-2	152	381	314	2921	635	30	0.73%	3.42%	9	2.0
63	Clark	D2-6	152	381	314	3048	762	30	0.61%	3.42%	10	2.4
64	Clark	D2-7	152	381	314	3048	762	28	0.61%	3.42%	10	2.4
65	Clark	D4-1-1	152	381	314	3048	762	27	0.49%	3.42%	10	2.4
66	Clark	D5-1	152	381	314	3048	762	28	0.37%	3.42%	10	2.4
67	Clark	D5-2	152	381	314	3048	762	29	0.37%	3.42%	10	2.4
68	Clark	D5-3	152	381	314	3048	762	27	0.37%	3.42%	10	2.4
69	Tan, Teng, Kong, and Lu	1-2.00/1.00	110	500	448	2000	500	71	0.48%	2.00%	4	1.1
70	Tan, Teng, Kong, and Lu	1-2.00/1.50	110	500	448	2500	750	72	0.48%	2.00%	6	1.7
71	Tan, Teng, Kong, and Lu	2-2.58/1.00	110	500	443	2000	500	68	0.48%	2.58%	5	1.1
72	Tan, Teng, Kong, and Lu	2-2.58/1.50	110	500	443	2500	750	68	0.48%	2.58%	6	1.7
73	Tan, Teng, Kong, and Lu	2-2.58/2.00	110	500	443	3000	1000	70	0.48%	2.58%	7	2.3
74	Higgins	8RA	254	610	521	2400	1048	29	0.50%	1.90%	5	2.0
75	Higgins	10RA	254	610	521	2400	1048	33	0.40%	1.90%	5	2.0
76	Higgins	12RA	254	610	521	2400	1048	30	0.33%	1.90%	5	2.0
77	Yun	Beam	203	508	417	2743	914	43	0.52%	2.72%	7	2.2
78	Aguilar et. al.	S1M-M	305	914	800	4065	915	28	0.31%	1.25%	5	1.1
79	Tan, Kong, Teng, and Weng	II-2N/1.00	110	500	443	2000	500	78	1.43%	2.58%	5	1.1
80	Tan, Kong, Teng, and Weng	III-2N/1.50	110	500	443	2500	750	78	1.43%	2.58%	6	1.7
81	Oh and Shin	H43A0	120	560	500	2000	625	51	0.13%	1.29%	1	1.3
82	Oh and Shin	U43A0	120	560	500	2000	625	74	0.13%	1.29%	4	1.3
83	Kong and Robbins	2-10	76	254	216	762	254	20	0.85%	1.73%	4	1.2
84	de Paiva and Seiss	G33S-12	76	229	203	610	203	20	1.09%	1.67%	3	1.0
85	de Paiva and Seiss	G33S-32	76	229	203	610	203	20	1.09%	2.58%	3	1.0
86	de Paiva and Seiss	F3S3	76	229	203	610	203	34	1.31%	1.67%	3	1.0

Num	Authors	Specimen	Width (mm)	Height (mm)	Effective Depth (mm)	Clear Span (mm)	Shear Span (mm)	Concrete Strength (MPa)	Shear Reinforcement Ratio (%)	Flexural Reinforcement Ratio	ln / d ratio	a/d ratio
87	Smith and Vansiotis	1B1-01	102	356	305	940	368	22	0.24%	1.94%	3	1.2
88	Smith and Vansiotis	2B1-05	102	356	305	940	368	19	0.42%	1.94%	3	1.2
89	Smith and Vansiotis	3B1-08	102	356	305	940	368	16	0.63%	1.94%	3	1.2
90	Smith and Vansiotis	3B1-36	102	356	305	940	368	20	0.77%	1.94%	3	1.2
91	Smith and Vansiotis	4B1-09	102	356	305	940	368	17	1.25%	1.94%	3	1.2
92	Smith and Vansiotis	1C1-14	102	356	305	1118	457	19	0.18%	1.94%	4	1.5
93	Smith and Vansiotis	2C1-17	102	356	305	1118	457	20	0.31%	1.94%	4	1.5
94	Smith and Vansiotis	3C1-20	102	356	305	1118	457	21	0.56%	1.94%	4	1.5
95	Smith and Vansiotis	4C1-24	102	356	305	1118	457	20	0.77%	1.94%	4	1.5

Num	Authors	Specimen	Experimental (kN)	Model Prediction (kN)	Model Prediction with effectiveness factor (kN)	Direct Strut Prediction (kN)	Experimental/Model Prediction	Experimental/Direct Strut Model Prediction with Effectiveness Factor	Experimental/Direct Strut Model Prediction
1	Shin, Lee, Moon, and Ghosh	MHB1.5-25	313	377	343	279	0.83	0.91	1.12
2	Shin, Lee, Moon, and Ghosh	MHB1.5-50	416	414	365	279	1.00	1.14	1.49
3	Shin, Lee, Moon, and Ghosh	MHB1.5-75	479	444	385	279	1.08	1.25	1.72
4	Shin, Lee, Moon, and Ghosh	MHB2.0-25	221	312	297	219	0.71	0.75	1.01
5	Shin, Lee, Moon, and Ghosh	MHB2.0-50	348	350	329	219	0.99	1.06	1.59
6	Shin, Lee, Moon, and Ghosh	MHB2.0-75	371	362	356	219	0.97	1.04	1.69
7	Shin, Lee, Moon, and Ghosh	MHB2.5-25	197	268	265	179	0.74	0.74	1.10
8	Shin, Lee, Moon, and Ghosh	MHB2.5-50	277	286	285	179	0.97	0.97	1.55
9	Shin, Lee, Moon, and Ghosh	MHB2.5-75	428	489	458	369	0.88	0.94	1.16
10	Shin, Lee, Moon, and Ghosh	HB1.5-25	492	529	483	369	0.93	1.02	1.33
11	Shin, Lee, Moon, and Ghosh	HB1.5-50	532	562	506	369	0.95	1.05	1.44
12	Shin, Lee, Moon, and Ghosh	HB1.5-75	561	589	527	369	0.95	1.06	1.52
13	Shin, Lee, Moon, and Ghosh	HB2.0-25	285	408	395	292	0.70	0.72	0.98
14	Shin, Lee, Moon, and Ghosh	HB2.0-50	392	454	435	292	0.86	0.90	1.34
15	Shin, Lee, Moon, and Ghosh	HB2.0-75	460	493	471	292	0.93	0.98	1.58
16	Shin, Lee, Moon, and Ghosh	HB2.0-100	484	527	502	292	0.92	0.96	1.66
17	Shin, Lee, Moon, and Ghosh	HB2.5-25	231	350	354	239	0.66	0.65	0.97
18	Shin, Lee, Moon, and Ghosh	HB2.5-50	298	375	380	239	0.79	0.78	1.25
19	Shin, Lee, Moon, and Ghosh	HB2.5-75	334	420	427	239	0.79	0.78	1.40
20	Shin, Lee, Moon, and Ghosh	HB2.5-100	368	459	467	239	0.80	0.79	1.54
21	Tan, Kong, Teng, and Guan	D-1.08-2.15	270	286	266	189	0.94	1.02	1.43
22	Tan, Kong, Teng, and Guan	D-1.08-3.23	280	264	243	173	1.06	1.15	1.62
23	Tan, Kong, Teng, and Guan	D-1.08-4.30	290	279	258	184	1.04	1.12	1.58
24	Tan, Kong, Teng, and Guan	D-1.08-5.38	290	285	265	189	1.02	1.09	1.53
25	Tan, Kong, Teng, and Guan	E-1.62-3.23	220	242	230	151	0.91	0.96	1.46
26	Tan, Kong, Teng, and Guan	E-1.62-4.30	190	219	206	132	0.87	0.92	1.44
27	Tan, Kong, Teng, and Guan	E-1.62-5.38	173	221	209	134	0.78	0.83	1.29
28	Tan, Kong, Teng, and Guan	F-2.16-4.30	150	200	202	95	0.75	0.74	1.58
29	Clark	B1-1	558	480	429	291	1.16	1.30	1.92
30	Clark	B1-2	513	518	468	323	0.99	1.10	1.59
31	Clark	B1-3	570	486	436	296	1.17	1.31	1.92
32	Clark	B1-4	536	479	428	290	1.12	1.25	1.85
33	Clark	B1-5	483	504	454	311	0.96	1.06	1.55
34	Clark	B6-1	759	781	735	526	0.97	1.03	1.44
35	Clark	C1-1	555	579	522	402	0.96	1.06	1.38
36	Clark	C1-2	622	584	528	405	1.07	1.18	1.54
37	Clark	C1-3	492	561	504	394	0.88	0.98	1.25
38	Clark	C1-4	572	607	551	417	0.94	1.04	1.37
39	Clark	C2-1	580	638	561	402	0.91	1.03	1.44
40	Clark	C2-2	602	631	555	399	0.95	1.08	1.51

Num	Authors	Specimen	Experimental (kN)	Model Prediction (kN)	Model Prediction with effectiveness factor (kN)	Direct Strut Prediction (kN)	Experimental/Model Prediction	Experimental/Direct Strut Model Prediction with Effectiveness Factor	Experimental/Direct Strut Model Prediction
41	Clark	C2-3	647	623	545	395	1.04	1.19	1.64
42	Clark	C2-4	576	670	593	417	0.86	0.97	1.38
43	Clark	C3-1	447	341	284	207	1.31	1.57	2.16
44	Clark	C3-2	401	335	278	202	1.20	1.44	1.98
45	Clark	C3-3	376	338	281	204	1.11	1.34	1.84
46	Clark	C4-1	619	541	475	374	1.14	1.30	1.65
47	Clark	C6-2	848	878	817	646	0.97	1.04	1.31
48	Clark	C6-3	870	874	812	644	1.00	1.07	1.35
49	Clark	C6-4	857	897	837	657	0.96	1.02	1.30
50	Clark	D1-1	602	615	541	436	0.98	1.11	1.38
51	Clark	D1-2	713	614	541	436	1.16	1.32	1.64
52	Clark	D1-3	513	597	524	428	0.86	0.98	1.20
53	Clark	D2-1	580	591	518	428	0.98	1.12	1.35
54	Clark	D2-2	624	612	538	434	1.02	1.16	1.44
55	Clark	D2-3	669	599	527	429	1.12	1.27	1.56
56	Clark	D2-4	670	596	523	429	1.12	1.28	1.56
57	Clark	D3-1	790	800	706	571	0.99	1.12	1.38
58	Clark	D4-1	624	633	543	421	0.99	1.15	1.48
59	Clark	D1-6	349	348	378	266	0.84	0.92	1.31
60	Clark	D1-7	358	422	383	270	0.85	0.94	1.33
61	Clark	D1-8	372	420	380	268	0.88	0.98	1.39
62	Clark	E1-2	444	472	432	286	0.94	1.03	1.55
63	Clark	D2-6	337	411	395	236	0.82	0.85	1.43
64	Clark	D2-7	315	397	381	225	0.79	0.83	1.40
65	Clark	D4-1_1	337	384	274	214	0.88	1.23	1.57
66	Clark	D5-1	292	359	278	218	0.81	1.05	1.34
67	Clark	D5-2	315	375	293	231	0.84	1.07	1.36
68	Clark	D5-3	315	352	271	211	0.89	1.16	1.49
69	Tan, Teng, Kong, and Lu	1-2.00/1.00	1000	880	828	632	1.14	1.21	1.58
70	Tan, Teng, Kong, and Lu	1-2.00/1.50	500	690	666	477	0.72	0.75	1.05
71	Tan, Teng, Kong, and Lu	2-2.58/1.00	500	909	857	695	0.55	0.58	0.72
72	Tan, Teng, Kong, and Lu	2-2.58/1.50	300	710	681	518	0.42	0.44	0.58
73	Tan, Teng, Kong, and Lu	2-2.58/2.00	260	582	585	410	0.45	0.44	0.63
74	Higgins	8RA	594	503	478	315	1.18	1.24	1.89
75	Higgins	10RA	578	546	522	327	1.06	1.11	1.77
76	Higgins	12RA	489	474	453	316	1.03	1.08	1.55
77	Yun	Beam	511	560	547	389	0.91	0.93	1.31
78	Aguilar et al.	STM-M	1277	1128	1083	802	1.13	1.18	1.59
79	Tan, Kong, Teng, and Weng	II-2N/1.00	520	566	528	404	0.92	0.98	1.29
80	Tan, Kong, Teng, and Weng	III-2N/1.50	335	490	465	302	0.68	0.72	1.11

Num	Authors	Specimen	Experimental (kN)	Model Prediction (kN)	Model Prediction with effectiveness factor (kN)	Direct Strut Prediction (kN)	Experimental/Model Prediction	Experimental/Direct Strut Model Prediction with Effectiveness Factor	Experimental/Direct Strut Model Prediction
81	Oh and Shin	H43A0	374	311	299	284	1.20	1.25	1.32
82	Oh and Shin	U43A0	408	391	380	366	1.04	1.07	1.11
83	Kong and Robbins	2-10	199	110	97	32	1.81	2.05	6.22
84	de Paiva and Seiss	G33S-12	169	149	129	90	1.13	1.31	1.88
85	de Paiva and Seiss	G33S-32	203	145	121	86	1.40	1.68	2.36
86	de Paiva and Seiss	F3S3	243	244	217	146	1.00	1.12	1.66
87	Smith and Vansiotis	1B1-01	295	243	213	172	1.21	1.38	1.72
88	Smith and Vansiotis	2B1-05	258	225	189	145	1.15	1.37	1.78
89	Smith and Vansiotis	3B1-08	262	205	164	117	1.28	1.60	2.24
90	Smith and Vansiotis	3B1-36	318	256	212	157	1.24	1.50	2.03
91	Smith and Vansiotis	4B1-09	307	226	181	126	1.36	1.70	2.44
92	Smith and Vansiotis	1C1-14	238	176	157	123	1.35	1.52	1.93
93	Smith and Vansiotis	2C1-17	248	207	178	128	1.20	1.39	1.94
94	Smith and Vansiotis	3C1-20	282	238	202	137	1.18	1.40	2.06
95	Smith and Vansiotis	4C1-24	293	238	198	126	1.23	1.48	2.33
						Average	0.98	1.09	1.56
						Standard Deviation	0.20	0.23	0.22
						COV	0.21	0.21	0.14

Appendix G

Strut and Tie Models

Researcher: Aguilar et. al, 2002 Specimen: STM-M

1. Geometry

$$\begin{aligned}
 h &:= 36\text{in} & f_c &:= 4130\text{psi} & F_y &:= 61\text{ksi} & b &:= 12\text{in} & A_s &:= 6 \cdot 0.79\text{in}^2 \\
 \alpha_1 &:= 0.85 - 0.0015 \cdot \frac{f_c}{1\text{MPa}} & \beta_1 &:= 0.97 - 0.0025 \cdot \frac{f_c}{1\text{MPa}} & d &:= h - \frac{3 \cdot 0.79\text{in}^2 \cdot 2.5\text{in} + 3 \cdot 0.79\text{in}^2 \cdot 6.5\text{in}}{6 \cdot 0.79\text{in}^2} \\
 x &:= \frac{A_s \cdot F_y}{\alpha_1 \cdot b \cdot f_c} & x &= 183.562\text{mm} & c &:= \frac{x}{\beta_1} & c &= 204.227\text{mm} & \rho &:= \frac{A_s}{b \cdot d} \\
 z &:= d - \frac{x}{2} & z &= 708.319\text{mm} & d_1 &:= h - d & l_b &:= 12\text{in} & a &:= 36\text{in} & \frac{a}{d} &= 1.143 \\
 A_v &:= 2 \cdot 0.11\text{in}^2 & s &:= 6\text{in} \\
 a_w &:= 0.85 \cdot a - \frac{z}{4} & a_w &= 600.16\text{mm} & \frac{a_w}{s} &= 3.938 & n &:= 2 & \text{Number of effective stirrup} & & & \text{as specified}
 \end{aligned}$$

2. Strut Dimensions

$$\chi := \sqrt{f_c} \frac{1}{\sqrt{\text{MPa}}} + 250 \cdot \sqrt{\rho \cdot \left(\frac{d}{a}\right)^5} \quad \psi := 1.67 \cdot \frac{\sqrt{f_c} \frac{1}{\sqrt{\text{MPa}}}}{\chi} \quad \psi = 0.351 \quad F_y := 65\text{ksi}$$

$$F_1 := \psi \cdot n \cdot F_y \cdot A_v$$

For strength of the strut: $f_{cu} := 0.6 \cdot f_c$ By Inspection, this will control

Bottom Strut

$$\alpha_{\text{TOP}} := \text{atan}\left(\frac{l_b}{x}\right) \quad \alpha_{\text{TOP}} = 58.942 \text{ deg}$$

$$\begin{aligned}
 \theta &:= \left[\begin{array}{l} \theta \leftarrow 50\text{deg} \\ \text{for } i \in 1 \dots 20 \\ \left| \begin{array}{l} C_1 \leftarrow \frac{F_1}{\sin(\theta)} \\ f_{cu} \leftarrow 0.6 \cdot f_c \\ w_{st} \leftarrow \frac{C_1}{b \cdot f_{cu}} \\ \beta \leftarrow \begin{cases} 90\text{deg} - \alpha_{\text{TOP}} + \theta & \text{if } \theta < \alpha_{\text{TOP}} \\ 90\text{deg} - \theta + \alpha_{\text{TOP}} & \text{otherwise} \end{cases} \\ \theta \leftarrow \text{atan}\left[\frac{d - \left(x - 0.5 \cdot w_{st} \cdot \frac{\cos(\alpha_{\text{TOP}})}{\sin(\beta)} \right)}{0.5a + 0.5 \cdot l_b - 0.5 \cdot w_{st} \cdot \frac{\sin(\alpha_{\text{TOP}})}{\sin(\beta)}} \right] \end{array} \right. \\ \theta \end{array} \right. \quad \theta = 45.72 \text{ deg}
 \end{aligned}$$

$$C_1 := \frac{F_1}{\sin(\theta)} \quad C_1 = 62.379 \text{ kN}$$

$$\text{Required strut Width: } w_{st} := \frac{C_1}{b \cdot f_{cu}} \quad w_{st} = 11.979 \text{ mm} \quad \frac{w_{st}}{2} = 5.989 \text{ mm}$$

$$\text{Length along node: } \beta_{TOP} := \begin{cases} 90\text{deg} - \alpha_{TOP} + \theta & \text{if } \theta < \alpha_{TOP} \\ 90\text{deg} - \theta + \alpha_{TOP} & \text{otherwise} \end{cases}$$

$$L_{TOP} := \frac{w_{st}}{\sin(\beta_{TOP})} \quad L_{TOP} = 12.305 \text{ mm}$$

Top Strut

$$\alpha_{BOT} := \text{atan}\left(\frac{l_b}{2 \cdot d_1}\right) \quad \alpha_{BOT} = 53.13 \text{ deg}$$

$$\theta := \begin{cases} 50\text{deg} \\ \text{for } i \in 1..40 \\ \left| \begin{array}{l} C_1 \leftarrow \frac{F_1}{\cos(\theta)} \\ f_{cu} \leftarrow 0.6 \cdot f_c \\ w_{st} \leftarrow \frac{C_1}{b \cdot f_{cu}} \\ \beta \leftarrow \begin{cases} 90\text{deg} - \alpha_{BOT} + \theta & \text{if } \theta < \alpha_{BOT} \\ 90\text{deg} - \theta + \alpha_{BOT} & \text{otherwise} \end{cases} \\ \theta \leftarrow 90\text{deg} - \text{atan}\left[\frac{h - 0.5x - \left(2d_1 - 0.5 \cdot w_{st} \cdot \frac{\cos(\alpha_{BOT})}{\sin(\beta)}\right)}{0.5a + 0.5 \cdot l_b - 0.5 \cdot w_{st} \cdot \frac{\sin(\alpha_{BOT})}{\sin(\beta)}}\right] \end{array} \right| \end{cases} \quad \theta = 45.332 \text{ deg}$$

$$C_1 := \frac{F_1}{\cos(\theta)} \quad C_1 = 63.527 \text{ kN}$$

$$\text{Required strut Width: } w_{st} := \frac{C_1}{b \cdot f_{cu}} \quad w_{st} = 12.199 \text{ mm} \quad \frac{w_{st}}{2} = 6.099 \text{ mm}$$

$$\text{Length along node: } \beta_{BOT} := \begin{cases} 90\text{deg} - \alpha_{BOT} + \theta & \text{if } \theta < \alpha_{BOT} \\ 90\text{deg} - \theta + \alpha_{BOT} & \text{otherwise} \end{cases}$$

$$L_{BOT} := \frac{w_{st}}{\sin(\beta_{BOT})} \quad L_{BOT} = 12.313 \text{ mm}$$

Direct Strut

Check Bottom Node:

$$\text{CCT Node: } w_{BOT} := \sqrt{l_b^2 + (2 \cdot d_1)^2} - L_{BOT} \quad f_{cu} := 0.75 \cdot f_c \quad C_{BOT} := f_{cu} \cdot b \cdot w_{BOT}$$

$$C_{BOT} = 2.4 \times 10^3 \text{ kN}$$

Check Top Node:

$$\text{CCC Node: } w_{TOP} := \sqrt{l_b^2 + x^2} - L_{TOP} \quad f_{cu} := 0.85 \cdot f_c \quad C_{TOP} := f_{cu} \cdot b \cdot w_{TOP}$$

$$C_{TOP} = 2.534 \times 10^3 \text{ kN}$$

Check the strength of the strut:

$$\theta_2 := \text{atan}\left(\frac{h - 0.5 \cdot w_{TOP} \cdot \cos(\alpha_{TOP}) - 0.5 \cdot w_{BOT} \cdot \cos(\alpha_{BOT})}{a - l_b + 0.5 \cdot w_{TOP} \cdot \sin(\alpha_{TOP}) + 0.5 \cdot w_{BOT} \cdot \sin(\alpha_{BOT})}\right) \quad \theta_2 = 38.342 \text{ deg}$$

$$\sigma_{cw} := 0.6 \cdot f_c \quad \sigma_{cw} = 17.085 \text{ MPa}$$

Calculate β for direct strut

$$\text{At Top Node: } \beta_{DTOP} := \begin{cases} 90\text{deg} - \alpha_{TOP} + \theta_2 & \text{if } \theta_2 < \alpha_{TOP} \\ 90\text{deg} - \theta_2 + \alpha_{TOP} & \text{otherwise} \end{cases} \quad \beta_{DTOP} = 69.4 \text{ deg}$$

$$\text{At Bottom Node: } \beta_{DBOT} := \begin{cases} 90\text{deg} - \alpha_{BOT} + \theta_2 & \text{if } \theta_2 < \alpha_{BOT} \\ 90\text{deg} - \theta_2 + \alpha_{BOT} & \text{otherwise} \end{cases} \quad \beta_{DBOT} = 75.212 \text{ deg}$$

$$w_{st} := \min(w_{BOT} \cdot \sin(\beta_{DBOT}), w_{TOP} \cdot \sin(\beta_{DTOP})) \quad w_{st} = 321.539 \text{ mm}$$

$$C_{Strut} := \sigma_{cw} \cdot w_{st} \cdot b \quad C_{Strut} = 1.674 \times 10^3 \text{ kN} \quad \text{Check2} := \begin{cases} \text{"Model Not Applicable"} & \text{if } C_{Strut} < 0 \\ \text{"OK"} & \text{otherwise} \end{cases}$$

$$C_2 := \min(C_{TOP}, C_{BOT}, C_{Strut}) \quad C_2 = 1.674 \times 10^3 \text{ kN}$$

Check main tension reinforcement

$$F_y := 61 \text{ ksi}$$

$$T := C_2 \cdot \cos(\theta_2) + C_1 \cdot \sin(\theta) \quad T = 1358 \text{ kN} \quad T_r := A_s \cdot F_y \quad T_r = 1286 \text{ kN}$$

$$\text{Check} := \begin{cases} \text{"OK"} & \text{if } T < T_r \\ \text{"NG"} & \text{otherwise} \end{cases}$$

$$F_2 := C_2 \cdot \sin(\theta_2) \quad F_2 = 1.039 \times 10^3 \text{ kN}$$

$$\text{Therefore: } V := F_1 + F_2 \quad V = 1083 \text{ kN} \quad \text{Check} = \text{"NG"} \quad \text{Check2} = \text{"OK"}$$

Close enough

Researcher: Clark, 1951 Specimen: C2-1

1. Geometry

$$A_s := 2 \cdot 1.267 \text{ in}^2 \quad d := 15.38 \text{ in} \quad \text{Backcalculated from test information} \quad b := 8 \text{ in} \quad h := 18 \text{ in}$$

$$f_c := 3720 \text{ psi} \quad \alpha_1 := 0.85 - 0.0015 \frac{f_c}{1 \text{ MPa}} \quad \beta_1 := 0.97 - 0.0025 \frac{f_c}{1 \text{ MPa}} \quad F_y := 46500 \text{ psi}$$

$$x := \frac{A_s \cdot F_y}{\alpha_1 \cdot b \cdot f_c} \quad x = 123.925 \text{ mm} \quad c := \frac{x}{\beta_1} \quad c = 136.8 \text{ mm} \quad \rho := \frac{A_s}{b \cdot d}$$

$$z := d - \frac{x}{2} \quad z = 328.69 \text{ mm} \quad d_1 := h - d \quad l_b := 3.5 \text{ in} \quad a := 24 \text{ in} \quad \frac{a}{d} = 1.56$$

$$A_v := 2 \cdot 0.111 \text{ in}^2 \quad s := 4 \text{ in} \quad a_w := 0.85a - \frac{z}{4} \quad a_w = 435.988 \text{ mm} \quad \frac{a_w}{s} = 4.291 \quad n := 5$$

2. Strut Dimensions

$$\chi := \sqrt{f_c} \frac{1}{\sqrt{\text{MPa}}} + 250 \cdot \sqrt{\rho \cdot \left(\frac{d}{a}\right)^5} \quad \psi := 1.67 \cdot \frac{\sqrt{f_c} \frac{1}{\sqrt{\text{MPa}}}}{\chi} \quad \psi = 0.502$$

$$F_y := 48020 \text{ psi} \quad F_1 := \psi \cdot n \cdot F_y \cdot A_v$$

For strength of the strut: $f_{cu} := 0.6 \cdot f_c$ By Inspection, this will control

Bottom Strut

$$\alpha_{\text{TOP}} := \text{atan}\left(\frac{l_b}{x}\right) \quad \alpha_{\text{TOP}} = 35.655 \text{ deg}$$

$$\theta := \theta \leftarrow 50 \text{ deg}$$

for $i \in 1 \dots 20$

$$C_1 \leftarrow \frac{F_1}{\sin(\theta)}$$

$$f_{cu} \leftarrow 0.6 \cdot f_c$$

$$w_{st} \leftarrow \frac{C_1}{b \cdot f_{cu}}$$

$$\beta \leftarrow \begin{cases} 90 \text{ deg} - \alpha_{\text{TOP}} + \theta & \text{if } \theta < \alpha_{\text{TOP}} \\ 90 \text{ deg} - \theta + \alpha_{\text{TOP}} & \text{otherwise} \end{cases}$$

$$\theta = 41.141 \text{ deg}$$

$$\theta \leftarrow \text{atan}\left[\frac{d - \left(x - 0.5 \cdot w_{st} \cdot \frac{\cos(\alpha_{\text{TOP}})}{\sin(\beta)}\right)}{0.5a + 0.5 \cdot l_b - 0.5 \cdot w_{st} \cdot \frac{\sin(\alpha_{\text{TOP}})}{\sin(\beta)}}\right]$$

θ

$$C_1 := \frac{F_1}{\sin(\theta)} \quad C_1 = 180.791 \text{ kN}$$

$$\text{Required strut Width: } w_{st} := \frac{C_1}{b \cdot f_{cu}} \quad w_{st} = 57.815 \text{ mm} \quad \frac{w_{st}}{2} = 28.907 \text{ mm}$$

$$\text{Length along node: } \beta_{TOP} := \begin{cases} 90\text{deg} - \alpha_{TOP} + \theta & \text{if } \theta < \alpha_{TOP} \\ 90\text{deg} - \theta + \alpha_{TOP} & \text{otherwise} \end{cases}$$

$$L_{TOP} := \frac{w_{st}}{\sin(\beta_{TOP})} \quad L_{TOP} = 58.081 \text{ mm}$$

Top Strut

$$\alpha_{BOT} := \text{atan}\left(\frac{l_b}{2 \cdot d_1}\right) \quad \alpha_{BOT} = 33.741 \text{ deg}$$

$$\theta := 50\text{deg}$$

for i ∈ 1 .. 40

$$C_1 \leftarrow \frac{F_1}{\cos(\theta)}$$

$$f_{cu} \leftarrow 0.6 \cdot f_c$$

$$w_{st} \leftarrow \frac{C_1}{b \cdot f_{cu}}$$

$$\beta \leftarrow \begin{cases} 90\text{deg} - \alpha_{BOT} + \theta & \text{if } \theta < \alpha_{BOT} \\ 90\text{deg} - \theta + \alpha_{BOT} & \text{otherwise} \end{cases}$$

$$\theta \leftarrow 90\text{deg} - \text{atan}\left[\frac{h - 0.5x - \left(2d_1 - 0.5 \cdot w_{st} \cdot \frac{\cos(\alpha_{BOT})}{\sin(\beta)}\right)}{0.5a + 0.5 \cdot l_b - 0.5 \cdot w_{st} \cdot \frac{\sin(\alpha_{BOT})}{\sin(\beta)}}\right]$$

$$\theta = 49.176 \text{ deg}$$

$$C_1 := \frac{F_1}{\cos(\theta)} \quad C_1 = 181.946 \text{ kN}$$

$$\text{Required strut Width: } w_{st} := \frac{C_1}{b \cdot f_{cu}} \quad w_{st} = 58.184 \text{ mm} \quad \frac{w_{st}}{2} = 29.092 \text{ mm}$$

$$\text{Length along node: } \beta_{BOT} := \begin{cases} 90\text{deg} - \alpha_{BOT} + \theta & \text{if } \theta < \alpha_{BOT} \\ 90\text{deg} - \theta + \alpha_{BOT} & \text{otherwise} \end{cases}$$

$$L_{BOT} := \frac{w_{st}}{\sin(\beta_{BOT})} \quad L_{BOT} = 60.361 \text{ mm}$$

Direct Strut

Check Bottom Node:

$$\text{CCT Node: } w_{\text{BOT}} := \sqrt{l_b^2 + (2 \cdot d_1)^2} - L_{\text{BOT}} \quad f_{\text{cu}} := 0.75 \cdot f_c \quad C_{\text{BOT}} := f_{\text{cu}} \cdot b \cdot w_{\text{BOT}} \\ C_{\text{BOT}} = 389.687 \text{ kN}$$

Check Top Node:

$$\text{CCC Node: } w_{\text{TOP}} := \sqrt{l_b^2 + x^2} - L_{\text{TOP}} \quad f_{\text{cu}} := 0.85 \cdot f_c \quad C_{\text{TOP}} := f_{\text{cu}} \cdot b \cdot w_{\text{TOP}} \\ C_{\text{TOP}} = 418.339 \text{ kN}$$

Check the strength of the strut:

$$\theta_2 := \text{atan} \left(\frac{h - 0.5 \cdot w_{\text{TOP}} \cdot \cos(\alpha_{\text{TOP}}) - 0.5 \cdot w_{\text{BOT}} \cdot \cos(\alpha_{\text{BOT}})}{a - l_b + 0.5 \cdot w_{\text{TOP}} \cdot \sin(\alpha_{\text{TOP}}) + 0.5 \cdot w_{\text{BOT}} \cdot \sin(\alpha_{\text{BOT}})} \right) \quad \theta_2 = 33.236 \text{ deg}$$

$$v_1 := 1 - \frac{47}{250} \quad v_1 = 0.812$$

$$\text{Check that width of bearing plate: } a_f := \frac{x}{\sin(\theta_2)} \cdot \left(\frac{v_1}{0.6 \cos(\theta_2)} - \cos(\theta_2) \right) \quad a_f = 176.719 \text{ mm}$$

Assume that a bearing plate of 125 mm will be ok.

$$\sigma_{\text{cw}} := 0.6 \cdot f_c \quad \sigma_{\text{cw}} = 15.389 \text{ MPa}$$

Calculate β for direct strut

$$\text{At Top Node: } \beta_{\text{DTOP}} := \begin{cases} 90 \text{ deg} - \alpha_{\text{TOP}} + \theta_2 & \text{if } \theta_2 < \alpha_{\text{TOP}} \\ 90 \text{ deg} - \theta_2 + \alpha_{\text{TOP}} & \text{otherwise} \end{cases} \quad \beta_{\text{DTOP}} = 87.582 \text{ deg}$$

$$\text{At Bottom Node: } \beta_{\text{DBOT}} := \begin{cases} 90 \text{ deg} - \alpha_{\text{BOT}} + \theta_2 & \text{if } \theta_2 < \alpha_{\text{BOT}} \\ 90 \text{ deg} - \theta_2 + \alpha_{\text{BOT}} & \text{otherwise} \end{cases} \quad \beta_{\text{DBOT}} = 89.496 \text{ deg}$$

$$w_{\text{st}} := \min(w_{\text{BOT}} \cdot \sin(\beta_{\text{DBOT}}), w_{\text{TOP}} \cdot \sin(\beta_{\text{DTOP}})) \quad w_{\text{st}} = 94.349 \text{ mm}$$

$$C_{\text{Strut}} := \sigma_{\text{cw}} \cdot w_{\text{st}} \cdot b \quad C_{\text{Strut}} = 295.035 \text{ kN} \quad \text{Check2} := \begin{cases} \text{"Model Not Applicable"} & \text{if } C_{\text{Strut}} < 0 \\ \text{"OK"} & \text{otherwise} \end{cases}$$
$$C_2 := \min(C_{\text{TOP}}, C_{\text{BOT}}, C_{\text{Strut}}) \quad C_2 = 295.035 \text{ kN}$$

Check main tension reinforcement

$$F_y := 46500 \text{ psi}$$

$$T := C_2 \cdot \cos(\theta_2) + C_1 \cdot \sin(\theta) \quad T = 384 \text{ kN} \quad T_r := A_s \cdot F_y \quad T_r = 524 \text{ kN}$$

$$\text{Check} := \begin{cases} \text{"OK"} & \text{if } T < T_r \\ \text{"NG"} & \text{otherwise} \end{cases} \quad F_2 := C_2 \cdot \sin(\theta_2) \quad F_2 = 161.706 \text{ kN}$$

$$\text{Therefore: } V := F_1 + F_2 \quad V = 280.651 \text{ kN}$$

$$P := 2 \cdot V \quad P = 561 \text{ kN} \quad \text{Check} = \text{"OK"} \quad \text{Check2} = \text{"OK"}$$

Researcher: de Paiva and Siess, 1965 Specimen: F3S3

1. Geometry

$$\begin{aligned}
 d &:= 8\text{in} & f_c &:= 4980\text{psi} & F_y &:= 47.4\text{ksi} & b &:= 3\text{in} & A_s &:= 2.020\text{in}^2 \\
 \alpha_1 &:= 0.85 - 0.0015 \cdot \frac{f_c}{1\text{MPa}} & \beta_1 &:= 0.97 - 0.0025 \cdot \frac{f_c}{1\text{MPa}} & h &:= 9\text{in} & \rho &:= \frac{A_s}{b \cdot d} \\
 x &:= \frac{A_s \cdot F_y}{\alpha_1 \cdot b \cdot f_c} & x &= 40.369\text{mm} & c &:= \frac{x}{\beta_1} & c &= 45.658\text{mm} & A_v &:= 2 \cdot \pi \cdot (0.5 \cdot 0.177\text{in})^2 \\
 z &:= d - \frac{x}{2} & z &= 183.015\text{mm} & d_1 &:= 1\text{in} & l_b &:= 4\text{in} & a &:= 8\text{in} & s &:= 1.25\text{in} \\
 a_w &:= 0.85 \cdot a - \frac{z}{4} & a_w &= 126.966\text{mm} & \frac{a_w}{s} &= 3.999 & n &:= 5 & \text{Number of effective stirrups}
 \end{aligned}$$

2. Strut Dimensions

$$\chi := \sqrt{f_c} \frac{1}{\sqrt{\text{MPa}}} + 250 \cdot \sqrt{\rho \cdot \left(\frac{d}{a}\right)^5} \quad \psi := 1.67 \cdot \frac{\sqrt{f_c} \frac{1}{\sqrt{\text{MPa}}}}{\chi} \quad \psi = 0.257$$

$$F_y := 32\text{ksi} \quad F_1 := \psi \cdot n \cdot F_y \cdot A_v$$

For strength of the strut: $f_{cu} := 0.6 \cdot f_c$ By Inspection, this will control

Bottom Strut

$$\alpha_{\text{TOP}} := \text{atan}\left(\frac{l_b}{x}\right) \quad \alpha_{\text{TOP}} = 68.33\text{deg}$$

$$\theta := \left\{ \begin{array}{l} \theta \leftarrow 50\text{deg} \\ \text{for } i \in 1..20 \\ \left| \begin{array}{l} C_1 \leftarrow \frac{F_1}{\sin(\theta)} \\ f_{cu} \leftarrow 0.6 \cdot f_c \\ w_{st} \leftarrow \frac{C_1}{b \cdot f_{cu}} \\ \beta \leftarrow \begin{cases} 90\text{deg} - \alpha_{\text{TOP}} + \theta & \text{if } \theta < \alpha_{\text{TOP}} \\ 90\text{deg} - \theta + \alpha_{\text{TOP}} & \text{otherwise} \end{cases} \\ \theta \leftarrow \text{atan}\left[\frac{d - \left(x - 0.5 \cdot w_{st} \cdot \frac{\cos(\alpha_{\text{TOP}})}{\sin(\beta)} \right)}{0.5a + 0.5 \cdot l_b - 0.5 \cdot w_{st} \cdot \frac{\sin(\alpha_{\text{TOP}})}{\sin(\beta)}} \right] \end{array} \right. \\ \theta \end{array} \right. \quad \theta = 47.887\text{deg}$$

$$C_1 := \frac{F_1}{\sin(\theta)} \quad C_1 = 12.116 \text{ kN}$$

$$\text{Required strut Width: } w_{st} := \frac{C_1}{b \cdot f_{cu}} \quad w_{st} = 7.718 \text{ mm} \quad \frac{w_{st}}{2} = 3.859 \text{ mm}$$

$$\text{Length along node: } \beta_{TOP} := \begin{cases} 90\text{deg} - \alpha_{TOP} + \theta & \text{if } \theta < \alpha_{TOP} \\ 90\text{deg} - \theta + \alpha_{TOP} & \text{otherwise} \end{cases}$$

$$L_{TOP} := \frac{w_{st}}{\sin(\beta_{TOP})} \quad L_{TOP} = 8.237 \text{ mm}$$

Top Strut

$$\alpha_{BOT} := \text{atan}\left(\frac{l_b}{2 \cdot d_1}\right) \quad \alpha_{BOT} = 63.435 \text{ deg}$$

$$\theta := 50\text{deg}$$

for i ∈ 1 .. 40

$$C_1 \leftarrow \frac{F_1}{\cos(\theta)}$$

$$f_{cu} \leftarrow 0.6 \cdot f_c$$

$$w_{st} \leftarrow \frac{C_1}{b \cdot f_{cu}}$$

$$\beta \leftarrow \begin{cases} 90\text{deg} - \alpha_{BOT} + \theta & \text{if } \theta < \alpha_{BOT} \\ 90\text{deg} - \theta + \alpha_{BOT} & \text{otherwise} \end{cases}$$

$$\theta = 42.989 \text{ deg}$$

$$\theta \leftarrow 90\text{deg} - \text{atan}\left[\frac{h - 0.5x - \left(2d_1 - 0.5 \cdot w_{st} \cdot \frac{\cos(\alpha_{BOT})}{\sin(\beta)}\right)}{0.5a + 0.5 \cdot l_b - 0.5 \cdot w_{st} \cdot \frac{\sin(\alpha_{BOT})}{\sin(\beta)}}\right]$$

$$C_1 := \frac{F_1}{\cos(\theta)} \quad C_1 = 12.287 \text{ kN}$$

$$\text{Required strut Width: } w_{st} := \frac{C_1}{b \cdot f_{cu}} \quad w_{st} = 7.827 \text{ mm} \quad \frac{w_{st}}{2} = 3.913 \text{ mm}$$

$$\text{Length along node: } \beta_{BOT} := \begin{cases} 90\text{deg} - \alpha_{BOT} + \theta & \text{if } \theta < \alpha_{BOT} \\ 90\text{deg} - \theta + \alpha_{BOT} & \text{otherwise} \end{cases}$$

$$L_{BOT} := \frac{w_{st}}{\sin(\beta_{BOT})} \quad L_{BOT} = 8.353 \text{ mm}$$

Direct Strut

Check Bottom Node:

$$\text{CCT Node: } w_{\text{BOT}} := \sqrt{l_b^2 + (2 \cdot d_1)^2} - L_{\text{BOT}} \quad f_{\text{cu}} := 0.75 \cdot f_c \quad C_{\text{BOT}} := f_{\text{cu}} \cdot b \cdot w_{\text{BOT}} \\ C_{\text{BOT}} = 206.51 \text{ kN}$$

Check Top Node:

$$\text{CCC Node: } w_{\text{TOP}} := \sqrt{l_b^2 + x^2} - L_{\text{TOP}} \quad f_{\text{cu}} := 0.85 \cdot f_c \quad C_{\text{TOP}} := f_{\text{cu}} \cdot b \cdot w_{\text{TOP}} \\ C_{\text{TOP}} = 224.817 \text{ kN}$$

Check the strength of the strut:

$$\theta_2 := \text{atan} \left(\frac{h - 0.5 \cdot w_{\text{TOP}} \cdot \cos(\alpha_{\text{TOP}}) - 0.5 \cdot w_{\text{BOT}} \cdot \cos(\alpha_{\text{BOT}})}{a - l_b + 0.5 \cdot w_{\text{TOP}} \cdot \sin(\alpha_{\text{TOP}}) + 0.5 \cdot w_{\text{BOT}} \cdot \sin(\alpha_{\text{BOT}})} \right) \quad \theta_2 = 43.616 \text{ deg}$$

$$\sigma_{\text{cw}} := 0.6 \cdot f_c \quad \sigma_{\text{cw}} = 20.602 \text{ MPa}$$

Calculate β for direct strut

$$\text{At Top Node: } \beta_{\text{DTOP}} := \begin{cases} 90\text{deg} - \alpha_{\text{TOP}} + \theta_2 & \text{if } \theta_2 < \alpha_{\text{TOP}} \\ 90\text{deg} - \theta_2 + \alpha_{\text{TOP}} & \text{otherwise} \end{cases} \quad \beta_{\text{DTOP}} = 65.285 \text{ deg}$$

$$\text{At Bottom Node: } \beta_{\text{DBOT}} := \begin{cases} 90\text{deg} - \alpha_{\text{BOT}} + \theta_2 & \text{if } \theta_2 < \alpha_{\text{BOT}} \\ 90\text{deg} - \theta_2 + \alpha_{\text{BOT}} & \text{otherwise} \end{cases} \quad \beta_{\text{DBOT}} = 70.181 \text{ deg}$$

$$w_{\text{st}} := \min(w_{\text{BOT}} \cdot \sin(\beta_{\text{DBOT}}), w_{\text{TOP}} \cdot \sin(\beta_{\text{DTOP}})) \quad w_{\text{st}} = 91.83 \text{ mm}$$

$$C_{\text{Strut}} := \sigma_{\text{cw}} \cdot w_{\text{st}} \cdot b \quad C_{\text{Strut}} = 144.158 \text{ kN} \quad \text{Check2} := \begin{cases} \text{"Model Not Applicable"} & \text{if } C_{\text{Strut}} < 0 \\ \text{"OK"} & \text{otherwise} \end{cases} \\ C_2 := \min(C_{\text{TOP}}, C_{\text{BOT}}, C_{\text{Strut}}) \quad C_2 = 144.158 \text{ kN}$$

Check main tension reinforcement

$$F_y := 47.4 \text{ ksi}$$

$$T := C_2 \cdot \cos(\theta_2) + C_1 \cdot \sin(\theta) \quad T = 113 \text{ kN} \quad T_r := A_s \cdot F_y \quad T_r = 84 \text{ kN}$$

$$\text{Check} := \begin{cases} \text{"OK"} & \text{if } T < T_r \\ \text{"NG"} & \text{otherwise} \end{cases} \quad \text{Assume that this is ok!}$$

$$F_2 := C_2 \cdot \sin(\theta_2) \quad F_2 = \text{■} \text{ kN}$$

$$\text{Therefore: } V := F_1 + F_2 \quad V = 108 \text{ kN} \quad \text{Check} = \text{"NG"} \quad \text{Check2} = \text{"OK"}$$

Researcher: Higgins and Farrow, 2006 Specimen: 8RA

1. Geometry

$$d := 20.5\text{in} \quad f_c := 29.3\text{MPa} \quad F_y := 417\text{MPa} \quad b := 10\text{in} \quad A_s := 5 \cdot \pi \cdot (0.5\text{in})^2$$

$$\alpha_1 := 0.85 - 0.0015 \frac{f_c}{1\text{MPa}} \quad \beta_1 := 0.97 - 0.0025 \frac{f_c}{1\text{MPa}} \quad h := 24\text{in} \quad \rho := \frac{A_s}{b \cdot d}$$

$$x := \frac{A_s \cdot F_y}{\alpha_1 \cdot b \cdot f_c} \quad x = 176.117\text{mm} \quad c := \frac{x}{\beta_1} \quad c = 196.394\text{mm} \quad A_v := 2 \cdot \pi \cdot (0.25\text{in})^2 \quad s := 8\text{in}$$

$$z := d - \frac{x}{2} \quad z = 432.642\text{mm} \quad d_1 := h - d \quad l_b := 100\text{mm} \quad a := 2.04d \quad \text{Assume 100 mm bearing plates}$$

$$a_w := 0.85a - \frac{z}{4} \quad a_w = 794.733\text{mm} \quad \frac{a_w}{s} = 3.911 \quad n := 4 \quad \text{Number of effective stirrups}$$

2. Strut Dimensions

$$\chi := \sqrt{f_c} \frac{1}{\sqrt{\text{MPa}}} + 250 \sqrt{\rho \cdot \left(\frac{d}{a}\right)^5} \quad \psi := 1.67 \cdot \frac{\sqrt{f_c} \frac{1}{\sqrt{\text{MPa}}}}{\chi} \quad \psi = 0.805$$

$$F_1 := \psi \cdot n \cdot F_y \cdot A_v$$

For strength of the strut: $f_{cu} := 0.6f_c$ By Inspection, this will control

$$\alpha_{\text{TOP}} := \text{atan}\left(\frac{l_b}{x}\right) \quad \alpha_{\text{TOP}} = 29.588\text{deg}$$

$$\theta := \left| \begin{array}{l} \theta \leftarrow 50\text{deg} \\ \text{for } i \in 1..20 \\ \left| \begin{array}{l} C_1 \leftarrow \frac{F_1}{\sin(\theta)} \\ f_{cu} \leftarrow 0.6f_c \\ w_{st} \leftarrow \frac{C_1}{b \cdot f_{cu}} \\ \beta \leftarrow \begin{cases} 90\text{deg} - \alpha_{\text{TOP}} + \theta & \text{if } \theta < \alpha_{\text{TOP}} \\ 90\text{deg} - \theta + \alpha_{\text{TOP}} & \text{otherwise} \end{cases} \\ \theta \leftarrow \text{atan}\left[\frac{d - \left(x - 0.5 \cdot w_{st} \cdot \frac{\cos(\alpha_{\text{TOP}})}{\sin(\beta)} \right)}{0.5a + 0.5l_b - 0.5 \cdot w_{st} \cdot \frac{\sin(\alpha_{\text{TOP}})}{\sin(\beta)}} \right] \end{array} \right. \\ \theta \end{array} \right. \quad \theta = 36.149\text{deg}$$

$$C_1 := \frac{F_1}{\sin(\theta)} \quad C_1 = 576.448 \text{ kN}$$

$$\text{Required strut Width: } w_{st} := \frac{C_1}{b \cdot f_{cu}} \quad w_{st} = 129.095 \text{ mm} \quad \frac{w_{st}}{2} = 64.547 \text{ mm}$$

$$\text{Length along node: } \beta_{TOP} := \begin{cases} 90\text{deg} - \alpha_{TOP} + \theta & \text{if } \theta < \alpha_{TOP} \\ 90\text{deg} - \theta + \alpha_{TOP} & \text{otherwise} \end{cases}$$

$$L_{TOP} := \frac{w_{st}}{\sin(\beta_{TOP})} \quad L_{TOP} = 129.946 \text{ mm}$$

Top Strut

$$\alpha_{BOT} := \text{atan}\left(\frac{l_b}{2 \cdot d_1}\right) \quad \alpha_{BOT} = 29.355 \text{ deg}$$

$$\theta := \begin{cases} 50\text{deg} \\ \text{for } i \in 1..40 \\ \left| \begin{array}{l} C_1 \leftarrow \frac{F_1}{\cos(\theta)} \\ f_{cu} \leftarrow 0.6 \cdot f_c \\ w_{st} \leftarrow \frac{C_1}{b \cdot f_{cu}} \\ \beta \leftarrow \begin{cases} 90\text{deg} - \alpha_{BOT} + \theta & \text{if } \theta < \alpha_{BOT} \\ 90\text{deg} - \theta + \alpha_{BOT} & \text{otherwise} \end{cases} \\ \theta \leftarrow 90\text{deg} - \text{atan}\left[\frac{h - 0.5x - \left(2d_1 - 0.5 \cdot w_{st} \cdot \frac{\cos(\alpha_{BOT})}{\sin(\beta)}\right)}{0.5a + 0.5 \cdot l_b - 0.5 \cdot w_{st} \cdot \frac{\sin(\alpha_{BOT})}{\sin(\beta)}}\right] \end{array} \right| \\ \theta \end{cases} \quad \theta = 53.481 \text{ deg}$$

$$C_1 := \frac{F_1}{\cos(\theta)} \quad C_1 = 571.414 \text{ kN}$$

$$\text{Required strut Width: } w_{st} := \frac{C_1}{b \cdot f_{cu}} \quad w_{st} = 127.967 \text{ mm} \quad \frac{w_{st}}{2} = 63.984 \text{ mm}$$

$$\text{Length along node: } \beta_{BOT} := \begin{cases} 90\text{deg} - \alpha_{BOT} + \theta & \text{if } \theta < \alpha_{BOT} \\ 90\text{deg} - \theta + \alpha_{BOT} & \text{otherwise} \end{cases}$$

$$L_{BOT} := \frac{w_{st}}{\sin(\beta_{BOT})} \quad L_{BOT} = 140.216 \text{ mm}$$

Direct Strut

Check Bottom Node:

$$\text{CCT Node: } w_{\text{BOT}} := \sqrt{l_b^2 + (2 \cdot d_1)^2} - L_{\text{BOT}} \quad f_{\text{cu}} := 0.75 \cdot f_c \quad C_{\text{BOT}} := f_{\text{cu}} \cdot b \cdot w_{\text{BOT}} \\ C_{\text{BOT}} = 355.978 \text{ kN}$$

Check Top Node:

$$\text{CCC Node: } w_{\text{TOP}} := \sqrt{l_b^2 + x^2} - L_{\text{TOP}} \quad f_{\text{cu}} := 0.85 \cdot f_c \quad C_{\text{TOP}} := f_{\text{cu}} \cdot b \cdot w_{\text{TOP}} \\ C_{\text{TOP}} = 459.138 \text{ kN}$$

Check the strength of the strut:

$$\theta_2 := \text{atan} \left(\frac{h - 0.5 \cdot w_{\text{TOP}} \cdot \cos(\alpha_{\text{TOP}}) - 0.5 \cdot w_{\text{BOT}} \cdot \cos(\alpha_{\text{BOT}})}{a - l_b + 0.5 \cdot w_{\text{TOP}} \cdot \sin(\alpha_{\text{TOP}}) + 0.5 \cdot w_{\text{BOT}} \cdot \sin(\alpha_{\text{BOT}})} \right) \quad \theta_2 = 28.924 \text{ deg}$$

$$\sigma_{\text{cw}} := 0.6 \cdot f_c \quad \sigma_{\text{cw}} = 17.58 \text{ MPa}$$

Calculate β for direct strut

$$\text{At Top Node: } \beta_{\text{DTOP}} := \begin{cases} 90 \text{deg} - \alpha_{\text{TOP}} + \theta_2 & \text{if } \theta_2 < \alpha_{\text{TOP}} \\ 90 \text{deg} - \theta_2 + \alpha_{\text{TOP}} & \text{otherwise} \end{cases} \quad \beta_{\text{DTOP}} = 89.336 \text{ deg}$$

$$\text{At Bottom Node: } \beta_{\text{DBOT}} := \begin{cases} 90 \text{deg} - \alpha_{\text{BOT}} + \theta_2 & \text{if } \theta_2 < \alpha_{\text{BOT}} \\ 90 \text{deg} - \theta_2 + \alpha_{\text{BOT}} & \text{otherwise} \end{cases} \quad \beta_{\text{DBOT}} = 89.569 \text{ deg}$$

$$w_{\text{st}} := \min(w_{\text{BOT}} \cdot \sin(\beta_{\text{DBOT}}), w_{\text{TOP}} \cdot \sin(\beta_{\text{DTOP}})) \quad w_{\text{st}} = 63.775 \text{ mm}$$

$$C_{\text{Strut}} := \sigma_{\text{cw}} \cdot w_{\text{st}} \cdot b \quad C_{\text{Strut}} = 284.774 \text{ kN} \quad \text{Check2} := \begin{cases} \text{"Model Not Applicable"} & \text{if } C_{\text{Strut}} < 0 \\ \text{"OK"} & \text{otherwise} \end{cases}$$

$$C_2 := \min(C_{\text{TOP}}, C_{\text{BOT}}, C_{\text{Strut}}) \quad C_2 = 284.774 \text{ kN}$$

Check main tension reinforcement

$$F_y := 417 \text{ MPa}$$

$$T := C_2 \cdot \cos(\theta_2) + C_1 \cdot \sin(\theta) \quad T = 708 \text{ kN} \quad T_r := A_s \cdot F_y \quad T_r = 1056 \text{ kN}$$

$$\text{Check} := \begin{cases} \text{"OK"} & \text{if } T < T_r \\ \text{"NG"} & \text{otherwise} \end{cases}$$

$$F_2 := C_2 \cdot \sin(\theta_2) \quad F_2 = 137.732 \text{ kN}$$

$$\text{Therefore: } V := F_1 + F_2 \quad V = 478 \text{ kN} \quad \text{Check} = \text{"OK"} \quad \text{Check2} = \text{"OK"}$$

Researcher: Kong and Robbins, 1970 Specimen: 2-10

1. Geometry

$$d := \frac{30\text{in}}{3.53} \quad f_c := 2920\text{psi} \quad F_y := 41600\text{psi} \quad b := 3\text{in} \quad A_s := \pi \cdot (0.5 \cdot 0.75\text{in})^2$$

$$\alpha_1 := 0.85 - 0.0015 \cdot \frac{f_c}{1\text{MPa}} \quad \beta_1 := 0.97 - 0.0025 \cdot \frac{f_c}{1\text{MPa}} \quad h := 10\text{in} \quad \rho := \frac{A_s}{b \cdot d}$$

$$x := \frac{A_s \cdot F_y}{\alpha_1 \cdot b \cdot f_c} \quad x = 65.002\text{mm} \quad c := \frac{x}{\beta_1} \quad c = 70.68\text{mm} \quad A_v := 2 \cdot \pi \cdot \left(0.5 \cdot \frac{5}{16}\text{in}\right)^2$$

$$z := d - \frac{x}{2} \quad z = 183.363\text{mm} \quad d_1 := 0.5 \cdot 1.5\text{in} \quad l_b := 3\text{in} \quad a := 10\text{in} \quad s := 6\text{in}$$

$$a_w := 0.85 \cdot a - \frac{z}{4} \quad a_w = 170.059\text{mm} \quad \frac{a_w}{s} = 1.116 \quad n := 1 \quad \text{Number of effective stirrups}$$

From Inspection this is the reinforcing steel that would be effective

2. Strut Dimensions

$$\chi := \sqrt{f_c} \frac{1}{\sqrt{\text{MPa}}} + 250 \cdot \sqrt{\rho \cdot \left(\frac{d}{a}\right)^5} \quad \psi := 1.67 \cdot \frac{\sqrt{f_c}}{\sqrt{\text{MPa}}} \frac{1}{\chi} \quad \psi = 0.284$$

$$F_y := 44\text{ksi} \quad F_1 := \psi \cdot n \cdot F_y \cdot A_v$$

For strength of the strut: $f_{cu} := 0.6 \cdot f_c$ By Inspection, this will control

Bottom Strut

$$\alpha_{\text{TOP}} := \text{atan}\left(\frac{l_b}{x}\right) \quad \alpha_{\text{TOP}} = 49.534\text{deg}$$

$$\theta := \theta \leftarrow 50\text{deg}$$

for $i \in 1..20$

$$C_1 \leftarrow \frac{F_1}{\sin(\theta)}$$

$$f_{cu} \leftarrow 0.6 \cdot f_c$$

$$w_{st} \leftarrow \frac{C_1}{b \cdot f_{cu}}$$

$$\beta \leftarrow \begin{cases} 90\text{deg} - \alpha_{\text{TOP}} + \theta & \text{if } \theta < \alpha_{\text{TOP}} \\ 90\text{deg} - \theta + \alpha_{\text{TOP}} & \text{otherwise} \end{cases}$$

$$\theta = 44.124\text{deg}$$

$$\theta \leftarrow \text{atan}\left[\frac{d - \left(x - 0.5 \cdot w_{st} \cdot \frac{\cos(\alpha_{\text{TOP}})}{\sin(\beta)}\right)}{0.5a + 0.5 \cdot l_b - 0.5 \cdot w_{st} \cdot \frac{\sin(\alpha_{\text{TOP}})}{\sin(\beta)}}\right]$$

θ

$$C_1 := \frac{F_1}{\sin(\theta)} \quad C_1 = 12.241 \text{ kN}$$

$$\text{Required strut Width: } w_{st} := \frac{C_1}{b \cdot f_{cu}} \quad w_{st} = 13.298 \text{ mm} \quad \frac{w_{st}}{2} = 6.649 \text{ mm}$$

$$\text{Length along node: } \beta_{TOP} := \begin{cases} 90\text{deg} - \alpha_{TOP} + \theta & \text{if } \theta < \alpha_{TOP} \\ 90\text{deg} - \theta + \alpha_{TOP} & \text{otherwise} \end{cases}$$

$$L_{TOP} := \frac{w_{st}}{\sin(\beta_{TOP})} \quad L_{TOP} = 13.358 \text{ mm}$$

Top Strut

$$\alpha_{BOT} := \text{atan}\left(\frac{l_b}{2 \cdot d_1}\right) \quad \alpha_{BOT} = 63.435 \text{ deg}$$

$$\theta := 50\text{deg}$$

for i ∈ 1..40

$$C_1 \leftarrow \frac{F_1}{\cos(\theta)}$$

$$f_{cu} \leftarrow 0.6 \cdot f_c$$

$$w_{st} \leftarrow \frac{C_1}{b \cdot f_{cu}}$$

$$\beta \leftarrow \begin{cases} 90\text{deg} - \alpha_{BOT} + \theta & \text{if } \theta < \alpha_{BOT} \\ 90\text{deg} - \theta + \alpha_{BOT} & \text{otherwise} \end{cases}$$

$$\theta = 40.504 \text{ deg}$$

$$\theta \leftarrow 90\text{deg} - \text{atan}\left[\frac{h - 0.5x - \left(2d_1 - 0.5 \cdot w_{st} \cdot \frac{\cos(\alpha_{BOT})}{\sin(\beta)}\right)}{0.5a + 0.5 \cdot l_b - 0.5 \cdot w_{st} \cdot \frac{\sin(\alpha_{BOT})}{\sin(\beta)}}\right]$$

$$C_1 := \frac{F_1}{\cos(\theta)} \quad C_1 = 11.208 \text{ kN}$$

$$\text{Required strut Width: } w_{st} := \frac{C_1}{b \cdot f_{cu}} \quad w_{st} = 12.176 \text{ mm} \quad \frac{w_{st}}{2} = 6.088 \text{ mm}$$

$$\text{Length along node: } \beta_{BOT} := \begin{cases} 90\text{deg} - \alpha_{BOT} + \theta & \text{if } \theta < \alpha_{BOT} \\ 90\text{deg} - \theta + \alpha_{BOT} & \text{otherwise} \end{cases}$$

$$L_{BOT} := \frac{w_{st}}{\sin(\beta_{BOT})} \quad L_{BOT} = 13.221 \text{ mm}$$

Direct Strut

Check Bottom Node:

$$\text{CCT Node: } w_{\text{BOT}} := \sqrt{l_b^2 + (2 \cdot d_1)^2} - L_{\text{BOT}} \quad f_{\text{cu}} := 0.75 \cdot f_c \quad C_{\text{BOT}} := f_{\text{cu}} \cdot b \cdot w_{\text{BOT}} \quad C_{\text{BOT}} = 82.811 \text{ kN}$$

Check Top Node:

$$\text{CCC Node: } w_{\text{TOP}} := \sqrt{l_b^2 + x^2} - L_{\text{TOP}} \quad f_{\text{cu}} := 0.85 \cdot f_c \quad C_{\text{TOP}} := f_{\text{cu}} \cdot b \cdot w_{\text{TOP}} \quad C_{\text{TOP}} = 113.187 \text{ kN}$$

Check the strength of the strut:

$$\theta_2 := \text{atan}\left(\frac{h - 0.5 \cdot w_{\text{TOP}} \cdot \cos(\alpha_{\text{TOP}}) - 0.5 \cdot w_{\text{BOT}} \cdot \cos(\alpha_{\text{BOT}})}{a - l_b + 0.5 \cdot w_{\text{TOP}} \cdot \sin(\alpha_{\text{TOP}}) + 0.5 \cdot w_{\text{BOT}} \cdot \sin(\alpha_{\text{BOT}})}\right) \quad \theta_2 = 40.798 \text{ deg}$$

$$\sigma_{\text{cw}} := 0.6 \cdot f_c \quad \sigma_{\text{cw}} = 12.08 \text{ MPa}$$

Calculate β for direct strut

$$\text{At Top Node: } \beta_{\text{DTOP}} := \begin{cases} 90\text{deg} - \alpha_{\text{TOP}} + \theta_2 & \text{if } \theta_2 < \alpha_{\text{TOP}} \\ 90\text{deg} - \theta_2 + \alpha_{\text{TOP}} & \text{otherwise} \end{cases} \quad \beta_{\text{DTOP}} = 81.263 \text{ deg}$$

$$\text{At Bottom Node: } \beta_{\text{DBOT}} := \begin{cases} 90\text{deg} - \alpha_{\text{BOT}} + \theta_2 & \text{if } \theta_2 < \alpha_{\text{BOT}} \\ 90\text{deg} - \theta_2 + \alpha_{\text{BOT}} & \text{otherwise} \end{cases} \quad \beta_{\text{DBOT}} = 67.363 \text{ deg}$$

$$w_{\text{st}} := \min(w_{\text{BOT}} \cdot \sin(\beta_{\text{DBOT}}), w_{\text{TOP}} \cdot \sin(\beta_{\text{DTOP}})) \quad w_{\text{st}} = 66.428 \text{ mm}$$

$$C_{\text{Strut}} := \sigma_{\text{cw}} \cdot w_{\text{st}} \cdot b \quad C_{\text{Strut}} = 61.145 \text{ kN} \quad \text{Check2} := \begin{cases} \text{"Model Not Applicable"} & \text{if } C_{\text{Strut}} < 0 \\ \text{"OK"} & \text{otherwise} \end{cases}$$
$$C_2 := \min(C_{\text{TOP}}, C_{\text{BOT}}, C_{\text{Strut}}) \quad C_2 = 61.145 \text{ kN}$$

Check main tension reinforcement

$$F_y := 41600 \text{ psi}$$

$$T := C_2 \cdot \cos(\theta_2) + C_1 \cdot \sin(\theta) \quad T = 54 \text{ kN} \quad T_r := A_s \cdot F_y \quad T_r = 82 \text{ kN}$$

$$\text{Check} := \begin{cases} \text{"OK"} & \text{if } T < T_r \\ \text{"NG"} & \text{otherwise} \end{cases}$$

$$F_2 := C_2 \cdot \sin(\theta_2) \quad F_2 = 39.952 \text{ kN}$$

$$\text{Therefore: } V := F_1 + F_2 \quad V = 48 \text{ kN} \quad \text{Check} = \text{"OK"} \quad \text{Check2} = \text{"OK"}$$

$$P_n := 44.8 \text{ kip} \quad P_n = 199 \text{ kN} \quad 2 \cdot V = 97 \text{ kN}$$

Researcher: Oh and Shin, 2001 Specimen: H43A0

1. Geometry

$$\begin{aligned}
 d &:= 500\text{mm} & f_c &:= 50.67\text{MPa} & F_y &:= 60\text{ksi} & b &:= 120\text{mm} & A_s &:= 2 \cdot 500\text{mm}^2 \\
 \alpha_1 &:= 0.85 - 0.0015 \cdot \frac{f_c}{1\text{MPa}} & \beta_1 &:= 0.97 - 0.0025 \cdot \frac{f_c}{1\text{MPa}} & h &:= 560\text{mm} & A_v &:= 2 \cdot \pi \cdot (0.5 \cdot 6\text{mm})^2 \\
 x &:= \frac{A_s \cdot F_y}{\alpha_1 \cdot b \cdot f_c} & x &= 87.902\text{mm} & c &:= \frac{x}{\beta_1} & c &= 104.233\text{mm} & \rho &:= \frac{A_s}{b \cdot d} & s &:= 222\text{mm} \\
 z &:= d - \frac{x}{2} & z &= 456.049\text{mm} & d_1 &:= h - d & l_b &:= 180\text{mm} & a &:= 1.25 \cdot d & \frac{a}{d} &= 1.25 \\
 a_w &:= 0.85 \cdot a - \frac{z}{4} & a_w &= 417.238\text{mm} & \frac{a_w}{s} &= 1.879 & n &:= 2 & \text{Number of effective stirrups}
 \end{aligned}$$

2. Strut Dimensions

$$\chi := \sqrt{f_c} \frac{1}{\sqrt{\text{MPa}}} + 250 \cdot \sqrt{\rho \cdot \left(\frac{d}{a}\right)^5} \quad \psi := 1.67 \cdot \frac{\sqrt{f_c} \frac{1}{\sqrt{\text{MPa}}}}{\chi} \quad \psi = 0.464$$

$$F_1 := \psi \cdot n \cdot F_y \cdot A_v$$

For strength of the strut: $f_{cu} := 0.6 \cdot f_c$ By Inspection, this will control

Bottom Strut

$$\alpha_{\text{TOP}} := \text{atan}\left(\frac{l_b}{x}\right) \quad \alpha_{\text{TOP}} = 63.972 \text{ deg}$$

$$\begin{aligned}
 \theta &:= \left| \begin{array}{l} \theta \leftarrow 50\text{deg} \\ \text{for } i \in 1 \dots 20 \\ \quad C_1 \leftarrow \frac{F_1}{\sin(\theta)} \\ \quad f_{cu} \leftarrow 0.6 \cdot f_c \\ \quad w_{st} \leftarrow \frac{C_1}{b \cdot f_{cu}} \\ \quad \beta \leftarrow \begin{cases} 90\text{deg} - \alpha_{\text{TOP}} + \theta & \text{if } \theta < \alpha_{\text{TOP}} \\ 90\text{deg} - \theta + \alpha_{\text{TOP}} & \text{otherwise} \end{cases} \\ \quad \theta \leftarrow \text{atan}\left[\frac{d - \left(x - 0.5 \cdot w_{st} \cdot \frac{\cos(\alpha_{\text{TOP}})}{\sin(\beta)} \right)}{0.5a + 0.5 \cdot l_b - 0.5 \cdot w_{st} \cdot \frac{\sin(\alpha_{\text{TOP}})}{\sin(\beta)}} \right] \\ \theta \end{array} \right. \quad \theta = 46.086 \text{ deg}
 \end{aligned}$$

$$C_1 := \frac{F_1}{\sin(\theta)} \quad C_1 = 30.166 \text{ kN}$$

$$\text{Required strut Width: } w_{st} := \frac{C_1}{b \cdot f_{cu}} \quad w_{st} = 8.269 \text{ mm} \quad \frac{w_{st}}{2} = 4.134 \text{ mm}$$

$$\text{Length along node: } \beta_{TOP} := \begin{cases} 90\text{deg} - \alpha_{TOP} + \theta & \text{if } \theta < \alpha_{TOP} \\ 90\text{deg} - \theta + \alpha_{TOP} & \text{otherwise} \end{cases}$$

$$L_{TOP} := \frac{w_{st}}{\sin(\beta_{TOP})} \quad L_{TOP} = 8.689 \text{ mm}$$

$$\text{Top Strut } l_b := 130 \text{ mm}$$

$$\alpha_{BOT} := \text{atan}\left(\frac{l_b}{2 \cdot d_1}\right) \quad \alpha_{BOT} = 47.291 \text{ deg}$$

$$\theta := \begin{cases} 50\text{deg} \\ \text{for } i \in 1..40 \\ \left[\begin{array}{l} C_1 \leftarrow \frac{F_1}{\cos(\theta)} \\ f_{cu} \leftarrow 0.6 \cdot f_c \\ w_{st} \leftarrow \frac{C_1}{b \cdot f_{cu}} \\ \beta \leftarrow \begin{cases} 90\text{deg} - \alpha_{BOT} + \theta & \text{if } \theta < \alpha_{BOT} \\ 90\text{deg} - \theta + \alpha_{BOT} & \text{otherwise} \end{cases} \\ \theta \leftarrow 90\text{deg} - \text{atan}\left[\frac{h - 0.5x - \left(2d_1 - 0.5 \cdot w_{st} \cdot \frac{\cos(\alpha_{BOT})}{\sin(\beta)}\right)}{0.5a + 0.5 \cdot l_b - 0.5 \cdot w_{st} \cdot \frac{\sin(\alpha_{BOT})}{\sin(\beta)}} \right] \end{array} \right] \\ \theta \end{cases} \quad \theta = 43.197 \text{ deg}$$

$$C_1 := \frac{F_1}{\cos(\theta)} \quad C_1 = 29.81 \text{ kN}$$

$$\text{Required strut Width: } w_{st} := \frac{C_1}{b \cdot f_{cu}} \quad w_{st} = 8.171 \text{ mm} \quad \frac{w_{st}}{2} = 4.085 \text{ mm}$$

$$\text{Length along node: } \beta_{BOT} := \begin{cases} 90\text{deg} - \alpha_{BOT} + \theta & \text{if } \theta < \alpha_{BOT} \\ 90\text{deg} - \theta + \alpha_{BOT} & \text{otherwise} \end{cases}$$

$$L_{BOT} := \frac{w_{st}}{\sin(\beta_{BOT})} \quad L_{BOT} = 8.192 \text{ mm}$$

Direct Strut

Check Bottom Node: $l_b := 180\text{mm}$

$$\text{CCT Node: } w_{\text{BOT}} := \sqrt{l_b^2 + (2 \cdot d_1)^2} - L_{\text{BOT}} \quad f_{\text{cu}} := 0.75 \cdot f_c \quad C_{\text{BOT}} := f_{\text{cu}} \cdot b \cdot w_{\text{BOT}} \quad C_{\text{BOT}} = 949.186 \text{ kN}$$

Check Top Node: $l_b := 130\text{mm}$

$$\text{CCC Node: } w_{\text{TOP}} := \sqrt{l_b^2 + x^2} - L_{\text{TOP}} \quad f_{\text{cu}} := 0.85 \cdot f_c \quad C_{\text{TOP}} := f_{\text{cu}} \cdot b \cdot w_{\text{TOP}} \quad C_{\text{TOP}} = 766.158 \text{ kN}$$

Check the strength of the strut:

$$\theta_2 := \text{atan} \left(\frac{h - 0.5 \cdot w_{\text{TOP}} \cdot \cos(\alpha_{\text{TOP}}) - 0.5 \cdot w_{\text{BOT}} \cdot \cos(\alpha_{\text{BOT}})}{a - l_b + 0.5 \cdot w_{\text{TOP}} \cdot \sin(\alpha_{\text{TOP}}) + 0.5 \cdot w_{\text{BOT}} \cdot \sin(\alpha_{\text{BOT}})} \right) \quad \theta_2 = 35.604 \text{ deg}$$

$$\sigma_{\text{cw}} := 0.6 \cdot f_c \quad \sigma_{\text{cw}} = 30.402 \text{ MPa}$$

Calculate β for direct strut

$$\text{At Top Node: } \beta_{\text{DTOP}} := \begin{cases} 90\text{deg} - \alpha_{\text{TOP}} + \theta_2 & \text{if } \theta_2 < \alpha_{\text{TOP}} \\ 90\text{deg} - \theta_2 + \alpha_{\text{TOP}} & \text{otherwise} \end{cases} \quad \beta_{\text{DTOP}} = 61.632 \text{ deg}$$

$$\text{At Bottom Node: } \beta_{\text{DBOT}} := \begin{cases} 90\text{deg} - \alpha_{\text{BOT}} + \theta_2 & \text{if } \theta_2 < \alpha_{\text{BOT}} \\ 90\text{deg} - \theta_2 + \alpha_{\text{BOT}} & \text{otherwise} \end{cases} \quad \beta_{\text{DBOT}} = 78.314 \text{ deg}$$

$$w_{\text{st}} := \min(w_{\text{BOT}} \cdot \sin(\beta_{\text{DBOT}}), w_{\text{TOP}} \cdot \sin(\beta_{\text{DTOP}})) \quad w_{\text{st}} = 130.44 \text{ mm}$$

$$C_{\text{Strut}} := \sigma_{\text{cw}} \cdot w_{\text{st}} \cdot b \quad C_{\text{Strut}} = 475.875 \text{ kN} \quad \text{Check2} := \begin{cases} \text{"Model Not Applicable"} & \text{if } C_{\text{Strut}} < 0 \\ \text{"OK"} & \text{otherwise} \end{cases}$$

$$C_2 := \min(C_{\text{TOP}}, C_{\text{BOT}}, C_{\text{Strut}}) \quad C_2 = 475.875 \text{ kN}$$

Check main tension reinforcement

$$F_y := 498.9 \text{ MPa}$$

$$T := C_2 \cdot \cos(\theta_2) + C_1 \cdot \sin(\theta) \quad T = 407 \text{ kN} \quad T_r := A_s \cdot F_y \quad T_r = 499 \text{ kN}$$

$$\text{Check} := \begin{cases} \text{"OK"} & \text{if } T < T_r \\ \text{"NG"} & \text{otherwise} \end{cases}$$

$$F_2 := C_2 \cdot \sin(\theta_2) \quad F_2 = 277.046 \text{ kN}$$

$$\text{Therefore: } V := F_1 + F_2 \quad V = 299 \text{ kN} \quad \text{Check} = \text{"OK"} \quad \text{Check2} = \text{"OK"}$$

Researcher: Smith and Vansiotis, 1982 Specimen: F3S3

1. Geometry

$$A_s := 0.93 \text{ in}^2 \quad a := 14.5 \text{ in} \quad a = 368.3 \text{ mm} \quad d := 12 \text{ in}$$

$$f_c := 3200 \text{ psi} \quad f_c = 22.063 \text{ MPa} \quad F_y := 431 \text{ MPa} \quad b := 4 \text{ in} \quad h := 14 \text{ in}$$

$$\alpha_1 := 0.85 - 0.0015 \cdot \frac{f_c}{1 \text{ MPa}} \quad \beta_1 := 0.97 - 0.0025 \cdot \frac{f_c}{1 \text{ MPa}} \quad \varepsilon_{cu} := 0.0035 \quad \rho := \frac{A_s}{b \cdot d}$$

$$x := \frac{A_s \cdot F_y}{\alpha_1 \cdot b \cdot f_c} \quad x = 141.219 \text{ mm} \quad c := \frac{x}{\beta_1} \quad c = 154.364 \text{ mm} \quad A_v := 2 \cdot 0.05 \text{ in}^2 \quad s := 10.5 \text{ in}$$

$$z := d - \frac{x}{2} \quad z = 234.19 \text{ mm} \quad d_1 := h - d \quad l_b := 4 \text{ in} \quad \frac{a}{d} = 1.208$$

$$a_w := 0.85 \cdot a - \frac{z}{4} \quad a_w = 254.507 \text{ mm} \quad \frac{a_w}{s} = 0.954 \quad n := 1 \text{ Number of effective stirrups}$$

2. Strut Dimensions

$$\chi := \sqrt{f_c} \frac{1}{\sqrt{\text{MPa}}} + 250 \cdot \sqrt{\rho \cdot \left(\frac{d}{a}\right)^5} \quad \psi := 1.67 \cdot \frac{\sqrt{f_c}}{\sqrt{\text{MPa}}} \quad \psi = 0.297$$

$$F_y := 437.4 \text{ MPa} \quad F_1 := \psi \cdot n \cdot F_y \cdot A_v$$

For strength of the strut: $f_{cu} := 0.6 \cdot f_c$ By Inspection, this will control

Bottom Strut

$$\alpha_{TOP} := \text{atan}\left(\frac{l_b}{x}\right) \quad \alpha_{TOP} = 35.733 \text{ deg}$$

$$\theta := \theta \leftarrow 50 \text{ deg}$$

for $i \in 1..20$

$$C_1 \leftarrow \frac{F_1}{\sin(\theta)}$$

$$f_{cu} \leftarrow 0.6 \cdot f_c$$

$$w_{st} \leftarrow \frac{C_1}{b \cdot f_{cu}}$$

$$\beta \leftarrow \begin{cases} 90 \text{ deg} - \alpha_{TOP} + \theta & \text{if } \theta < \alpha_{TOP} \\ 90 \text{ deg} - \theta + \alpha_{TOP} & \text{otherwise} \end{cases}$$

$$\theta \leftarrow \text{atan} \left[\frac{d - \left(x - 0.5 \cdot w_{st} \cdot \frac{\cos(\alpha_{TOP})}{\sin(\beta)} \right)}{0.5a + 0.5 \cdot l_b - 0.5 \cdot w_{st} \cdot \frac{\sin(\alpha_{TOP})}{\sin(\beta)}} \right]$$

$$\theta = 35.912 \text{ deg}$$

θ

$$C_1 := \frac{F_1}{\sin(\theta)} \quad C_1 = 14.307 \text{ kN}$$

$$\text{Required strut Width: } w_{st} := \frac{C_1}{b \cdot f_{cu}} \quad w_{st} = 10.637 \text{ mm} \quad \frac{w_{st}}{2} = 5.319 \text{ mm}$$

$$\text{Length along node: } \beta_{TOP} := \begin{cases} 90\text{deg} - \alpha_{TOP} + \theta & \text{if } \theta < \alpha_{TOP} \\ 90\text{deg} - \theta + \alpha_{TOP} & \text{otherwise} \end{cases}$$

$$L_{TOP} := \frac{w_{st}}{\sin(\beta_{TOP})} \quad L_{TOP} = 10.637 \text{ mm}$$

Top Strut

$$\alpha_{BOT} := \text{atan}\left(\frac{l_b}{2 \cdot d_1}\right) \quad \alpha_{BOT} = 45 \text{ deg}$$

$$\theta := \begin{cases} 50\text{deg} \\ \text{for } i \in 1..40 \\ \left| \begin{array}{l} C_1 \leftarrow \frac{F_1}{\cos(\theta)} \\ f_{cu} \leftarrow 0.6 \cdot f_c \\ w_{st} \leftarrow \frac{C_1}{b \cdot f_{cu}} \\ \beta \leftarrow \begin{cases} 90\text{deg} - \alpha_{BOT} + \theta & \text{if } \theta < \alpha_{BOT} \\ 90\text{deg} - \theta + \alpha_{BOT} & \text{otherwise} \end{cases} \\ \theta \leftarrow 90\text{deg} - \text{atan}\left[\frac{h - 0.5x - \left(2d_1 - 0.5 \cdot w_{st} \cdot \frac{\cos(\alpha_{BOT})}{\sin(\beta)}\right)}{0.5a + 0.5 \cdot l_b - 0.5 \cdot w_{st} \cdot \frac{\sin(\alpha_{BOT})}{\sin(\beta)}}\right] \end{array} \right. \\ \theta \end{cases} \quad \theta = 51.072 \text{ deg}$$

$$C_1 := \frac{F_1}{\cos(\theta)} \quad C_1 = 13.355 \text{ kN}$$

$$\text{Required strut Width: } w_{st} := \frac{C_1}{b \cdot f_{cu}} \quad w_{st} = 9.929 \text{ mm} \quad \frac{w_{st}}{2} = 4.965 \text{ mm}$$

$$\text{Length along node: } \beta_{BOT} := \begin{cases} 90\text{deg} - \alpha_{BOT} + \theta & \text{if } \theta < \alpha_{BOT} \\ 90\text{deg} - \theta + \alpha_{BOT} & \text{otherwise} \end{cases}$$

$$L_{BOT} := \frac{w_{st}}{\sin(\beta_{BOT})} \quad L_{BOT} = 9.986 \text{ mm}$$

Direct Strut

Check Bottom Node:

$$\text{CCT Node: } w_{\text{BOT}} := \sqrt{l_b^2 + (2 \cdot d_1)^2} - L_{\text{BOT}} \quad f_{\text{cu}} := 0.75 \cdot f_c \quad C_{\text{BOT}} := f_{\text{cu}} \cdot b \cdot w_{\text{BOT}} \quad C_{\text{BOT}} = 224.776 \text{ kN}$$

Check Top Node:

$$\text{CCC Node: } w_{\text{TOP}} := \sqrt{l_b^2 + x^2} - L_{\text{TOP}} \quad f_{\text{cu}} := 0.85 \cdot f_c \quad C_{\text{TOP}} := f_{\text{cu}} \cdot b \cdot w_{\text{TOP}} \quad C_{\text{TOP}} = 311.21 \text{ kN}$$

Check the strength of the strut:

$$\theta_2 := \text{atan} \left(\frac{h - 0.5 \cdot w_{\text{TOP}} \cdot \cos(\alpha_{\text{TOP}}) - 0.5 \cdot w_{\text{BOT}} \cdot \cos(\alpha_{\text{BOT}})}{a - l_b + 0.5 \cdot w_{\text{TOP}} \cdot \sin(\alpha_{\text{TOP}}) + 0.5 \cdot w_{\text{BOT}} \cdot \sin(\alpha_{\text{BOT}})} \right) \quad \theta_2 = 33.792 \text{ deg}$$

$$\sigma_{\text{cw}} := 0.6 \cdot f_c \quad \sigma_{\text{cw}} = 13.238 \text{ MPa}$$

Calculate β for direct strut

$$\text{At Top Node: } \beta_{\text{DTOP}} := \begin{cases} 90 \text{ deg} - \alpha_{\text{TOP}} + \theta_2 & \text{if } \theta_2 < \alpha_{\text{TOP}} \\ 90 \text{ deg} - \theta_2 + \alpha_{\text{TOP}} & \text{otherwise} \end{cases} \quad \beta_{\text{DTOP}} = 88.059 \text{ deg}$$

$$\text{At Bottom Node: } \beta_{\text{DBOT}} := \begin{cases} 90 \text{ deg} - \alpha_{\text{BOT}} + \theta_2 & \text{if } \theta_2 < \alpha_{\text{BOT}} \\ 90 \text{ deg} - \theta_2 + \alpha_{\text{BOT}} & \text{otherwise} \end{cases} \quad \beta_{\text{DBOT}} = 78.792 \text{ deg}$$

$$w_{\text{st}} := \min(w_{\text{BOT}} \cdot \sin(\beta_{\text{DBOT}}), w_{\text{TOP}} \cdot \sin(\beta_{\text{DTOP}})) \quad w_{\text{st}} = 131.149 \text{ mm}$$

$$C_{\text{Strut}} := \sigma_{\text{cw}} \cdot w_{\text{st}} \cdot b \quad C_{\text{Strut}} = 176.392 \text{ kN} \quad \text{Check2} := \begin{cases} \text{"Model Not Applicable"} & \text{if } C_{\text{Strut}} < 0 \\ \text{"OK"} & \text{otherwise} \end{cases}$$

$$C_2 := \min(C_{\text{TOP}}, C_{\text{BOT}}, C_{\text{Strut}}) \quad C_2 = 176.392 \text{ kN}$$

Check main tension reinforcement

$$F_y := 437.4 \text{ MPa}$$

$$T := C_2 \cdot \cos(\theta_2) + C_1 \cdot \sin(\theta) \quad T = 157 \text{ kN} \quad T_r := A_s \cdot F_y \quad T_r = 262 \text{ kN}$$

$$\text{Check} := \begin{cases} \text{"OK"} & \text{if } T < T_r \\ \text{"NG"} & \text{otherwise} \end{cases}$$

$$F_2 := C_2 \cdot \sin(\theta_2) \quad F_2 = 98.105 \text{ kN}$$

$$\text{Therefore: } V := F_1 + F_2 \quad V = 106 \text{ kN} \quad \text{Check} = \text{"OK"} \quad \text{Check2} = \text{"OK"}$$

Researcher: Shin, Lee, Moon, and Ghosh, 1999 Specimen: HB1.5-25

1. Geometry

$$A_s := 2.509\text{mm}^2 \quad d := 215\text{mm} \quad f_c := 73\text{MPa} \quad F_y := 414\text{MPa} \quad b := 125\text{mm} \quad d_b := 25\text{mm}$$

$$\alpha_1 := 0.85 - 0.0015 \cdot \frac{f_c}{1\text{MPa}} \quad \beta_1 := 0.97 - 0.0025 \cdot \frac{f_c}{1\text{MPa}} \quad h := 250\text{mm} \quad \rho := \frac{A_s}{b \cdot d}$$

$$x := \frac{A_s \cdot F_y}{\alpha_1 \cdot b \cdot f_c} \quad x = 62.372\text{mm} \quad c := \frac{x}{\beta_1} \quad c = 79.203\text{mm}$$

$$z := d - \frac{x}{2} \quad z = 183.814\text{mm} \quad d_1 := h - d \quad l_b := 45\text{mm} \quad a := 1.5 \cdot d \quad a = 322.5\text{mm}$$

$$A_v := 2 \cdot 0.05\text{in}^2 \quad \rho_v := 0.0045 \quad s := \frac{A_v}{b \cdot \rho_v} \quad s = 115\text{mm}$$

$$a_w := 0.85 \cdot a - \frac{z}{4} \quad a_w = 228.172\text{mm} \quad \frac{a_w}{s} = 1.989 \quad n := 3 \quad \text{Number of effective stirrups}$$

2. Strut Dimensions

$$\chi := \sqrt{f_c} \frac{1}{\sqrt{\text{MPa}}} + 250 \cdot \sqrt{\rho \cdot \left(\frac{d}{a}\right)^5} \quad \psi := 1.67 \cdot \frac{\sqrt{f_c} \frac{1}{\sqrt{\text{MPa}}}}{\chi} \quad \psi = 0.545 \quad F_1 := \psi \cdot n \cdot F_y \cdot A_v$$

For strength of the strut: $f_{cu} := 0.6 \cdot f_c$ By Inspection, this will control

$$\alpha_{\text{TOP}} := \text{atan}\left(\frac{l_b}{x}\right) \quad \alpha_{\text{TOP}} = 35.81\text{ deg}$$

$$\theta := \left| \begin{array}{l} \theta \leftarrow 50\text{deg} \\ \text{for } i \in 1..20 \\ \quad C_1 \leftarrow \frac{F_1}{\sin(\theta)} \\ \quad f_{cu} \leftarrow 0.6 \cdot f_c \\ \quad w_{\text{st}} \leftarrow \frac{C_1}{b \cdot f_{cu}} \\ \quad \beta \leftarrow \begin{cases} 90\text{deg} - \alpha_{\text{TOP}} + \theta & \text{if } \theta < \alpha_{\text{TOP}} \\ 90\text{deg} - \theta + \alpha_{\text{TOP}} & \text{otherwise} \end{cases} \\ \quad \theta \leftarrow \text{atan}\left[\frac{d - \left(x - 0.5 \cdot w_{\text{st}} \cdot \frac{\cos(\alpha_{\text{TOP}})}{\sin(\beta)} \right)}{0.5a + 0.5 \cdot l_b - 0.5 \cdot w_{\text{st}} \cdot \frac{\sin(\alpha_{\text{TOP}})}{\sin(\beta)}} \right] \\ \theta \end{array} \right| \quad \theta = 41.166\text{ deg}$$

$$C_1 := \frac{F_1}{\sin(\theta)} \quad C_1 = 66.292 \text{ kN}$$

$$\text{Required strut Width: } w_{st} := \frac{C_1}{b \cdot f_{cu}} \quad w_{st} = 12.108 \text{ mm} \quad \frac{w_{st}}{2} = 6.054 \text{ mm}$$

$$\text{Length along node: } \beta_{TOP} := \begin{cases} 90\text{deg} - \alpha_{TOP} + \theta & \text{if } \theta < \alpha_{TOP} \\ 90\text{deg} - \theta + \alpha_{TOP} & \text{otherwise} \end{cases}$$

$$L_{TOP} := \frac{w_{st}}{\sin(\beta_{TOP})} \quad L_{TOP} = 12.161 \text{ mm}$$

Top Strut

$$\alpha_{BOT} := \text{atan}\left(\frac{l_b}{2 \cdot d_1}\right) \quad \alpha_{BOT} = 32.735 \text{ deg}$$

$$\theta := 50\text{deg}$$

for i ∈ 1 .. 40

$$C_1 \leftarrow \frac{F_1}{\cos(\theta)}$$

$$f_{cu} \leftarrow 0.6 \cdot f_c$$

$$w_{st} \leftarrow \frac{C_1}{b \cdot f_{cu}}$$

$$\beta \leftarrow \begin{cases} 90\text{deg} - \alpha_{BOT} + \theta & \text{if } \theta < \alpha_{BOT} \\ 90\text{deg} - \theta + \alpha_{BOT} & \text{otherwise} \end{cases}$$

$$\theta \leftarrow 90\text{deg} - \text{atan}\left[\frac{h - 0.5x - \left(2d_1 - 0.5 \cdot w_{st} \cdot \frac{\cos(\alpha_{BOT})}{\sin(\beta)}\right)}{0.5a + 0.5 \cdot l_b - 0.5 \cdot w_{st} \cdot \frac{\sin(\alpha_{BOT})}{\sin(\beta)}}\right]$$

$$\theta = 49.46 \text{ deg}$$

$$C_1 := \frac{F_1}{\cos(\theta)} \quad C_1 = 67.136 \text{ kN}$$

$$\text{Required strut Width: } w_{st} := \frac{C_1}{b \cdot f_{cu}} \quad w_{st} = 12.262 \text{ mm} \quad \frac{w_{st}}{2} = 6.131 \text{ mm}$$

$$\text{Length along node: } \beta_{BOT} := \begin{cases} 90\text{deg} - \alpha_{BOT} + \theta & \text{if } \theta < \alpha_{BOT} \\ 90\text{deg} - \theta + \alpha_{BOT} & \text{otherwise} \end{cases}$$

$$L_{BOT} := \frac{w_{st}}{\sin(\beta_{BOT})} \quad L_{BOT} = 12.804 \text{ mm}$$

Direct Strut

Check Bottom Node:

$$\text{CCT Node: } w_{\text{BOT}} := \sqrt{l_b^2 + (2 \cdot d_1)^2} - L_{\text{BOT}} \quad f_{\text{cu}} := 0.75 \cdot f_c \quad C_{\text{BOT}} := f_{\text{cu}} \cdot b \cdot w_{\text{BOT}} \quad C_{\text{BOT}} = 481.887 \text{ kN}$$

Check Top Node:

$$\text{CCC Node: } w_{\text{TOP}} := \sqrt{l_b^2 + x^2} - L_{\text{TOP}} \quad f_{\text{cu}} := 0.85 \cdot f_c \quad C_{\text{TOP}} := f_{\text{cu}} \cdot b \cdot w_{\text{TOP}} \quad C_{\text{TOP}} = 502.213 \text{ kN}$$

Check the strength of the strut:

$$\theta_2 := \text{atan} \left(\frac{h - 0.5 \cdot w_{\text{TOP}} \cdot \cos(\alpha_{\text{TOP}}) - 0.5 \cdot w_{\text{BOT}} \cdot \cos(\alpha_{\text{BOT}})}{a - l_b + 0.5 \cdot w_{\text{TOP}} \cdot \sin(\alpha_{\text{TOP}}) + 0.5 \cdot w_{\text{BOT}} \cdot \sin(\alpha_{\text{BOT}})} \right) \quad \theta_2 = 31.606 \text{ deg}$$

$$v_1 := 1 - \frac{47}{250} \quad v_1 = 0.812$$

$$\text{Check that width of bearing plate: } a_f := \frac{x}{\sin(\theta_2)} \cdot \left(\frac{v_1}{0.6 \cos(\theta_2)} - \cos(\theta_2) \right) \quad a_f = 87.756 \text{ mm}$$

$$\sigma_{\text{cw}} := 0.6 \cdot f_c \quad \sigma_{\text{cw}} = 43.8 \text{ MPa}$$

Calculate β for direct strut

$$\text{At Top Node: } \beta_{\text{DTOP}} := \begin{cases} 90\text{deg} - \alpha_{\text{TOP}} + \theta_2 & \text{if } \theta_2 < \alpha_{\text{TOP}} \\ 90\text{deg} - \theta_2 + \alpha_{\text{TOP}} & \text{otherwise} \end{cases} \quad \beta_{\text{DTOP}} = 85.796 \text{ deg}$$

$$\text{At Bottom Node: } \beta_{\text{DBOT}} := \begin{cases} 90\text{deg} - \alpha_{\text{BOT}} + \theta_2 & \text{if } \theta_2 < \alpha_{\text{BOT}} \\ 90\text{deg} - \theta_2 + \alpha_{\text{BOT}} & \text{otherwise} \end{cases} \quad \beta_{\text{DBOT}} = 88.871 \text{ deg}$$

$$w_{\text{st}} := \min(w_{\text{BOT}} \cdot \sin(\beta_{\text{DBOT}}), w_{\text{TOP}} \cdot \sin(\beta_{\text{DTOP}})) \quad w_{\text{st}} = 64.575 \text{ mm}$$

$$C_{\text{Strut}} := \sigma_{\text{cw}} \cdot w_{\text{st}} \cdot b \quad C_{\text{Strut}} = 353.55 \text{ kN} \quad \text{Check2} := \begin{cases} \text{"Model Not Applicable"} & \text{if } C_{\text{Strut}} < 0 \\ \text{"OK"} & \text{otherwise} \end{cases}$$

$$C_2 := \min(C_{\text{TOP}}, C_{\text{BOT}}, C_{\text{Strut}}) \quad C_2 = 353.55 \text{ kN}$$

Check main tension reinforcement

$$T := C_2 \cdot \cos(\theta_2) + C_1 \cdot \sin(\theta) \quad T = 352 \text{ kN} \quad T_r := A_s \cdot F_y \quad T_r = 421 \text{ kN}$$

$$\text{Check} := \begin{cases} \text{"OK"} & \text{if } T < T_r \\ \text{"NG"} & \text{otherwise} \end{cases}$$

$$F_2 := C_2 \cdot \sin(\theta_2) \quad F_2 = 185.287 \text{ kN}$$

$$\text{Therefore: } V := F_1 + F_2 \quad V = 228.923 \text{ kN}$$

$$P := 2 \cdot V \quad P = 458 \text{ kN} \quad \text{Check} = \text{"OK"} \quad \text{Check2} = \text{"OK"}$$

Researcher: Tan, Kong, Teng, and Guan, 1995 Specimen: D-1.08-2.15

1. Geometry

$$A_s := 628\text{mm}^2 \quad d := 463\text{mm} \quad f_c := 48.2\text{MPa} \quad F_y := 504.8\text{MPa} \quad b := 110\text{mm} \quad \rho := \frac{A_s}{b \cdot d}$$

$$\alpha_1 := 0.85 - 0.0015 \frac{f_c}{1\text{MPa}} \quad \beta_1 := 0.97 - 0.0025 \frac{f_c}{1\text{MPa}} \quad \epsilon_{cu} := 0.0035 \quad h := 500\text{mm}$$

$$x := \frac{A_s \cdot F_y}{\alpha_1 \cdot b \cdot f_c} \quad x = 76.882\text{mm} \quad c := \frac{x}{\beta_1} \quad c = 90.503\text{mm} \quad A_v := 2 \cdot \pi \cdot (5\text{mm})^2 \quad s := 300\text{mm}$$

$$z := d - \frac{x}{2} \quad z = 424.559\text{mm} \quad d_1 := h - d \quad l_b := 100\text{mm} \quad a := 500\text{mm} \quad \text{Assume 100 mm bearing plates}$$

$$a_w := 0.85a - \frac{z}{4} \quad a_w = 318.86\text{mm} \quad \frac{a_w}{s} = 1.063 \quad n := 2 \quad \text{Number of effective stirrups}$$

2. Strut Dimensions

$$\chi := \sqrt{f_c} \frac{1}{\sqrt{\text{MPa}}} + 250 \cdot \sqrt{\rho \cdot \left(\frac{d}{a}\right)^5} \quad \psi := 1.67 \cdot \frac{\sqrt{f_c}}{\sqrt{\text{MPa}}} \quad \psi = 0.388$$

$$F_y := 375.2\text{MPa} \quad F_1 := \psi \cdot n \cdot F_y \cdot A_v$$

For strength of the strut: $f_{cu} := 0.6f_c$ By Inspection, this will control

Bottom Strut

$$\alpha_{TOP} := \text{atan}\left(\frac{l_b}{x}\right) \quad \alpha_{TOP} = 52.446\text{deg}$$

$$\theta := \left| \begin{array}{l} \theta \leftarrow 50\text{deg} \\ \text{for } i \in 1..20 \\ \left| \begin{array}{l} C_1 \leftarrow \frac{F_1}{\sin(\theta)} \\ f_{cu} \leftarrow 0.6f_c \\ w_{st} \leftarrow \frac{C_1}{b \cdot f_{cu}} \\ \beta \leftarrow \begin{cases} 90\text{deg} - \alpha_{TOP} + \theta & \text{if } \theta < \alpha_{TOP} \\ 90\text{deg} - \theta + \alpha_{TOP} & \text{otherwise} \end{cases} \\ \theta \leftarrow \text{atan}\left[\frac{d - \left(x - 0.5 \cdot w_{st} \cdot \frac{\cos(\alpha_{TOP})}{\sin(\beta)} \right)}{0.5a + 0.5l_b - 0.5 \cdot w_{st} \cdot \frac{\sin(\alpha_{TOP})}{\sin(\beta)}} \right] \end{array} \right. \\ \theta \end{array} \right. \quad \theta = 53.207 \text{ deg}$$

$$C_1 := \frac{F_1}{\sin(\theta)} \quad C_1 = 57.173 \text{ kN}$$

$$\text{Required strut Width: } w_{st} := \frac{C_1}{b \cdot f_{cu}} \quad w_{st} = 17.972 \text{ mm} \quad \frac{w_{st}}{2} = 8.986 \text{ mm}$$

$$\text{Length along node: } \beta_{TOP} := \begin{cases} 90\text{deg} - \alpha_{TOP} + \theta & \text{if } \theta < \alpha_{TOP} \\ 90\text{deg} - \theta + \alpha_{TOP} & \text{otherwise} \end{cases}$$

$$L_{TOP} := \frac{w_{st}}{\sin(\beta_{TOP})} \quad L_{TOP} = 17.974 \text{ mm}$$

Top Strut

$$\alpha_{BOT} := \text{atan}\left(\frac{l_b}{2 \cdot d_1}\right) \quad \alpha_{BOT} = 53.499 \text{ deg}$$

$$\theta := \begin{cases} 50\text{deg} \\ \text{for } i \in 1..40 \\ \left| \begin{array}{l} C_1 \leftarrow \frac{F_1}{\cos(\theta)} \\ f_{cu} \leftarrow 0.6 \cdot f_c \\ w_{st} \leftarrow \frac{C_1}{b \cdot f_{cu}} \\ \beta \leftarrow \begin{cases} 90\text{deg} - \alpha_{BOT} + \theta & \text{if } \theta < \alpha_{BOT} \\ 90\text{deg} - \theta + \alpha_{BOT} & \text{otherwise} \end{cases} \\ \theta \leftarrow 90\text{deg} - \text{atan}\left[\frac{h - 0.5x - \left(2d_1 - 0.5 \cdot w_{st} \cdot \frac{\cos(\alpha_{BOT})}{\sin(\beta)}\right)}{0.5a + 0.5 \cdot l_b - 0.5 \cdot w_{st} \cdot \frac{\sin(\alpha_{BOT})}{\sin(\beta)}} \right] \end{array} \right| \\ \theta \end{cases} \quad \theta = 36.647 \text{ deg}$$

$$C_1 := \frac{F_1}{\cos(\theta)} \quad C_1 = 57.065 \text{ kN}$$

$$\text{Required strut Width: } w_{st} := \frac{C_1}{b \cdot f_{cu}} \quad w_{st} = 17.938 \text{ mm} \quad \frac{w_{st}}{2} = 8.969 \text{ mm}$$

$$\text{Length along node: } \beta_{BOT} := \begin{cases} 90\text{deg} - \alpha_{BOT} + \theta & \text{if } \theta < \alpha_{BOT} \\ 90\text{deg} - \theta + \alpha_{BOT} & \text{otherwise} \end{cases}$$

$$L_{BOT} := \frac{w_{st}}{\sin(\beta_{BOT})} \quad L_{BOT} = 18.743 \text{ mm}$$

Direct Strut

Check Bottom Node:

$$\text{CCT Node: } w_{\text{BOT}} := \sqrt{l_b^2 + (2 \cdot d_1)^2} - L_{\text{BO}} \cdot f_{\text{cu}} := 0.75 \cdot f_c \quad C_{\text{BOT}} := f_{\text{cu}} \cdot b \cdot w_{\text{BOT}} \quad C_{\text{BOT}} = 420.155 \text{ kN}$$

Check Top Node:

$$\text{CCC Node: } w_{\text{TOP}} := \sqrt{l_b^2 + x^2} - L_{\text{TOP}} \quad f_{\text{cu}} := 0.85 \cdot f_c \quad C_{\text{TOP}} := f_{\text{cu}} \cdot b \cdot w_{\text{TOP}} \quad C_{\text{TOP}} = 487.466 \text{ kN}$$

Check the strength of the strut:

$$\theta_2 := \text{atan} \left(\frac{h - 0.5 \cdot w_{\text{TOP}} \cdot \cos(\alpha_{\text{TOP}}) - 0.5 \cdot w_{\text{BOT}} \cdot \cos(\alpha_{\text{BOT}})}{a - l_b + 0.5 \cdot w_{\text{TOP}} \cdot \sin(\alpha_{\text{TOP}}) + 0.5 \cdot w_{\text{BOT}} \cdot \sin(\alpha_{\text{BOT}})} \right) \quad \theta_2 = 41.909 \text{ deg}$$

$$\sigma_{\text{cw}} := 0.6 \cdot f_c \quad \sigma_{\text{cw}} = 28.92 \text{ MPa}$$

Calculate β for direct strut

$$\text{At Top Node: } \beta_{\text{DTOP}} := \begin{cases} 90 \text{ deg} - \alpha_{\text{TOP}} + \theta_2 & \text{if } \theta_2 < \alpha_{\text{TOP}} \\ 90 \text{ deg} - \theta_2 + \alpha_{\text{TOP}} & \text{otherwise} \end{cases} \quad \beta_{\text{DTOP}} = 79.463 \text{ deg}$$

$$\text{At Bottom Node: } \beta_{\text{DBOT}} := \begin{cases} 90 \text{ deg} - \alpha_{\text{BOT}} + \theta_2 & \text{if } \theta_2 < \alpha_{\text{BOT}} \\ 90 \text{ deg} - \theta_2 + \alpha_{\text{BOT}} & \text{otherwise} \end{cases} \quad \beta_{\text{DBOT}} = 78.41 \text{ deg}$$

$$w_{\text{st}} := \min(w_{\text{BOT}} \cdot \sin(\beta_{\text{DBOT}}), w_{\text{TOP}} \cdot \sin(\beta_{\text{DTOP}})) \quad w_{\text{st}} = 103.505 \text{ mm}$$

$$C_{\text{Strut}} := \sigma_{\text{cw}} \cdot w_{\text{st}} \cdot b \quad C_{\text{Strut}} = 329.271 \text{ kN} \quad \text{Check2} := \begin{cases} \text{"Model Not Applicable"} & \text{if } C_{\text{Strut}} < 0 \\ \text{"OK"} & \text{otherwise} \end{cases}$$

$$C_2 := \min(C_{\text{TOP}}, C_{\text{BOT}}, C_{\text{Strut}}) \quad C_2 = 329.271 \text{ kN}$$

Check main tension reinforcement

$$F_y := 504.8 \text{ MPa}$$

$$T := C_2 \cdot \cos(\theta_2) + C_1 \cdot \sin(\theta) \quad T = 279 \text{ kN} \quad T_r := A_s \cdot F_y \quad T_r = 317 \text{ kN}$$

$$\text{Check} := \begin{cases} \text{"OK"} & \text{if } T < T_r \\ \text{"NG"} & \text{otherwise} \end{cases}$$

$$F_2 := C_2 \cdot \sin(\theta_2) \quad F_2 = 219.937 \text{ kN}$$

$$\text{Therefore: } V := F_1 + F_2 \quad V = 266 \text{ kN} \quad \text{Check} = \text{"OK"} \quad \text{Check2} = \text{"OK"}$$

Researcher: Tan, Teng, Kong, and Lu, 1997 Specimen: 1-2.00-1.00

1. Geometry

$$d := 448.2\text{mm} \quad f_c := 71.2\text{MPa} \quad F_y := 538\text{MPa} \quad b := 110\text{mm} \quad \rho := 2\% \quad A_s := \rho \cdot b \cdot d$$

$$\alpha_1 := 0.85 - 0.0015 \cdot \frac{f_c}{1\text{MPa}} \quad \beta_1 := 0.97 - 0.0025 \cdot \frac{f_c}{1\text{MPa}} \quad h := 500\text{mm} \quad \rho := \frac{A_s}{b \cdot d}$$

$$x := \frac{A_s \cdot F_y}{\alpha_1 \cdot b \cdot f_c} \quad x = 91.138\text{mm} \quad c := \frac{x}{\beta_1} \quad c = 115.073\text{mm} \quad A_v := 2 \cdot \pi \cdot (5\text{mm})^2 \quad s := 300\text{mm}$$

$$z := d - \frac{x}{2} \quad z = 402.631\text{mm} \quad d_1 := h - d \quad l_b := 100\text{mm} \quad a := 500\text{mm} \quad \text{Assume 100 mm bearing plates}$$

$$a_w := 0.85 \cdot a - \frac{z}{4} \quad a_w = 324.342\text{mm} \quad \frac{a_w}{s} = 1.081 \quad n := 2 \quad \text{Number of effective stirrups}$$

2. Strut Dimensions

$$\chi := \sqrt{f_c} \frac{1}{\sqrt{\text{MPa}}} + 250 \cdot \sqrt{\rho \cdot \left(\frac{d}{a}\right)^5} \quad \psi := 1.67 \cdot \frac{\sqrt{f_c}}{\sqrt{\text{MPa}}} \frac{1}{\chi} \quad \psi = 0.399$$

$$F_y := 385\text{MPa} \quad F_1 := \psi \cdot n \cdot F_y \cdot A_v$$

For strength of the strut: $f_{cu} := 0.6 \cdot f_c$ By Inspection, this will control

Bottom Strut

$$\alpha_{TOP} := \text{atan}\left(\frac{l_b}{x}\right) \quad \alpha_{TOP} = 47.655\text{deg}$$

$$\theta := \left\{ \begin{array}{l} \theta \leftarrow 50\text{deg} \\ \text{for } i \in 1 \dots 20 \\ \left| \begin{array}{l} C_1 \leftarrow \frac{F_1}{\sin(\theta)} \\ f_{cu} \leftarrow 0.6 \cdot f_c \\ w_{st} \leftarrow \frac{C_1}{b \cdot f_{cu}} \\ \beta \leftarrow \begin{cases} 90\text{deg} - \alpha_{TOP} + \theta & \text{if } \theta < \alpha_{TOP} \\ 90\text{deg} - \theta + \alpha_{TOP} & \text{otherwise} \end{cases} \\ \theta \leftarrow \text{atan}\left[\frac{d - \left(x - 0.5 \cdot w_{st} \cdot \frac{\cos(\alpha_{TOP})}{\sin(\beta)} \right)}{0.5a + 0.5 \cdot l_b - 0.5 \cdot w_{st} \cdot \frac{\sin(\alpha_{TOP})}{\sin(\beta)}} \right] \end{array} \right. \\ \theta \end{array} \right. \quad \theta = 50.777\text{deg}$$

$$C_1 := \frac{F_1}{\sin(\theta)} \quad C_1 = 62.263 \text{ kN}$$

$$\text{Required strut Width: } w_{st} := \frac{C_1}{b \cdot f_{cu}} \quad w_{st} = 13.25 \text{ mm} \quad \frac{w_{st}}{2} = 6.625 \text{ mm}$$

$$\text{Length along node: } \beta_{TOP} := \begin{cases} 90\text{deg} - \alpha_{TOP} + \theta & \text{if } \theta < \alpha_{TOP} \\ 90\text{deg} - \theta + \alpha_{TOP} & \text{otherwise} \end{cases}$$

$$L_{TOP} := \frac{w_{st}}{\sin(\beta_{TOP})} \quad L_{TOP} = 13.269 \text{ mm}$$

Top Strut

$$\alpha_{BOT} := \text{atan}\left(\frac{l_b}{2 \cdot d_1}\right) \quad \alpha_{BOT} = 43.987 \text{ deg}$$

$$\theta := \begin{cases} 50\text{deg} \\ \text{for } i \in 1..40 \\ \left[\begin{array}{l} C_1 \leftarrow \frac{F_1}{\cos(\theta)} \\ f_{cu} \leftarrow 0.6 \cdot f_c \\ w_{st} \leftarrow \frac{C_1}{b \cdot f_{cu}} \\ \beta \leftarrow \begin{cases} 90\text{deg} - \alpha_{BOT} + \theta & \text{if } \theta < \alpha_{BOT} \\ 90\text{deg} - \theta + \alpha_{BOT} & \text{otherwise} \end{cases} \\ \theta \leftarrow 90\text{deg} - \text{atan}\left[\frac{h - 0.5x - \left(2d_1 - 0.5 \cdot w_{st} \cdot \frac{\cos(\alpha_{BOT})}{\sin(\beta)}\right)}{0.5a + 0.5 \cdot l_b - 0.5 \cdot w_{st} \cdot \frac{\sin(\alpha_{BOT})}{\sin(\beta)}} \right] \end{array} \right] \\ \theta \end{cases} \quad \theta = 39.709 \text{ deg}$$

$$C_1 := \frac{F_1}{\cos(\theta)} \quad C_1 = 62.699 \text{ kN}$$

$$\text{Required strut Width: } w_{st} := \frac{C_1}{b \cdot f_{cu}} \quad w_{st} = 13.342 \text{ mm} \quad \frac{w_{st}}{2} = 6.671 \text{ mm}$$

$$\text{Length along node: } \beta_{BOT} := \begin{cases} 90\text{deg} - \alpha_{BOT} + \theta & \text{if } \theta < \alpha_{BOT} \\ 90\text{deg} - \theta + \alpha_{BOT} & \text{otherwise} \end{cases}$$

$$L_{BOT} := \frac{w_{st}}{\sin(\beta_{BOT})} \quad L_{BOT} = 13.38 \text{ mm}$$

Direct Strut

Check Bottom Node:

$$\text{CCT Node: } w_{\text{BOT}} := \sqrt{l_b^2 + (2 \cdot d_1)^2} - L_{\text{BO}} \quad f_{\text{cu}} := 0.75 \cdot f_c \quad C_{\text{BOT}} := f_{\text{cu}} \cdot b \cdot w_{\text{BOT}} \quad C_{\text{BOT}} = 767.201 \text{ kN}$$

Check Top Node:

$$\text{CCC Node: } w_{\text{TOP}} := \sqrt{l_b^2 + x^2} - L_{\text{TOP}} \quad f_{\text{cu}} := 0.85 \cdot f_c \quad C_{\text{TOP}} := f_{\text{cu}} \cdot b \cdot w_{\text{TOP}} \quad C_{\text{TOP}} = 812.383 \text{ kN}$$

Check the strength of the strut:

$$\theta_2 := \text{atan} \left(\frac{h - 0.5 \cdot w_{\text{TOP}} \cdot \cos(\alpha_{\text{TOP}}) - 0.5 \cdot w_{\text{BOT}} \cdot \cos(\alpha_{\text{BOT}})}{a - l_b + 0.5 \cdot w_{\text{TOP}} \cdot \sin(\alpha_{\text{TOP}}) + 0.5 \cdot w_{\text{BOT}} \cdot \sin(\alpha_{\text{BOT}})} \right) \quad \theta_2 = 40.026 \text{ deg}$$

$$\sigma_{\text{cw}} := 0.6 \cdot f_c \quad \sigma_{\text{cw}} = 42.72 \text{ MPa}$$

Calculate β for direct strut

$$\text{At Top Node: } \beta_{\text{DTOP}} := \begin{cases} 90 \text{ deg} - \alpha_{\text{TOP}} + \theta_2 & \text{if } \theta_2 < \alpha_{\text{TOP}} \\ 90 \text{ deg} - \theta_2 + \alpha_{\text{TOP}} & \text{otherwise} \end{cases} \quad \beta_{\text{DTOP}} = 82.371 \text{ deg}$$

$$\text{At Bottom Node: } \beta_{\text{DBOT}} := \begin{cases} 90 \text{ deg} - \alpha_{\text{BOT}} + \theta_2 & \text{if } \theta_2 < \alpha_{\text{BOT}} \\ 90 \text{ deg} - \theta_2 + \alpha_{\text{BOT}} & \text{otherwise} \end{cases} \quad \beta_{\text{DBOT}} = 86.039 \text{ deg}$$

$$w_{\text{st}} := \min(w_{\text{BOT}} \cdot \sin(\beta_{\text{DBOT}}), w_{\text{TOP}} \cdot \sin(\beta_{\text{DTOP}})) \quad w_{\text{st}} = 120.951 \text{ mm}$$

$$C_{\text{Strut}} := \sigma_{\text{cw}} \cdot w_{\text{st}} \cdot b \quad C_{\text{Strut}} = 568.371 \text{ kN} \quad \text{Check2} := \begin{cases} \text{"Model Not Applicable"} & \text{if } C_{\text{Strut}} < 0 \\ \text{"OK"} & \text{otherwise} \end{cases}$$

$$C_2 := \min(C_{\text{TOP}}, C_{\text{BOT}}, C_{\text{Strut}}) \quad C_2 = 568.371 \text{ kN}$$

Check main tension reinforcement

$$F_y := 538 \text{ MPa}$$

$$T := C_2 \cdot \cos(\theta_2) + C_1 \cdot \sin(\theta) \quad T = 475 \text{ kN} \quad T_r := A_s \cdot F_y \quad T_r = 530 \text{ kN}$$

$$\text{Check} := \begin{cases} \text{"OK"} & \text{if } T < T_r \\ \text{"NG"} & \text{otherwise} \end{cases}$$

$$F_2 := C_2 \cdot \sin(\theta_2) \quad F_2 = 365.538 \text{ kN}$$

$$\text{Therefore: } V := F_1 + F_2 \quad V = 414 \text{ kN} \quad \text{Check} = \text{"OK"} \quad \text{Check2} = \text{"OK"}$$

$$P := 2 \cdot V \quad P = 828 \text{ kN}$$

Researcher: Tan, Kong, Teng, and Weng, 1997 Specimen: 1-2N-1.00

1. Geometry

$$d := 442.5\text{mm} \quad f_c := 77.6\text{MPa} \quad F_y := 498.9\text{MPa} \quad b := 110\text{mm} \quad A_s := 4.300\text{mm}^2$$

$$\alpha_1 := 0.85 - 0.0015 \cdot \frac{f_c}{1\text{MPa}} \quad \beta_1 := 0.97 - 0.0025 \cdot \frac{f_c}{1\text{MPa}} \quad h := 500\text{mm} \quad A_v := 2 \cdot 0.11\text{in}^2 \quad s := 100\text{mm}$$

$$x := \frac{A_s \cdot F_y}{\alpha_1 \cdot b \cdot f_c} \quad x = 95.605\text{mm} \quad c := \frac{x}{\beta_1} \quad c = 123.202\text{mm} \quad \rho := \frac{A_s}{b \cdot d}$$

$$z := d - \frac{x}{2} \quad z = 394.697\text{mm} \quad d_1 := h - d \quad l_b := 150\text{mm} \quad a := 500\text{mm} \quad \frac{a}{d} = 1.13$$

$$a_w := 0.85 \cdot a - \frac{z}{4} \quad a_w = 326.326\text{mm} \quad \frac{a_w}{s} = 3.263 \quad n := 4 \quad \text{Number of effective stirrups (two stirrups used in beam)}$$

2. Strut Dimensions

$$\chi := \sqrt{f_c} \frac{1}{\sqrt{\text{MPa}}} + 250 \cdot \sqrt{\rho \cdot \left(\frac{d}{a}\right)^5} \quad \psi := 1.67 \cdot \frac{\sqrt{f_c}}{\sqrt{\text{MPa}}} \quad \psi = 0.39$$

$$F_y := 353.2\text{MPa} \quad F_1 := \psi \cdot n \cdot F_y \cdot A_v$$

For strength of the strut: $f_{cu} := 0.6 \cdot f_c$ By Inspection, this will control

Bottom Strut

$$\alpha_{\text{TOP}} := \text{atan}\left(\frac{l_b}{x}\right) \quad \alpha_{\text{TOP}} = 57.488 \text{ deg}$$

$$\theta := \left\{ \begin{array}{l} \theta \leftarrow 50\text{deg} \\ \text{for } i \in 1 \dots 20 \\ \left| \begin{array}{l} C_1 \leftarrow \frac{F_1}{\sin(\theta)} \\ f_{cu} \leftarrow 0.6 \cdot f_c \\ w_{st} \leftarrow \frac{C_1}{b \cdot f_{cu}} \\ \beta \leftarrow \begin{cases} 90\text{deg} - \alpha_{\text{TOP}} + \theta & \text{if } \theta < \alpha_{\text{TOP}} \\ 90\text{deg} - \theta + \alpha_{\text{TOP}} & \text{otherwise} \end{cases} \\ \theta \leftarrow \text{atan}\left[\frac{d - \left(x - 0.5 \cdot w_{st} \cdot \frac{\cos(\alpha_{\text{TOP}})}{\sin(\beta)} \right)}{0.5a + 0.5 \cdot l_b - 0.5 \cdot w_{st} \cdot \frac{\sin(\alpha_{\text{TOP}})}{\sin(\beta)}} \right] \end{array} \right. \end{array} \right. \quad \theta = 48.103 \text{ deg}$$

$$C_1 := \frac{F_1}{\sin(\theta)} \quad C_1 = 105.037 \text{ kN}$$

$$\text{Required strut Width: } w_{st} := \frac{C_1}{b \cdot f_{cu}} \quad w_{st} = 20.509 \text{ mm} \quad \frac{w_{st}}{2} = 10.254 \text{ mm}$$

$$\text{Length along node: } \beta_{TOP} := \begin{cases} 90\text{deg} - \alpha_{TOP} + \theta & \text{if } \theta < \alpha_{TOP} \\ 90\text{deg} - \theta + \alpha_{TOP} & \text{otherwise} \end{cases}$$

$$L_{TOP} := \frac{w_{st}}{\sin(\beta_{TOP})} \quad L_{TOP} = 20.787 \text{ mm}$$

$$\text{Top Strut } l_b := 100 \text{ mm}$$

$$\alpha_{BOT} := \text{atan}\left(\frac{l_b}{2 \cdot d_1}\right) \quad \alpha_{BOT} = 41.009 \text{ deg}$$

$$\theta := \begin{cases} 50\text{deg} \\ \text{for } i \in 1..40 \\ \left| \begin{array}{l} C_1 \leftarrow \frac{F_1}{\cos(\theta)} \\ f_{cu} \leftarrow 0.6 \cdot f_c \\ w_{st} \leftarrow \frac{C_1}{b \cdot f_{cu}} \\ \beta \leftarrow \begin{cases} 90\text{deg} - \alpha_{BOT} + \theta & \text{if } \theta < \alpha_{BOT} \\ 90\text{deg} - \theta + \alpha_{BOT} & \text{otherwise} \end{cases} \\ \theta \leftarrow 90\text{deg} - \text{atan}\left[\frac{h - 0.5x - \left(2d_1 - 0.5 \cdot w_{st} \cdot \frac{\cos(\alpha_{BOT})}{\sin(\beta)}\right)}{0.5a + 0.5 \cdot l_b - 0.5 \cdot w_{st} \cdot \frac{\sin(\alpha_{BOT})}{\sin(\beta)}}\right] \end{array} \right| \\ \theta \end{cases} \quad \theta = 40.401 \text{ deg}$$

$$C_1 := \frac{F_1}{\cos(\theta)} \quad C_1 = 102.666 \text{ kN}$$

$$\text{Required strut Width: } w_{st} := \frac{C_1}{b \cdot f_{cu}} \quad w_{st} = 20.046 \text{ mm} \quad \frac{w_{st}}{2} = 10.023 \text{ mm}$$

$$\text{Length along node: } \beta_{BOT} := \begin{cases} 90\text{deg} - \alpha_{BOT} + \theta & \text{if } \theta < \alpha_{BOT} \\ 90\text{deg} - \theta + \alpha_{BOT} & \text{otherwise} \end{cases}$$

$$L_{BOT} := \frac{w_{st}}{\sin(\beta_{BOT})} \quad L_{BOT} = 20.047 \text{ mm}$$

Direct Strut

Check Bottom Node: $l_b := 100\text{mm}$

$$\text{CCT Node: } w_{\text{BOT}} := \sqrt{l_b^2 + (2 \cdot d_1)^2} - L_{\text{BOT}} \quad f_{\text{cu}} := 0.75 \cdot f_c \quad C_{\text{BOT}} := f_{\text{cu}} \cdot b \cdot w_{\text{BOT}} \quad C_{\text{BOT}} = 847.309 \text{ kN}$$

Check Top Node: $l_b := 150\text{mm}$

$$\text{CCC Node: } w_{\text{TOP}} := \sqrt{l_b^2 + x^2} - L_{\text{TOP}} \quad f_{\text{cu}} := 0.85 \cdot f_c \quad C_{\text{TOP}} := f_{\text{cu}} \cdot b \cdot w_{\text{TOP}} \quad C_{\text{TOP}} = 1139.786 \text{ kN}$$

Check the strength of the strut:

$$\theta_2 := \text{atan} \left(\frac{h - 0.5 \cdot w_{\text{TOP}} \cdot \cos(\alpha_{\text{TOP}}) - 0.5 \cdot w_{\text{BOT}} \cdot \cos(\alpha_{\text{BOT}})}{a - l_b + 0.5 \cdot w_{\text{TOP}} \cdot \sin(\alpha_{\text{TOP}}) + 0.5 \cdot w_{\text{BOT}} \cdot \sin(\alpha_{\text{BOT}})} \right) \quad \theta_2 = 41.582 \text{ deg}$$

$$\sigma_{\text{cw}} := 0.6 \cdot f_c \quad \sigma_{\text{cw}} = 46.56 \text{ MPa}$$

Calculate β for direct strut

$$\text{At Top Node: } \beta_{\text{DTOP}} := \begin{cases} 90\text{deg} - \alpha_{\text{TOP}} + \theta_2 & \text{if } \theta_2 < \alpha_{\text{TOP}} \\ 90\text{deg} - \theta_2 + \alpha_{\text{TOP}} & \text{otherwise} \end{cases} \quad \beta_{\text{DTOP}} = 74.094 \text{ deg}$$

$$\text{At Bottom Node: } \beta_{\text{DBOT}} := \begin{cases} 90\text{deg} - \alpha_{\text{BOT}} + \theta_2 & \text{if } \theta_2 < \alpha_{\text{BOT}} \\ 90\text{deg} - \theta_2 + \alpha_{\text{BOT}} & \text{otherwise} \end{cases} \quad \beta_{\text{DBOT}} = 89.427 \text{ deg}$$

$$w_{\text{st}} := \min(w_{\text{BOT}} \cdot \sin(\beta_{\text{DBOT}}), w_{\text{TOP}} \cdot \sin(\beta_{\text{DTOP}})) \quad w_{\text{st}} = 132.344 \text{ mm}$$

$$C_{\text{Strut}} := \sigma_{\text{cw}} \cdot w_{\text{st}} \cdot b \quad C_{\text{Strut}} = 677.813 \text{ kN} \quad \text{Check2} := \begin{cases} \text{"Model Not Applicable"} & \text{if } C_{\text{Strut}} < 0 \\ \text{"OK"} & \text{otherwise} \end{cases}$$

$$C_2 := \min(C_{\text{TOP}}, C_{\text{BOT}}, C_{\text{Strut}}) \quad C_2 = 677.813 \text{ kN}$$

Check main tension reinforcement

$$F_y := 498.9 \text{ MPa}$$

$$T := C_2 \cdot \cos(\theta_2) + C_1 \cdot \sin(\theta) \quad T = 574 \text{ kN} \quad T_r := A_s \cdot F_y \quad T_r = 599 \text{ kN}$$

$$\text{Check} := \begin{cases} \text{"OK"} & \text{if } T < T_r \\ \text{"NG"} & \text{otherwise} \end{cases}$$

$$F_2 := C_2 \cdot \sin(\theta_2) \quad F_2 = 449.86 \text{ kN}$$

$$\text{Therefore: } V := F_1 + F_2 \quad V = 528 \text{ kN} \quad \text{Check} = \text{"OK"} \quad \text{Check2} = \text{"OK"}$$

Researcher: Yun, 2000 Specimen: Beam

1. Geometry

$$d := 417\text{mm} \quad f_c := 6.2\text{ksi} \quad F_y := 67\text{ksi} \quad b := 8\text{in} \quad A_s := 2 \cdot 1\text{in}^2 + 2 \cdot 0.79\text{in}^2 \quad \rho := \frac{A_s}{b \cdot d}$$

$$\alpha_1 := 0.85 - 0.0015 \cdot \frac{f_c}{1\text{MPa}} \quad \beta_1 := 0.97 - 0.0025 \cdot \frac{f_c}{1\text{MPa}} \quad h := 20\text{in} \quad A_v := 2 \cdot 0.11\text{in}^2 \quad s := 5.25\text{in}$$

$$x := \frac{A_s \cdot F_y}{\alpha_1 \cdot b \cdot f_c} \quad x = 156.298\text{mm} \quad c := \frac{x}{\beta_1} \quad c = 181.083\text{mm}$$

$$z := d - \frac{x}{2} \quad z = 338.851\text{mm} \quad d_1 := h - d \quad l_b := 10\text{in} \quad a := 36\text{in} \quad \frac{a}{d} = 2.193$$

$$a_w := 0.85 \cdot a - \frac{z}{4} \quad a_w = 692.527\text{mm} \quad \frac{a_w}{s} = 5.193 \quad n := 6 \quad \text{Number of effective stirrups}$$

2. Strut Dimensions

$$\chi := \sqrt{f_c} \frac{1}{\sqrt{\text{MPa}}} + 250 \cdot \sqrt{\rho \cdot \left(\frac{d}{a}\right)^5} \quad \psi := 1.67 \cdot \frac{\sqrt{f_c}}{\sqrt{\text{MPa}}} \quad \psi = 0.885 \quad F_y := 77.5\text{ksi}$$

$$F_1 := \psi \cdot n \cdot F_y \cdot A_v$$

For strength of the strut: $f_{cu} := 0.6 \cdot f_c$ By Inspection, this will control

Bottom Strut

$$\alpha_{\text{TOP}} := \text{atan}\left(\frac{l_b}{x}\right) \quad \alpha_{\text{TOP}} = 58.394\text{deg}$$

$$\theta := \left| \begin{array}{l} \theta \leftarrow 50\text{deg} \\ \text{for } i \in 1..20 \\ \left| \begin{array}{l} C_1 \leftarrow \frac{F_1}{\sin(\theta)} \\ f_{cu} \leftarrow 0.6 \cdot f_c \\ w_{st} \leftarrow \frac{C_1}{b \cdot f_{cu}} \\ \beta \leftarrow \begin{cases} 90\text{deg} - \alpha_{\text{TOP}} + \theta & \text{if } \theta < \alpha_{\text{TOP}} \\ 90\text{deg} - \theta + \alpha_{\text{TOP}} & \text{otherwise} \end{cases} \\ \theta \leftarrow \text{atan}\left[\frac{d - \left(x - 0.5 \cdot w_{st} \cdot \frac{\cos(\alpha_{\text{TOP}})}{\sin(\beta)} \right)}{0.5a + 0.5 \cdot l_b - 0.5 \cdot w_{st} \cdot \frac{\sin(\alpha_{\text{TOP}})}{\sin(\beta)}} \right] \end{array} \right. \end{array} \right. \quad \theta = 30.82\text{deg}$$

$$C_1 := \frac{F_1}{\sin(\theta)} \quad C_1 = 786.206 \text{ kN}$$

$$w_{st} := \frac{C_1}{b \cdot f_{cu}} \quad w_{st} = 150.852 \text{ mm} \quad \frac{w_{st}}{2} = 75.426 \text{ mm}$$

Length along node: $\beta_{TOP} := \begin{cases} 90\text{deg} - \alpha_{TOP} + \theta & \text{if } \theta < \alpha_{TOP} \\ 90\text{deg} - \theta + \alpha_{TOP} & \text{otherwise} \end{cases}$

Required strut Width:

$$L_{TOP} := \frac{w_{st}}{\sin(\beta_{TOP})} \quad L_{TOP} = 170.182 \text{ mm}$$

Top Strut $l_b := 4\text{in}$

$$\alpha_{BOT} := \text{atan}\left(\frac{l_b}{2 \cdot d_1}\right) \quad \alpha_{BOT} = 29.172 \text{ deg}$$

$$\theta := 50\text{deg}$$

for $i \in 1..40$

$$C_1 \leftarrow \frac{F_1}{\cos(\theta)}$$

$$f_{cu} \leftarrow 0.6 \cdot f_c$$

$$w_{st} \leftarrow \frac{C_1}{b \cdot f_{cu}}$$

$$\beta \leftarrow \begin{cases} 90\text{deg} - \alpha_{BOT} + \theta & \text{if } \theta < \alpha_{BOT} \\ 90\text{deg} - \theta + \alpha_{BOT} & \text{otherwise} \end{cases}$$

$$\theta = 56.113 \text{ deg}$$

$$\theta \leftarrow 90\text{deg} - \text{atan}\left[\frac{h - 0.5x - \left(2d_1 - 0.5 \cdot w_{st} \cdot \frac{\cos(\alpha_{BOT})}{\sin(\beta)}\right)}{0.5a + 0.5 \cdot l_b - 0.5 \cdot w_{st} \cdot \frac{\sin(\alpha_{BOT})}{\sin(\beta)}}\right]$$

$$C_1 := \frac{F_1}{\cos(\theta)} \quad C_1 = 722.458 \text{ kN}$$

Required strut Width: $w_{st} := \frac{C_1}{b \cdot f_{cu}} \quad w_{st} = 138.62 \text{ mm} \quad \frac{w_{st}}{2} = 69.31 \text{ mm}$

Length along node: $\beta_{BOT} := \begin{cases} 90\text{deg} - \alpha_{BOT} + \theta & \text{if } \theta < \alpha_{BOT} \\ 90\text{deg} - \theta + \alpha_{BOT} & \text{otherwise} \end{cases}$

$$L_{BOT} := \frac{w_{st}}{\sin(\beta_{BOT})} \quad L_{BOT} = 155.496 \text{ mm}$$

Direct Strut

Check Bottom Node: $l_b := 4\text{in}$

$$\text{CCT Node: } w_{\text{BOT}} := \sqrt{l_b^2 + (2 \cdot d_1)^2} - L_{\text{BO}} \cdot f_{\text{cu}} := 0.75 \cdot f_c \quad C_{\text{BOT}} := f_{\text{cu}} \cdot b \cdot w_{\text{BOT}} \quad C_{\text{BOT}} = 344.904 \text{ kN}$$

Check Top Node: $l_b := 10\text{in}$

$$\text{CCC Node: } w_{\text{TOP}} := \sqrt{l_b^2 + x^2} - L_{\text{TOP}} \quad f_{\text{cu}} := 0.85 \cdot f_c \quad C_{\text{TOP}} := f_{\text{cu}} \cdot b \cdot w_{\text{TOP}} \quad C_{\text{TOP}} = 945.472 \text{ kN}$$

Check the strength of the strut:

$$\theta_2 := \text{atan} \left(\frac{h - 0.5 \cdot w_{\text{TOP}} \cdot \cos(\alpha_{\text{TOP}}) - 0.5 \cdot w_{\text{BOT}} \cdot \cos(\alpha_{\text{BOT}})}{a - l_b + 0.5 \cdot w_{\text{TOP}} \cdot \sin(\alpha_{\text{TOP}}) + 0.5 \cdot w_{\text{BOT}} \cdot \sin(\alpha_{\text{BOT}})} \right) \quad \theta_2 = 31.803 \text{ deg}$$

$$\sigma_{\text{cw}} := 0.6 \cdot f_c \quad \sigma_{\text{cw}} = 25.648 \text{ MPa}$$

Calculate β for direct strut

$$\text{At Top Node: } \beta_{\text{DTOP}} := \begin{cases} 90\text{deg} - \alpha_{\text{TOP}} + \theta_2 & \text{if } \theta_2 < \alpha_{\text{TOP}} \\ 90\text{deg} - \theta_2 + \alpha_{\text{TOP}} & \text{otherwise} \end{cases} \quad \beta_{\text{DTOP}} = 63.409 \text{ deg}$$

$$\text{At Bottom Node: } \beta_{\text{DBOT}} := \begin{cases} 90\text{deg} - \alpha_{\text{BOT}} + \theta_2 & \text{if } \theta_2 < \alpha_{\text{BOT}} \\ 90\text{deg} - \theta_2 + \alpha_{\text{BOT}} & \text{otherwise} \end{cases} \quad \beta_{\text{DBOT}} = 87.369 \text{ deg}$$

$$w_{\text{st}} := \min(w_{\text{BOT}} \cdot \sin(\beta_{\text{DBOT}}), w_{\text{TOP}} \cdot \sin(\beta_{\text{DTOP}})) \quad w_{\text{st}} = 52.887 \text{ mm}$$

$$C_{\text{Strut}} := \sigma_{\text{cw}} \cdot w_{\text{st}} \cdot b \quad C_{\text{Strut}} = 275.633 \text{ kN} \quad \text{Check2} := \begin{cases} \text{"Model Not Applicable"} & \text{if } C_{\text{Strut}} < 0 \\ \text{"OK"} & \text{otherwise} \end{cases}$$

$$C_2 := \min(C_{\text{TOP}}, C_{\text{BOT}}, C_{\text{Strut}}) \quad C_2 = 275.633 \text{ kN}$$

Check main tension reinforcement

$$F_y := 67\text{ksi}$$

$$T := C_2 \cdot \cos(\theta_2) + C_1 \cdot \sin(\theta) \quad T = 834 \text{ kN} \quad T_r := A_s \cdot F_y \quad T_r = 1 \times 10^3 \text{ kN}$$

$$\text{Check} := \begin{cases} \text{"OK"} & \text{if } T < T_r \\ \text{"NG"} & \text{otherwise} \end{cases}$$

$$F_2 := C_2 \cdot \sin(\theta_2) \quad F_2 = 145.259 \text{ kN}$$

$$\text{Therefore: } V := F_1 + F_2 \quad V = 548 \text{ kN} \quad \text{Check} = \text{"OK"} \quad \text{Check2} = \text{"OK"}$$

Appendix H
Corrosion Strut and Tie Model

Specimen L-1.0-R

1. Geometry

$$A_s := 2.500\text{mm}^2 \quad d := 300\text{mm} \quad f_c := 45.4\text{MPa} \quad F_y := 400\text{MPa} \quad b := 125\text{mm} \quad \rho := \frac{A_s}{b \cdot d}$$

$$w_c := 0.3\text{mm} \quad b := 125\text{mm} - 2 \cdot 22.5\text{mm}$$

$$\alpha_1 := 0.85 - 0.0015 \cdot 30 \quad \beta_1 := 0.97 - 0.0025 \cdot 30 \quad \varepsilon_{cu} := 0.0035 \quad h := 350\text{mm}$$

$$x := \frac{A_s \cdot F_y}{\alpha_1 \cdot b \cdot f_c} \quad x = 136.81\text{mm} \quad c := \frac{x}{\beta_1} \quad c = 152.86\text{mm} \quad A_v := 2 \cdot 100\text{mm}^2$$

$$z := d - \frac{x}{2} \quad z = 231.595\text{mm} \quad d_1 := 50\text{mm} \quad l_b := 125\text{mm} \quad a := 300\text{mm} \quad L := 1500\text{mm}$$

2. Strut Dimensions

$$\chi := \sqrt{f_c} \frac{1}{\sqrt{\text{MPa}}} + 250 \cdot \sqrt{\rho \cdot \left(\frac{d}{a}\right)^5} \quad \psi := 1.67 \cdot \frac{\sqrt{f_c} \frac{1}{\sqrt{\text{MPa}}}}{\chi} \quad \psi = 0.237$$

Yield Strength of Stirrups: $F_y := 417\text{MPa} \quad F_1 := \psi \cdot 76\text{kN}$

For strength of the strut: $f_{cu} := 0.6 \cdot f_c - 11 \frac{\text{MPa}}{\text{mm}} w_c \quad f_{cu} = 23.94\text{MPa}$

Bottom Strut

$$\alpha_{\text{TOP}} := \text{atan}\left(\frac{l_b}{x}\right) \quad \alpha_{\text{TOP}} = 42.417\text{deg}$$

$$\theta := \left| \begin{array}{l} \theta \leftarrow 50\text{deg} \\ \text{for } i \in 1..20 \\ \quad C_1 \leftarrow \frac{F_1}{\sin(\theta)} \\ \quad f_{cu} \leftarrow 0.6 \cdot f_c \\ \quad w_{st} \leftarrow \frac{C_1}{b \cdot f_{cu}} \\ \quad \beta \leftarrow \begin{cases} 90\text{deg} - \alpha_{\text{TOP}} + \theta & \text{if } \theta < \alpha_{\text{TOP}} \\ 90\text{deg} - \theta + \alpha_{\text{TOP}} & \text{otherwise} \end{cases} \\ \quad \theta \leftarrow \text{atan}\left[\frac{d - \left(x - 0.5 \cdot w_{st} \cdot \frac{\cos(\alpha_{\text{TOP}})}{\sin(\beta)} \right)}{0.5a + 0.5 \cdot l_b - 0.5 \cdot w_{st} \cdot \frac{\sin(\alpha_{\text{TOP}})}{\sin(\beta)}} \right] \\ \theta \end{array} \right| \quad \theta = 38.927\text{deg}$$

$$C_1 := \frac{F_1}{\sin(\theta)} \quad C_1 = 28.616 \text{ kN}$$

$$\text{Required strut Width: } w_{st} := \frac{C_1}{b \cdot f_{cu}} \quad w_{st} = 14.941 \text{ mm} \quad \frac{w_{st}}{2} = 7.471 \text{ mm}$$

$$\text{Length along node: } \beta_{TOP} := \begin{cases} 90\text{deg} - \alpha_{TOP} + \theta & \text{if } \theta < \alpha_{TOP} \\ 90\text{deg} - \theta + \alpha_{TOP} & \text{otherwise} \end{cases}$$

$$L_{TOP} := \frac{w_{st}}{\sin(\beta_{TOP})} \quad L_{TOP} = 14.969 \text{ mm}$$

Top Strut

$$\alpha_{BOT} := \text{atan}\left(\frac{l_b}{2 \cdot d_1}\right) \quad \alpha_{BOT} = 51.34 \text{ deg}$$

$$\theta := \begin{cases} 50\text{deg} \\ \text{for } i \in 1..40 \\ \left[\begin{array}{l} C_1 \leftarrow \frac{F_1}{\cos(\theta)} \\ f_{cu} \leftarrow 0.6 \cdot f_c \\ w_{st} \leftarrow \frac{C_1}{b \cdot f_{cu}} \\ \beta \leftarrow \begin{cases} 90\text{deg} - \alpha_{BOT} + \theta & \text{if } \theta < \alpha_{BOT} \\ 90\text{deg} - \theta + \alpha_{BOT} & \text{otherwise} \end{cases} \\ \theta \leftarrow 90\text{deg} - \text{atan}\left[\frac{h - 0.5x - \left(2d_1 - 0.5 \cdot w_{st} \cdot \frac{\cos(\alpha_{BOT})}{\sin(\beta)}\right)}{0.5a + 0.5 \cdot l_b - 0.5 \cdot w_{st} \cdot \frac{\sin(\alpha_{BOT})}{\sin(\beta)}} \right] \end{array} \right] \end{cases} \quad \theta = 48.23 \text{ deg}$$

$$C_1 := \frac{F_1}{\cos(\theta)} \quad C_1 = 26.991 \text{ kN}$$

$$\text{Required strut Width: } w_{st} := \frac{C_1}{b \cdot f_{cu}} \quad w_{st} = 14.093 \text{ mm} \quad \frac{w_{st}}{2} = 7.047 \text{ mm}$$

$$\text{Length along node: } \beta_{BOT} := \begin{cases} 90\text{deg} - \alpha_{BOT} + \theta & \text{if } \theta < \alpha_{BOT} \\ 90\text{deg} - \theta + \alpha_{BOT} & \text{otherwise} \end{cases}$$

$$L_{BOT} := \frac{w_{st}}{\sin(\beta_{BOT})} \quad L_{BOT} = 14.114 \text{ mm}$$

Direct Strut

Check Bottom Node:

$$\text{CCT Node: } w_{BOT} := \sqrt{l_b^2 + (2 \cdot d_1)^2} - L_{BOT} \quad f_{cu} := 0.75 \cdot f_c \quad C_{BOT} := f_{cu} \cdot b \cdot w_{BOT} \quad C_{BOT} = 397.606 \text{ kN}$$

Check Top Node:

$$\text{CCC Node: } w_{TOP} := \sqrt{l_b^2 + x^2} - L_{TOP} \quad f_{cu} := 0.85 \cdot f_c \quad C_{TOP} := f_{cu} \cdot b \cdot w_{TOP} \quad C_{TOP} = 525.895 \text{ kN}$$

Check the strength of the strut:

$$\theta_2 := \text{atan} \left(\frac{h - 0.5 \cdot w_{TOP} \cdot \cos(\alpha_{TOP}) - 0.5 \cdot w_{BOT} \cdot \cos(\alpha_{BOT})}{a - l_b + 0.5 \cdot w_{TOP} \cdot \sin(\alpha_{TOP}) + 0.5 \cdot w_{BOT} \cdot \sin(\alpha_{BOT})} \right) \quad \theta_2 = 39.844 \text{ deg}$$

$$f_{cu} := 0.6 \cdot f_c - 11 \frac{\text{MPa}}{\text{mm}} w_c$$

Calculate β for direct strut

$$\text{At Top Node: } \beta_{DTOP} := \begin{cases} 90 \text{ deg} - \alpha_{TOP} + \theta_2 & \text{if } \theta_2 < \alpha_{TOP} \\ 90 \text{ deg} - \theta_2 + \alpha_{TOP} & \text{otherwise} \end{cases} \quad \beta_{DTOP} = 87.427 \text{ deg}$$

$$\text{At Bottom Node: } \beta_{DBOT} := \begin{cases} 90 \text{ deg} - \alpha_{BOT} + \theta_2 & \text{if } \theta_2 < \alpha_{BOT} \\ 90 \text{ deg} - \theta_2 + \alpha_{BOT} & \text{otherwise} \end{cases} \quad \beta_{DBOT} = 78.504 \text{ deg}$$

$$w_{st} := \min(w_{BOT} \cdot \sin(\beta_{DBOT}), w_{TOP} \cdot \sin(\beta_{DTOP})) \quad w_{st} = 143.036 \text{ mm}$$

$$C_{Strut} := f_{cu} \cdot w_{st} \cdot b \quad C_{Strut} = 273.942 \text{ kN} \quad \text{Check2} := \begin{cases} \text{"Model Not Applicable"} & \text{if } C_{Strut} < 0 \\ \text{"OK"} & \text{otherwise} \end{cases}$$

$$C_2 := \min(C_{TOP}, C_{BOT}, C_{Strut}) \quad C_2 = 273.942 \text{ kN}$$

$$F_2 := C_2 \cdot \sin(\theta_2) \quad F_2 = 175.514 \text{ kN}$$

Check Main Reinforcement

$$T := C_2 \cdot \cos(\theta_2) + C_1 \cdot \sin(\theta) \quad T = 230 \text{ kN} \quad T_r := A_s \cdot F_y \quad T_r = 417 \text{ kN}$$

$$\text{Check} := \begin{cases} \text{"OK"} & \text{if } T < T_r \\ \text{"NG"} & \text{otherwise} \end{cases}$$

$$\text{Therefore: } V := F_1 + F_2 \quad V = 193.494 \text{ kN}$$

$$P := \frac{V \cdot L}{L - a} \quad P = 242 \text{ kN} \quad \text{Check} = \text{"OK"} \quad \text{Check2} = \text{"OK"}$$

Specimen L-1.5-R

1. Geometry

$$A_s := 2 \cdot 500 \text{mm}^2 \quad d := 300 \text{mm} \quad f_c := 45.4 \text{MPa} \quad F_y := 400 \text{MPa} \quad b := 125 \text{mm} \quad \rho := \frac{A_s}{b \cdot d}$$

$$w_c := 0.3 \text{mm} \quad b := 125 \text{mm} - 2 \cdot 22.5 \text{mm}$$

$$\alpha_1 := 0.85 - 0.0015 \cdot \frac{f_c}{\text{MPa}} \quad \beta_1 := 0.97 - 0.0025 \cdot \frac{f_c}{\text{MPa}} \quad h := 350 \text{mm}$$

$$x := \frac{A_s \cdot F_y}{\alpha_1 \cdot b \cdot f_c} \quad x = 140.852 \text{mm} \quad c := \frac{x}{\beta_1} \quad c = 164.451 \text{mm} \quad A_v := 2 \cdot 100 \text{mm}^2$$

$$z := d - \frac{x}{2} \quad z = 229.574 \text{mm} \quad d_1 := 50 \text{mm} \quad l_b := 125 \text{mm} \quad a := 450 \text{mm} \quad L := 1500 \text{mm}$$

2. Strut Dimensions

$$\chi := \sqrt{f_c} \frac{1}{\sqrt{\text{MPa}}} + 250 \cdot \sqrt{\rho \cdot \left(\frac{d}{a}\right)^5} \quad \psi := 1.67 \cdot \frac{\sqrt{f_c}}{\sqrt{\text{MPa}}} \frac{1}{\chi} \quad \psi = 0.522$$

Yield Strength of Stirrups: $F_y := 417 \text{MPa} \quad F_1 := \psi \cdot 152 \text{kN}$

For strength of the strut: $f_{cu} := 0.6 \cdot f_c - 11 \frac{\text{MPa}}{\text{mm}} w_c \quad f_{cu} = 23.94 \text{MPa}$

Bottom Strut

$$\alpha_{\text{TOP}} := \text{atan}\left(\frac{l_b}{x}\right) \quad \alpha_{\text{TOP}} = 41.588 \text{deg}$$

$$\theta := \left| \begin{array}{l} \theta \leftarrow 50 \text{deg} \\ \text{for } i \in 1 \dots 20 \\ \left| \begin{array}{l} C_1 \leftarrow \frac{F_1}{\sin(\theta)} \\ f_{cu} \leftarrow 0.6 \cdot f_c \\ w_{st} \leftarrow \frac{C_1}{b \cdot f_{cu}} \\ \beta \leftarrow \begin{cases} 90 \text{deg} - \alpha_{\text{TOP}} + \theta & \text{if } \theta < \alpha_{\text{TOP}} \\ 90 \text{deg} - \theta + \alpha_{\text{TOP}} & \text{otherwise} \end{cases} \\ \theta \leftarrow \text{atan} \left[\frac{d - \left(x - 0.5 \cdot w_{st} \cdot \frac{\cos(\alpha_{\text{TOP}})}{\sin(\beta)} \right)}{0.5a + 0.5 \cdot l_b - 0.5 \cdot w_{st} \cdot \frac{\sin(\alpha_{\text{TOP}})}{\sin(\beta)}} \right] \end{array} \right. \\ \theta \end{array} \right. \quad \theta = 34.571 \text{deg}$$

$$C_1 := \frac{F_1}{\sin(\theta)} \quad C_1 = 139.854 \text{ kN}$$

$$\text{Required strut Width: } w_{st} := \frac{C_1}{b \cdot f_{cu}} \quad w_{st} = 73.023 \text{ mm} \quad \frac{w_{st}}{2} = 36.512 \text{ mm}$$

$$\text{Length along node: } \beta_{TOP} := \begin{cases} 90\text{deg} - \alpha_{TOP} + \theta & \text{if } \theta < \alpha_{TOP} \\ 90\text{deg} - \theta + \alpha_{TOP} & \text{otherwise} \end{cases}$$

$$L_{TOP} := \frac{w_{st}}{\sin(\beta_{TOP})} \quad L_{TOP} = 73.574 \text{ mm}$$

Top Strut

$$\alpha_{BOT} := \text{atan}\left(\frac{l_b}{2 \cdot d_1}\right) \quad \alpha_{BOT} = 51.34 \text{ deg}$$

$$\theta := \begin{array}{l} 50\text{deg} \\ \text{for } i \in 1 \dots 40 \\ \left| \begin{array}{l} C_1 \leftarrow \frac{F_1}{\cos(\theta)} \\ f_{cu} \leftarrow 0.6 \cdot f_c \\ w_{st} \leftarrow \frac{C_1}{b \cdot f_{cu}} \\ \beta \leftarrow \begin{cases} 90\text{deg} - \alpha_{BOT} + \theta & \text{if } \theta < \alpha_{BOT} \\ 90\text{deg} - \theta + \alpha_{BOT} & \text{otherwise} \end{cases} \\ \theta \leftarrow 90\text{deg} - \text{atan}\left[\frac{h - 0.5x - \left(2d_1 - 0.5 \cdot w_{st} \cdot \frac{\cos(\alpha_{BOT})}{\sin(\beta)}\right)}{0.5a + 0.5 \cdot l_b - 0.5 \cdot w_{st} \cdot \frac{\sin(\alpha_{BOT})}{\sin(\beta)}}\right] \end{array} \right. \\ \theta \end{array} \quad \theta = 53.044 \text{ deg}$$

$$C_1 := \frac{F_1}{\cos(\theta)} \quad C_1 = 131.997 \text{ kN}$$

$$\text{Required strut Width: } w_{st} := \frac{C_1}{b \cdot f_{cu}} \quad w_{st} = 68.921 \text{ mm} \quad \frac{w_{st}}{2} = 34.46 \text{ mm}$$

$$\text{Length along node: } \beta_{BOT} := \begin{cases} 90\text{deg} - \alpha_{BOT} + \theta & \text{if } \theta < \alpha_{BOT} \\ 90\text{deg} - \theta + \alpha_{BOT} & \text{otherwise} \end{cases}$$

$$L_{BOT} := \frac{w_{st}}{\sin(\beta_{BOT})} \quad L_{BOT} = 68.951 \text{ mm}$$

Direct Strut

Check Bottom Node:

$$\text{CCT Node: } w_{\text{BOT}} := \sqrt{l_b^2 + (2 \cdot d_1)^2} - L_{\text{BOT}} \quad f_{\text{cu}} := 0.75 \cdot f_c \quad C_{\text{BOT}} := f_{\text{cu}} \cdot b \cdot w_{\text{BOT}} \quad C_{\text{BOT}} = 248.23 \text{ kN}$$

Check Top Node:

$$\text{CCC Node: } w_{\text{TOP}} := \sqrt{l_b^2 + x^2} - L_{\text{TOP}} \quad f_{\text{cu}} := 0.85 \cdot f_c \quad C_{\text{TOP}} := f_{\text{cu}} \cdot b \cdot w_{\text{TOP}} \quad C_{\text{TOP}} = 354.241 \text{ kN}$$

Check the strength of the strut:

$$\theta_2 := \text{atan} \left(\frac{h - 0.5 \cdot w_{\text{TOP}} \cdot \cos(\alpha_{\text{TOP}}) - 0.5 \cdot w_{\text{BOT}} \cdot \cos(\alpha_{\text{BOT}})}{a - l_b + 0.5 \cdot w_{\text{TOP}} \cdot \sin(\alpha_{\text{TOP}}) + 0.5 \cdot w_{\text{BOT}} \cdot \sin(\alpha_{\text{BOT}})} \right) \quad \theta_2 = 34.95 \text{ deg}$$

$$f_{\text{cu}} := 0.6 \cdot f_c - 11 \frac{\text{MPa}}{\text{mm}} w_c$$

Calculate β for direct strut

$$\text{At Top Node: } \beta_{\text{DTOP}} := \begin{cases} 90 \text{deg} - \alpha_{\text{TOP}} + \theta_2 & \text{if } \theta_2 < \alpha_{\text{TOP}} \\ 90 \text{deg} - \theta_2 + \alpha_{\text{TOP}} & \text{otherwise} \end{cases} \quad \beta_{\text{DTOP}} = 83.362 \text{ deg}$$

$$\text{At Bottom Node: } \beta_{\text{DBOT}} := \begin{cases} 90 \text{deg} - \alpha_{\text{BOT}} + \theta_2 & \text{if } \theta_2 < \alpha_{\text{BOT}} \\ 90 \text{deg} - \theta_2 + \alpha_{\text{BOT}} & \text{otherwise} \end{cases} \quad \beta_{\text{DBOT}} = 73.61 \text{ deg}$$

$$w_{\text{st}} := \min(w_{\text{BOT}} \cdot \sin(\beta_{\text{DBOT}}), w_{\text{TOP}} \cdot \sin(\beta_{\text{DTOP}})) \quad w_{\text{st}} = 87.424 \text{ mm}$$

$$C_{\text{Strut}} := f_{\text{cu}} \cdot w_{\text{st}} \cdot b \quad C_{\text{Strut}} = 167.434 \text{ kN} \quad \text{Check2} := \begin{cases} \text{"Model Not Applicable"} & \text{if } C_{\text{Strut}} < 0 \\ \text{"OK"} & \text{otherwise} \end{cases}$$

$$C_2 := \min(C_{\text{TOP}}, C_{\text{BOT}}, C_{\text{Strut}}) \quad C_2 = 167.434 \text{ kN}$$

$$F_2 := C_2 \cdot \sin(\theta_2) \quad F_2 = 95.916 \text{ kN}$$

Check Main Reinforcement

$$T := C_2 \cdot \cos(\theta_2) + C_1 \cdot \sin(\theta) \quad T = 243 \text{ kN} \quad T_r := A_s \cdot F_y \quad T_r = 417 \text{ kN}$$

$$\text{Check} := \begin{cases} \text{"OK"} & \text{if } T < T_r \\ \text{"NG"} & \text{otherwise} \end{cases}$$

$$\text{Therefore: } V := F_1 + F_2 \quad V = 175.273 \text{ kN}$$

$$P := \frac{V \cdot L}{L - a} \quad \boxed{P = 250 \text{ kN}} \quad \text{Check} = \text{"OK"} \quad \text{Check2} = \text{"OK"}$$

Specimen L-2.0-R

1. Geometry

$$A_s := 2.500\text{mm}^2 \quad d := 300\text{mm} \quad f_c := 45.4\text{MPa} \quad F_y := 400\text{MPa} \quad b := 125\text{mm} \quad \rho := \frac{A_s}{b \cdot d}$$

$$w_c := 0.3\text{mm} \quad b := 125\text{mm} - 2 \cdot 22.5\text{mm}$$

$$\alpha_1 := 0.85 - 0.0015 \cdot 30 \quad \beta_1 := 0.97 - 0.0025 \cdot 30 \quad \varepsilon_{cu} := 0.0035 \quad h := 350\text{mm}$$

$$x := \frac{A_s \cdot F_y}{\alpha_1 \cdot b \cdot f_c} \quad x = 137\text{mm} \quad c := \frac{x}{\beta_1} \quad c = 153\text{mm} \quad A_v := 2.100\text{mm}^2$$

$$z := d - \frac{x}{2} \quad z = 232\text{mm} \quad d_1 := 50\text{mm} \quad l_b := 125\text{mm} \quad a := 600\text{mm} \quad L := 1500\text{mm}$$

2. Strut Dimensions

$$\chi := \sqrt{f_c} \frac{1}{\sqrt{\text{MPa}}} + 250 \cdot \sqrt{\rho \cdot \left(\frac{d}{a}\right)^5} \quad \psi := 1.67 \cdot \frac{\sqrt{f_c}}{\sqrt{\text{MPa}}} \quad \psi = 1$$

$$\text{Yield Strength of Stirrups: } F_y := 417\text{MPa} \quad F_1 := \psi \cdot 228\text{kN}$$

$$\text{For strength of the strut: } f_{cu} := 0.6 \cdot f_c - 11 \frac{\text{MPa}}{\text{mm}} w_c \quad f_{cu} = 24\text{MPa}$$

Bottom Strut

$$\alpha_{TOP} := \text{atan}\left(\frac{l_b}{x}\right) \quad \alpha_{TOP} = 42\text{deg}$$

$$\theta := \left\{ \begin{array}{l} \theta \leftarrow 50\text{deg} \\ \text{for } i \in 1..20 \\ \left| \begin{array}{l} C_1 \leftarrow \frac{F_1}{\sin(\theta)} \\ f_{cu} \leftarrow 0.6 \cdot f_c \\ w_{st} \leftarrow \frac{C_1}{b \cdot f_{cu}} \\ \beta \leftarrow \left\{ \begin{array}{l} 90\text{deg} - \alpha_{TOP} + \theta \text{ if } \theta < \alpha_{TOP} \\ 90\text{deg} - \theta + \alpha_{TOP} \text{ otherwise} \end{array} \right. \\ \theta \leftarrow \text{atan}\left[\frac{d - \left(x - 0.5 \cdot w_{st} \cdot \frac{\cos(\alpha_{TOP})}{\sin(\beta)} \right)}{0.5a + 0.5 \cdot l_b - 0.5 \cdot w_{st} \cdot \frac{\sin(\alpha_{TOP})}{\sin(\beta)}} \right] \end{array} \right. \\ \theta \end{array} \right. \quad \theta = 35\text{deg}$$

$$C_1 := \frac{F_1}{\sin(\theta)} \quad C_1 = 321 \text{ kN}$$

$$\text{Required strut Width:} \quad w_{st} := \frac{C_1}{b \cdot f_{cu}} \quad w_{st} = 168 \text{ mm} \quad \frac{w_{st}}{2} = 84 \text{ mm}$$

$$\text{Length along node:} \quad \beta_{TOP} := \begin{cases} 90\text{deg} - \alpha_{TOP} + \theta & \text{if } \theta < \alpha_{TOP} \\ 90\text{deg} - \theta + \alpha_{TOP} & \text{otherwise} \end{cases}$$

$$L_{TOP} := \frac{w_{st}}{\sin(\beta_{TOP})} \quad L_{TOP} = 169 \text{ mm}$$

Top Strut

$$\alpha_{BOT} := \text{atan}\left(\frac{l_b}{2 \cdot d_1}\right) \quad \alpha_{BOT} = 51 \text{ deg}$$

$$\theta := \begin{cases} 50\text{deg} \\ \text{for } i \in 1..40 \\ \left[\begin{array}{l} C_1 \leftarrow \frac{F_1}{\cos(\theta)} \\ f_{cu} \leftarrow 0.6 \cdot f_c \\ w_{st} \leftarrow \frac{C_1}{b \cdot f_{cu}} \\ \beta \leftarrow \begin{cases} 90\text{deg} - \alpha_{BOT} + \theta & \text{if } \theta < \alpha_{BOT} \\ 90\text{deg} - \theta + \alpha_{BOT} & \text{otherwise} \end{cases} \\ \theta \leftarrow 90\text{deg} - \text{atan}\left[\frac{h - 0.5x - \left(2d_1 - 0.5 \cdot w_{st} \cdot \frac{\cos(\alpha_{BOT})}{\sin(\beta)} \right)}{0.5a + 0.5 \cdot l_b - 0.5 \cdot w_{st} \cdot \frac{\sin(\alpha_{BOT})}{\sin(\beta)}} \right] \end{array} \right] \\ \theta \end{cases} \quad \theta = 54 \text{ deg}$$

$$C_1 := \frac{F_1}{\cos(\theta)} \quad C_1 = 310 \text{ kN}$$

$$\text{Required strut Width:} \quad w_{st} := \frac{C_1}{b \cdot f_{cu}} \quad w_{st} = 162 \text{ mm} \quad \frac{w_{st}}{2} = 81 \text{ mm}$$

$$\text{Length along node:} \quad \beta_{BOT} := \begin{cases} 90\text{deg} - \alpha_{BOT} + \theta & \text{if } \theta < \alpha_{BOT} \\ 90\text{deg} - \theta + \alpha_{BOT} & \text{otherwise} \end{cases}$$

$$L_{BOT} := \frac{w_{st}}{\sin(\beta_{BOT})} \quad L_{BOT} = 162 \text{ mm}$$

Direct Strut

Check Bottom Node:

$$\text{CCT Node: } w_{\text{BOT}} := \sqrt{l_b^2 + (2 \cdot d_1)^2} - L_{\text{BOT}} \quad f_{\text{cu}} := 0.75 \cdot f_c \quad C_{\text{BOT}} := f_{\text{cu}} \cdot b \cdot w_{\text{BOT}} \quad C_{\text{BOT}} = -5 \text{ kN}$$

Check Top Node:

$$\text{CCC Node: } w_{\text{TOP}} := \sqrt{l_b^2 + x^2} - L_{\text{TOP}} \quad f_{\text{cu}} := 0.85 \cdot f_c \quad C_{\text{TOP}} := f_{\text{cu}} \cdot b \cdot w_{\text{TOP}} \quad C_{\text{TOP}} = 50 \text{ kN}$$

Check the strength of the strut:

$$\theta_2 := \text{atan} \left(\frac{h - 0.5 \cdot w_{\text{TOP}} \cdot \cos(\alpha_{\text{TOP}}) - 0.5 \cdot w_{\text{BOT}} \cdot \cos(\alpha_{\text{BOT}})}{a - l_b + 0.5 \cdot w_{\text{TOP}} \cdot \sin(\alpha_{\text{TOP}}) + 0.5 \cdot w_{\text{BOT}} \cdot \sin(\alpha_{\text{BOT}})} \right) \quad \theta_2 = 36 \text{ deg}$$

$$f_{\text{cu}} := 0.6 \cdot f_c - 11 \frac{\text{MPa}}{\text{mm}} w_c$$

Calculate β for direct strut

$$\text{At Top Node: } \beta_{\text{DTOP}} := \begin{cases} 90 \text{ deg} - \alpha_{\text{TOP}} + \theta_2 & \text{if } \theta_2 < \alpha_{\text{TOP}} \\ 90 \text{ deg} - \theta_2 + \alpha_{\text{TOP}} & \text{otherwise} \end{cases} \quad \beta_{\text{DTOP}} = 83 \text{ deg}$$

$$\text{At Bottom Node: } \beta_{\text{DBOT}} := \begin{cases} 90 \text{ deg} - \alpha_{\text{BOT}} + \theta_2 & \text{if } \theta_2 < \alpha_{\text{BOT}} \\ 90 \text{ deg} - \theta_2 + \alpha_{\text{BOT}} & \text{otherwise} \end{cases} \quad \beta_{\text{DBOT}} = 74 \text{ deg}$$

$$w_{\text{st}} := \min(w_{\text{BOT}} \cdot \sin(\beta_{\text{DBOT}}), w_{\text{TOP}} \cdot \sin(\beta_{\text{DTOP}})) \quad w_{\text{st}} = -2 \text{ mm}$$

$$C_{\text{Strut}} := f_{\text{cu}} \cdot w_{\text{st}} \cdot b \quad C_{\text{Strut}} = -4 \text{ kN} \quad \text{Check2} := \begin{cases} \text{"Model Not Applicable"} & \text{if } C_{\text{Strut}} < 0 \\ \text{"OK"} & \text{otherwise} \end{cases}$$

$$C_2 := \min(C_{\text{TOP}}, C_{\text{BOT}}, C_{\text{Strut}}) \quad C_2 = -5 \text{ kN}$$

$$F_2 := C_2 \cdot \sin(\theta_2) \quad F_2 = -3 \text{ kN}$$

Check Main Reinforcement

$$T := C_2 \cdot \cos(\theta_2) + C_1 \cdot \sin(\theta) \quad T = 245 \text{ kN} \quad T_r := A_s \cdot F_y \quad T_r = 417 \text{ kN}$$

$$\text{Check} := \begin{cases} \text{"OK"} & \text{if } T < T_r \\ \text{"NG"} & \text{otherwise} \end{cases}$$

$$\text{Therefore: } V := F_1 + F_2 \quad V = 181 \text{ kN}$$

$$R := \frac{V \cdot a}{L - a} \quad R = 121 \text{ kN}$$

$$P := V + R \quad \boxed{P = 301 \text{ kN}} \quad \text{Check} = \text{"OK"} \quad \text{Check2} = \text{"Model Not Applicable"} \\ \text{Close Enough}$$

Specimen M-1.0-R

1. Geometry

$$A_s := 2 \cdot 500 \text{mm}^2 \quad d := 300 \text{mm} \quad f_c := 40.5 \text{MPa} \quad F_y := 400 \text{MPa} \quad b := 125 \text{mm} \quad \rho := \frac{A_s}{b \cdot d}$$

$$w_c := 0.5 \text{mm} \quad b := 125 \text{mm} - 2 \cdot 22.5 \text{mm}$$

$$\alpha_1 := 0.85 - 0.0015 \cdot 30 \quad \beta_1 := 0.97 - 0.0025 \cdot 30 \quad \epsilon_{cu} := 0.0035 \quad h := 350 \text{mm}$$

$$x := \frac{A_s \cdot F_y}{\alpha_1 \cdot b \cdot f_c} \quad x = 153.362 \text{mm} \quad c := \frac{x}{\beta_1} \quad c = 171.355 \text{mm} \quad A_v := 2 \cdot 100 \text{mm}^2$$

$$z := d - \frac{x}{2} \quad z = 223.319 \text{mm} \quad d_1 := 50 \text{mm} \quad l_b := 125 \text{mm} \quad a := 300 \text{mm} \quad L := 1500 \text{mm}$$

2. Strut Dimensions

$$\chi := \sqrt{f_c} \frac{1}{\sqrt{\text{MPa}}} + 250 \cdot \sqrt{\rho \cdot \left(\frac{d}{a}\right)^5} \quad \psi := 1.67 \cdot \frac{\sqrt{f_c} \frac{1}{\sqrt{\text{MPa}}}}{\chi} \quad \psi = 0.225$$

Yield Strength of Stirrups: $F_y := 417 \text{MPa} \quad F_1 := \psi \cdot 73 \text{kN}$

For strength of the strut: $f_{cu} := 0.6 \cdot f_c - 11 \frac{\text{MPa}}{\text{mm}} w_c \quad f_{cu} = 18.8 \text{MPa}$

Bottom Strut

$$\alpha_{\text{TOP}} := \text{atan}\left(\frac{l_b}{x}\right) \quad \alpha_{\text{TOP}} = 39.182 \text{deg}$$

$$\theta := \left\{ \begin{array}{l} \theta \leftarrow 50 \text{deg} \\ \text{for } i \in 1..20 \\ \left| \begin{array}{l} C_1 \leftarrow \frac{F_1}{\sin(\theta)} \\ f_{cu} \leftarrow 0.6 \cdot f_c \\ w_{st} \leftarrow \frac{C_1}{b \cdot f_{cu}} \\ \beta \leftarrow \begin{cases} 90 \text{deg} - \alpha_{\text{TOP}} + \theta & \text{if } \theta < \alpha_{\text{TOP}} \\ 90 \text{deg} - \theta + \alpha_{\text{TOP}} & \text{otherwise} \end{cases} \\ \theta \leftarrow \text{atan} \left[\frac{d - \left(x - 0.5 \cdot w_{st} \cdot \frac{\cos(\alpha_{\text{TOP}})}{\sin(\beta)} \right)}{0.5a + 0.5 \cdot l_b - 0.5 \cdot w_{st} \cdot \frac{\sin(\alpha_{\text{TOP}})}{\sin(\beta)}} \right] \end{array} \right. \quad \theta = 36.197 \text{deg} \\ \theta \end{array} \right.$$

$$C_1 := \frac{F_1}{\sin(\theta)} \quad C_1 = 27.839 \text{ kN}$$

$$\text{Required strut Width: } w_{st} := \frac{C_1}{b \cdot f_{cu}} \quad w_{st} = 18.51 \text{ mm} \quad \frac{w_{st}}{2} = 9.255 \text{ mm}$$

$$\text{Length along node: } \beta_{TOP} := \begin{cases} 90\text{deg} - \alpha_{TOP} + \theta & \text{if } \theta < \alpha_{TOP} \\ 90\text{deg} - \theta + \alpha_{TOP} & \text{otherwise} \end{cases}$$

$$L_{TOP} := \frac{w_{st}}{\sin(\beta_{TOP})} \quad L_{TOP} = 18.535 \text{ mm}$$

Top Strut

$$\alpha_{BOT} := \text{atan}\left(\frac{l_b}{2 \cdot d_1}\right) \quad \alpha_{BOT} = 51.34 \text{ deg}$$

$$\theta := \begin{array}{l} 50\text{deg} \\ \text{for } i \in 1..40 \\ \left| \begin{array}{l} C_1 \leftarrow \frac{F_1}{\cos(\theta)} \\ f_{cu} \leftarrow 0.6 \cdot f_c \\ w_{st} \leftarrow \frac{C_1}{b \cdot f_{cu}} \\ \beta \leftarrow \begin{cases} 90\text{deg} - \alpha_{BOT} + \theta & \text{if } \theta < \alpha_{BOT} \\ 90\text{deg} - \theta + \alpha_{BOT} & \text{otherwise} \end{cases} \\ \theta \leftarrow 90\text{deg} - \text{atan}\left[\frac{h - 0.5x - \left(2d_1 - 0.5 \cdot w_{st} \cdot \frac{\cos(\alpha_{BOT})}{\sin(\beta)}\right)}{0.5a + 0.5 \cdot l_b - 0.5 \cdot w_{st} \cdot \frac{\sin(\alpha_{BOT})}{\sin(\beta)}}\right] \end{array} \right. \end{array} \quad \theta = 49.463 \text{ deg}$$

$$C_1 := \frac{F_1}{\cos(\theta)} \quad C_1 = 25.296 \text{ kN}$$

$$\text{Required strut Width: } w_{st} := \frac{C_1}{b \cdot f_{cu}} \quad w_{st} = 16.819 \text{ mm} \quad \frac{w_{st}}{2} = 8.41 \text{ mm}$$

$$\text{Length along node: } \beta_{BOT} := \begin{cases} 90\text{deg} - \alpha_{BOT} + \theta & \text{if } \theta < \alpha_{BOT} \\ 90\text{deg} - \theta + \alpha_{BOT} & \text{otherwise} \end{cases}$$

$$L_{BOT} := \frac{w_{st}}{\sin(\beta_{BOT})} \quad L_{BOT} = 16.828 \text{ mm}$$

Direct Strut

Check Bottom Node:

$$\text{CCT Node: } w_{\text{BOT}} := \sqrt{l_b^2 + (2 \cdot d_1)^2} - L_{\text{BOT}} \quad f_{\text{cu}} := 0.75 \cdot f_c \quad C_{\text{BOT}} := f_{\text{cu}} \cdot b \cdot w_{\text{BOT}} \quad C_{\text{BOT}} = 348.097 \text{ kN}$$

Check Top Node:

$$\text{CCC Node: } w_{\text{TOP}} := \sqrt{l_b^2 + x^2} - L_{\text{TOP}} \quad f_{\text{cu}} := 0.85 \cdot f_c \quad C_{\text{TOP}} := f_{\text{cu}} \cdot b \cdot w_{\text{TOP}} \quad C_{\text{TOP}} = 493.835 \text{ kN}$$

Check the strength of the strut:

$$\theta_2 := \text{atan} \left(\frac{h - 0.5 \cdot w_{\text{TOP}} \cdot \cos(\alpha_{\text{TOP}}) - 0.5 \cdot w_{\text{BOT}} \cdot \cos(\alpha_{\text{BOT}})}{a - l_b + 0.5 \cdot w_{\text{TOP}} \cdot \sin(\alpha_{\text{TOP}}) + 0.5 \cdot w_{\text{BOT}} \cdot \sin(\alpha_{\text{BOT}})} \right) \quad \theta_2 = 39.346 \text{ deg}$$

$$f_{\text{cu}} := 0.6 \cdot f_c - 11 \frac{\text{MPa}}{\text{mm}} w_c$$

Calculate β for direct strut

$$\text{At Top Node: } \beta_{\text{DTOP}} := \begin{cases} 90 \text{ deg} - \alpha_{\text{TOP}} + \theta_2 & \text{if } \theta_2 < \alpha_{\text{TOP}} \\ 90 \text{ deg} - \theta_2 + \alpha_{\text{TOP}} & \text{otherwise} \end{cases} \quad \beta_{\text{DTOP}} = 89.837 \text{ deg}$$

$$\text{At Bottom Node: } \beta_{\text{DBOT}} := \begin{cases} 90 \text{ deg} - \alpha_{\text{BOT}} + \theta_2 & \text{if } \theta_2 < \alpha_{\text{BOT}} \\ 90 \text{ deg} - \theta_2 + \alpha_{\text{BOT}} & \text{otherwise} \end{cases} \quad \beta_{\text{DBOT}} = 78.005 \text{ deg}$$

$$w_{\text{st}} := \min(w_{\text{BOT}} \cdot \sin(\beta_{\text{DBOT}}), w_{\text{TOP}} \cdot \sin(\beta_{\text{DTOP}})) \quad w_{\text{st}} = 140.122 \text{ mm}$$

$$C_{\text{Strut}} := f_{\text{cu}} \cdot w_{\text{st}} \cdot b \quad C_{\text{Strut}} = 210.744 \text{ kN} \quad \text{Check2} := \begin{cases} \text{"Model Not Applicable"} & \text{if } C_{\text{Strut}} < 0 \\ \text{"OK"} & \text{otherwise} \end{cases}$$

$$C_2 := \min(C_{\text{TOP}}, C_{\text{BOT}}, C_{\text{Strut}}) \quad C_2 = 210.744 \text{ kN}$$

$$F_2 := C_2 \cdot \sin(\theta_2) \quad F_2 = 133.611 \text{ kN}$$

Check Main Reinforcement

$$T := C_2 \cdot \cos(\theta_2) + C_1 \cdot \sin(\theta) \quad T = 182 \text{ kN} \quad T_r := A_s \cdot F_y \quad T_r = 417 \text{ kN}$$

$$\text{Check} := \begin{cases} \text{"OK"} & \text{if } T < T_r \\ \text{"NG"} & \text{otherwise} \end{cases}$$

$$\text{Therefore: } V := F_1 + F_2 \quad V = 150.052 \text{ kN}$$

$$P := \frac{V \cdot L}{L - a} \quad \boxed{P = 188 \text{ kN}} \quad \text{Check} = \text{"OK"} \quad \text{Check2} = \text{"OK"}$$

Specimen M-1.5-R

1. Geometry

$$A_s := 2 \cdot 500 \text{mm}^2 \quad d := 300 \text{mm} \quad f_c := 40.5 \text{MPa} \quad F_y := 400 \text{MPa} \quad b := 125 \text{mm} \quad \rho := \frac{A_s}{b \cdot d}$$

$$w_c := 0.3 \text{mm} \quad b := 125 \text{mm} - 2 \cdot 22.5 \text{mm}$$

$$\alpha_1 := 0.85 - 0.0015 \cdot 30 \quad \beta_1 := 0.97 - 0.0025 \cdot 30 \quad \varepsilon_{cu} := 0.0035 \quad h := 350 \text{mm}$$

$$x := \frac{A_s \cdot F_y}{\alpha_1 \cdot b \cdot f_c} \quad x = 153.362 \text{mm} \quad c := \frac{x}{\beta_1} \quad c = 171.355 \text{mm} \quad A_v := 2 \cdot 100 \text{mm}^2$$

$$z := d - \frac{x}{2} \quad z = 223.319 \text{mm} \quad d_1 := 50 \text{mm} \quad l_b := 125 \text{mm} \quad a := 450 \text{mm} \quad L := 1500 \text{mm}$$

2. Strut Dimensions

$$\chi := \sqrt{f_c} \frac{1}{\sqrt{\text{MPa}}} + 250 \cdot \sqrt{\rho \cdot \left(\frac{d}{a}\right)^5} \quad \psi := 1.67 \cdot \frac{\sqrt{f_c} \frac{1}{\sqrt{\text{MPa}}}}{\chi} \quad \psi = 0.502$$

Yield Strength of Stirrups: $F_y := 417 \text{MPa} \quad F_1 := \psi \cdot 152 \text{kN}$

For strength of the strut: $f_{cu} := 0.6 \cdot f_c - 11 \frac{\text{MPa}}{\text{mm}} w_c \quad f_{cu} = 21 \text{MPa}$

Bottom Strut

$$\alpha_{TOP} := \text{atan}\left(\frac{l_b}{x}\right) \quad \alpha_{TOP} = 39.182 \text{ deg}$$

$$\theta := \begin{cases} \theta \leftarrow 50 \text{deg} \\ \text{for } i \in 1..20 \\ \quad C_1 \leftarrow \frac{F_1}{\sin(\theta)} \\ \quad w_{st} \leftarrow \frac{C_1}{b \cdot f_{cu}} \\ \quad \beta \leftarrow \begin{cases} 90 \text{deg} - \alpha_{TOP} + \theta & \text{if } \theta < \alpha_{TOP} \\ 90 \text{deg} - \theta + \alpha_{TOP} & \text{otherwise} \end{cases} \\ \quad \theta_i \leftarrow \text{atan}\left[\frac{d - \left(x - 0.5 \cdot w_{st} \cdot \frac{\cos(\alpha_{TOP})}{\sin(\beta)}\right)}{0.5a + 0.5 \cdot l_b - 0.5 \cdot w_{st} \cdot \frac{\sin(\alpha_{TOP})}{\sin(\beta)}}\right] \\ \quad \text{break if } |\theta - \theta_i| < 0.0001 \text{ deg} \\ \quad \theta \leftarrow \theta_i \\ \theta \end{cases} \quad \theta = 34.211 \text{ deg}$$

$$C_1 := \frac{F_1}{\sin(\theta)} \quad C_1 = 135.665 \text{ kN}$$

$$\text{Required strut Width: } w_{st} := \frac{C_1}{b \cdot f_{cu}} \quad w_{st} = 80.753 \text{ mm} \quad \frac{w_{st}}{2} = 40.377 \text{ mm}$$

$$\text{Length along node: } \beta_{TOP} := \begin{cases} 90\text{deg} - \alpha_{TOP} + \theta & \text{if } \theta < \alpha_{TOP} \\ 90\text{deg} - \theta + \alpha_{TOP} & \text{otherwise} \end{cases}$$

$$L_{TOP} := \frac{w_{st}}{\sin(\beta_{TOP})} \quad L_{TOP} = 81.058 \text{ mm}$$

Top Strut

$$\alpha_{BOT} := \text{atan}\left(\frac{l_b}{2 \cdot d_1}\right) \quad \alpha_{BOT} = 51.34 \text{ deg}$$

$$\theta := \begin{cases} 50\text{deg} \\ \text{for } i \in 1..40 \\ \left| \begin{array}{l} C_1 \leftarrow \frac{F_1}{\cos(\theta)} \\ f_{cu} \leftarrow 0.6 \cdot f_c \\ w_{st} \leftarrow \frac{C_1}{b \cdot f_{cu}} \\ \beta \leftarrow \begin{cases} 90\text{deg} - \alpha_{BOT} + \theta & \text{if } \theta < \alpha_{BOT} \\ 90\text{deg} - \theta + \alpha_{BOT} & \text{otherwise} \end{cases} \\ \theta \leftarrow 90\text{deg} - \text{atan}\left[\frac{h - 0.5x - \left(2d_1 - 0.5 \cdot w_{st} \cdot \frac{\cos(\alpha_{BOT})}{\sin(\beta)}\right)}{0.5a + 0.5 \cdot l_b - 0.5 \cdot w_{st} \cdot \frac{\sin(\alpha_{BOT})}{\sin(\beta)}}\right] \end{array} \right| \\ \theta \end{cases} \quad \theta = 53.467 \text{ deg}$$

$$C_1 := \frac{F_1}{\cos(\theta)} \quad C_1 = 128.132 \text{ kN}$$

$$\text{Required strut Width: } w_{st} := \frac{C_1}{b \cdot f_{cu}} \quad w_{st} = 76.269 \text{ mm} \quad \frac{w_{st}}{2} = 38.134 \text{ mm}$$

$$\text{Length along node: } \beta_{BOT} := \begin{cases} 90\text{deg} - \alpha_{BOT} + \theta & \text{if } \theta < \alpha_{BOT} \\ 90\text{deg} - \theta + \alpha_{BOT} & \text{otherwise} \end{cases}$$

$$L_{BOT} := \frac{w_{st}}{\sin(\beta_{BOT})} \quad L_{BOT} = 76.321 \text{ mm}$$

Direct Strut

Check Bottom Node:

$$\text{CCT Node: } w_{\text{BOT}} := \sqrt{l_b^2 + (2 \cdot d_1)^2} - L_{\text{BOT}} \quad f_{\text{cu}} := 0.75 \cdot f_c \quad C_{\text{BOT}} := f_{\text{cu}} \cdot b \cdot w_{\text{BOT}} \quad C_{\text{BOT}} = 203.529 \text{ kN}$$

Check Top Node:

$$\text{CCC Node: } w_{\text{TOP}} := \sqrt{l_b^2 + x^2} - L_{\text{TOP}} \quad f_{\text{cu}} := 0.85 \cdot f_c \quad C_{\text{TOP}} := f_{\text{cu}} \cdot b \cdot w_{\text{TOP}} \quad C_{\text{TOP}} = 321.648 \text{ kN}$$

Check the strength of the strut:

$$\theta_2 := \text{atan} \left(\frac{h - 0.5 \cdot w_{\text{TOP}} \cdot \cos(\alpha_{\text{TOP}}) - 0.5 \cdot w_{\text{BOT}} \cdot \cos(\alpha_{\text{BOT}})}{a - l_b + 0.5 \cdot w_{\text{TOP}} \cdot \sin(\alpha_{\text{TOP}}) + 0.5 \cdot w_{\text{BOT}} \cdot \sin(\alpha_{\text{BOT}})} \right) \quad \theta_2 = 35.221 \text{ deg}$$

$$f_{\text{cu}} := 0.6 \cdot f_c - 11 \frac{\text{MPa}}{\text{mm}} w_c$$

Calculate β for direct strut

$$\text{At Top Node: } \beta_{\text{DTOP}} := \begin{cases} 90 \text{deg} - \alpha_{\text{TOP}} + \theta_2 & \text{if } \theta_2 < \alpha_{\text{TOP}} \\ 90 \text{deg} - \theta_2 + \alpha_{\text{TOP}} & \text{otherwise} \end{cases} \quad \beta_{\text{DTOP}} = 86.039 \text{ deg}$$

$$\text{At Bottom Node: } \beta_{\text{DBOT}} := \begin{cases} 90 \text{deg} - \alpha_{\text{BOT}} + \theta_2 & \text{if } \theta_2 < \alpha_{\text{BOT}} \\ 90 \text{deg} - \theta_2 + \alpha_{\text{BOT}} & \text{otherwise} \end{cases} \quad \beta_{\text{DBOT}} = 73.881 \text{ deg}$$

$$w_{\text{st}} := \min(w_{\text{BOT}} \cdot \sin(\beta_{\text{DBOT}}), w_{\text{TOP}} \cdot \sin(\beta_{\text{DTOP}})) \quad w_{\text{st}} = 80.464 \text{ mm}$$

$$C_{\text{Strut}} := f_{\text{cu}} \cdot w_{\text{st}} \cdot b \quad C_{\text{Strut}} = 135.179 \text{ kN} \quad \text{Check2} := \begin{cases} \text{"Model Not Applicable"} & \text{if } C_{\text{Strut}} < 0 \\ \text{"OK"} & \text{otherwise} \end{cases}$$

$$C_2 := \min(C_{\text{TOP}}, C_{\text{BOT}}, C_{\text{Strut}}) \quad C_2 = 135.179 \text{ kN}$$

$$F_2 := C_2 \cdot \sin(\theta_2) \quad F_2 = 77.962 \text{ kN}$$

Check Main Reinforcement

$$T := C_2 \cdot \cos(\theta_2) + C_1 \cdot \sin(\theta) \quad T = 213 \text{ kN} \quad T_r := A_s \cdot F_y \quad T_r = 417 \text{ kN}$$

$$\text{Check} := \begin{cases} \text{"OK"} & \text{if } T < T_r \\ \text{"NG"} & \text{otherwise} \end{cases}$$

$$\text{Therefore: } V := F_1 + F_2 \quad V = 154.238 \text{ kN}$$

$$P := \frac{V \cdot L}{L - a} \quad P = 220 \text{ kN} \quad \text{Check} = \text{"OK"} \quad \text{Check2} = \text{"OK"}$$

Specimen M-2.0-R

1. Geometry

$$A_s := 2 \cdot 500 \text{mm}^2 \quad d := 300 \text{mm} \quad f_c := 40.5 \text{MPa} \quad F_y := 400 \text{MPa} \quad b := 125 \text{mm} \quad \rho := \frac{A_s}{b \cdot d}$$

$$w_c := 0.35 \text{mm} \quad b := 125 \text{mm} - 22.5 \text{mm}$$

$$\alpha_1 := 0.85 - 0.0015 \cdot 30 \quad \beta_1 := 0.97 - 0.0025 \cdot 30 \quad \varepsilon_{cu} := 0.0035 \quad h := 350 \text{mm}$$

$$x := \frac{A_s \cdot F_y}{\alpha_1 \cdot b \cdot f_c} \quad x = 120 \text{mm} \quad c := \frac{x}{\beta_1} \quad c = 134 \text{mm} \quad A_v := 2 \cdot 100 \text{mm}^2$$

$$z := d - \frac{x}{2} \quad z = 240 \text{mm} \quad d_1 := 50 \text{mm} \quad l_b := 125 \text{mm} \quad a := 600 \text{mm} \quad L := 1500 \text{mm}$$

2. Strut Dimensions

$$\chi := \sqrt{f_c} \frac{1}{\sqrt{\text{MPa}}} + 250 \cdot \sqrt{\rho \cdot \left(\frac{d}{a}\right)^5} \quad \psi := 1.67 \cdot \frac{\sqrt{f_c} \frac{1}{\sqrt{\text{MPa}}}}{\chi} \quad \psi = 1$$

Yield Strength of Stirrups: $F_y := 417 \text{MPa} \quad F_1 := \psi \cdot 226 \text{kN}$

For strength of the strut: $f_{cu} := 0.6 \cdot f_c - 11 \frac{\text{MPa}}{\text{mm}} w_c \quad f_{cu} = 20 \text{MPa}$

Bottom Strut

$$\alpha_{\text{TOP}} := \text{atan}\left(\frac{l_b}{x}\right) \quad \alpha_{\text{TOP}} = 46 \text{deg}$$

$$\theta := \left\{ \begin{array}{l} \theta \leftarrow 50 \text{deg} \\ \text{for } i \in 1..20 \\ \quad \left\{ \begin{array}{l} C_1 \leftarrow \frac{F_1}{\sin(\theta)} \\ f_{cu} \leftarrow 0.6 \cdot f_c \\ w_{st} \leftarrow \frac{C_1}{b \cdot f_{cu}} \\ \beta \leftarrow \left\{ \begin{array}{l} 90 \text{deg} - \alpha_{\text{TOP}} + \theta \text{ if } \theta < \alpha_{\text{TOP}} \\ 90 \text{deg} - \theta + \alpha_{\text{TOP}} \text{ otherwise} \end{array} \right. \\ \theta \leftarrow \text{atan}\left[\frac{d - \left(x - 0.5 \cdot w_{st} \cdot \frac{\cos(\alpha_{\text{TOP}})}{\sin(\beta)} \right)}{0.5a + 0.5 \cdot l_b - 0.5 \cdot w_{st} \cdot \frac{\sin(\alpha_{\text{TOP}})}{\sin(\beta)}} \right] \end{array} \right. \\ \theta \end{array} \right. \quad \theta = 35 \text{deg}$$

$$C_1 := \frac{F_1}{\sin(\theta)} \quad C_1 = 307 \text{ kN}$$

$$\text{Required strut Width:} \quad w_{st} := \frac{C_1}{b \cdot f_{cu}} \quad w_{st} = 146 \text{ mm} \quad \frac{w_{st}}{2} = 73 \text{ mm}$$

$$\text{Length along node:} \quad \beta_{TOP} := \begin{cases} 90\text{deg} - \alpha_{TOP} + \theta & \text{if } \theta < \alpha_{TOP} \\ 90\text{deg} - \theta + \alpha_{TOP} & \text{otherwise} \end{cases}$$

$$L_{TOP} := \frac{w_{st}}{\sin(\beta_{TOP})} \quad L_{TOP} = 149 \text{ mm}$$

Top Strut

$$\alpha_{BOT} := \text{atan}\left(\frac{l_b}{2 \cdot d_1}\right) \quad \alpha_{BOT} = 51 \text{ deg}$$

$$\theta := \begin{cases} 50\text{deg} \\ \text{for } i \in 1..40 \\ \left| \begin{array}{l} C_1 \leftarrow \frac{F_1}{\cos(\theta)} \\ f_{cu} \leftarrow 0.6 \cdot f_c \\ w_{st} \leftarrow \frac{C_1}{b \cdot f_{cu}} \\ \beta \leftarrow \begin{cases} 90\text{deg} - \alpha_{BOT} + \theta & \text{if } \theta < \alpha_{BOT} \\ 90\text{deg} - \theta + \alpha_{BOT} & \text{otherwise} \end{cases} \\ \theta \leftarrow 90\text{deg} - \text{atan}\left[\frac{h - 0.5x - \left(2d_1 - 0.5 \cdot w_{st} \cdot \frac{\cos(\alpha_{BOT})}{\sin(\beta)}\right)}{0.5a + 0.5 \cdot l_b - 0.5 \cdot w_{st} \cdot \frac{\sin(\alpha_{BOT})}{\sin(\beta)}}\right] \end{array} \right. \\ \theta \end{cases} \quad \theta = 54 \text{ deg}$$

$$C_1 := \frac{F_1}{\cos(\theta)} \quad C_1 = 302 \text{ kN}$$

$$\text{Required strut Width:} \quad w_{st} := \frac{C_1}{b \cdot f_{cu}} \quad w_{st} = 144 \text{ mm} \quad \frac{w_{st}}{2} = 72 \text{ mm}$$

$$\text{Length along node:} \quad \beta_{BOT} := \begin{cases} 90\text{deg} - \alpha_{BOT} + \theta & \text{if } \theta < \alpha_{BOT} \\ 90\text{deg} - \theta + \alpha_{BOT} & \text{otherwise} \end{cases}$$

$$L_{BOT} := \frac{w_{st}}{\sin(\beta_{BOT})} \quad L_{BOT} = 144 \text{ mm}$$

Direct Strut

Check Bottom Node:

$$\text{CCT Node: } w_{\text{BOT}} := \sqrt{l_b^2 + (2 \cdot d_1)^2} - L_{\text{BOT}} \quad f_{\text{cu}} := 0.75 \cdot f_c \quad C_{\text{BOT}} := f_{\text{cu}} \cdot b \cdot w_{\text{BOT}} \quad C_{\text{BOT}} = 50 \text{ kN}$$

Check Top Node:

$$\text{CCC Node: } w_{\text{TOP}} := \sqrt{l_b^2 + x^2} - L_{\text{TOP}} \quad f_{\text{cu}} := 0.85 \cdot f_c \quad C_{\text{TOP}} := f_{\text{cu}} \cdot b \cdot w_{\text{TOP}} \quad C_{\text{TOP}} = 84 \text{ kN}$$

Check the strength of the strut:

$$\theta_2 := \text{atan} \left(\frac{h - 0.5 \cdot w_{\text{TOP}} \cdot \cos(\alpha_{\text{TOP}}) - 0.5 \cdot w_{\text{BOT}} \cdot \cos(\alpha_{\text{BOT}})}{a - l_b + 0.5 \cdot w_{\text{TOP}} \cdot \sin(\alpha_{\text{TOP}}) + 0.5 \cdot w_{\text{BOT}} \cdot \sin(\alpha_{\text{BOT}})} \right) \quad \theta_2 = 35 \text{ deg}$$

$$f_{\text{cu}} := 0.6 \cdot f_c - 11 \frac{\text{MPa}}{\text{mm}} w_c$$

Calculate β for direct strut

$$\text{At Top Node: } \beta_{\text{DTOP}} := \begin{cases} 90 \text{ deg} - \alpha_{\text{TOP}} + \theta_2 & \text{if } \theta_2 < \alpha_{\text{TOP}} \\ 90 \text{ deg} - \theta_2 + \alpha_{\text{TOP}} & \text{otherwise} \end{cases} \quad \beta_{\text{DTOP}} = 78 \text{ deg}$$

$$\text{At Bottom Node: } \beta_{\text{DBOT}} := \begin{cases} 90 \text{ deg} - \alpha_{\text{BOT}} + \theta_2 & \text{if } \theta_2 < \alpha_{\text{BOT}} \\ 90 \text{ deg} - \theta_2 + \alpha_{\text{BOT}} & \text{otherwise} \end{cases} \quad \beta_{\text{DBOT}} = 73 \text{ deg}$$

$$w_{\text{st}} := \min(w_{\text{BOT}} \cdot \sin(\beta_{\text{DBOT}}), w_{\text{TOP}} \cdot \sin(\beta_{\text{DTOP}})) \quad w_{\text{st}} = 15 \text{ mm}$$

$$C_{\text{Strut}} := f_{\text{cu}} \cdot w_{\text{st}} \cdot b \quad C_{\text{Strut}} = 32 \text{ kN} \quad \text{Check2} := \begin{cases} \text{"Model Not Applicable"} & \text{if } C_{\text{Strut}} < 0 \\ \text{"OK"} & \text{otherwise} \end{cases}$$

$$C_2 := \min(C_{\text{TOP}}, C_{\text{BOT}}, C_{\text{Strut}}) \quad C_2 = 32 \text{ kN}$$

$$F_2 := C_2 \cdot \sin(\theta_2) \quad F_2 = 18 \text{ kN}$$

Check Main Reinforcement

$$T := C_2 \cdot \cos(\theta_2) + C_1 \cdot \sin(\theta) \quad T = 271 \text{ kN} \quad T_r := A_s \cdot F_y \quad T_r = 417 \text{ kN}$$

$$\text{Check} := \begin{cases} \text{"OK"} & \text{if } T < T_r \\ \text{"NG"} & \text{otherwise} \end{cases}$$

$$\text{Therefore: } V := F_1 + F_2$$

$$R := \frac{V \cdot a}{L - a} \quad R = 130 \text{ kN}$$

$$P := V + R \quad \boxed{P = 325 \text{ kN}} \quad \text{Check} = \text{"OK"} \quad \text{Check2} = \text{"OK"}$$

Specimen H-1.0-R

1. Geometry

$$A_s := 2.500\text{mm}^2 \quad d := 300\text{mm} \quad f_c := 43\text{MPa} \quad F_y := 400\text{MPa} \quad b := 125\text{mm} \quad \rho := \frac{A_s}{b \cdot d}$$

$$w_c := 0.9\text{mm} \quad b := 125\text{mm} - 2 \cdot 22.5\text{mm}$$

$$\alpha_1 := 0.85 - 0.0015 \cdot 30 \quad \beta_1 := 0.97 - 0.0025 \cdot 30 \quad h := 350\text{mm}$$

$$x := \frac{A_s \cdot F_y}{\alpha_1 \cdot b \cdot f_c} \quad x = 144.446\text{mm} \quad c := \frac{x}{\beta_1} \quad c = 161.392\text{mm} \quad A_v := 2 \cdot 100\text{mm}^2$$

$$z := d - \frac{x}{2} \quad z = 227.777\text{mm} \quad d_1 := 50\text{mm} \quad l_b := 125\text{mm} \quad a := 300\text{mm} \quad L := 1500\text{mm}$$

2. Strut Dimensions

$$\chi := \sqrt{f_c} \frac{1}{\sqrt{\text{MPa}}} + 250 \cdot \sqrt{\rho \cdot \left(\frac{d}{a}\right)^5} \quad \psi := 1.67 \cdot \frac{\sqrt{f_c} \frac{1}{\sqrt{\text{MPa}}}}{\chi} \quad \psi = 0.231$$

Yield Strength of Stirrups: $F_y := 417\text{MPa} \quad F_1 := \psi \cdot 68\text{ kN}$

For strength of the strut: $f_{cu} := 0.6 \cdot f_c - 11 \frac{\text{MPa}}{\text{mm}} w_c \quad f_{cu} = 15.9\text{MPa}$

Bottom Strut

$$\alpha_{\text{TOP}} := \text{atan}\left(\frac{l_b}{x}\right) \quad \alpha_{\text{TOP}} = 40.872\text{ deg}$$

$$\theta := \left| \begin{array}{l} \theta \leftarrow 50\text{deg} \\ \text{for } i \in 1 \dots 20 \\ \left| \begin{array}{l} C_1 \leftarrow \frac{F_1}{\sin(\theta)} \\ f_{cu} \leftarrow 0.6 \cdot f_c \\ w_{st} \leftarrow \frac{C_1}{b \cdot f_{cu}} \\ \beta \leftarrow \begin{cases} 90\text{deg} - \alpha_{\text{TOP}} + \theta & \text{if } \theta < \alpha_{\text{TOP}} \\ 90\text{deg} - \theta + \alpha_{\text{TOP}} & \text{otherwise} \end{cases} \\ \theta \leftarrow \text{atan}\left[\frac{d - \left(x - 0.5 \cdot w_{st} \cdot \frac{\cos(\alpha_{\text{TOP}})}{\sin(\beta)} \right)}{0.5a + 0.5 \cdot l_b - 0.5 \cdot w_{st} \cdot \frac{\sin(\alpha_{\text{TOP}})}{\sin(\beta)}} \right] \end{array} \right. \\ \theta \end{array} \right. \quad \theta = 37.564\text{ deg}$$

$$C_1 := \frac{F_1}{\sin(\theta)} \quad C_1 = 25.779 \text{ kN}$$

$$\text{Required strut Width: } w_{st} := \frac{C_1}{b \cdot f_{cu}} \quad w_{st} = 20.267 \text{ mm} \quad \frac{w_{st}}{2} = 10.133 \text{ mm}$$

$$\text{Length along node: } \beta_{TOP} := \begin{cases} 90\text{deg} - \alpha_{TOP} + \theta & \text{if } \theta < \alpha_{TOP} \\ 90\text{deg} - \theta + \alpha_{TOP} & \text{otherwise} \end{cases}$$

$$L_{TOP} := \frac{w_{st}}{\sin(\beta_{TOP})} \quad L_{TOP} = 20.3 \text{ mm}$$

Top Strut

$$\alpha_{BOT} := \text{atan}\left(\frac{l_b}{2 \cdot d_1}\right) \quad \alpha_{BOT} = 51.34 \text{ deg}$$

$$\theta := \begin{cases} 50\text{deg} \\ \text{for } i \in 1..40 \\ \left| \begin{array}{l} C_1 \leftarrow \frac{F_1}{\cos(\theta)} \\ f_{cu} \leftarrow 0.6 \cdot f_c \\ w_{st} \leftarrow \frac{C_1}{b \cdot f_{cu}} \\ \beta \leftarrow \begin{cases} 90\text{deg} - \alpha_{BOT} + \theta & \text{if } \theta < \alpha_{BOT} \\ 90\text{deg} - \theta + \alpha_{BOT} & \text{otherwise} \end{cases} \\ \theta \leftarrow 90\text{deg} - \text{atan}\left[\frac{h - 0.5x - \left(2d_1 - 0.5 \cdot w_{st} \cdot \frac{\cos(\alpha_{BOT})}{\sin(\beta)}\right)}{0.5a + 0.5 \cdot l_b - 0.5 \cdot w_{st} \cdot \frac{\sin(\alpha_{BOT})}{\sin(\beta)}}\right] \end{array} \right. \end{cases} \quad \theta = 48.904 \text{ deg}$$

$$C_1 := \frac{F_1}{\cos(\theta)} \quad C_1 = 23.909 \text{ kN}$$

$$\text{Required strut Width: } w_{st} := \frac{C_1}{b \cdot f_{cu}} \quad w_{st} = 18.797 \text{ mm} \quad \frac{w_{st}}{2} = 9.398 \text{ mm}$$

$$\text{Length along node: } \beta_{BOT} := \begin{cases} 90\text{deg} - \alpha_{BOT} + \theta & \text{if } \theta < \alpha_{BOT} \\ 90\text{deg} - \theta + \alpha_{BOT} & \text{otherwise} \end{cases}$$

$$L_{BOT} := \frac{w_{st}}{\sin(\beta_{BOT})} \quad L_{BOT} = 18.814 \text{ mm}$$

Direct Strut

Check Bottom Node:

$$\text{CCT Node: } w_{\text{BOT}} := \sqrt{l_b^2 + (2 \cdot d_1)^2} - L_{\text{BOT}} \quad f_{\text{cu}} := 0.75 \cdot f_c \quad C_{\text{BOT}} := f_{\text{cu}} \cdot b \cdot w_{\text{BOT}} \quad C_{\text{BOT}} = 364.462 \text{ kN}$$

Check Top Node:

$$\text{CCC Node: } w_{\text{TOP}} := \sqrt{l_b^2 + x^2} - L_{\text{TOP}} \quad f_{\text{cu}} := 0.85 \cdot f_c \quad C_{\text{TOP}} := f_{\text{cu}} \cdot b \cdot w_{\text{TOP}} \quad C_{\text{TOP}} = 499.192 \text{ kN}$$

Check the strength of the strut:

$$\theta_2 := \text{atan} \left(\frac{h - 0.5 \cdot w_{\text{TOP}} \cdot \cos(\alpha_{\text{TOP}}) - 0.5 \cdot w_{\text{BOT}} \cdot \cos(\alpha_{\text{BOT}})}{a - l_b + 0.5 \cdot w_{\text{TOP}} \cdot \sin(\alpha_{\text{TOP}}) + 0.5 \cdot w_{\text{BOT}} \cdot \sin(\alpha_{\text{BOT}})} \right) \quad \theta_2 = 40.157 \text{ deg}$$

$$f_{\text{cu}} := 0.6 \cdot f_c - 11 \frac{\text{MPa}}{\text{mm}} w_c$$

Calculate β for direct strut

$$\text{At Top Node: } \beta_{\text{DTOP}} := \begin{cases} 90 \text{deg} - \alpha_{\text{TOP}} + \theta_2 & \text{if } \theta_2 < \alpha_{\text{TOP}} \\ 90 \text{deg} - \theta_2 + \alpha_{\text{TOP}} & \text{otherwise} \end{cases} \quad \beta_{\text{DTOP}} = 89.285 \text{ deg}$$

$$\text{At Bottom Node: } \beta_{\text{DBOT}} := \begin{cases} 90 \text{deg} - \alpha_{\text{BOT}} + \theta_2 & \text{if } \theta_2 < \alpha_{\text{BOT}} \\ 90 \text{deg} - \theta_2 + \alpha_{\text{BOT}} & \text{otherwise} \end{cases} \quad \beta_{\text{DBOT}} = 78.816 \text{ deg}$$

$$w_{\text{st}} := \min(w_{\text{BOT}} \cdot \sin(\beta_{\text{DBOT}}), w_{\text{TOP}} \cdot \sin(\beta_{\text{DTOP}})) \quad w_{\text{st}} = 138.582 \text{ mm}$$

$$C_{\text{Strut}} := f_{\text{cu}} \cdot w_{\text{st}} \cdot b \quad C_{\text{Strut}} = 176.276 \text{ kN}$$

$$C_2 := \min(C_{\text{TOP}}, C_{\text{BOT}}, C_{\text{Strut}}) \quad C_2 = 176.276 \text{ kN}$$

$$F_2 := C_2 \cdot \sin(\theta_2) \quad F_2 = 113.677 \text{ kN}$$

$$\text{Check2} := \begin{cases} \text{"Model Not Applicable"} & \text{if } C_{\text{Strut}} < 0 \\ \text{"OK"} & \text{otherwise} \end{cases}$$

Check Main Reinforcement

$$T := C_2 \cdot \cos(\theta_2) + C_1 \cdot \sin(\theta) \quad T = 153 \text{ kN} \quad T_r := A_s \cdot F_y \quad T_r = 417 \text{ kN}$$

$$\text{Check} := \begin{cases} \text{"OK"} & \text{if } T < T_r \\ \text{"NG"} & \text{otherwise} \end{cases}$$

$$\text{Therefore: } V := F_1 + F_2 \quad V = 129.393 \text{ kN}$$

$$R := \frac{V \cdot a}{L - a} \quad R = 32.348 \text{ kN}$$

$$P := V + R \quad \boxed{P = 162 \text{ kN}} \quad \text{Check} = \text{"OK"} \quad \text{Check2} = \text{"OK"}$$

Specimen H-1.5-R

1. Geometry

$$A_s := 2 \cdot 500 \text{mm}^2 \quad d := 300 \text{mm} \quad f_c := 43 \text{MPa} \quad F_y := 400 \text{MPa} \quad b := 125 \text{mm} \quad \rho := \frac{A_s}{b \cdot d}$$

$$w_c := 1.00 \text{mm} \quad b := 125 \text{mm} - 2 \cdot 22.5 \text{mm}$$

$$\alpha_1 := 0.85 - 0.0015 \cdot 30 \quad \beta_1 := 0.97 - 0.0025 \cdot 30 \quad \varepsilon_{cu} := 0.0035 \quad h := 350 \text{mm}$$

$$x := \frac{A_s \cdot F_y}{\alpha_1 \cdot b \cdot f_c} \quad x = 144.446 \text{mm} \quad c := \frac{x}{\beta_1} \quad c = 161.392 \text{mm} \quad A_v := 2 \cdot 100 \text{mm}^2$$

$$z := d - \frac{x}{2} \quad z = 227.777 \text{mm} \quad d_1 := 50 \text{mm} \quad l_b := 125 \text{mm} \quad a := 450 \text{mm} \quad L := 1500 \text{mm}$$

2. Strut Dimensions

$$\chi := \sqrt{f_c} \frac{1}{\sqrt{\text{MPa}}} + 250 \cdot \sqrt{\rho \cdot \left(\frac{d}{a}\right)^5} \quad \psi := 1.67 \cdot \frac{\sqrt{f_c} \frac{1}{\sqrt{\text{MPa}}}}{\chi} \quad \psi = 0.512$$

$$\text{Yield Strength of Stirrups: } F_y := 417 \text{MPa} \quad F_1 := \psi \cdot 133 \text{kN}$$

$$\text{For strength of the strut: } f_{cu} := 0.6 \cdot f_c - 11 \frac{\text{MPa}}{\text{mm}} w_c \quad f_{cu} = 14.8 \text{MPa}$$

Bottom Strut

$$\alpha_{\text{TOP}} := \text{atan}\left(\frac{l_b}{x}\right) \quad \alpha_{\text{TOP}} = 40.872 \text{deg}$$

$$\theta := \begin{cases} \theta \leftarrow 50 \text{deg} \\ \text{for } i \in 1 \dots 20 \\ \quad \left| \begin{array}{l} C_1 \leftarrow \frac{F_1}{\sin(\theta)} \\ w_{\text{st}} \leftarrow \frac{C_1}{b \cdot f_{cu}} \\ \beta \leftarrow \begin{cases} 90 \text{deg} - \alpha_{\text{TOP}} + \theta & \text{if } \theta < \alpha_{\text{TOP}} \\ 90 \text{deg} - \theta + \alpha_{\text{TOP}} & \text{otherwise} \end{cases} \\ \theta_i \leftarrow \text{atan}\left[\frac{d - \left(x - 0.5 \cdot w_{\text{st}} \cdot \frac{\cos(\alpha_{\text{TOP}})}{\sin(\beta)} \right)}{0.5a + 0.5 \cdot l_b - 0.5 \cdot w_{\text{st}} \cdot \frac{\sin(\alpha_{\text{TOP}})}{\sin(\beta)}} \right] \\ \text{break if } |\theta - \theta_i| < 0.0001 \text{deg} \\ \theta \leftarrow \theta_i \end{array} \right. \\ \theta \end{cases} \quad \theta = 36.856 \text{deg}$$

$$C_1 := \frac{F_1}{\sin(\theta)} \quad C_1 = 113.616 \text{ kN}$$

$$\text{Required strut Width: } w_{st} := \frac{C_1}{b \cdot f_{cu}} \quad w_{st} = 95.959 \text{ mm} \quad \frac{w_{st}}{2} = 47.98 \text{ mm}$$

$$\text{Length along node: } \beta_{TOP} := \begin{cases} 90\text{deg} - \alpha_{TOP} + \theta & \text{if } \theta < \alpha_{TOP} \\ 90\text{deg} - \theta + \alpha_{TOP} & \text{otherwise} \end{cases}$$

$$L_{TOP} := \frac{w_{st}}{\sin(\beta_{TOP})} \quad L_{TOP} = 96.195 \text{ mm}$$

Top Strut

$$\alpha_{BOT} := \text{atan}\left(\frac{l_b}{2 \cdot d_1}\right) \quad \alpha_{BOT} = 51.34 \text{ deg}$$

$$\theta := \begin{cases} 50\text{deg} \\ \text{for } i \in 1..40 \\ \left| \begin{array}{l} C_1 \leftarrow \frac{F_1}{\cos(\theta)} \\ f_{cu} \leftarrow 0.6 \cdot f_c \\ w_{st} \leftarrow \frac{C_1}{b \cdot f_{cu}} \\ \beta \leftarrow \begin{cases} 90\text{deg} - \alpha_{BOT} + \theta & \text{if } \theta < \alpha_{BOT} \\ 90\text{deg} - \theta + \alpha_{BOT} & \text{otherwise} \end{cases} \\ \theta \leftarrow 90\text{deg} - \text{atan}\left[\frac{h - 0.5x - \left(2d_1 - 0.5 \cdot w_{st} \cdot \frac{\cos(\alpha_{BOT})}{\sin(\beta)}\right)}{0.5a + 0.5 \cdot l_b - 0.5 \cdot w_{st} \cdot \frac{\sin(\alpha_{BOT})}{\sin(\beta)}}\right] \end{array} \right| \\ \theta \end{cases} \quad \theta = 53.696 \text{ deg}$$

$$C_1 := \frac{F_1}{\cos(\theta)} \quad C_1 = 115.101 \text{ kN}$$

$$\text{Required strut Width: } w_{st} := \frac{C_1}{b \cdot f_{cu}} \quad w_{st} = 97.214 \text{ mm} \quad \frac{w_{st}}{2} = 48.607 \text{ mm}$$

$$\text{Length along node: } \beta_{BOT} := \begin{cases} 90\text{deg} - \alpha_{BOT} + \theta & \text{if } \theta < \alpha_{BOT} \\ 90\text{deg} - \theta + \alpha_{BOT} & \text{otherwise} \end{cases}$$

$$L_{BOT} := \frac{w_{st}}{\sin(\beta_{BOT})} \quad L_{BOT} = 97.296 \text{ mm}$$

Direct Strut

Check Bottom Node:

$$\text{CCT Node: } w_{\text{BOT}} := \sqrt{l_b^2 + (2 \cdot d_1)^2} - L_{\text{BOT}} \quad f_{\text{cu}} := 0.75 \cdot f_c \quad C_{\text{BOT}} := f_{\text{cu}} \cdot b \cdot w_{\text{BOT}} \quad C_{\text{BOT}} = 161.977 \text{ kN}$$

Check Top Node:

$$\text{CCC Node: } w_{\text{TOP}} := \sqrt{l_b^2 + x^2} - L_{\text{TOP}} \quad f_{\text{cu}} := 0.85 \cdot f_c \quad C_{\text{TOP}} := f_{\text{cu}} \cdot b \cdot w_{\text{TOP}} \quad C_{\text{TOP}} = 277.275 \text{ kN}$$

Check the strength of the strut:

$$\theta_2 := \text{atan} \left(\frac{h - 0.5 \cdot w_{\text{TOP}} \cdot \cos(\alpha_{\text{TOP}}) - 0.5 \cdot w_{\text{BOT}} \cdot \cos(\alpha_{\text{BOT}})}{a - l_b + 0.5 \cdot w_{\text{TOP}} \cdot \sin(\alpha_{\text{TOP}}) + 0.5 \cdot w_{\text{BOT}} \cdot \sin(\alpha_{\text{BOT}})} \right) \quad \theta_2 = 37.74 \text{ deg}$$

$$f_{\text{cu}} := 0.6 \cdot f_c - 11 \frac{\text{MPa}}{\text{mm}} w_c$$

Calculate β for direct strut

$$\text{At Top Node: } \beta_{\text{DTOP}} := \begin{cases} 90 \text{deg} - \alpha_{\text{TOP}} + \theta_2 & \text{if } \theta_2 < \alpha_{\text{TOP}} \\ 90 \text{deg} - \theta_2 + \alpha_{\text{TOP}} & \text{otherwise} \end{cases} \quad \beta_{\text{DTOP}} = 86.868 \text{ deg}$$

$$\text{At Bottom Node: } \beta_{\text{DBOT}} := \begin{cases} 90 \text{deg} - \alpha_{\text{BOT}} + \theta_2 & \text{if } \theta_2 < \alpha_{\text{BOT}} \\ 90 \text{deg} - \theta_2 + \alpha_{\text{BOT}} & \text{otherwise} \end{cases} \quad \beta_{\text{DBOT}} = 76.4 \text{ deg}$$

$$w_{\text{st}} := \min(w_{\text{BOT}} \cdot \sin(\beta_{\text{DBOT}}), w_{\text{TOP}} \cdot \sin(\beta_{\text{DTOP}})) \quad w_{\text{st}} = 61.021 \text{ mm}$$

$$C_{\text{Strut}} := f_{\text{cu}} \cdot w_{\text{st}} \cdot b \quad C_{\text{Strut}} = 72.249 \text{ kN} \quad \text{Check2} := \begin{cases} \text{"Model Not Applicable"} & \text{if } C_{\text{Strut}} < 0 \\ \text{"OK"} & \text{otherwise} \end{cases}$$

$$C_2 := \min(C_{\text{TOP}}, C_{\text{BOT}}, C_{\text{Strut}}) \quad C_2 = 72.249 \text{ kN}$$

$$F_2 := C_2 \cdot \sin(\theta_2) \quad F_2 = 44.222 \text{ kN}$$

Check Main Reinforcement

$$T := C_2 \cdot \cos(\theta_2) + C_1 \cdot \sin(\theta) \quad T = 150 \text{ kN} \quad T_{\text{r}} := A_s \cdot F_y \quad T_{\text{r}} = 417 \text{ kN}$$

$$\text{Check} := \begin{cases} \text{"OK"} & \text{if } T < T_{\text{r}} \\ \text{"NG"} & \text{otherwise} \end{cases}$$

$$\text{Therefore: } V := F_1 + F_2 \quad V = 112.37 \text{ kN}$$

$$P := \frac{V \cdot L}{L - a} \quad \boxed{P = 161 \text{ kN}} \quad \text{Check} = \text{"OK"} \quad \text{Check2} = \text{"OK"}$$

Appendix I Case Study

To illustrate the use of the proposed model, a case study of a real structure that has deteriorated from the effects of corrosion is presented in this section. The structure is a pier bent that supports a ramp for a major expressway. The structure was constructed in 1963.

The structure is 95.75 in (2.432 m) high from the top of the footing to the bottom of the bearing seat on the south side of the pier structure. The cap beam is 21 ft (6.401 m) long and the column is 12 ft (3.658 m) long. The column is 44 in (1.118 m) wide and the cap beam is 48 in (1.219 m) wide. An elevation drawing of the structure is provided in Figure 1.

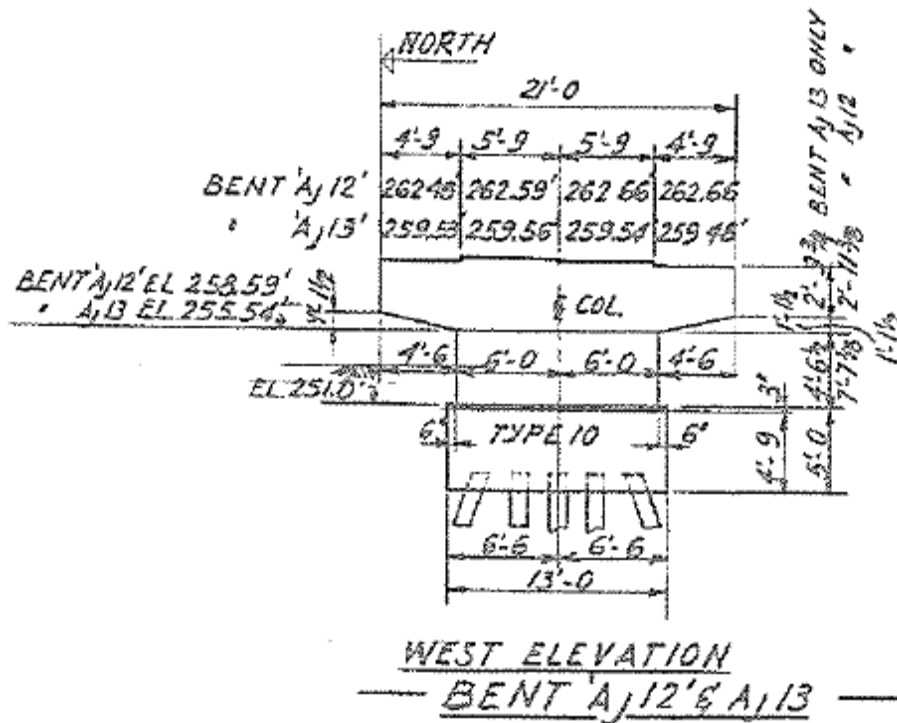


Figure 1 Case Study Structure Dimensions (McCormick Rankin Corporation)

The structure supports four girders which are simply supported at each pier bent. The girders are supported on expansion and fixed bearings. The length of the bearing plate along the cap beam is 3ft (0.914 m). The concrete compressive strength was assumed to be 25 MPa. The reinforcement yield

strength was assumed to be 230 MPa. Shown in Figure 2 are the east face of the structure and a field sketch of the deterioration.

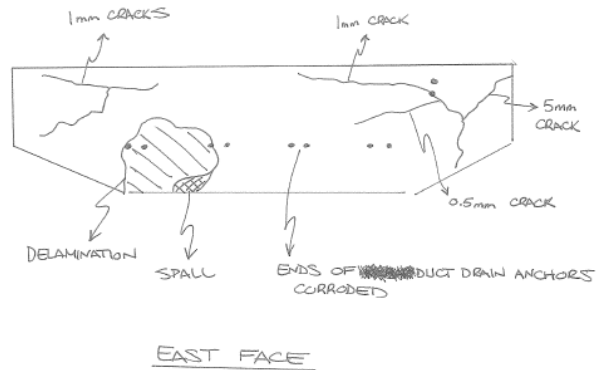


Figure 2 East Face of Structure (McCormick Rankin Corporation)

Wide cracks in the concrete that varied from 0.5 mm to 6 mm were recorded. In addition, an area of delamination and minor spalling was noted. It is not clear whether these deteriorations were caused by corrosion. The structure has been repaired, so it is likely that corrosion has played a role in the life of the structure.

A strut and tie model of the structure was developed is shown in Figure 3. The strength of the cantilever portion of the cap beam was modelled using a direct strut from the girder loading point to the outside edge of the column. A tension tie is provided between the two upper nodes, and a reinforced compression strut is necessary between the two bottom nodes. The length of the nodes (3ft (0.914 m)) is based on the bearing length at the girder supports; all of the nodes were assumed to have the same length. The depth of the nodes (7 in (0.178 m)) is assumed to be twice the depth to the centroid of the main reinforcing steel.

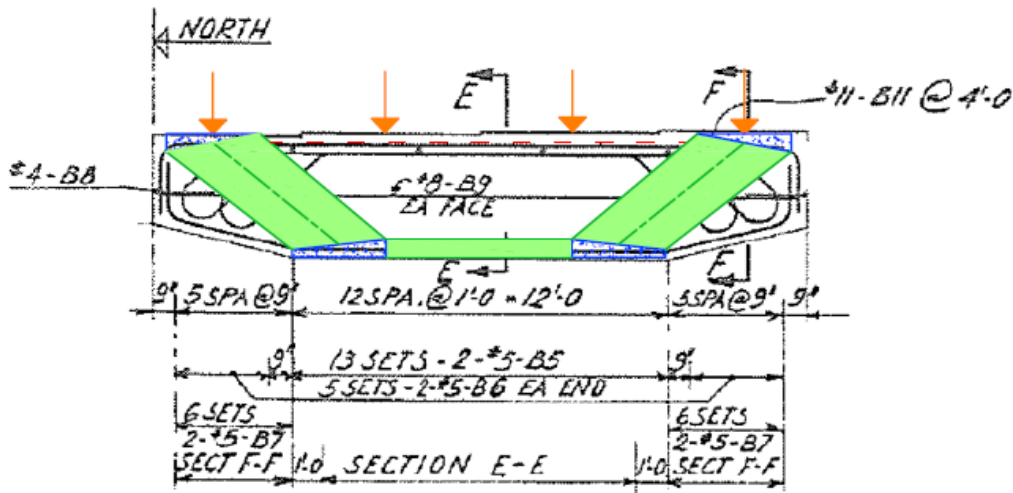


Figure 3 Case Study Strut and Tie Model

Table 1 summarizes the factored strengths of the elements in the strut and tie model. The applied loads in the nodes, top tension tie, and bottom compression strut are based on the strength of the diagonal compressive strut. The compressive strength of the diagonal compressive strut was reduced to account for the effects of a 1 mm wide crack in the concrete. The resistance of the top tension tie is less than the applied load, but this difference will not affect the overall strength of the pier bent. The reaction that can be supported by the pier bent for the outside girder was found to be 2003 kN.

Table 1 Case Study Strut and Tie Model Loads

Element	Applied Load (kN)	Resistance (kN)
Diagonal Compressive Strut	--	3116
Top Tension Tie	2387	2350
Bottom Compressive Strut	2413	2860
Top Node (Critical)	3116	12473

The truck loading specified by CSA S6-06 is a CL-625 truck load. The total weight of the truck is 625 kN. The two spans supported by this pier are equal in length. Consequently, if one truck was on each span the sum of the reactions from the four girders would be 625 kN. It is clear that the deteriorated pier bent is strong enough to support the applied loads, so no strengthening is required. This example illustrates that the formulations provided in Chapter 6 can be easily used by an engineer

to evaluate the strength of a deteriorated structure. A copy of the case study calculations is provided below.

Case Study

1. Geometry

$$A_s := 8 \cdot 1.56 \text{ in}^2 \quad d := 44.5 \text{ in} \quad f_c := 25 \text{ MPa} \quad F_y := 230 \text{ MPa} \quad b := 4 \text{ ft}$$

Assume: $c := 50 \text{ mm}$ $b := b - 2 \cdot c$ **STEP 3**

$$\alpha_1 := 0.85 - 0.0015 \cdot \frac{f_c}{\text{MPa}} \quad \beta_1 := 0.97 - 0.0025 \cdot \frac{f_c}{\text{MPa}} \quad h := 48 \text{ in} \quad \phi_s := 0.85 \quad \phi_c := 0.65$$

$$x := \frac{A_s \cdot F_y}{\alpha_1 \cdot b \cdot f_c} \quad x = 81.459 \text{ mm} \quad c := \frac{x}{\beta_1} \quad c = 89.762 \text{ mm}$$

$$x = 3.207 \text{ in} \quad d_1 := 3.5 \text{ in} \quad l_b := 36 \text{ in} \quad a := 450 \text{ mm} \quad w_c := 1 \text{ mm}$$

2. Strut Capacity

$$\alpha_s := 50.75 \text{ deg} \quad \text{Assume tension steel close to yielding} \quad \epsilon_s := 0.002$$

$$\epsilon_1 := \epsilon_s + (\epsilon_s + 0.002) \cdot \cot(\alpha_s)^2 \quad \epsilon_1 = 0.00467$$

$$f_{cu} := \min\left(0.85 \cdot f_c, \frac{f_c}{0.8 + 170 \cdot \epsilon_1}\right) \quad f_{cu} = 15.684 \text{ MPa} \quad 0.85 \cdot f_c = 21.25 \text{ MPa}$$

$$f_{cu} := f_{cu} - 11 \frac{\text{MPa}}{\text{mm}} w_c \quad f_{cu} = 4.684 \text{ MPa} \quad \text{STEP 2}$$

From AutoCAD:

$$A_{cu} := b \cdot 36 \text{ in} \quad A_{cu} = 1023396 \text{ mm}^2$$

$$D := \phi_c \cdot A_{cu} \cdot f_{cu} \quad D = 3116 \text{ kN}$$

3. Check Tension Tie

For the top Tie: $T_1 := D \cdot \sin(50 \text{ deg}) \quad T_1 = 2387 \text{ kN}$

$$A_s := 12 \cdot 1.56 \text{ in}^2 \quad d_b := 1.41 \text{ in} \quad \alpha := 2 \text{ mm}$$

$$\Delta A_{s0} := A_s \cdot \left[1 - \left[1 - \frac{\alpha}{d_b} \cdot \left(7.53 + 9.32 \cdot \frac{c}{d_b} \right) \cdot 10^{-3} \right]^2 \right] \quad \Delta A_{s0} = 41.63 \text{ mm}^2$$

$$K := 0.0575 \text{ mm}^{-1} \quad \Delta A_s := \frac{w_c}{K} + \Delta A_{s0} \quad \Delta A_s = 59.022 \text{ mm}^2$$

$$A_s := A_s - \Delta A_s \quad \text{STEP 1}$$

$$F_y := 230\text{MPa} \quad T_s := \phi_s \cdot A_s \cdot F_y \quad T_s = 2350\text{kN}$$

$$\text{Check1} := \begin{cases} \text{"NOT OK"} & \text{if } T_1 > T_s \\ \text{"OK"} & \text{otherwise} \end{cases}$$

4. Check Bottom Compression Strut

$$\alpha_s := 90\text{deg} \quad \text{Assume tension steel close to yielding} \quad \epsilon_s := 0.002$$

$$\epsilon_1 := \epsilon_s + (\epsilon_s + 0.002) \cdot \cot(\alpha_s)^2 \quad \epsilon_1 = 0.002$$

$$\text{Use compressive strength of sound concrete: } f_{cu} := \min\left(0.85 \cdot f_c, \frac{f_c}{0.8 + 170 \cdot \epsilon_1}\right) \quad f_{cu} = 21.25\text{MPa}$$

$$A_{cu} := b \cdot 7\text{in} \quad C := D \cdot \cos(39.25\text{deg}) \quad C = 2413\text{kN}$$

As per clause 11.4.2.4 and clause 7.6.5:

Tie spacing not to exceed:

$$d_b := 0.75\text{in} \quad d_t := 0.625\text{in} \quad s_{\max} := \min(16 \cdot d_b, 48 \cdot d_t, h) \quad s_{\max} = 12\text{in} \quad s_{\text{prov}} := 12\text{in}$$

OK, therefore use a reinforced bottom strut:

$$A_s := 2 \cdot 0.44\text{in}^2 \quad C_r := \phi_c \cdot A_{cu} \cdot f_{cu} + \phi_s \cdot A_s \cdot F_y \quad C_r = 2860\text{kN} \quad \text{Check2} := \begin{cases} \text{"NOT OK"} & \text{if } C > C_r \\ \text{"OK"} & \text{otherwise} \end{cases}$$

5. Check Nodal Capacity

$$\text{Top node critical -- CCT Node: } f_{cu} := 0.75 \cdot \phi_c \cdot f_c \quad f_{cu} = 12.188\text{MPa}$$

$$A_{cu} := b \cdot 36\text{in} \quad A_{cu} = 1023396\text{mm}^2$$

$$\text{NODE}_{\text{Capacity}} := A_{cu} \cdot f_{cu} \quad \text{NODE}_{\text{Capacity}} = 12473\text{kN}$$

$$\text{Check3} := \begin{cases} \text{"NOT OK"} & \text{if } D > \text{NODE}_{\text{Capacity}} \\ \text{"OK"} & \text{otherwise} \end{cases}$$

6. Summary

The point load capacity of the pier bent for the outside girders is:

$$P := D \cdot \cos(50\text{deg}) \quad P = 2003\text{kN}$$

Check1 = "NOT OK" Close Enough

Check2 = "OK"

Check3 = "OK"